Final Report

Navigating the Moon

AE3200
Group 22

Delft University of Technology

TU Delft

Final Report

Navigating the Moon

by

Group 22

Student Name	Student Number
Matei Dinescu	5260248
Jasper Geijsberts	5331587
Ian Maes	5216931
Serban Nedelcu	5324491
Andreas Van Parys	5089263
Lennart van der Peet	5280168
Nikolaus Oliver Ricker Chong	5274737
Kyle Scherpenzeel	5310210
Carl Spichal	5222397
Mathijs Vereycken	5324661

Instructor:	W. van der Wal
Coaches:	E. Gülçin & Z. Jingjing
Project Duration:	April 2023 - June 2023
Faculty:	Faculty of Aerospace Engineering, Delft

Cover: European Space Agency. *A constellation of satellites around the Moon*

Style: TU Delft Report Style, with modifications by Daan Zwaneveld

TU Delft

Contents

Nomenclature

All acronyms used in the document are clickable and link to this table.

Acronym	Definition
ADCS	Attitude Determination Control System
AFS	Augmented Forward Signal
BLT	Ballistic Lunar Transfer
BOL	Begin of Life
CAD	Computer Aided Design
CALT	China Academy of Launch Vehicle Technology
CDH	Command and Data Handling
CMCU	Clock Monitoring and Control Unit
CMG	Control Moment Gyro
CoG	Center of Gravity
CPI	Cost Performance Index
CPU	Central Processing Unit
DMIPS	Dhrystone Million Instructions Per Second
DOD	Depth of Discharge
DOP	Dilution of Precision
DSAC	Deep Space Atomic Clock
EM	Engineering Model
EP	Electrical Propulsion
EPS	Electrical Power System
ESA	European Space Agency
ESTEC	European Space research TEchnology Centre
EOL	End of Life
FLCA	Future Lunar Communications Architecture
FEM	Finite Element Methods
FGUU	Frequency Generator and Upconverter Unit
FM	Flight Model
FOC	Full Operational Capability
FOV	Field of View
FSS	Fine Sun Sensor
GDOP	Geometric Dilution of Precision
GNSS	Global Navigation Satellite System
GPIM	Green Propulsion Infusion Mission
GPS	Global Positioning System
GS	Ground Station
HALO	Habitation and Logistic Outpost
HET	Hall Effect Thrusters
HDOP	Horizontal Dilution of Precision
HHDOP	Height Constrained Horizontal Dilution of Precision
IA&T	Integration Testing and Assembling
IMM-α	Inverted Metamorphic Multi-junction
IT	Information Technology
IOC	Initial Operational Capability
IOV	In-Orbit Validation
IPS	Instructions Per Second
JIT	Just in Time
LEO	Low Earth Orbit
LOI	Lunar Orbit Insertion
LL1	Lunar Lagrange point 1
LL2	Lunar Lagrange point 2
LNSS	Lunar Navigation Space System
LNS	Lunar Navigation Satellite
LRC	Lunar Relay Constellation
LRS	Lunar Relay Satellites
LRT	Lunar Reference Time
LV	Launch Vehicle
MCS	Master Control Station
MIPS	Million Instructions Per Second
MMOI	Mass Moment of Inertia
NASA	The National Aeronautics and Space Administration
NCR	Non-Conformance Report
NRHO	Near-Rectilinear Halo Orbit
NSGU	Navigation Signal Generation Unit
NSPTF	National Space Propulsion Test Facility
OBC NG	On Board Computer Next Generation
OBDH	On Board Data Handling
ODTS	Orbit Determination & Time Synchronisation
OG	Original Constellation
OISL	Optical Inter-Satellite Links.
OWR	One-Way Ranging
PCDU	Power Conditioning and Distribution Unit
PDOP	Position Dilution of Precision
PPE	Power and Propulsion Element
PRU	Power Regulation Unit
PVT	Position Velocity Time
RAAN	Right Ascension of the Ascending Node
RAMS	Reliability, Availability, Maintainability and Safety
R&D	Research & Development
RINEX	Receiver Independent Exchange Format
ROI	Return on Investment
RF	Radio Frequency
RP-1	Refined Petroleum-1
RTG	Radioisotope Thermoelectric Generator
SMAD	Space Mission Analysis and Design
SNR	Signal-to-Noise Ratio
SOI	Sphere of Influence
SOC	Streets of Coverage
SSD	Sum of the Square of the differences
STM	Structural and Thermal Model
SWOT	Strengths, Weaknesses, Opportunities & Threats
TBD	To Be Determined
TCS	Thermal Control System
TLI	Trans-Lunar Injection
TRL	Technology Readiness Level
TDOP	Time Dilution of Precision
TS	Time Dissemination
TSU	Thermal Storage Unit
TT&C	Telemetry Tracking and Command
TUDAT	TU Delft Astrodynamics Toolbox
TWM	Two way Measurements
UERE	User Equivalent Range Error
UEVE	User Equivalent Velocity Error
ULS	User Lunar Segment
USA	United States of America
UTC	Universal Time Coordinated
V&V	Verification & Validation
VDOP	Vertical Dilution of Precision

1

Executive Overview

By C.A.G.C. Spichal, I. Maes, N. Ricker

In the last few decades, a large increase in interest in space and particularly the Moon has taken place. The Moon is seen as a gateway to the rest of the Solar System. Missions to the Moon will inevitably lead to technological and scientific advancements. These would help in humanity's mission to explore and develop habitats in the Solar System. Companies see economic opportunities in these places for activities such as the acquisition of rare Earth materials, as well as commercialising space travel. Furthermore, countries see these accomplishments as a sort of international competition while also collaborating with other nations. The mission design presented here aims to facilitate these objectives by providing the necessary navigation support to any future mission on or around the Moon.

The Design Synthesis Project (DSE) is the final exercise performed during the Bachelor programme at Delft University of Technology. It is a 10-week project, where 10 students design a solution to a problem statement set by a tutor. It is an intensive set of sessions, accounting for almost 4000 working hours, where the prospective engineers must study, plan, design, and report a conceptual mission design.

There are multiple people involved in the project. The tutor, coaches, and students are directly connected to a project. Some professors and Teaching Assistants act as a link between the Bachelor and mission objectives. They provide the general information on deliverables and objectives of the DSE. Finally, companies and field experts are external components aiding in achieving the target. The DSE aims to provide an opportunity for students to apply the knowledge and skills developed throughout their Bachelor in a real-life environment. It combines multiple disciplines to solve a complex problem.

The topic of the DSE developed in this overview is "Navigating the Moon". This project aims to design a Lunar navigation system capable of offering full coverage of the Moon's surface. It is a mission inspired by a similar project currently being developed at the European Space Agency (ESA), named "Moonlight". Even though the project is not performed in collaboration with ESA, it is still considered the main stakeholder in the design. The tutor in charge is Dr.ir. W. van der Wal, along with coaches MSc. J. Zhao and Dr. G. Ermiş.

The Moonlight Project is a Lunar communications and navigation system aiming to provide reliable communications and accurate positioning for several Lunar missions. ESA is currently inviting companies to show "expressions of interest to contribute to commercial satellite services for the Moon" [1]. This will be taken in consideration for future development and production of the mission. The DSE team acts as one of the companies studying conceptual designs. It is an ambitious project, for which the scope had to be reduced to adapt it to the previous knowledge and objectives of the course. The main difference between the team and the companies concerns the data relay: contrary to the ESA mission, the current DSE only develops the navigation component of the mission. The original mission need statement from ESA is [1]:

Enable the implementation of European Communication and Navigation capability through a European-led private delivery of Services that will support the current and next generation of institutional and commercial Lunar explorers.

After making the necessary changes to the original mission, a new mission need statement was produced. This mission need statement focuses more on this DSE project group's mission, not necessarily ESA's mission. This statement drives the design and choices made throughout the project, always aiming to reach the goal in the

[1] https://www.esa.int/Applications/Connectivity_and_Secure_Communications/Who_s_ready_to_serve_the_lunar_missions

most efficient way. The mission need statement for the DSE project is:

Produce a conceptual design for a navigation system on the Moon that is capable of providing service to Lunar missions, starting deployment by 2028.

Furthermore, there are certain user requirements that help the team focus on certain aspects of the mission. Before taking these into account however, the objectives are researched for their feasibility. Some requirements are changed with the agreement of the tutor, including the velocity and position requirement for landers. Afterwards, the main technical objectives are listed. These main technical objectives are about providing accurate positioning for orbiters, landers, and surface elements on the Moon, with accuracy of 100 m for orbiters, 50 m (horizontally) and 100 m (vertically) for landers and 10 m for surface users. These accuracies need to be combined with a PVT service availability of 95% over a course of 3 months. The PVT service provides any user on or around the Moon with the position, velocity and time. Along with these requirements, there are certain constraints to consider, also set by the user. First, the complete mission has an economic budget of 10 billion euros. Second, the first launch of the deployment phase must take place in 2028. Finally, the mission design and operation must be environmentally and socially sustainable.

The Project Plan discusses the organisational approach to complete the mission. This includes an organogram which provides the desired structure to perform all tasks efficiently. By assigning specific tasks to the members, better communication and efficiency is achieved. The Project Plan effectively discusses all the steps that must be taken to produce a successful design. These steps are divided per week, considering deliverables and milestones, along with several sub-processes and decision-making steps. In the following paragraphs, a summarised version of this plan is explained.

During the first week of DSE, the team focuses on understanding the topic and creating the organisational structure. Among this structure, a Gantt chart, Workflow diagram, Work Breakdown Structure and Organogram are created. Furthermore, the mission needs are studied, a mission need statement is built, and the stakeholder requirements are discussed and analysed. In the second week, the literature review takes place. This allows to understand the mission functions, such that the team understands the various steps the mission will perform during operation. The functional requirements for the mission are also defined and used to find viable design options.

After defining the organisational structure, the mission design is started. From the mission need statement and problem requirements, a general solution can be implemented. A lot of options need to be researched. Therefore, a design options analysis is performed using a design options tree. It is done to study all possibilities and get the best solution possible. This means looking into all general solutions as well as variations of smaller systems within these general solutions.

The next step consists in defining the technical mission requirements. This set of requirements define what the mission should accomplish, without providing solutions to it. For this process, a set of requirements provided by ESA was used as a complementary document. These ESA requirements are a base for the navigation requirements and will be considered for the group's design. There are certain driving requirements, these have a large influence on design decisions and will be the most important to consider during the designing process. Some of these requirements are:

- The LNSS shall provide navigation service for surface stationary/mobile, descending, ascending, and orbiting users.
- The navigation services shall be broadcast with a radio Augmented Forward Signal (AFS).
- The service shall allow the user to compute position and velocity and time offset at least once per second.
- The service shall provide position errors smaller than or equal to 10 m for surface users.
- The service shall provide velocity errors smaller or equal than 0.1m/s for surface users.
- The system shall not depend on other services or processes required by users.
- The system shall not pose a risk to humans, equipment, or environment on the Moon at the End of Life.
- Budgets shall include costs of offsetting atmospheric pollution through greenhouse gases or hazardous substances.
- The LNSS shall be redundant against 2 nodes failures.
- The service shall comply with legal and ethical regulations.

The requirements above encompass the most relevant aspects of the mission to be complied with. They are also used during the study of viable design options. Given the novelty of the mission and the difference in environment, a large range of possibilities are checked. The main categories revolve around Earth based ranging, Lunar based ranging, and Space based ranging. Earth based turns out to be not feasible, generally due to accuracy issues or lack of Moon coverage. Some other options could be feasible, such as setting Lunar towers, surface sensors, or body beacons. Finally, deep space reflectors, continuous space probes among others could work. There are usually concerns related to accuracy or costs in the previously mentioned scenarios. Nonetheless, some of these scenarios are further studied to prove their feasibility.

One main group of designs proved to be viable and efficient, a Lunar constellation. In this group, there are various parameters to study, such as the use of one or more ground stations, number of satellites, orbit inclination, altitude, and number of orbit planes. Through a detailed design and a trade-off, the parameters are further explored and optimised to reduce errors, while considering cost, reliability, and sustainability. Some variations or combinations of a Lunar constellation are also considered, such as using Lagrange points to provide the data relay intermediate point from the Moon constellation back to Earth.

Along with designing requirements and studying designs, a preliminary market analysis is performed. It gives a general idea of the competition and costs. There are several future Lunar missions which serve as a basis to estimate how the future market will look like: Lunar Gateway, LunaNet, and Artemis. They might not have the same objectives, but share characteristics. By performing a SWOT analysis, the following results were found:

- **Strengths**: First in the market, accounting for a large market share. ESA is an already established agency, and the system would aid in scientific advances.
- **Weaknesses**: There are multiple uncertainties due to the novelty of the design. It involves a long development phase, which leads to the likelihood of overshooting the budget.
- **Opportunities**: There is potential in the development of a Lunar economy, from military to commercial applications. It could also provide usage to other agencies, while providing jobs and collaboration.
- **Threats**: Given the innovative technology, there are higher risks, such as new regulations, political conflicts, or even a space disaster. There are also risks of an unstable market interest.

A preliminary total mission cost margin of $4.10\,\text{B€} - 6.83\,\text{B€}$ was calculated based on cost values from GNSS, Earth and Moon based scientific satellites. A rule of thumb is then applied to obtain the first order estimation of the constellation cost.

A technical risk assessment of the mission after finding feasible designs showed relevant risks at all stages of the mission: Research & Development, Production, Verification & Validation, Launch, Operation, and End of Life. Relevant analysis of human error, technical errors, and external factors were compared to generate a risk map. The main risks are: bad/incomplete requirements, oversimplification of the analysis, and clock failure of the node. Mitigation strategies were developed to lower the risks. Even though there are no high-risk situations after mitigation, each situation is reassessed at launch and operations.

Finally, certain strategies are developed for the next stages of the mission design. Resource allocation considers the use of sources of supply and how to allocate them correctly along the process. A plan to keep track of them is created. The resources discussed are money, time, natural resources, human power, and energy. They are limited either by the user, or by the sustainability objectives set. From the study, production, and launch are the stages with the highest resource allocation, while End of Life needs the least resources.

Strategies for margins and budgets are also considered. They do not state values but explain procedures to obtain them in the next steps. Both mission and spacecraft margins and budgets will be needed for the design. In general, margins are large at the initial stages and become smaller as the design progresses. The budgets are generally obtained from historical data and as the design iterates, they become more accurate by using analytical expressions.

Finally, a sustainability strategy is developed. In this, the technical aspects are considered, and environmental and social concerns are linked. It introduces a general structure which can be used in other stages to consider sustainability in the design. The main concerns relate to production and launch. There are suggested mitigation strategies which can be further developed. These plans are created, so the team understands the risks' relevance, and where the critical points lie to study. This concludes the first stage of the design, where the plans are set, the mission studied, a clear path designed, the team structured, and the general technical

overview of the mission understood. The team can further focus on developing the mission and spacecraft in detail.

Earlier in the Baseline Report, several contenders for the design were outlined. After eliminating the unfeasible and non-developable ones, the team made a decision to perform two segments in parallel: space and ground. Each one is developed independently through two stages, a first stage reassessing the feasibility of the design, and a second stage studying the detailed aspects, concluding with a trade-off. The space segment designs are:

- **Moon Constellation**: Lunar orbiters in a constellation providing PVT services. This design is very similar to current GNSS constellations.
- **Moon/Lagrange Constellation**: The standard Moon constellation is supported by navigation satellites in orbit around the Moon-Earth Lagrange points LL1 and LL2. It could potentially reduce the required number of satellites.
- **Moon Tower/Moon Constellation**: The standard Moon constellation would incorporate a tower on the Moon's surface to support with coverage. These towers would be placed in areas of high interest to improve accuracy.
- **Earth Constellation**: Satellites orbiting the Earth at altitudes similar to the Earth-Moon distance with different inclinations, combined with satellites at LL1 and LL2.

Three different designs are considered for the control segment of the mission. These are:

- **Base Lunar Stations**: Six ground stations would be located on the Moon, capable of communicating with the constellation, updating the ephemeris information locally or relaying it to the Earth.
- **Lunar Relay Constellation**: Use of relay satellites in LL1 and LL2. They would directly contact all navigation satellites. These would serve the same function as the ground stations.
- **Self-Control Satellites**: The satellites would update each other with the use of reference marks. In this design, the satellite constellation would act independently for operation functions. They would communicate with a relay satellite for monitoring purposes from the Earth's surface.

In the stage 1 design process, basic calculations are made for the necessary amount of satellites and their orbital planes for each conceptual design. The Moon Tower/Moon constellation was eliminated. This was due to the complex and costly deployment method required. Due to the number of towers that needed to be transported, a large amount of high payload launchers are needed for the transportation to the Moon. Then getting the towers to the correct locations is another difficulty. This would require a whole other project to be designed and greatly exceed the budget cap of the project. Lastly, the ground stations on the Moon design option was eliminated. The ground stations had similar problems to the Moon towers, due to the complex and costly deployment method.

In the stage 2 design of the orbit segment, models and simulations are created to simulate coverage, perturbation, and accuracy properties of orbits as well as the Lagrange points. This is done by simulations within the group's GitHub. The Earth constellation is also eliminated due to coverage issues, making the design not meet the requirements. These models are then used to find optimal orbits for the different stage 1 designs. Simulations of propagating the orbits of the different design concepts give an insight into the ΔV that is needed for orbit maintenance. This is an important consideration for the trade-off later on. Other parameters like PDOP and the amount of coverage can be calculated using the models and can be used later on for the trade-off.

After the remaining orbit concepts are designed, the Moon constellation and Lagrange/Moon constellation, the trade-off is performed. First, the characteristics of the missions are investigated. These characteristics are used to find significant differences between the design options in terms of these criteria.
Trade-off criteria are selected that offer a good comparison between the designs. A brief discussion of the differences and results of the analysis is included. It can be seen here:

- **Technology Readiness Level**: This criterion came out better for the Moon constellation. Mainly because of the more proven constellation type and similarities to GNSS constellations.
- **Reliability**: The Lagrange point environment is less explored than Lunar orbits, there are also 2 points of failure with the Lagrange satellites. These satellites are not simple to replace. These two downsides give the upper hand to the Moon constellation in this criteria.

- **Mission Complexity**: Mainly due to the manoeuvre complexity of EOL operations for the Lagrange satellites, and the lack thereof for the Moon constellation, the Moon constellation is considered to be less complex.
- **Maintenance** ΔV: The 2 satellites at the Lagrange points in halo orbits will require less ΔV than the ones in Lunar orbits. This gives a slight edge to the Lagrange/Moon constellation regarding Maintenance ΔV.
- **Coverage**: The number of satellites in view (also called the coverage fold) for the Moon constellation (7-12 fold) is slightly higher than the coverage fold for the Lagrange/Moon constellation (6-11 fold). This provides advantages for redundancy and accuracies. Therefore, the Moon constellation is considered best for this criteria.
- **Positioning Accuracy**: The positioning accuracies including dilution of precision (DOP) values are fairly similar for both design options. However, the allowable orbit ephemeris errors are smaller in the Moon constellation. This gives the Moon constellation the upper hand.

For the trade-off, each criterion was assigned a weight based on its relative importance. These are defined by taking each individual team member's opinion into account. Now the designs are given scores for the different criteria based on the analysis, which a brief description can be seen in the summation of criteria. This is done by taking every team member's opinion into account, specifically, the members that analysed those specific criteria. Finally, a trade-off table is made where the final design is chosen. The selected design option is the Moon constellation due to its many advantages for the different criteria.

The control segment is designed for the trade-off. For this trade-off, the same procedures as before are used. The trade-off criteria and a brief description of their results are given here:

- **Technology Readiness Level**: The relay satellite to MCS option has been proven in GNSS constellations multiple times, while self-control has only been tested in the BeiDou [2] GNSS system. Therefore, the relay to MCS design options is considered to be the best for this criteria.
- **Cost**: The self-control system will have lower operations and deployment costs since these tasks can be performed by the control system itself. The relay satellite to MCS system will need an operations segment, which will cost more. Therefore, the self-control system is considered best.
- **Temporal Performance**: Self-control has the advantage of transmitting at a much shorter distance when compared to first sending the data to Earth, meaning a higher update frequency of satellite ephemeris data can be achieved. This is the main reason the self-control outperforms the relay satellite to MCS in this criteria.
- **Sustainability**: Both designs are considered to perform similarly in this category. The self-control needs fewer launches, but the satellites will have a higher mass. On the other hand, the other design options need more launches, but the satellites will have a lower mass. In total, they are given the same score for this criteria.
- **Reliability**: Overall, self-control is considered to be the more reliable. It is less complex and straightforward with redundancy built-in, but has a lower TRL. Despite the lower TRL, it is still considered to be more reliable.
- **Market Potential**: The self-control is considered to be more scalable due to its lower dependency on a MCS and provides more interesting technology for future missions when compared to the relay satellite to MCS option. Therefore, it is considered to be better in the category.

These assigned weights are done similarly to the space segment trade-off. Afterwards, assigning scores is done by taking into account the group's opinions. Using the scores that were given to both designs for the different criteria, the final design is selected. The selected design option is the ODTS self-control system.

After both choices are made using the trade-off, they are combined into a final design that will be developed into further stages. An N^2 chart, hardware, software, and communication & data handling diagrams are made to provide a base for the further analysis of the final design. Also, throughout the three weeks, certain verification and validation procedures are set and tested. The risk and sustainability strategy is updated. This entails many of the risks and sustainability planning included in the baseline report. Now that the final design has been decided upon, the subsystems can be designed.

The navigation subsystem looks into the accuracy to which the position of any user on the Lunar surface or in Lunar orbit can be determined. This means that the errors in the position of each satellite in orbit are also

studied. The constellation is always set up in such a way that the requirements are met. A set of different frozen orbits, orbits for which the satellite remains in orbit without having to burn any propellant, are analysed. The optimal set is deduced from it. After the selection of the satellite constellation, one of the clocks with the best specific performance and the highest frequency stability, the Deep Space Atomic Clock, is selected. This clock is chosen based on the reasoning that it must measure time as accurately as possible to provide the best possible position data and the highest allowable ephemeris error, which is a crucial part for the design as the perturbations around the Moon are much greater

The Telemetry, Tracking & Command subsystem aims to provide the user with the necessary signals for navigation. The spacecraft uses four S-band antennas positioned in a phased array to provide the ephemeris data to the users. Another S-band antenna is used to relay position, velocity, and health data to the Lunar Pathfinder. This is done to monitor the system, and intervene if it is not operating nominally. The self-control requires two lasers mounted on gimbals. One laser is used to communicate with other satellites and exchange its ephemeris data. The other laser is used for two-way ranging with retroreflectors on the Moon. The gimbals provide a good range of motion and accuracy for these lasers to point in the necessary direction of the neighbouring satellites. The rate at which the ephemeris of each satellite is updated amounts to about one and a half hours. This enables the ephemeris error to reset to zero after that time, thus not deviating more than the allowed one of 0.9494 m.

The Command Data Handling subsystem mainly focuses on the selection of an on-board computer that provides sufficient performance and reliability to perform all the necessary computations. These computations include the update of its position and the ones coming from the other satellites. The first iterations look into values coming from literature and providing typical computer mass and power densities. The final computer that is selected is named OBC NG and has a memory of 512 MiB.

The propulsion subsystem entails the selection of a type of propellant as well as a propulsion system that results from the propellant used. All the types of propulsion that can be implemented for the mission are looked at and narrowed down to the two most promising options: electrical and green mono-propulsion. Unlike hydrazine, green propellants are non-toxic propellants that can be used for the mission. In the final trade-off, mono-propulsion is selected based on the reasoning that the power required to feed an electrical propulsion system is too important. The mission phases on which the most substantial mass savings are made are the LOI and EOL. The components present a lower mass compared to the propellant one and are not as much of a driving factor in the total mass of the propulsion system. The total propellant mass amounts to 244 kg. The final mono-propellant that is chosen is called AF-M315E. 1 N and 22 N thrusters are selected to provide for the mission's necessary manoeuvres.

The Attitude Determination and Control System (ADCS) focuses on the maintenance of the satellite in its required orientation and position within the orbit. However, the first constraint to look at is related to the pointing accuracy of the lasers, given that they need to point specifically into the direction of the neighbouring satellites as well as towards the reflectors that help the satellite determine its position. The accuracy at which the position is to be determined is found to be $0.46°$. The next step consists in identifying the disturbances that must be counteracted in order to keep the satellite in its desired orientation. In the case of the Moon, only radiation disturbances present substantial effects. The actuators used to correct those disturbances are Control Moment Gyros (CMG). Because CMG can only reach a certain maximum speed, thrusters are added to desaturate the CMGs. Sensors are also implemented to measure the actual orientation of the satellite based on the position of the stars and the Sun.

The Electrical Power System (EPS) deals with the supply of power and electricity to all the components that are in need of it. To gain an idea of the needed power, the average of power required for other navigation satellites is used. Then, after the first design stage, a new power is estimated with values for preliminary components. The power is supplied by solar arrays, paired with batteries when the spacecraft is not exposed to sunlight. The batteries, therefore, need to be sized first according to the longest time during which no sunlight comes in. After that, the solar arrays are sized. The most challenging factor to account for is the efficiency at which solar cells can transform photon energy into electric energy. Quadruple Junction Solar Cells used in the JUICE mission are selected for each of the Navigating the Moon satellites. The total beginning of life power provided by the EPS amounts to 2340 W. The second to last hardware component to be designed is the Power Control and Distribution Unit (PCDU). The PCDU makes sure to distribute the power to each component in a regulated way. The selected model is the Terma PCDU. Finally, the entire cable harness that makes up the 'veins' of the

spacecraft system is estimated to be 100 kg.

The Thermal Control System (TCS) controls the temperature of the system, such that, every component is within their operating range and can perform nominally. To deduce the necessary coating, heaters and radiators that must be implemented, the absorptivity, as well as the emissivity are analysed. The use of a coating to increase reflectivity and increase thermal efficiency is analysed. The combination of the heat energy produced and dissipated amounts to an operational temperature range of 290 K to 308 K.

The Structure subsystem of the satellite focuses on the critical loads applied to the spacecraft that could potentially damage it permanently. The most critical phase is the launch. During the launch, natural frequencies pose a great threat to the integrity of the satellite. The yield and ultimate stress must also be analysed to select the appropriate material. Based on a short trade-off that accounts for cost, manufacturability, mass and thermal expansion coefficient, aluminium and titanium alloys are selected as the final materials. The next step that is looked into is the design of a solar array support structure that can carry the bending loads. With all the load constraints in mind, the cube shape with a 1 m side dimension is selected as an initial design that will be built upon.

Due to the subsystems' interconnected design, the spacecraft used for the Lunar navigation satellite constellation is optimised for its objectives. It is designed for a lifetime of 12 years, meaning that the satellite will provide its functions for the constellation for an extensive amount of time. The satellite has a mass of 1047.9 kg and an unstowed size of approximately 9.7 m x 3.1 m x 1.6 m. Six of these satellites fit into one Falcon Heavy by using a triangular support structure.

With the completion of the design phase for all mission systems, the key characteristics of the mission can be discussed. The constellation consists out of seven orbits. Four of these planes have almost the same Kepler elements, except the right ascension of the ascending node, which is evenly phased. The satellites within the planes are also evenly phased w.r.t. their true anomaly to gain the highest performance. They have a semi major axis of 5701.2 km and an inclination of $40.78°$. Two orbits in the same orbital plane are used, primarily for improved coverage of the North and South Pole. These orbits are highly eccentric, with an eccentricity of 0.6. They have a semi-major axis of 6541.4 km and an inclination of $56.2°$. Finally, a low inclination orbit is used to improve accuracy and coverage around the equator. This orbit has a semi major axis $10\,000$ km with an inclination $10°$. Using these seven orbits, an update frequency of approximately once every 1.5 h is needed to meet the navigation requirements.

Compared to the proposed frozen orbit constellation by F. Pereira and Daniel Selva [3], more accurate results have been obtained with this design for the entire Moon surface. To improve the DOPs and thereby meeting the accuracy requirements for the polar regions, by adding the polar orbits as proposed by T. Ely [4]. Additionally, service volumes up to 200 km altitude are investigated, again showing that the requirements are adhered to. The [4]

The timeline for the mission consists of six phases. The first phase, Phase A which starts in 2023, addresses the feasibility of the mission design. Concepts for the mission are tested for the first time. Shortly afterwards, in phase B, the system requirements and interfaces are finalised. Subsystems and some general mission aspects are designed. In 2025, phase C starts. The first physical models representing the spacecraft are produced. These are used to validate the design previously made. Phase D which starts in 2026, goes into the qualification and production process. The satellites are produced, and a prototype is launched. During Phase E starting in 2028, the deployment of the constellation takes place. This allows for the early operational capabilities, where the navigation service can be used for the first time in 2035. Later during this phase, full operational capabilities are reached in 2037 and the services can be used at the designed performance.

The fully operational constellation consists of the satellites that will provide the navigation service. Starting it implies generating/obtaining power, which may vary depending on the design. There will be one or more reference fixed points of which the position is known, such that the node has references for its orientation. Once the system is oriented in the correct attitude, it will be able to contact base (main operations centre). The base will confirm this connection and check the satellite position. Later, orbit insertion and final positioning will happen by translating the node to the desired space.

Once all satellites are set into position, the navigation network will be synchronised, so it can start providing ser-

vice. To accomplish this, the clocks must have the same time, so the ground station on Earth will synchronise them with the system time by sending correction factors. Then the initial position parameters are calculated for each satellite, values which are used by the customers of the navigation system. Base performs all calculations and updates the parameters at the same moment. Finally, all values are validated to ensure there were no errors.

Providing service is the most important function of the system. It consists of sending a signal to the users continuously such that they can calculate their approximate position. To perform this, the orientation of the node must be correct, followed by modulating the necessary data the user needs for positioning. It involves encrypting the information, converting it into a wave and combining it with a carrier wave and a unique pseudo-random wave, to then be sent to the Moon's surface. The *operations function* assists the *service function* by updating the orbital parameters of the nodes periodically. This is done to keep the positioning service accurate and reduce errors in the system.

Finally, maintenance functions take care of multiple disturbing situations. It also manages the changes required by the base and checks the system for issues. This last component is the most complex, given the isolated situation. If an error is found, a reparation protocol starts. Depending on the risk of the issue, either an automated change will be applied, or the service will stop, and a manual solution will be attempted. If the issue is not solved, then the component will be discarded, or the node decommissioned. In those cases, base must come up with solutions to maintain providing reliable service. Lastly, Phase F, which is started at the end of the mission, instigates the end of life procedures of the satellites.

During the design process, a lot of thought is put into the cost of each aspect of the mission. Due to the more detailed design, the preliminary cost can be updated or replaced by a more detailed investigation. An extensive analysis is performed on the cost of the mission during its different stages. It is split up into five categories: The spacecraft production, mission development, integration, assembly and testing, mission launch and operations. The spacecraft is investigated on a subsystem level. The most expensive stages of the mission are the spacecraft production and the operations. These make up two thirds of the complete mission cost. The budget requirement **NTM-USER-09** limits the total mission cost to $\$\ 10\,\mathrm{B}$. This requirement is met even after adding 2σ to the total cost.

Table 1.1: Mission Cost

Mission stage	Cost [B$]	SSD [B$]
Development	1.134	0.283
Spacecraft Production	1.538	0.418
IA&T	0.263	0.089
Launch	0.717	0.036
Operations	2.537	0.634
Carbon Footprint	0.003	0.001
Mission Total	6.192	1.461

The Return on Investment (ROI) for these high costs should not be missed. In general, the service will help smaller European companies to have a stake in future Lunar market. By providing them with access to crucial navigation services, these companies can participate in space exploration and benefit from potential Commerical opportunities. Such inclusivity would have a positive effect on European taxpayers, as it would promote economic growth and job creation. Furthermore, valuable knowledge can be gathered to expand scientific understanding on different topics.

Sustainability is taken into account during the whole mission lifetime. This includes the early stages of the design process. The R&D has a larger impact than most would expect initially. When considering sustainability early on, it can have positive effects during the following stages of the mission. Sustainability in the R&D phase leads to conceptual sustainability throughout the manufacturing, launch, operation, EOL and end of mission phases. The CO_2 emissions of the launch and spacecraft production are calculated, these are found to be $\$\ 3\,\mathrm{M\,kg}$. This is not a vast amount in terms of space missions. The operations stage also has a considerable effect on the sustainability of the design. For the operations of the propulsion subsystem, only electrical and green propellants are considered. To reduce emissions, the ADCS uses natural forces for maintenance operations as much as possible. Additionally, Radioisotope Thermoelectric Generators (RTG) shall not be used for

power generation.

Overall, the design aims to optimise the use of satellites in several orbital planes to provide the coverage needed for navigation services. This concludes the conceptual design for a navigation system on the Moon that is capable of providing service to Lunar missions.

2 Introduction

By L.D. van der Peet, N. Ricker

The Moon has always been a source of interest for humanity. Since the last Apollo mission in 1972, human Lunar exploration has been on hold. Recently, the interest in returning to the Moon has been on the rise. This is accentuated by the Artemis missions and several planned rovers to extract valuable resources.

Lunar navigation is one of the critical pillars that enable future exploration of the Moon. With the development of a navigation network, individual missions are liberated from the effort and cost associated with singular solutions. The introduction of this network will enable more and smaller missions to take place, stimulate the growth of the Lunar economy and open up opportunities for interplanetary exploration.

The purpose of this report is to finalise the orbits of the constellation, which builds on research performed previously [5] and design a compliant Lunar Navigation Satellite (LNS). First the mission outline in chapter 3 explores the need of the mission with a market analysis, together with the objects, and describes the previously established design concept. Then, chapter 4 investigates the potential of frozen orbits. The viability of these orbits are evaluated on the required manoeuvres and their associated updating frequency to remain within accuracy requirements. This chapter additionally concludes the orbit design, such that LNS can be designed for predefined orbital parameters. Afterwards, chapter 5 establishes requirements and initial estimates of the system. Furthermore, an analysis of the risks for the subsystems is performed. Then, chapter 6 starts with the design of the subsystems. Each subsystem is first designed individually by selecting initial components in a first stage design. After which, iterations between subsystems are performed to achieve a better optimised design. Chapter 7 summarises the important parameters from the design, as well as mission, and explains steps for the mission after the design stage. Additionally, the subsystems are integrated into a final design, and are shown in the internal and external lay-out of the spacecraft. Finally, in Appendix B, the technical drawing is shown in combination with important mission diagrams.

3 Mission Overview

While this report focuses mainly on the subsystem design of the satellites, said design is dictated by the overall mission and the events within it. Therefore, this chapter aims to give a good overview of the mission and all the decisions taken to arrive at the current state. Firstly, a reminder of the mission objectives will be given and the mission need statement in section 3.1. Next, a brief description and its most important components will be presented in section 3.2. Following this, a market analysis is done that shows economic potential of this

mission in the marketplace. The final section includes the operations and logistics side of the satellite design. It dictates the distribution of the goods and materials within a specified time frame.

3.1. Mission Objectives

By N. Ricker, J.K. Geijsberts, M. Dinescu

For the project to flow towards a single goal, a mission need statement needs to be made. It is seen below.

Produce a conceptual design for a navigation system on the Moon that is capable of providing service to Lunar missions, starting deployment by 2028.

This mission need statement, combined with the technical mission objectives determined in the Baseline report [6], summarises what the team is effectively trying to achieve with this design. The mission objectives are as follows:

1. "To design a navigation system capable of providing accurate positioning for orbiters, landers, and surface users on the Moon."
2. "To design a navigation system capable of providing accurate velocity measurements for orbiters, landers, and surface users on the Moon."
3. "To design a navigation system capable of providing accurate time for orbiters, landers, and surface users on the Moon."
4. "To design a navigation system capable of covering the entire Moon for 95% of the time."
5. "To design a robust system that is able to perform securely on and around the Moon, capable of resisting the harsh environment."
6. "To design a system capable of communicating with its base and receiving updates in a self-sufficient manner."
7. "To design a system capable of coordinating all its provider nodes to perform efficiently."
8. "To design a system that can provide navigation services for as long as possible."
9. "To design a failure-resistant system."
10. "To design a self-sufficient system, which can sustain the system's power needs without the need for operations."
11. "To design a system that is as environmentally sustainable as possible, and when it generates a negative impact on the environment, active mitigation procedures are implemented."

3.2. Mission Description

By J.K. Geijsberts, M. Dinescu

This section provides a brief description of the mission, including all the important aspects of previous reports, crucial for understanding the future design decisions for each subsystem. The main aspect of the mission is the orbits as they are the leading factor in ensuring the success of provision of the navigation services. Following this, the relay satellites are introduced as it is imperative for Earth communication. Lastly, the launcher selection is discussed as it is the method of bringing the navigation satellites to their correct positions.

3.2.1. Design Concept

In previous reports, the conceptual design of the mission was determined. This was done by the use of two trade-offs, one being the space segment trade-off, and the other being the ground segment trade-off. For the space segment, one choice had to be made out of four options. For the ground segment, one choice had to be made out of three options. Using simulation which was done with Python code, and through two general trade-offs of both the space and control segment, the conceptual design was chosen. This was chosen to be the Moon constellation with one relay satellite at a Lagrange point. The usage of self-control is present in the form of ODTS. ODTS is a method that determines the location of the navigation satellites in their orbits through altimetry with the Moon and onboard calculations. For the links between satellites, which all communicate with each other, the use of optical inter-satellite links (through lasers) is used. Next to that, for the functioning of the ODTS, the use of a Moon reflector (also through lasers) is used for the determination of the satellite altitude and positioning with respect to the Moon. By the use of ODTS, no ground station is needed to perform any calculations. Additional calculations for updating ephemeris parameters (a crucial part of GNSS) are also done onboard.

3.2.2. Navigation Satellite
The actual navigation satellite had its parameters estimated in previous reports, as a zero-stage design. The mass, power, and volume of the whole spacecraft are estimated. Next to that, all the individual subsystem masses and powers are estimated. Components are not yet chosen, but these specifications were used to estimate other parts of the mission, like which launcher was to be used, which can be seen in subsection 3.2.4.

3.2.3. Relay
The relay satellite provides the Earth with health and coordinates of the LNSS satellites for the monitoring part of the mission. This satellite was a spacecraft at a Lagrange point that would function as a relay for communication with Earth. This spacecraft is supposed to be designed by itself to function as a custom relay. Any communication from and to Earth of the navigation satellites is first passed to the relay, which then passes it towards Earth.

3.2.4. Launcher
The launch vehicles that have been considered in previous reports are the Ariane 6, the Long March 5, the Falcon Heavy and the Falcon 9. Other LVs have not been considered due to their TRL level as well as if they are still in service. Next to that, not all launch vehicles can launch to the Moon. Out of the launch vehicles considered, the Falcon 9 is the lowest-cost and the Falcon Heavy can carry the most and is after the Falcon 9 the lowest cost. Knowing that the Falcon Heavy can carry more mass than the Ariane 6, and costs less, the size will need to be checked as the Ariane 6 has a bigger payload fairing. Long March 5 was not considered as it is produced by the CALT, which is not an ESA partner. In the previous reports, the estimated size of the spacecraft indicated that the Falcon Heavy and Falcon 9, or a combination of both were chosen as a launch vehicle.

3.3. Market Analysis
Performed by L.D. van der Peet, K. Scherpenzeel. Written by L.D. van der Peet
A market analysis assists in understanding the need and the bigger picture of the mission. By analysing the market, it should become clear that the service provided has potential and contributes to the success of other missions. This analysis starts with an overview of the market and its segmentation, i.e. what the type and number of upcoming missions. Then, the position of the service in the market is determined with a Strengths, Weaknesses, Opportunities, and Threats (SWOT) analysis.

3.3.1. Market Size
The service provided will be offered around the Lunar surface and therefore can be seen as part of the Lunar economy. As it stands, the Lunar economy has a market value of about $3\,\mathrm{B}\,\$$. However, it is estimated that the Moon will accumulate around $100\,\mathrm{B}\,\$$ of investment over the 2021-2031 period [7]. By 2040 this shall already surpass $142\,\mathrm{B}\,\$$ according to PWC[1]. Currently, the Lunar surface is solely roamed by rovers. With the introduction of the Artemis programme, by 2025 human presence on the Moon is aimed to once more be established[2].

As the Lunar economy continues to grow, so does the market for Lunar navigation. Current predictions expect around 6 to 10 mission launches per year, as seen in Figure 3.1. Many of these launches are part of the Artemis missions. More than $50\,\%$ of the 2030-2035 Lunar transportation market will come from rover missions. Together with landers, they make up nearly the whole market, as evidenced by Figure 3.2.

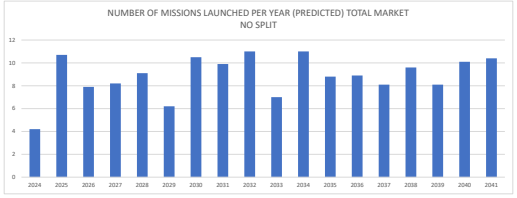

Figure 3.1: Number of predicted launches per year [8]

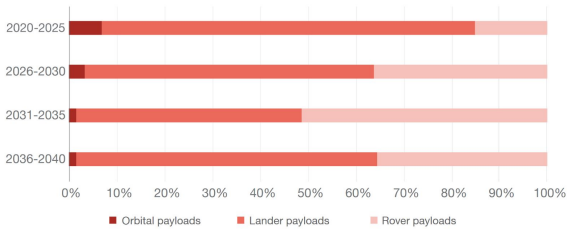

Figure 3.2: Division of the Lunar market [9]

[1] https://space-economy.esa.int/article/119/pwcs-lunar-market-assessment-market-trends-and-challenges-in-the-development-of-
[2] https://www.space.com/artemis-3-moon-landing-mission

3.3.2. Market Segmentation and Potential

The concept of the 'Moonlight programme' by ESA originates from the rejuvenated interest in the Moon. The interest is spread out widely, ranging from human habitation plans to commercial endeavours. To obtain a clear overview of the size of the market, potential customers, mission types and their goals are evaluated.

Identification of Customers

More than half of the projected $100\,\mathrm{B}\,\$$ of revenue is expected to be generated from commercial expeditions [8]. This includes extraction of valuable resources such as Hydrogen (H_2) and Oxygen (O_2). Additionally, scientific rovers form a large contribution to current Lunar activities, and will continue to do so, with at least five rover initiatives planned[3]. The full list of potential market customers together with their benefit from LNSS can be seen in Table 3.1 below.

Table 3.1: Upcoming missions that benefit from Lunar Navigation services

Goal	Rationale	Benefit	Example missions
Human missions to the Moon	To establish the possibility of extraterrestrial habitats and prepare for human planetary exploration	Provide accurate positions to navigate to desired locations	Artemis[4], Moon Village[5], HERACLES EL3[6]
Rover missions	To autonomously explore the back side of the Moon, and extend the reach of surface exploration missions	Provide navigation for the autonomous rovers	VIPER[7] LRP[8]
Scientific orbiters	Map the surface of the Moon and explore seismological activity, heat, or Hydrogen locations	Accurately determine the location of orbiter and pinpoint the viewed location	LunaH-map[9] LGN[10] Lunar trailblazer[11]
Lunar communication network	Provide coverage of the Lunar service volumes	Increased performance by combining navigation services	LunaNet[12]
Space transportation	Explore the possibility of humans travelling to extraterrestrial bodies such as Mars	Allow to make a stop on the Moon and travel towards the final target.	Artemis
In situ resource utilisation	Extraction and mining of valuable resources on the Moon	Locating of sources and guiding equipment	Caterpillar Moxie[13]
Commercial missions	Deliver payload to the Moon	Guiding landers to their designated landing zone	Astrobotic Peregrine[14]

The overarching benefits of a LNSS constellation are derived from the ability to enable various missions to carry out data intensive research, without requiring custom transmitting infrastructure. Previously, all Lunar assets relied on individual communication and navigating solutions, thus costly and wasteful development was required to perform the objective. A singular solution also leads to more and smaller (budget) missions to be developed, unlocking new opportunities to the Lunar market, and thereby stimulating growth in the Lunar economy, and in turn enabling more science per mission.

[3] https://www.smithsonianmag.com/science-nature/these-five-innovative-rovers-will-soon-explore-the-moon-180980819/
[4] https://www.nasa.gov/specials/artemis/
[5] https://www.esa.int/About_Us/Ministerial_Council_2016/Moon_Village
[6] https://tinyurl.com/HERACLES-ESA
[7] https://www.nasa.gov/viper/overview
[8] https://www.nasa.gov/resource-prospector
[9] https://nssdc.gsfc.nasa.gov/nmc/spacecraft/display.action?id=LUNAH-MAP
[10] https://solarsystem.nasa.gov/studies/203/lunar-geophysical-network-lgn/
[11] https://www.jpl.nasa.gov/missions/lunar-trailblazer
[12] https://www.nasa.gov/feature/goddard/2021/lunanet-empowering-artemis-with-communications-and-navigation-interoperability
[13] https://mars.nasa.gov/mars2020/spacecraft/instruments/moxie/
[14] https://www.astrobotic.com/lunar-delivery/landers/peregrine-lander/

3.3.3. Market Position

Clearly, there is a large potential for the market. Now it is essential to evaluate the market share and position available for Navigating the Moon. Currently, there are no other plans to establish a Lunar navigation system. As a NASA collaborative project, LunaNet aims to establish a communications and navigation network on the Moon[12]. As part of this mission, the 'Moonlight programme' has initiated. 'Moonlight' will provide navigation services to the Lunar surface and is therein the sole provider. Being sole provider does not mean taking the total market share. For this, the service must provide a need, which can not be resolved more efficiently by customers. Some helpful and harmful aspects of the market are highlighted in the SWOT analysis in Figure 3.3.

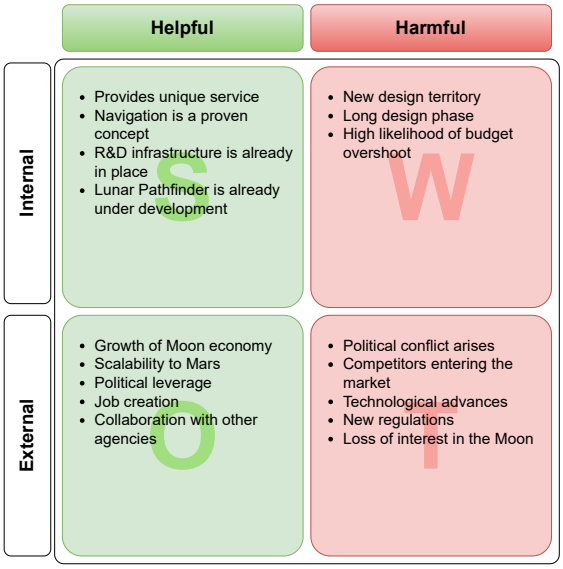

Figure 3.3: SWOT analysis of Navigating the Moon's market position

In addition to the navigation service provided, with the existing inter-satellite links for self-control, a communications network can be established. This means that Navigating the Moon enters a new, and potentially bigger market. All missions that experience benefits from existing navigation services, will also benefit from communications by relaying large data messaged back to Earth. This infrastructure may be enabled due to the existing links, but is not part of the current mission. Therefore, this will not be investigated and could potentially be evaluated in future research.

3.4. Operations & Logistics

By N. Ricker

"The field of operations and logistics focuses on making sure that the right amount and quality of materials and goods are produced and delivered to the correct recipients according to schedule" [15]. It ensures the mission is accomplished from a managerial perspective. This section studies relevant aspects of the mission, starting with the supply chain and manufacturing, including testing in subsection 3.4.1, launch in subsection 3.4.2, nominal operations including user support and business strategy is revised in subsection 3.4.3, to finally conclude with End of Mission in subsection 3.4.4. Each subsection includes a diagram representing the process, along with an analysis of it.

On top of the non-technical mission aspects studied in the section, a mission outline is defined through a Functional Flow Diagram and a Functional Breakdown Structure. They can be found in section B.2. These diagrams study the technical operations of the system, from launch to end of life (EOL).

3.4.1. Manufacturing and Production

This stage in the mission starts after the main design is in place. After the board has given the green light, manufacturing and production take place. A general overview is introduced below.

[15] https://firsthand.co/industries/operations-and-logistics

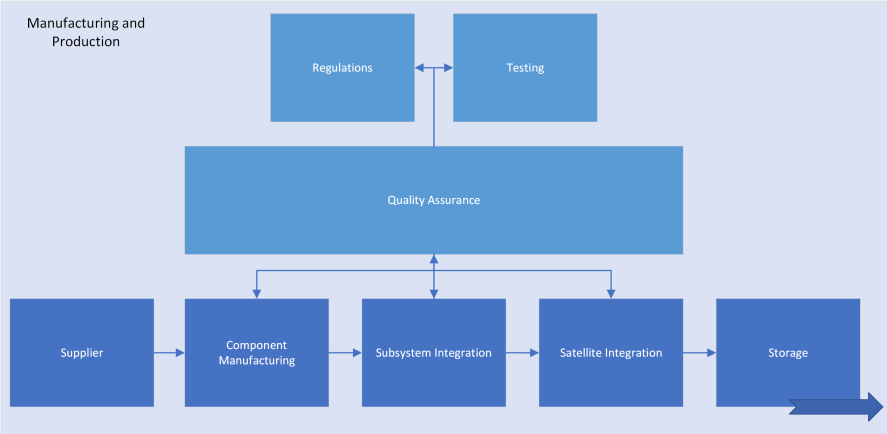

Figure 3.4: Manufacturing and Production Diagram

Figure 3.4 presents most aspects of the supply chain, except for ”Shipping”, which is introduced later. This stage requires special attention during the first years of development. There is a high need for adaptability, but as the process standardises, the complexity reduces. More detailed aspects are considered in section 7.7, while this subsection focuses on the nodes enabling the process. Given the large number of satellites (34) to produce, this stage is cyclic until the system is fully operational, and if the service is successful, there will be a requirement for spare satellites in the near future.

The suppliers are the initial link in the chain. After a contract is made, they supply raw materials or off-the-shelf components. In this stage, there is usually a need for a competitive process to obtain the best quality-cost performance. Once this is ensured, satellite manufacturing begins. The process involves the manufacturing of specific components, integration between subsystems, and the final product assembly. Throughout the whole process, there must be quality assurance techniques in place for the product.

Quality is a complex feature to assess. The team must develop a Quality Policy, stating the overall intentions of the organisation. During production, the satellite must be manufactured in a modular way, to have a better overview of the product. As well, a quality control system must be in place, where sufficient tests are performed. These can be either destructive or non-destructive, though both are advised [10]. Once the product is accepted, it can be packed and kept in a storage facility until launch. The storage conditions must also be monitored, to avoid degrading the system beforehand.

Furthermore, there are regulations to follow and standards to meet. Compliance is a sensitive topic to manage, and a specialised team is in charge of managing it. It must be constantly monitored and performing audits provide reliability on the final outcome [16]. This topic is present in all sectors: economics, manufacturing, and sustainability. The quality management team should receive regular ”Non-Conformance Reports” (NCR) to study the current situation and develop plans to avoid them in the future[17].

Finally, the production process aims to reduce waste at all times. This is referred to as ”lean manufacturing” and shall be applied throughout the whole supply chain. As seen in the timeline, the production phase is long, for which the concept of ”Just in Time” (JIT) is vital. Based on the production plan, and the learning curve of the workforce, the required amount of satellites (4-6) must be produced just before the determined launch window. In this way, the storage volume is reduced, reducing costs. As the launch approaches, the next phase takes place.

3.4.2. Launch and Deployment

The next stage in the mission is one of the riskiest and must be dealt with carefully. Launch and deployment are short-duration but have the most people operating at once. The diagram shows an overview of the most relevant aspects to consider.

[16] https://www.cioinsight.com/leadership/meet-regulatory-compliance/
[17] https://www.eclipsesuite.com/non-conformance-report/

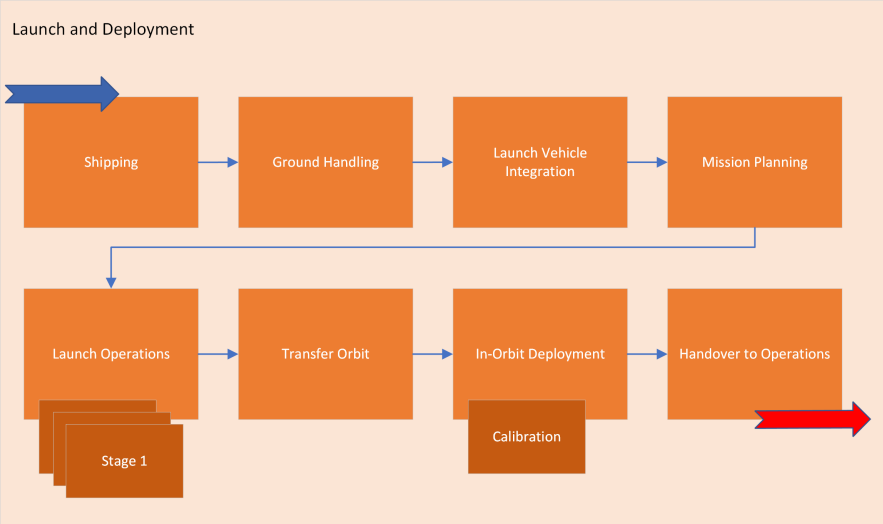

Figure 3.5: Launch and Deployment Diagram [11]

First, the transportation of a satellite needs the following considerations. The satellite undergoes careful packaging to reduce the risk for the most sensitive devices, protecting them against moisture and temperature changes. There must be qualified workers capable of handling and driving the satellite to its destination. Given the transportation of hazardous materials, the team must comply with country regulations. Finally, upon arrival, it should go to a clean room for careful unpacking [18].

Ground handling focuses on pre-launch preparations, such as setting up the equipment, and performing verification of the system's integrity. Then, the satellite is integrated with the launcher and undergoes several tests for connection. During this step, any necessary changes to the satellite or adapter are performed. Once the integration is complete, the mission planning takes place, where the launch window and procedures are discussed. Launch operations are a logistical challenge, where all subteams must be in sync. This step includes loading the propellant, engine ignition, lift-off and launch stages including separation. All systems must be closely monitored and high efficiency is required to react rapidly to any unexpected situation.

The last stages are mainly related to monitoring and verifying the outcome. After the destination is reached, deployment occurs, for which the team must monitor and solve any arising issues. Health checks are performed for all components, along with some refinement of the calibration systems. Once everything is nominal, the operations team takes over.

3.4.3. Operations and Control

This stage is the longest, however, given the self-control capability of the system, it does not require as much effort. It focuses on monitoring the satellites, while in parallel offering a service to the user and managing a project from a business side. The first part is shown in Figure 3.6.

[18] https://www.freightwaves.com/news/ground-control-inside-story-of-shipping-a-3-ton-satellite

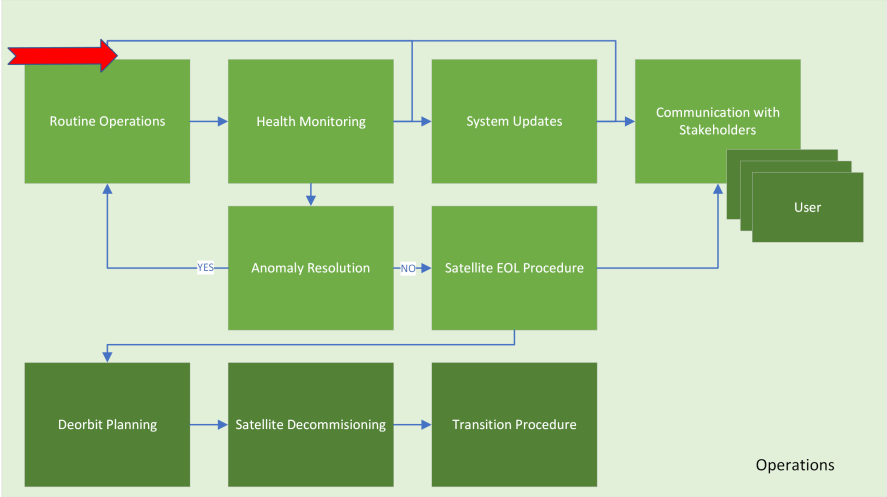

Figure 3.6: Operations Diagram

The ground segment obtains its data from the Lunar Pathfinder, for which no specific ground station is required. The data relay section is taken care of by the Lunar Pathfinder. A group of engineers on the ground monitor the constellation, doing routine checks on the system's health. When an anomaly occurs, a troubleshooting procedure takes place. If the issue is not resolved, there can be a need for an End of Life (EOL) procedure. In this scenario, the team must plan the satellite's decommissioning considering the sustainability requirements set. Here, all options are assessed to reduce damage to the environment and other missions. Once it is performed, there shall be a transition in place to substitute the satellite, either by using one of the spare satellites or by planning a new launch for replenishing the constellation.

Based on the data obtained from the constellation, some software updates may be available to increase efficiency. In such cases, there shall be proper planning for a proven system update and good communication with the relay satellite. This must be done considering the coverage navigation requirements.

User Support and Services
In parallel with the technical operations performed on the constellation, the team must have good communication with all stakeholders. It shall consider regulation changes, possible conflicts that may arise on Earth, upcoming missions and user feedback. Since the mission has as its main objective to provide a navigation service, continuous feedback from the users is necessary.

The team should develop a Customer Relationship Management strategy to nurture the connections with clients and potential customers. Through this strategy, they improve relations, promote growth and increase client retention [19]. Potential customers for the service are divided into three categories: ESA, ESA partners, and third parties[1]. They should all have a say in the path the service will take.

A final aspect to consider regarding users is the reliability of the service, and the security measures considered. The team must provide a rapid response to any support requirements. All users should be trained to minimise risks and use the system effectively. Regarding security, the Legal, and Information Technology (IT) departments shall work together to ensure updated security policies are in order, ranging from data transmission to authentication techniques and third-party assessments.

Mission Lifetime
By M. Vereycken
As no clear end of mission life is stated, the option to upgrade and replace the LNSS should be feasible. Current GNSS, like GPS already showed the possibility to upgrade and replace satellites to maintain and even improve the service quality. The LNS will only have a limited lifetime, the chance of extending the mission life past the satellite lifetime is likely. Multiple missions to the Moon are already planned and more will come as the Lunar interest only increases [20]. This is advantageous as it facilitates the launch of a new LNS generation by combining the initiation of Lunar missions and the new LNS, hence reducing the cost significantly. Furthermore,

[19] https://www.techtarget.com/searchcustomerexperience/definition/CRM-customer-relationship-management
[20] https://lunarresourcesregistry.com/list-of-planned-mission-to-the-moon/

this approach shows efficient resource utilisation to maximise sustainability. Additionally, it ensures future mission success and a continuous and reliable LNSS.

Marketing and Business Strategy
The last element in the nominal operations of the mission involves the business and marketing strategies. These are performed by the marketing, business development, and sales departments. This team should do a market analysis, following the 7Ps of marketing [21]. Then, sufficient coverage for the service is vital to incentivise space exploration and increase interest. Promotional campaigns, such as school visits, are common ways of achieving the desired result.

3.4.4. End of Mission

Even though the mission has no clearly defined operational period, a formal procedure is required to provide an easy transition for all stakeholders. Figure 3.7 introduces a general overview.

Figure 3.7: End of Mission Diagram

Once the end of operations has been defined, planning takes place. It involves informing users, employees and shareholders, designing a timeline for cease of service, and a transition phase for current users. This transition must be as smooth as possible to avoid limiting the users. It can be achieved by having a new generation of satellites or decommissioning the constellation throughout a longer time period.

Once the mission concludes, the team must develop a Post-Mission Analysis, where the overall performance is assessed. Proper documentation shall be produced, including accomplishments, learnings, and data collected. Given the objectives of the mission, there is also a high opportunity to share data obtained with partner organisations and the scientific community. Employees and other stakeholders should also be reassigned. Afterwards, the mission is officially over, along with all logistics and operations required.

4

Orbits and Navigation Service Design

In order to perform the mission successfully, and within requirements, the satellites positions in the constellation have to be considered carefully. Thus, the orbital characteristics must be designed for very precisely. Firstly, the requirements taken into account for this mission aspect are described in section 4.1. It is followed by an iteration in section 4.2 including assumptions and a change in orbits compared to the initial design found in [12], due to sustainability considerations. This iteration is done by looking into Lunar frozen orbits, which were found in [3] and verifying using a personally developed dynamic model based on TUDAT, if these comply with the requirements found in the Baseline Report [6]. Since this analysis yielded a non-compliance of the accuracy and availability (**NTM-NAV-OWR-03**, **NTM-NAV-TWM-03**, **NTM-NAV-PVT-02**, **NTM-NAV-PVT-04** and **NTM-NAV-TS-04**) requirements, the team added other frozen orbits and satellites such that they would meet the needs while trying to keep in mind sustainability by keeping to a minimum number of orbital planes and thus launches. Then, a part describing the final configuration of the orbits including all the navigation, which is considered to be the payload of the mission, aspects derived from the orbital results is added in section 4.3.

[21] https://www.optimizely.com/optimization-glossary/marketing-strategy/#:~:text=A%20marketing%20strategy%20is%20a,use%20to%20reach%20those%20customers.

4.1. Navigation Requirements

By S. Nedelcu, K. Scherpenzeel

The requirements for navigation are critical since it is the payload and the primary goal of the mission. They are derived from the technical requirements found in the Baseline report [6], and can be seen in Table A.2 in Appendix A. Some concepts present in the requirements shall be explained in the list below in accordance with [13], the ESA Moonlight mission requirements.

- The service volumes are described in Figure 4.1. As it can be seen, SV1 includes the whole Moon surface, including the South Pole and the back of the Moon. SV2 covers the volume starting from the Lunar surface area until an altitude of 200 km.
- Availability: The navigation service is available when the satellites meet all the technical requirements for accuracy. To achieve this, errors are relevant, along with the health and quality indicators.

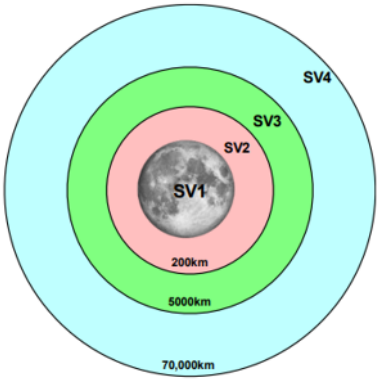

Figure 4.1: Service Volumes Definition according to [13].

4.2. Iteration Process

Initially, the orbits of the constellation from [12] chosen in the Midterm report [5], were circular and included 24 satellites in six planes which could fulfil the requirements. However, the increment in velocity (ΔV) for orbit keeping was estimated at $0.5\,\mathrm{km\,s^{-1}}$ per year. This does not take into consideration the sustainability requirements of the propulsion subsystem, thus an iteration to this initial design has to be made. In order to perform this iteration, two models are needed, a static one and a dynamic one. For those models, some assumptions have been made, which will be discussed first in subsection 4.2.1, followed by the two models in subsection 4.2.2 and subsection 4.2.3 and finally the iteration process will be described in subsection 4.2.4. This section presents only the process that was utilised in order to arrive at the results which are shown in the final design section 4.3.

4.2.1. Assumptions

By K. Scherpenzeel

The assumptions used by the two models described in subsection 4.2.1.

Table 4.1: Assumptions for the Orbit Design

ID	Assumption	Reasoning
ODA-01	The Moon is a perfect sphere.	An elevation angle was taken into account to nullify the effects of a rough surface.
ODA-02	Minimum 10° elevation angle for line of sight	This angle is used by ESA[14] and a sensitivity analysis will be performed for verification.
ODA-03	Satellites project circular areas to the surface.	Omnidirectional antennas will be used, and every user will receive the same type of signal.
ODA-04	No maximum distance the satellite signal can reach.	The subsystem design will design for the requirement imposed from the outcome of the mission design.
ODA-05	Moon is a spherical harmonic gravity model with an order of 10.	Main perturbations from the non-uniform field, therefore modelled at high order.
ODA-06	Earth is a spherical harmonic gravity model with an order of 5.	Only minor perturbations from Earth, therefore, an order of 5 was deemed sufficient.
ODA-07	Radiation pressure from the Sun, with the spacecraft assumed to be a sphere.	Allowed for quick iteration, as the area could easily be changed.
ODA-08	Schwarzschild relativity is used for acceleration due to relativity.	Common relativity solution and already implemented in TUDAT.
ODA-09	The Sun is assumed to be a point mass.	It is very far from the Moon, thus increasing the degree of its gravity field would have a very small effect.
ODA-10	The time step used in the simulation of 1 second.	Higher than $10\,$s yields wrong results.
ODA-11	10000 evenly distributed locations on the Moon were analysed.	More points would yield a too high computational time.
ODA-12	1σ receiver noise, and resolution error assumed to be $0.1\,$m.	From literature[15].
ODA-13	1σ multipath error assumed to be $0.2\,$m.	From literature[15].
ODA-14	1σ differential group delay error assumed to be $0.15\,$m.	From literature[15].
ODA-15	1σ clock error assumed to be $0.03\,$m.	The clock chosen is the Deep Space Atomic Clock in subsection 4.2.4, which is 50 times more accurate than Galileo's clock [16][15].
ODA-16	Troposphere and ionosphere error assumed to be 0.	The Moon does not have an atmosphere, so these errors do not have to be taken into account.
ODA-17	All satellites have the same weight in the position determination of the user.	A minimum elevation angle of 10° is already assumed for the satellite to be considered in view of the ULS.

4.2.2. Static Model

Performed by N. Ricker. Written by K. Scherpenzeel.

To inspect the accuracy and therefore, the requirements of the design, for the entire Lunar surface, the Moon is discretised in 10000 points. The requirements at the bottom level, all need the DOP values at all these points. A static model had to be created to get the line of sight distance to each satellite, which could then be utilised for the DOP calculations. A visualisation option was also added in order to inspect the surface to pinpoint the locations where the requirements were not met. The model outputs every type of DOP for all 10000 points for further analysis in later parts.

4.2.3. Dynamic Model

Performed by K. Scherpenzeel, S. Nedelcu. Written by K. Scherpenzeel.

To inspect the requirements in time and therefore also the updating frequency, a dynamic model had to be created. This model utilised the TUDAT package in python to propagate the orbits over time. This had to be done to verify the requirements over time to see if the required threshold was met at every point. The dynamic model outputs the positional elements of every satellite for a certain period of time, with a user-chosen time

step. These points could then be used in the static model to calculate the performance of the system at each time step. The different points in time could then be sent back to the static model to analyse the systems' performance over a certain time period. This could then be used to verify the requirements over time for all points.

4.2.4. Iteration

Performed by K. Scherpenzeel, S. Nedelcu. Written by S. Nedelcu., K Scherpenzeel

The iteration that is considered is designing a constellation consisting of frozen orbits to limit the need of ΔV for orbit-keeping. The following paragraphs will have this structure: first, a small part about the computations of the DOPs will be done, since they are used in all the following paragraphs. Then, the analysis of the frozen orbits will be clarified. Furthermore, the position, velocity, and timing accuracy and availability requirements have to be verified, and not only the instantaneous ones. To do so, the different accuracies have to be quantified and propagated in time for the duration of one period of the furthest satellite from the Moon. Thus, as a third part, the HHDOP will be propagated in time (to verify availability of 95% of the time). In this part, how redundancy is taken into account will also be explained. Then, for the position and timing accuracies in time, an explanation on how they were computed is shown. Velocity calculations are also mentioned in the previous part. In addition, the previously mentioned calculations imply other requirements on updating frequency and navigation message content, which are presented in a following fragment. Finally, a last consideration must be made for the orbiting and landing users.

DOP Calculations

First, defining the DOPs, the HHDOP, height constrained horizontal dilution of precision is calculated as seen in Equation 4.1. In the first matrix of Equation 4.1, the elements are the unit vectors of the range between the LNSS satellites and the user in three directions : East, North and Up. The other DOPs are computed similarly to the HHDOP, however in the first matrix, the last row, which constrains the height direction, is not included. The other DOPs are GDOP : geometrical which includes all three directions and time; position (three directions), horizontal (x and y directions), vertical and time. The PDOP is used to verify requirements **NTM-SYS-NAV-PVT-07**, **NTM-SYS-NAV-PVT-08**, **NTM-SYS-NAV-PVT-15** and **NTM-SYS-NAV-PVT-16** which are about position and velocity requirements for surface and orbiting users. They can be found in Table A.2, in Appendix A. HDOP is used for **NTM-SYS-NAV-PVT-10** and **NTM-SYS-NAV-PVT-12** which are about horizontal position and velocity requirements during landing. VDOP is used for **NTM-SYS-NAV-PVT-11** and **NTM-SYS-NAV-PVT-13** which are about vertical position and velocity requirements during landing. Finally, TDOP is necessary for **NTM-SYS-NAV-PVT-09**, **NTM-SYS-NAV-PVT-14**, **NTM-SYS-NAV-PVT-17** and **NTM-SYS-NAV-TS-03** which are about the timing accuracy for all type of users and for the time dissemination service.

$$HH = \begin{bmatrix} u_{E_1} & u_{N_1} & u_{U_1} & 1 \\ \vdots & \vdots & \vdots & \vdots \\ u_{E_m} & u_{N_m} & u_{U_m} & 1 \\ 0 & 0 & 1 & 0 \end{bmatrix} \qquad HC = [(HH)^T(HH)]^{-1} = \begin{bmatrix} C_{H11} & 0 & 0 & 0 \\ 0 & C_{H22} & 0 & 0 \\ 0 & 0 & C_{H33} & 0 \\ 0 & 0 & 0 & C_{H44} \end{bmatrix}$$

$$HHDOP = \sqrt{C_{H11}^2 + C_{H22}^2} \tag{4.1}$$

Frozen Orbits Analysis

From literature, a list of 49 possible frozen orbits are compiled. At first, a genetic algorithm was started to optimise the combination of the orbits for the least amount of satellites to meet the requirements. This was quickly scrapped as a research paper was found [3] that created the optimal frozen orbit constellations to obtain the lowest GDOP with minimum satellites. This source [3] presented 13 different constellations, seen in Figure 4.2 which are all put in the model built by the team to verify which one would perform best in terms of Dilution Of Precision.

Architectures							
ID	SMA [km]	# SV	# Planes	Phasing	Eccentricity	Inclination [deg]	Argument of periapsis
1	8025.9	20	5	0	0.004	39.53	270
2	8148.8	20	5	0	0.004	39.51	90
3	7298.6	21	3	1	0.001	39.71	270
4	8669.2	24	4	0	0.024	39.46	270
5	8916.6	24	4	1	0	39.41	90
6	8904.4	24	4	1	0	39.41	90
7	7434.8	21	3	1	0	39.67	270
8	7298.6	21	3	1	0.001	39.71	90
9	8954.2	24	4	1	0.002	39.40	90
10	8536.0	24	4	0	0.025	39.47	270
11	5701.2	24	4	1	0.002	40.78	90
12	8855.4	24	4	0	0.023	39.43	270
13	8904.4	24	4	1	0	39.41	90

Figure 4.2: 13 Possible Frozen Orbits Constellations for Moon Navigation [3]

After analysing all the frozen orbits, which entails computing the six different DOPs, a lack in the required HHDOP in **NTM-SYS-NAV-PVT-03** is observed. This is seen especially in the polar and equatorial regions. This means that more satellites have to be added to meet requirements. This is done by considering some earlier found orbits by adding them to the constellation after choosing the best performing orbit from [3], which is the 11^{th} one in Figure 4.2, since it has the smallest HHDOP and according to [3], the ΔV necessary to maintain this constellation is equal to $0\,\mathrm{m\,s^{-1}}$. First, ESA South Pole orbits found in [17] orbits were considered, but they did not meet the 95% availability requirements over time. Two different polar orbits are then added to the original constellation, for the North, and the South Pole [4] with three satellites in each. After adding these orbits, the required performance around the equator is not met either. This causes 3 low inclination orbit satellites to be added to improve performance, which are found in [18]. This causes the initial design to have 33 satellites. The two polar orbits could have one satellite taken out because this allowed the requirements to be met, still with only 31 satellites.

HHDOP Calculations in Time

The calculation of the HHDOP in Equation 4.1 is instantaneous, meaning it yields a result for a single position of the satellites. However, availability requirements which include **NTM-SYS-NAV-OWR-03**, **NTM-SYS-NAV-PVT-04** and **NTM-SYS-NAV-TS-04**, mean that the HHDOP has to be smaller or equal to 3.5 on every point of the Moon, at any time step during the maximum period time of all satellites (which occurs at the furthest one from the Moon). For this, the dynamic model was used where the time steps are taken to be one second and the duration was the orbital period of the equator orbits from [18], since their semi-major axis is greater than North/South poles orbits [4] and the original constellations orbits [3] semi-major axes. From the coordinates of the LNSS satellites at those one second time steps, the six DOPs including HHDOP are computed at every point for bigger time steps, since they took a computational time of 10 hours for a DOP calculation at every 1000s already. This was also due to the redundancy, where any possible combination of two satellites failing had to be analysed. Then, for each point on the Moon surface, all time evolutions of the HHDOP that are exactly at 95% of the maximum HHDOP (in time) are scattered in boxplots, and all of them have to be under 3.5 in order to meet the availability requirements.

In order to take into consideration the redundancy requirement, **NTM-RED-01**, which states that “The LNSS shall be redundant against two provider node failures”. If this is taken into account, the model is run with additional satellites and a loop is made where any combination of two satellites do not function and the HHDOP requirement again has to be fulfilled. Boxplots of all combinations for every time evolutions of the spatial points that are exactly at 95% of the maximum HHDOP is done again and all of them shall be under 3.5.

Allowable Ephemeris Error for Surface Users

For position and time, the other DOPs have to be calculated. They are then multiplied by the UERE [19] and by a factor of two to take into account the two-sigma standard deviation of the required accuracy. This result should be smaller or equal to the required two-sigma accuracy. It is shown in Equation 4.2, where the factor of two comes from the required accuracy has to be within two sigma standard deviation.

$$\text{Required 2 Sigma Accuracy} = 2 \cdot UERE \cdot DOP \tag{4.2}$$

Where the UERE is defined in Equation 4.3 below. The errors (e_i) taken into account, consist of clock error, receiver noise and resolution, multipath error and differential group delay as stated in the assumptions in subsection 4.2.1. $\sum e_i^2$ is the sum of all errors squared, which is done like that because they are assumed not to be correlated, according to the assumptions ODA-12 to ODA-16. The result of $\sum e_i^2$ is 0.0734 m and is used throughout all the calculations.

$$UERE = \sqrt{\sum e_i^2 + \text{Allowable Ephemeris Error}^2} \tag{4.3}$$

Finally, the allowable satellite error in position can be obtained from Equation 4.4, below.

$$\text{Allowable Ephemeris Error} = \sqrt{\frac{\text{Required 2 Sigma Accuracy}^2}{(2 \cdot DOP)^2} - \sum e_i^2} \tag{4.4}$$

This equation imposes a constraint or a further requirement on the allowable ephemeris error in order to comply with the required accuracy which is $10\,\text{m}$ for the position and $c\delta t = 3 \cdot 10^8 \cdot 0.4 \cdot 10^{-6} = 120m$ (where c is the speed of light) for timing according to **NTM-SYS-NAV-PVT-15** and **NTM-SYS-NAV-PVT-17** respectively for surface users. This allowable ephemeris error is, indeed, the error in the LNSS satellite positioning. Thus, in Equation 4.4, the DOP value is replaced by PDOP first and then TDOP in order to compute the smallest allowable satellite error, which will be the constraining one. This also takes into account availability, since the DOP value taken is the maximum of the 95% worst of all DOP spatial points. Finally, results are obtained for the allowable ephemeris error for timing and position.

After finding new requirements for position and timing, the velocity also had to be taken into account since there are also requirements for its accuracy (**NTM-SYS-NAV-PVT-08**, **NTM-SYS-NAV-PVT-12**, **NTM-SYS-NAV-PVT-13** and **NTM-SYS-NAV-PVT-16**). This is done in a similar fashion as for the position accuracy, with the Doppler shift. From [20], it can be seen that a similar matrix to the first one in Equation 4.1 can be constructed for velocity as well. It is shown in Equation 4.5 as U and where m is the number of satellites in view.

$$\begin{bmatrix} \dot{\rho}_1 \\ \vdots \\ \dot{\rho}_m \end{bmatrix} = U \cdot \begin{bmatrix} \dot{x} \\ \dot{y} \\ \dot{z} \\ c\delta\dot{t} \end{bmatrix} + \dot{U} \cdot \begin{bmatrix} x \\ y \\ z \\ c\delta t \end{bmatrix} \quad where, \quad U = \begin{bmatrix} u_{E_1} & u_{N_1} & u_{U_1} & 1 \\ \vdots & \vdots & \vdots & \vdots \\ u_{E_m} & u_{N_m} & u_{U_m} & 1 \end{bmatrix} \tag{4.5}$$

By subtracting U at time t_0 (when the satellites are in their initial position) from U at time t_1 and dividing by dt which is equal to one second, according to assumption ODA-10, on two different randomly picked points on the Moon, the maximum is found to be 0.0011. The product of this value with the user position vector is a lot smaller than the product of the U matrix with the user velocity vector. Thus, the second term in Equation 4.5 can be neglected. As a recommendation, in order to have a more reliable result, the simulation could be run for a whole period and the derivative of U should be computed over all Moon points. However, this result is also validated by [20], since they only take into account the first term of Equation 4.5. Thus, the DOPs for the velocity are computed in the same way as for the position, so they are equal to the position ones because the U matrix is the same. Finally, in order to calculate the allowable ephemeris error the following equation is used: Equation 4.6, in accordance with a discussion with Wouter van der Wal [1].

$$\text{Required 2 Sigma Velocity Accuracy} = 2 \cdot UEVE \cdot DOP \tag{4.6}$$

Where UEVE contains the allowable velocity ephemeris error and the measurement noise σ in the same way as Equation 4.3. This σ is computed with the following Equation 4.7 from [21].

$$\sigma = \sigma_{@45dB-Hz} \cdot 10^{-\frac{C/N_0 - 45}{20}} \tag{4.7}$$

With, $\sigma_{@45dB-Hz} = 0.01\,\text{m s}^{-1}$ being "typical value for GPS range-rate measurements" [21]. Furthermore, C/N_0 is the carrier-to-noise ratio which is given by the signal-to-noise ratio, SNR, added to the bandwidth,

[1] Communication with Wouter van der Wal, dd. 16/06/2023

BW, according to [22] both found in section 6.2: TT&C. This gives a $C/N_0 = 78dB$ and finally a noise for the range-rate measurements of $0.000\,223\,9\,\mathrm{m\,s^{-1}}$. This equation is however empirical, so to be able to verify it, another source computing this noise for range-rate measurements is needed. The paper [23] suggests a σ of $0.06\,\mathrm{m\,s^{-1}}$, which seems to be more conservative, thus it will be the one that is chosen to verify the update period requirements. It is in accordance with [24], which states that the measurement noise is in the order of centimetres per second. This paper also states that there is a systematic error that shall also be taken into account, but it is smaller than the noise (millimetres per second), thus it can be neglected [24]. However, these values are found for Earth navigation systems, therefore, it is more advisable, as a recommendation, to conduct practical testing or simulations in the specific Moon atmosphere to obtain accurate estimates of the range rate measurement noise. As a further recommendation, a more thorough search about the UEVE shall be conducted in order to find all the different components and check if they are larger than the measurement noise for the Moon. This could be done, for example, by modelling a signal from the satellite to the user and analysing the losses. The receiver should also be analysed to see how accurately frequency can be measured, which in turn is how well the Doppler shift can be computed. Then, running the dynamic model, the constraining ephemeris error is the one with the smallest time to update, which could be velocity, position or timing.

Update Frequency and Data Content

This ephemeris error has to be included in the satellite and mission design. In fact, the time it takes for the orbit to deviate from the initial orbit with a deviation equal to the allowable ephemeris error shall be the updating period. This is the case because if the satellites deviate by more than that distance w.r.t the perfect orbit, then the user position will not be accurate enough to meet the requirements. However, this situation's effect can be completely mitigated by updating the parameters on board of the spacecraft (every time the allowable error is reached) and sending these new parameters to the user, and therefore comply to the requirements. This timeline is also shown in Figure 4.3 and is further explained below.

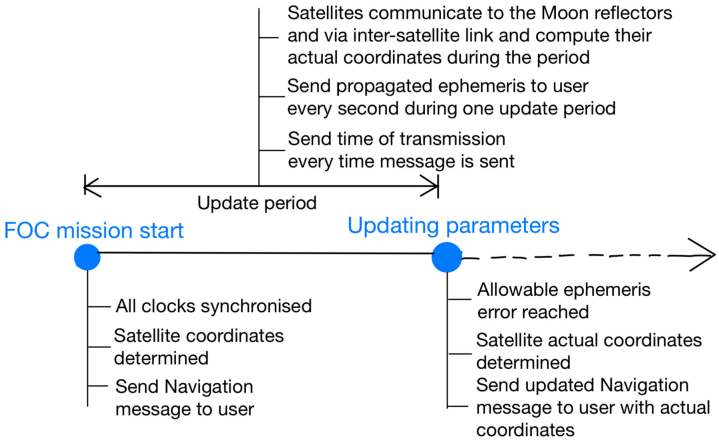

Figure 4.3: Timeline of the system from the cold start to the first updating time

At the beginning of the mission (at FOC meaning all satellites are in their respective orbits and functional), which is represented by the first blue dot in Figure 4.3, the satellites must have their clocks synchronised, and their absolute positions determined in the selenocentric reference frame. The first Navigation message is thus sent to the user. What the Navigation message includes is the satellite's Kepler coordinates (ephemeris data) at the moment the mission starts, which were calculated by using the Moon reflectors and inter-satellite linking (both with lasers) as stated in subsection 3.2.1 and the time the message was sent is also included in the Navigation message. Other data will also be included, and this is chosen in section 4.3.

Then, during the update period, the ephemeris data that is sent, is propagated in time with an integration time of one second in order to comply with **NTM-SYS-NAV-PVT-01**. This propagation has initial coordinates at $t = 0$, which are the actual ones computed at FOC or after every update period. Then, every second, they are simulated with the desired accuracy. These propagated or simulated coordinates are sent once per second to the user. In addition to sending the Kepler coordinates, the time the signal was sent is also included in the message in order for the user to compute the pseudo-range (distance from itself to the satellite). Also, health and quality indicators are continuously sent to the user in that message in order to comply with **NTM-SYS-NAV-02**.

At the same time, the satellites communicate with each other with inter-satellite linking and with the Moon reflectors in order to recompute their position. At the end of the period, this computation has to be done and new satellites coordinates are sent to the user, before the allowable ephemeris error is reached. From that point on, the coordinates of the satellites are real and they are sent to the user once, then every second propagated until the next update, where the real ones are sent, then simulated and so on. When the real ones are computed and the update period is reached, the real coordinates are overtaking the place of the propagated coordinates in the Navigation message.

Finally, about the accuracy of the propagation, if the Sun, the Earth, and the Moon are considered as point masses and no perturbations are included, then the propagation calculations performed in the spacecraft are for an ideal orbit. Thus, the deviation from this ideal orbit to the actual precise orbit containing all the perturbations and the higher order gravity fields of the Moon and the Earth is equal to the allowable ephemeris error. However, if the ideal orbit is used for the simulation during the update periods, then the deviation to the simulation with perturbations (included in the assumptions) is of 9 m in 50 s is reached. This value is too high, considering the fact that allowable ephemeris error in the requirements of OWR and TWM is 10 m. This means that every 50 seconds the satellites would have to recompute their position and send that new information to the user, which would result in impossible requirements on the Command and Data Handling(CDH) and TT&C subsystems because the satellites would have to point the lasers to all surrounding satellites and to the Moon reflectors in that period and perform the computations. Thus, the accuracy of the propagation has to be defined and is chosen in the final orbital and navigation design in section 4.3.

Orbiting and Landing Users

Finally, a last consideration for the design to be complete and in order to comply with most of the requirements, the orbiting and landing users have to be taken into account. Thus, the static and dynamic model are used with a radius equal to the Moon radius plus 200 km, due to requirement **NTM-SYS-NAV-06**. Also, the elevation angle is reduced to zero because there is no Moon surface to block the signals, and there will be more satellites in view per user. Thus, the accuracy should be higher for the orbiting users at that altitude. The model was not run for other orbit altitudes because it would have taken too long to run, discretising all spheres at all different heights until 200 km. As a recommendation, the model could be run to simulate all different orbit altitudes at which the users could be, in order to provide a more accurate result.

For landing users, the requirements for position and velocity are split into two directions: horizontal and vertical, thus Equation 4.2 and Equation 4.6 are used by replacing DOP with the HDOP and VDOP. Then, the same approach as explained above is applied. The height of the landing can be assumed at 1.5 km according to [17]. However, since more satellites will be in view at that point due to the Moon surface not getting in the way, it is assumed the landing altitude is on the Moon surface, at touchdown, in order to be more conservative.

Moreover, ESA researched a constellation of three satellites in [17] which would provide PVT for orbiting and landing users on the South Pole only of the Moon. With only these three satellites and "using a multi-epoch stacking approach within the navigation filter in the lander navigation unit, [...] it is possible to achieve below 100 m 3-sigma position precision from around 1.5 km above the Lunar surface and reaching 200 m 3-sigma horizontal precision at touchdown" [17]. This complies with the requirements, thus with the constellation chosen here, consisting of 34 satellites, and which complies with 10 m 2-sigma position precision on the surface of the Moon at any point for 95% of the time, it can be said that the landing requirements (50 m 2-sigma horizontal and 100 m 2-sigma vertical) are met at touchdown.

4.3. Orbits and Navigation Final Design

Performed by S. Nedelcu, K. Scherpenzeel

With the iterations being performed, a final design is obtained. This final design is the outcome of the steps seen in section 4.2 by complying to the requirements and minimising the amount of satellites needed. This section will take the following form. First, the orbital considerations will be shown including the orbits chosen, followed by the navigation ones and finally the V&V will be described. Also, the recommendations to make the orbits and navigation design more accurate are given in text.

4.3.1. Orbit Characteristics

Written by S. Nedelcu

The final design chosen for the orbits of the navigation satellites is described in Table 4.2, below. These were chosen as explained in section 4.2, by adding one North and one South Pole observation orbit (which are on the same plane) [4] and one low inclination orbit [18] to the original constellation [3]. This amounts to a total of 34

satellites, which accounts for redundancy as well. These orbits are all frozen and were chosen over the initial design which included 24 satellites in circular, non-frozen orbits, because of unreasonable ΔV requirements, which would not comply to the spacecraft design and sustainability considerations.

Table 4.2: Final Orbits Parameters

Orbit	Characteristic	Value	Unit
Original Orbit Constellation	Orbit plane number	4	[-]
	Satellite number	24	[-]
	Semi-major axis	5701.2	[km]
	Eccentricity	0.002	[-]
	Inclination	40.78	[deg]
	Argument of Periapsis	90	[deg]
	Starting True Anomaly	0	[deg]
	ΔV	0	[m/s]
Low Inclination Orbit	Orbit plane number	1	[-]
	Satellite number	4	[-]
	Semi-major axis	10000	[km]
	Eccentricity	0.038	[-]
	Inclination	10	[deg]
	Argument of Periapsis	90	[deg]
	Starting true Anomaly	30	[deg]
	ΔV	0	[m/s]
South/North Pole Orbits	Orbit plane number	1	[-]
	Satellite number	6	[-]
	Semi-major axis	6541.4	[km]
	Eccentricity	0.6	[-]
	Inclination	56.2	[deg]
	Argument of Periapsis	90/270	[deg]
	Starting true Anomaly	0	[deg]
	ΔV	0	[m/s]
All	Total Orbit plane number	6	[-]
	Total Satellite number	34	[-]
	Min Distance to Moon	2616.56	[km]
	Max Distance to Moon	10466.24	[km]

Some comments about this table can be made. First, the starting true anomaly is the angle at which the first satellite of the orbit is located at $t = 0$. The following satellites are located at starting true anomaly $+ sat * 360/n$, where sat is the number of the satellite in that particular orbit and n is the total number of satellites in that same orbit. It can be seen that for the low inclination orbits, the starting true anomaly is not equal to zero. That was done to take into account redundancy: only three satellites are added to the initial 31, one in each North/South poles orbits and one in the low inclination orbit. However, if the starting true anomaly for the latter is left at zero, requirements are still not met, thus adding $30\,°$ to all of them is found from studying the DOP values plotted on the Moon 10000 points map. The same goes for the Right Ascension of the Ascending Node (RAAN) : it is $0\,°$ for all of them, except for the original constellation, which contains four planes. Thus, the RAAN for those are $0\,°$, $90\,°$, $180\,°$ and $270\,°$.

Furthermore, the ΔV is zero for all the orbits because frozen orbits about the Moon are periodic (even though they deviate from the initial one, they return to the starting point after some time) according to [25]. Thus, orbit-keeping is not needed, but a margin of $63\,\mathrm{m\,s^{-1}}$ for the total lifetime of the spacecraft, per satellite still has been used for the propulsion subsystem in subsection 6.4.3. Finally, the maximum and minimum distance from the Moon centre are both from the South/North Pole orbits and are used for TT&C calculations in section 6.2.

These orbits and satellites can be seen visually in Figure 4.4. The low inclination orbit is seen in cyan, the North, and South Pole orbits are very eccentric in brown and green respectively. The rest of them are part of the original satellite constellation.

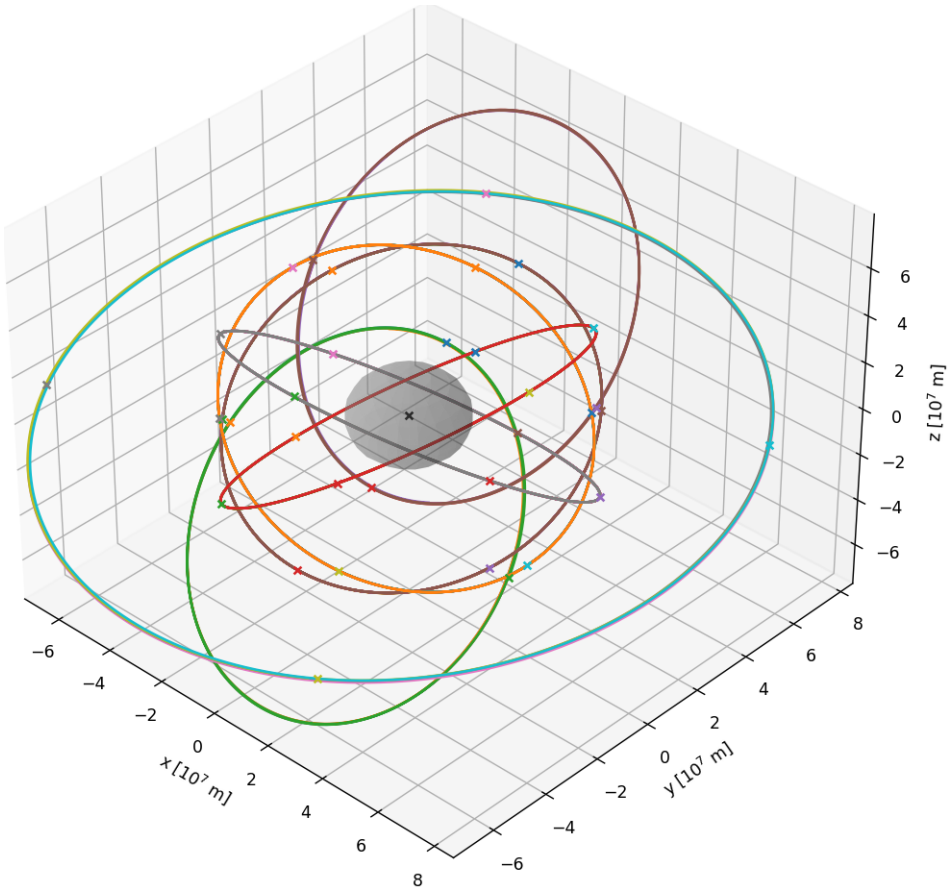

Figure 4.4: Frozen Orbits and Satellites

4.3.2. Navigation Characteristics

By analysing the performance of these orbits, many parameters are computed, and the clock is chosen which lead to compliance with most requirements. First, the main Navigation component will be chosen : the clock. Furthermore, the parameters calculated include the DOPs, the UERE and UEVE, the allowable ephemeris error, the updating frequency which will be once every update period and the data content. A final section about the subsystem requirements is also included.

Clock Choice

Written by K. Scherpenzeel

Accurate clocks are one of the most important aspects when it comes to navigation design. Clock errors in current GNSS technology can account for 0.3-1.9m of error, contributing to the UERE [19]. Mitigating this error allows for more precise PVT measurements for the users and thus, increase the overall performance of the system. This is why NASA developed the Deep Space Atomic Clock (DSAC) which will be utilised, as it performs 50 times better than the best atomic clock currently on the market [16]. The mass versus performance of the clock is also much higher than current clocks, which can be seen in Figure 4.5. The DSAC has been fully tested, and operational models have been sent to space in missions to prove the technology in a relevant environment, and therefore completed its TRL 7 certification [27]. The clock has a much better performance and the UERE 1σ error is taken conservatively as 0.03 m as it is 50 times better than current technology. The mission design includes three clocks, as this allows for a high level redundancy in the system and therefore guarantee the effectiveness of the design. The specifications that are being considered are the mass of 16 kg, power of 50 W, dimensions

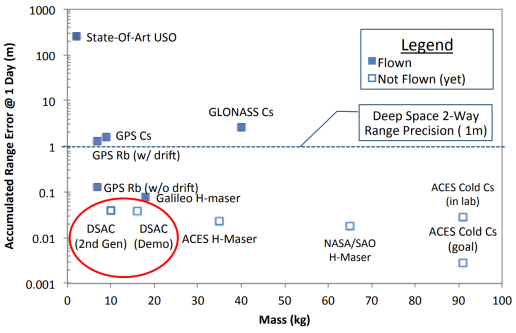

Figure 4.5: Performance Graph Atomic Clocks[26]

of 29 by 27 by 23 cm, TRL of 7, and finally the Allan Deviation 3×10^{-15} d^{-1}, which is the measurement metric for frequency stability in clocks[28]: an important part of the clock error budget. The summarised specifications can be seen in Table 4.3 with a picture of a laboratory model in Figure 4.6[2].

Table 4.3: DSAC Specifications

Parameter	Value
Mass	16 kg [29]
Power	50 W [30]
Dimensions	29 cm x 27 cm x 23 cm[29]
Allan Deviation[28]	3×10^{-15} d^{-1}[30]
TRL	7 [27]

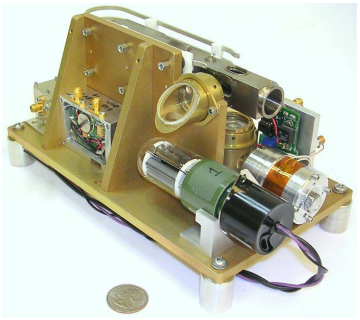

Figure 4.6: DSAC Laboratory Test Model

DOP Calculations

Written by S. Nedelcu, K. Scherpenzeel

To meet the 95 % threshold in time requirement for all points, the satellites have to be propagated and the DOPs calculated at each time point. This is done using the models described in section 4.2 and then for all 10000 points getting a singular 95 % point w.r.t the maximum in time propagated. This calculation is performed for the largest period of the satellites, being the low inclination satellites. To measure the performance of the design and therefore analyse their ability to meet requirements, the surface points are plotted in a boxplot, this can be seen in Figure 4.7. In addition, this boxplot is also for the worst case scenario if two satellites fail at the same time, as explained in section 4.2, so redundancy is also taken into account.

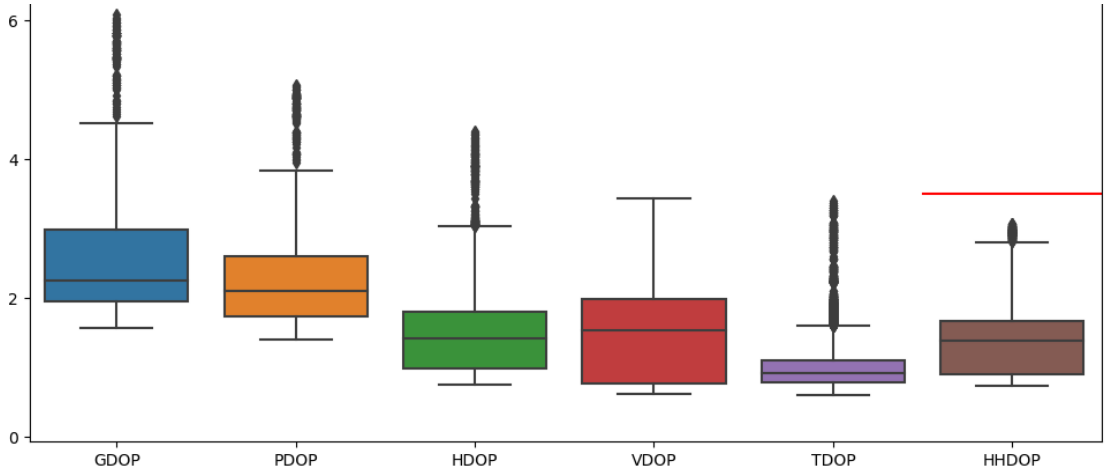

Figure 4.7: 95^{th} Percentile of HHDOP Values for all 10000 Points on the Moon for the Final Design

At the risk of repeating, the frozen orbits satellites are chosen over the initial circular ones because they require considerably less ΔV for orbit-keeping. Still, there are 10 fewer satellites in the initial constellation, so one could think sustainability is balanced. The same plot is produced for the initial orbits in Figure 4.8. It can be seen that the requirements for HHDOP are not met for 95 % of the time, and the DOPs are a lot larger than for the chosen frozen orbits, thus new satellites need to be added. Also, redundancy needs to be taken care of, so in the end a similar number of satellites would be needed for the initial constellation as for the frozen orbits one. This is why the frozen orbit constellation is chosen in the end.

[2] https://www.nasa.gov/mission_pages/tdm/clock/images.html

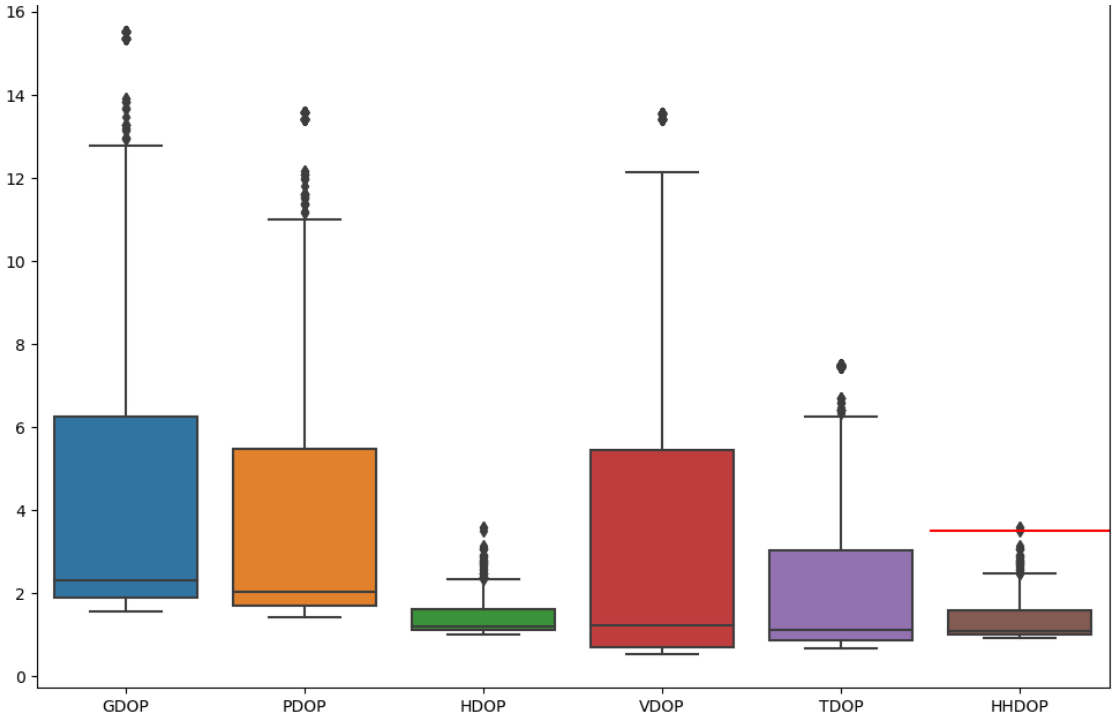

Figure 4.8: 95^{th} Percentile of HHDOP Values for all 10000 Points on the Moon for the Initial Circular Constellation

The red line in Figure 4.7 represents the 3.5 hard requirement **NTM-SYS-NAV-PVT-03**. As it can be seen all 95^{th} percentile points are underneath that line, thus for all points on the Moon, that requirement is complied with. The 95^{th} percentile HHDOP values are also plotted on the Moon surface, so it can be seen which regions are the worst performing, while still being within requirements. This Moon surface plot is seen in Figure 4.9. This map is made in the worst case scenario, which means if the worst combination of two satellites fail to account for redundancy. As it can be seen, the 'worst' performing regions are at the equator, which is most likely when two of the four low inclination satellites fail.

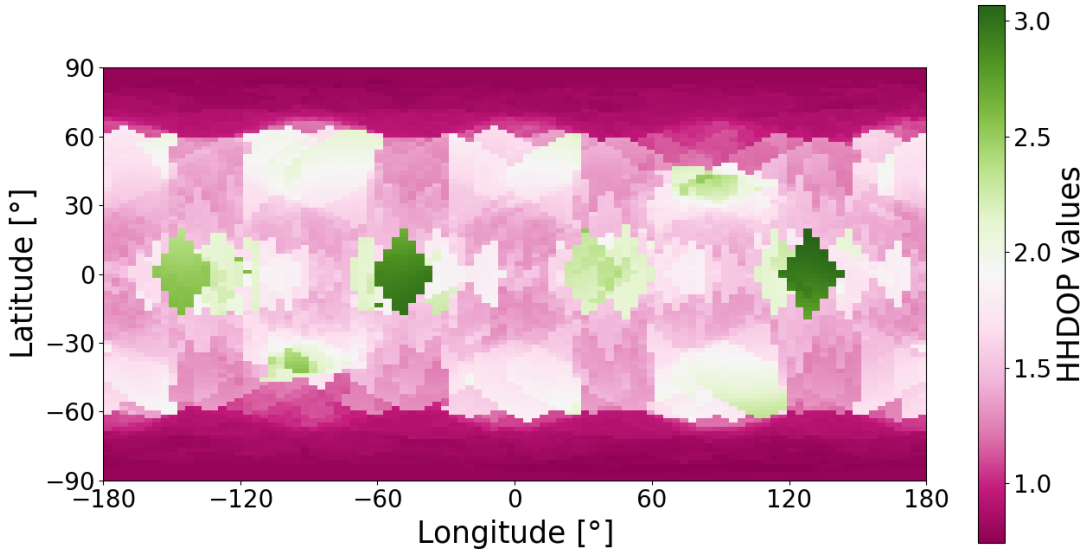

Figure 4.9: 95^{th} percentile of HHDOP values on the Moon 2D surface

Allowable Ephemeris Error from Accuracy Requirements

Written by S. Nedelcu

After computing all the different DOPs in time, the allowable ephemeris error can be computed for position and velocity with Equation 4.4 and Equation 4.6. For this, the parameters needed in these equations and their specific requirement are shown in Table 4.4, for all types of users. The DOP value used is the maximum of the 95^{th} percentile points in order to take into account the least well covered point on the Moon. When the requirement is about velocity, the same DOP is used as for the position, however it is then multiplied by the UEVE instead of the UERE, as explained in section 4.2.

Table 4.4: DOP and **NTM-SYS-NAV** Requirement Values Leading to Allowable Ephemeris Error

User	Requirement	Requirement Value	DOP Used	DOP Value	Allowable Ephemeris Error
Surface	**PVT-15**	$10\,$m	PDOP	5.064	$0.9494\,$m
Surface	**PVT-16**	$1\,$m s^{-1}	PDOP	5.064	$0.078\,41\,$m s^{-1}
Surface	**PVT-17**	c $\cdot\, 0.4\,$µs = $120\,$m	TDOP	3.408	$17.60\,$m
Landing	**PVT-10**	$50\,$m	HDOP	4.407	$5.666\,$m
Landing	**PVT-11**	$100\,$m	VDOP	3.433	$14.56\,$m
Landing	**PVT-12**	$1\,$m s^{-1}	HDOP	4.407	$0.096\,28\,$m s^{-1}
Landing	**PVT-13**	$2\,$m s^{-1}	VDOP	3.433	$0.2851\,$m s^{-1}
Landing	**PVT-14**	c$\cdot 15\,$ms = $4500\,$km	TDOP	3.408	$660.2\,$km
Orbiting	**PVT-07**	$100\,$m	PDOP	5.064	$9.870\,$m
Orbiting	**PVT-08**	$1\,$m s^{-1}	PDOP	5.064	$0.078\,41\,$m s^{-1}
Orbiting	**PVT-09**	c $\cdot\, 15\,$ms = $4500\,$km	TDOP	3.408	$660.2\,$km
All	**TS-03**	c $\cdot\, 1\,$µs = $300\,$m	TDOP	3.408	$44.01\,$m

As it can be seen, some values are higher than others, such as the allowable position ephemeris error for the timing accuracy for landing and orbiting users. This is normal, since the accuracy required is 10^5 lower than for the surface users ($15\,$ms compared to $0.4\,$µs) [13]. Furthermore, the allowable position ephemeris error is more constraining than the time one as it can be seen, the most constraining one is for the position surface users $0.9494\,$m, thus this one will be taken into account for the updating period. For the allowable velocity ephemeris error, the most constraining one is again for surface users and for orbiting users, since they have the same velocity accuracy requirement. This allowable velocity deviation is $0.078\,41\,$m s^{-1} and will be used to check whether it is more constraining in terms of update period than the position one. As a final check, the requirements for position and velocity error of the LNSS satellites given by the OWR and TWM services are the following : **NTM-SYS-NAV-OWR-01** and **NTM-SYS-NAV-TWM-07** which allow an error of $10\,$m and **NTM-SYS-NAV-OWR-02** and **NTM-SYS-NAV-TWM-08**, which allow an error of $0.1\,$m s^{-1}. As it can be seen, the requirements found from the model, in order to make sure the user accuracy requirements are met, are more constraining, thus are used to find the updating period.

Updating Period

Written by S. Nedelcu

From the results above, the updating period can be computed as explained in section 4.2. However, first, the accuracy of the propagated coordinates has to be chosen. Taking the Moon as point mass and no perturbations gives a deviation from the simulated orbit propagation in the dynamic model (with 10 degree Moon spherical harmonic gravity field, 5 degree Earth gravity spherical harmonic field, Sun point mass and relativistic and solar radiation pressure perturbations) of $9\,$m in $50\,$s, a more accurate propagation during the update period has to be chosen. The period results in Table 4.5 are computed with a 3 degree accurate Moon gravity field, Earth and Sun as point mass, and no additional perturbations and calculation the deviation from it to the more accurate orbit.

This period has to be computed for all different satellites orbits since they have different parameters, thus will have different perturbations. Some of them can nonetheless be grouped. Three different results are thus obtained : one for the original orbit constellation, one for the South/North poles orbits and one in the low inclination orbits. As a recommendation, with more time, these update period calculations should be made for all satellites without grouping them, because they could have different perturbations even though they follow the same orbits. The results are presented below in Table 4.5.

Table 4.5: Update Frequency

Orbit	Allowable ephemeris error	Update period	Error at the smallest time
Original Constellation	$0.9494\,\text{m}$	1h55min58sec	$0.9492\,\text{m}$
Original Constellation	$0.078\,41\,\text{m}\,\text{s}^{-1}$	> 1 period	$0.000\,337\,0\,\text{m}\,\text{s}^{-1}$
South/North poles	$0.9494\,\text{m}$	1h36min11sec	$0.949\,36\,\text{m}$
South/North poles	$0.078\,41\,\text{m}\,\text{s}^{-1}$	> 1 period	$0.000\,274\,6\,\text{m}\,\text{s}^{-1}$
Low inclination	$0.9494\,\text{m}$	1h49min29sec	$0.949\,36\,\text{m}$
Low inclination	$0.078\,41\,\text{m}\,\text{s}^{-1}$	> 1 period	$0.000\,281\,7\,\text{m}\,\text{s}^{-1}$

Some comments can be made about these results. First, the allowable ephemeris errors for position and velocity were taken to be the most constraining ones from the previous paragraph. For the velocity deviations, it can be seen that they are less constraining than the position ones, even after a full orbital period, they do not reach the allowable ephemeris error, thus the update period requirement comes from the position deviation. The final update frequency of this constellation shall thus be once every **1h 36min 11sec** for the accuracy of position, time, and velocity of the user to be within the system requirements. A last aspect must be taken into account : the LNSS satellites' clock drift. This drift is very minor, according to [16] : 1 second every 10 million years. How much it deviates within this updating period can be calculated thus with a simple cross product. The result is $18.29\,\text{ps}$ which is smaller than the most constraining required timing accuracy of $0.4\,\mu\text{s}$. Therefore, all requirements stated in Table 4.4 are fulfilled if this update frequency is chosen.

Data Content and Size
Written by K. Scherpenzeel

The satellites send similar data to the users w.r.t the data sent from current GNSS satellites. However, there are some dissimilarities between the two different systems. The system that has been designed first calculates propagated coordinates with less accuracy than the real orbit on board for each satellite, utilising the 3rd order spherical harmonic gravitational field. This is done such that the user can comply with the requirements set without itself computing the propagation every second, since it will have less computational power than the on-board computer. This method thus allows for faster position, velocity, and time calculations for the user. The final data sent to the user will have the new Receiver Independent Exchange Format (RINEX) data type[31]. This is the newest data format that is compatible with current GNSS systems and is very efficient with the data that has to be sent. The data that is sent includes can be seen in Table 4.6.

Table 4.6: Navigation Message Content Parameters

Data	Data Size [bits]	Type
Satellite ID	6	Service Parameters[19]
Satellite Health, Quality and Availability	6	
$\sqrt{a}$	32	Orbit Parameters[19]
e	32	
i	32	
Ω	32	
ω	32	
ν	32	
Time of Signal Transmission	16	Time and Clock Correction Parameters[3]
Clock Correction	72	
Broadcast Group Delay	32	
DSAC-UTC Conversion	99	
Ephemeris Accuracy	8	Integrity[4]

The total data that is being sent is not only for the user but also for the monitoring of the system on Earth. The satellite health and ephemeris accuracy is used for the observation of the system, where if there are any problems, the ground segment can intervene. The data is sent in five subframes, similarly to the current GNSS [19]. The five subframes will all have a size of less than 100 bits each. The first frame sent, includes the service parameters, integrity, time of signal transmission, and the broadcast group delay. This frame will then

[3] https://gssc.esa.int/navipedia/index.php/Galileo_Navigation_Message
[4] https://gssc.esa.int/navipedia/index.php/Galileo_Navigation_Message

be composed of 68 bits. The next two frames, will include half the orbit parameters and will therefore be 96 bits. The last two frames will in order be: clock correction and DSAC time to UTC conversion. They will consist out of 72 and 99 bits respectively. The clock correction and differential group delay is used by the user to mitigate for the errors for position determination. The relativistic effects are already mitigated by taking them into account in the dynamic model. The size of the data for the final chosen navigation design is much smaller than what is found in current GNSS literature, as there are less correction parameters. The reason for this design having less correction parameters is that there is no atmosphere to correct for, and that a lot of parameters are corrected for on the satellites by doing the propagation calculations.

4.3.3. Orbits and Navigation Service Verification and Validation

Performed by K. Scherpenzeel, S. Nedelcu

Verification and validation is an integral part to any design, and therefore is also performed for this design. Most of the groundwork of the navigation code has already been verified and validated in the midterm report[5]. The new code includes an interface between the static and dynamic model, that allows the DOPs to be analysed over time. The static and dynamic model both have been verified and therefore, only the interaction between the two have to be verified and validated.

Verification

Written by K. Scherpenzeel

This interaction is analysed by creating unit tests, module tests, and a separate sensitivity analysis is performed for the mask angle. The unit tests that have been performed include tests where, the shape of the outputs are analysed, and wrong parameters are put to check value errors. These tests combined with the initial tests being performed in the midterm report give confidence that the results required are accurate.

The Moon has a very rough surface and therefore, a mask angle has to be implemented to account for any craters and mountains. A range with steps of size of 5 degrees from 0-35 have been analysed to see the effects of changing the mask angle on the design. It can be seen in Figure 4.10 that varying the mask angle, there is little to even no effect on the performance of the system. However, it must be noted that these are only 9 points in time, which flattens the curves more at some points. The assumption of having a 10 degree mask angle clearly holds, as increasing it barely affects the performance of the system.

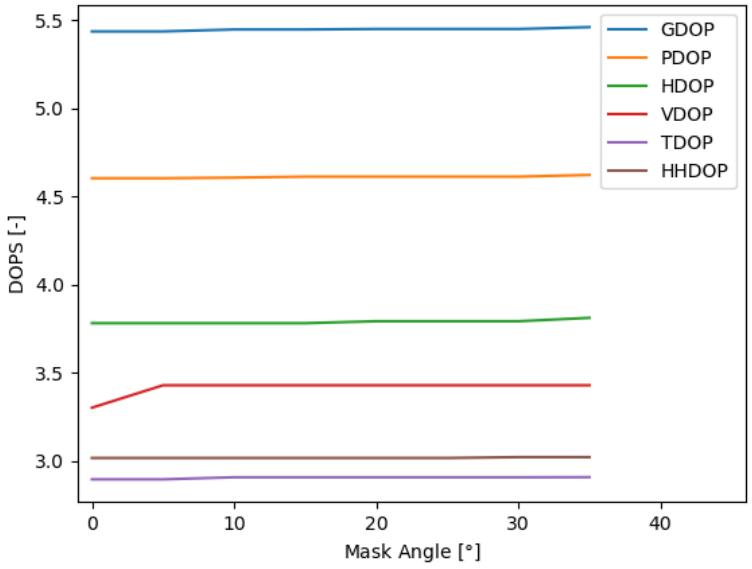

Figure 4.10: Mask Angle Versus Max DOPs

Requirements Verification

Written by S. Nedelcu

The requirements found in Table A.2 in Appendix A for the Navigation subsystem can be verified in order to show the design complies with them. A third column is added to that table also showing if it complies or not, however, a small rationale on how the final orbital and navigation design meets the requirements is added.

NTM-SYS-NAV-01, **NTM-SYS-NAV-06**, **NTM-SYS-NAV-07**, **NTM-SYS-NAV-TWM-01**, **NTM-SYS-NAV-TWM-02** and **NTM-SYS-NAV-TWM-09** are all complied with because the navigation service is provided for all users, in SV1 and SV2 and continuously and TWM is done in SV1 and SV2, more than 18 hours in a day in order for the satellites to obtain their Kepler coordinates. **NTM-SYS-NAV-02**, **NTM-SYS-NAV-03**, **NTM-SYS-NAV-04**, **NTM-SYS-NAV-05**, **NTM-SYS-NAV-TS-01** and **NTM-SYS-NAV-TS-02** are also met. The first one (health quality and availability) is included in the Navigation message, as explained previously. For the next two, the Kepler coordinates are provided to the user in the selenocentric frame, and it can make the frame transformation to Lunar inertial reference frame easily. For the last three, also in the message content, is included the conversion from the DSAC time to UTC and the user can easily convert from UTC to LRT. **NTM-SYS-NAV-OWR-01**, **NTM-SYS-NAV-OWR-02**, **NTM-SYS-NAV-TWM-07** and **NTM-SYS-NAV-TWM-08** are about the ephemeris errors which are higher than the ones taken into account for the update period calculations, thus they are complied with. **NTM-SYS-NAV-PVT-03**, **NTM-SYS-NAV-PVT-07** to **NTM-SYS-NAV-PVT-17** and **NTM-SYS-NAV-TS-03** are the user HDOP, position, velocity, and time accuracy requirements and they are all complied with as stated in the sections above. Finally, the user is able to compute its position, velocity and time offset using AFS at least once per second with the Kepler elements being propagated with a time step of one second and then sent to the user through a signal (AFS), thus **NTM-SYS-NAV-PVT-01** is complied with. The PVT providing service also works continuously more than 15 hours of the day, thus **NTM-SYS-NAV-PVT-02** is also a requirement that is fulfilled.

Finally, all the requirements that were not designed to include all the availability requirements computed over three months or a year : **NTM-SYS-NAV-OWR-03**, **NTM-SYS-NAV-OWR-04**, **NTM-SYS-NAV-PVT-04**, **NTM-SYS-NAV-PVT-05** and **NTM-SYS-NAV-TS-04**. This is due to the fact that running the dynamic model for a long period of time took too much computational time and memory. In order to reduce it, the time step was changed to be higher than 1 second, however, this flawed the results since the integration time was too large and the propagation of the orbits was not accurate enough any more. They were ran for the largest period out of all the different constellations and for that time, all requirements were met : the service is available more than 95% of the time calculated over the largest period (24h55min16s). As a recommendation, if more time was allocated, these different propagating durations (3 months and a year) would be done, in order to also verify these availability requirements. Furthermore, **NTM-SYS-NAV-TWM-03** and **NTM-SYS-NAV-TWM-05** were not considered in this design at all, due to time constraints. Finally, cold start has not been designed in this system, so **NTM-SYS-NAV-PVT-06** cannot be verified.

A last category are the requirements that were not designed for in this subsystem but are verified by others, such as TT&C or CDH in section 6.2 or section 6.3 respectively. These include the TWM requirements : **NTM-SYS-NAV-TWM-04** and **NTM-SYS-NAV-TWM-06**, which are thus verified.

Validation

Written by S. Nedelcu

The two models used (static and dynamic) have to be validated. The first paragraph will be about the static one, and the second will validate the dynamic model.

For the static model, a paper by Arcia, A. [12] is used as an already validated reference model. It introduces interesting orbits which should have full Moon coverage. The numbers in [12] are input in the static model, and similar results are found. Thus, the static model is considered validated, providing reliability to the software. Furthermore, this was a basis for error calculations, where further validation techniques are used. The results were positive, and the model can be used for the design of the mission.

For the dynamic model, some perturbations assumptions can be analysed. First, for the Moon gravity field degree, the accelerations for a point mass, 5th degree and 10th degree have been plotted in time as can be seen in Figure 4.11 and Figure 4.12.

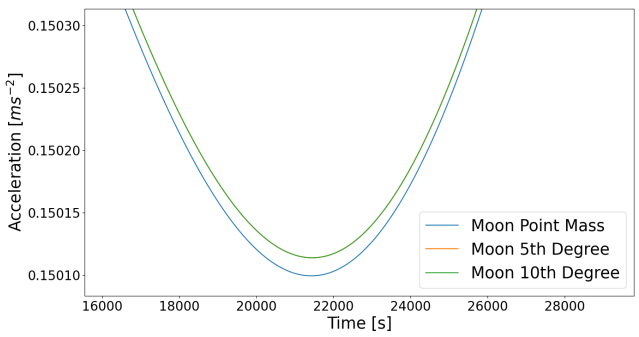

Figure 4.11: Moon gravity field acceleration

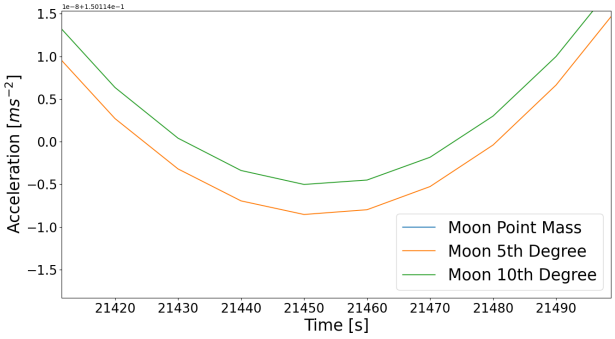

Figure 4.12: Zoomed in Moon gravity field acceleration

From these figures, it can be seen that the difference between the Moon as a point mass and other two (5th and 10th order) is quite high, thus a higher order is necessary. Between 5th and 10th degree, the difference is in the order of 10^{-8}. By plotting the same for the Earth accelerations, between point mass and 5th degree, the difference is also in the order of 10^{-8}, however between 5th and 10th order gravity field, the acceleration is almost the same (smaller than 10^{-12}), hence a higher degree than 5 is not used for the Earth gravity field. Furthermore, 10^{-8} is a significant difference because if the accelerations in time for the remaining perturbations : relativistic and solar radiation pressure are respectively in the order of $10^{-8}ms^{-2}$ and $10^{-12}ms^{-2}$. Finally, for the integration time of one second, the Kepler elements in time output by the dynamic model are very similar in values and variation as the results of [32], if the orbits in that paper are input in the dynamic model. If the time step is increased to more than 10 seconds, the Kepler elements start to deviate and the orbit is not even frozen any more.

5

Spacecraft Overview

5.1. Spacecraft Requirements

Performed by Everyone, Written by S. Nedelcu

After defining the mission in its general form, the system requirements for the spacecraft can be derived. These include only nine general requirements, since most of the subsystems have more specific requirements in their respective sections. These spacecraft requirements are seen in Table 5.1.

Table 5.1: Navigation Payload Requirements

General Spacecraft Requirements	
NTM-SYS-GEN-01:	The spacecraft shall not exceed a mass of 2300 kg.
NTM-SYS-GEN-02:	The spacecraft dimensions shall not exceed 2 × 3.5 × 3.5 m.
NTM-SYS-GEN-03:	The spacecraft shall have a lifetime of at least 12 years.
NTM-SYS-GEN-04:	The failure rate of a system shall be lower than 0.017 per year.
NTM-SYS-GEN-05:	The spacecraft shall have an EOL procedure for debris mitigation.
NTM-SYS-GEN-06:	The spacecraft manufacturing shall compensate for CO2 emissions.
NTM-SYS-GEN-07:	The spacecraft shall communicate with its neighbouring satellites.
NTM-SYS-GEN-08:	The spacecraft shall be able to communicate with the data relay satellite.

NTM-SYS-GEN-09:	The spacecraft shall provide an AFS signal to users on the Moon's surface and low orbits.

The rationale for **NTM-SYS-GEN-01** comes from the fact that there are 34 total satellites, with maximum six per orbital plane, as explained in section 4.3. Thus, six satellites shall fit in the Falcon Heavy[1], since it is the launch vehicle chosen in subsection 3.2.4. The dimensions requirement **NTM-SYS-GEN-02**, also comes from there[2]. The third spacecraft requirement is reasoned by finding lifetimes of GNSS satellites such as GPS : 13.9 years [33], Galileo : more than 12 years [3]. **NTM-SYS-GEN-04** is from Galileo's failure rate per year, which is 0.017 [4]. The rest of the requirements flow down from the user requirements.

5.2. Spacecraft Risk Analysis

By M. Dinescu

In this section, the risks that can occur during the mission to individual subsystems and their impact will be discussed. Firstly, in subsection 5.2.1, risks per subsystem will be identified. Finally, in subsection 5.2.2, the risks with the highest threat to the success of the mission will be mitigated.

5.2.1. Risk Identification

This subsection presents the subsystem risks. As can be seen in Table 5.2, the risks are split into different subsystems, and are ordered with the riskiest at the top. Note that, there are not a significant amount of risks for the navigation subsystem because the majority of the navigation failures are resultant of the failures of other subsystems. It can be interpreted that the rest of the risk for the other subsystems are also risks to the Navigation subsystem.

Table 5.2: Risk identification for each subsystem.

Navigation Subsystem risks			
ID	**Cause**	**Event**	**Result**
N1	Clock EOL	Clock fails	Inaccuracy
N2	Temperature fluctuations beyond nominal operation	Time synchronisation failure	Timing error to large
N3	Software malfunction	computation error	Wrong orbit
Propulsion risks			
ID	**Cause**	**Event**	**Result**
P1	Tank leakage	Improper flow of propellant	Burn is not performed properly. In addition less Δ V available
P2	Engine manufacturing defects	Engine failure.	Burn is not performed properly
P3	Insufficient propellant	Engine failure	Burn is nor performed properly
P4	Software malfunction	Incorrect burn calculation	Incorrect orbit
P5	Valve/ filter malfunction	Improper flow of propellant	Burn does not occur properly
P6	Space Debris	Nozzle blocked or damaged	Burn is not performed properly
Attitude, Determination & Control Subsystem risks			
ID	**Cause**	**Event**	**Result**
A1	Actuator dysfunction	Disturbance torque destabilises spacecraft	Spacecraft enters highly unstable rotation
A2	Solar rays blind the star sensor	Star sensor malfunction	Attitude cannot be determined
A3	Sun is not visible	Sun sensor malfunction	Attitude cannot be determined

[1] https://www.spacex.com/vehicles/falcon-heavy/
[2] https://www.spacex.com/vehicles/falcon-heavy/
[3] https://www.esa.int/Applications/Navigation/Galileo/Facts_and_figures
[4] https://www.eoportal.org/satellite-missions/galileo-foc#spacecraft-of-the-foc-series

A4	Sensor malfunction	Incorrect antenna pointing direction	User does not receive data
A5	Material degradation	CMG failure	Spacecraft experience unstable rotation
A6	Space debris	Sensor malfunction due to collision	Attitude cannot be determined
A7	Software malfunction	Attitude calculation incorrect	User does not receive data
A8	Space Debris	Collision alters attitude	User does not receive message
Tele-communcation, Telemetry & Command Subsystem risks			
ID	**Cause**	**Event**	**Result**
TT1	Deployable mechanism failure	Antenna is not deployed	Loss of coverage
TT2	Gimbal dysfunction	Wrong antenna pointing direction	Laser update is not possible
TT3	Laser malfunction	Laser cannot be fired	Loss of communication
TT4	Space Debris	Laser is damaged	Loss of communication
TT5	Space Debris	Laser is obstructed	Temporary loss of communication
Command & Data Handling Subsystem risks			
ID	**Cause**	**Event**	**Result**
C1	Data errors	Wrong information sent to the user	User gets wrong PVT.
C2	Data errors	Wrong updating information	Large user error
C3	Presence of a solar flare	Computers fail	The system breaks
C4	Power exceeded or TC incorrect	Component overheats	Component malfunction
C5	Radiation	Bit error	Wrong information sent to the user
C6	Presence of a geomagnetic storm	Computers fail	The system breaks
Electrical Power Subsystem risks			
ID	**Cause**	**Event**	**Result**
E1	Deployable mechanism failure	Solar Panels do not deploy or rotate	Power required not met.
E2	Emergency or unforeseen situation	Temporary increase in power required	power supply insufficient
E3	Cable plugged incorrectly	Power cannot travel through cable	Power required not met
E4	Pre damaged connections	Failure of a number of solar cells	Power required not met
E5	PCDU malfunction	Power shortage	Power required not met
E6	PCDU malfunction	Power surge	Components damaged
E7	Cable overheats	Cable burns through	Component will not receive power
E8	Space Debris	Solar Panel failure	Power required not met
E9	Leak	Battery cell failure	Loss of power during eclipse
Thermal Control Subsystem risks			
ID	**Cause**	**Event**	**Result**
TH1	Mechanism failure	Radiator is not deployed	Temperature requirement not met

TH2	Software malfunction	Radiator fails	Temperature requirement not met
TH3	Material degradation	Valve malfunction	Active control system fails
TH4	Space Debris	Radiator fails	Temperature requirement not met
TH5	Leakage/ blockage.	Fluid system failure	Temperature requirement not met
TH6	Coating degradation	Exposure to external conditions	Temperature requirement not met
Structures Subsystem risks			
ID	**Cause**	**Event**	**Result**
S1	Connection with Payload adapter fails	Spacecrafts move freely inside launcher	Launch fails
S2	Connection with payload adapter fails	Satellites not deployed	Deployment failed or delayed
S3	Launcher prepared incorrectly or damaged	Satellites experience large launch loads	Satellites fail
S4	Space Debris	Spacecraft body damaged	Interior components exposed to extreme environment
S5	Unknown hole or other stress concentration inducers	Large strss concentrations	Satellite damaged or fails
S6	Extreme environment	Tank material degradation	Leakage or component loss of connection

All the risks above in Table 5.2 are compiled in to a clear risk map below. The colour coding is identical to the risk identification for the simplicity.

Table 5.3: Risk map for all subsystem risks.

Consequence \ Likelihood	Very Low	Low	Medium	High	Very High
Catastrophic	S4	P2, P3, A5	N1, P1, A1, TT1, E2, S1, S2, S3		
Critical	P6, A7, C6, E8, TH4	N2, N3, TT3, C3, S5	A4, TT2, C1, C2, E3, TH2	A2, E1, TH1	
Moderate	A8, TT4	A6, C4, C5, E7, E9, TH3, TH5, S6	P4, P5, E4, E5, E6		A3
Marginal	TT5		TH6		
Negligible					

5.2.2. Risk Mitigation

The risks in the red zone were considered to be too risky to leave alone, therefore some mitigation methods are selected and analysed below in the table. Once again, it is ordered from the riskiest to the most docile risks.

Table 5.4: The risk mitigation for each subsystem.

ID	Mitigation of Navigation risks
N1	Have extra clocks for redundancy. Perform tests to estimate lifetime and reliability of clocks.
ID	**Mitigation of Propulsion Risks**
P1	Have experts perform experiments, such as stress tests, simulating expected environment and perform checks prior to launch to ensure no unknown holes.
P2	Have experts perform necessary tests and experiments simulating expected environment prior to installation to reduce chance of initial defects. Also have multiple engines for redundancy.
P3	Compute mass of spacecraft to ensure sufficient propellant is on board. Also add a bit of extra propellant as a margin.
ID	**Mitigation of ADCS Risks**
A1	Have experts perform experiments simulating expected environments prior to launch to verify the actuators are functioning and are not defect. Also have extra actuators for redundancy.
A5	Have extra CMG as redundancy. Also perform experiments to predict lifetime of CMG.
A2	Have experts perform experiments simulating the expected environment and measure performance. The sensors should be attempted to be placed such that the solar rays are not within the baffle sun exclusion angle. Also, multiple star sensors can be used for redundancy. Also have other forms of attitude determination during the sunlit periods.

A3	Place sun sensors in a configuration such that it covers the spacecraft as much as possible. Have more sun sensors for redundancy and use other forms of sensors during eclipse period.
A4	Have experts perform experiments simulating expected different environments prior to launch to verify the sensors are functioning and are not defect. Also have extra sensors for redundancy.
ID	**Mitigation of TT & C Risks**
TT1	Perform experiments with mechanism under expected environments. Tests should be done before that the joint allows movement. Also have extra satellite and multiple fold coverage for redundancy.
TT2	Perform experiments with mechanism under expected environments. Tests should be done before that the joint allows movement. Also have extra satellites for redundancy.
ID	**Mitigation of CD& H Risks**
C1	Software checks prior to launch. Extra programs with attempt to reboot or solve system.
C2	Software checks prior to launch. Extra programs with attempt to reboot or solve system.
ID	**Mitigation of EPS Risks**
E1	Perform experiments with mechanism under expected environments. Tests should be done before that the joint allows movement. Also have extra satellite for redundancy.
E2	Checks should be done prior to launch to ensure that the battery is functioning, and no defects are present. In addition, there should be extra batteries for redundancy.
E3	Checks should be done prior to launch to ensure every component receives power.
ID	**Mitigation of TCS Risks**
TH1	Perform experiments with mechanism under expected environments. Tests should be done before that the joint allows movement. Also have extra satellite for redundancy.
TH2	Checks should be done prior to launch that radiator functions properly. Also have additional radiators as redundancy.
ID	**Mitigation of Structures Risks**
S1	Assessment done prior to launch to ensure that adapter connections are fastened securely. Stress experiments on payload adapters to ensure security.
S2	Assessment done prior to launch to ensure that adapter connections are fastened securely.Stress experiments on payload adapters to ensure security.
S3	Assessment of Launcher prior to launch such that it is ensured that launch loads are not being applied to the payload due to structural malfunctions.

As can be seen, all the risks are now in the 'safe' zone. The majority of the mitigations were either of the form of redundancy, adding a margin or experiment and testing. The first one is the most optimal one, as it reduces both the consequence and the likelihood. For example, if a component fails, if a layer of redundancy is present, then it means that there will be another component should be able to replace it. Hence, the likelihood, that the subsystem will fail during the mission lifetime reduces. Similarly, as there is an extra component, it means that the subsystem can continue functioning as normal suggesting that the severity of said component failing is reduced as it no longer guarantees the failure of the subsystem. The other two mitigation simply reduce the likelihood by providing extra knowledge on the reliability or by increasing the amount of the resource. The reason it is selected sometimes over redundancy, is because in some cases it is not possible, (cannot make propellant redundant, can only add margin), or because it will introduce many more complexities and hence might cause more damage than good, (adding multiple propellant tanks increases the complexity far too much). Below, you can find the final risk map after the implemented risk mitigations. It should be noted that even though only the most dangerous risks were mitigated, during each individual subsystem design, the respective teams took margins and other extra redundancies not mentioned here meaning that some other safer risks were also indirectly mitigated. This will be seen in the subsystem design section.

Table 5.5: Subsystem risk map after risk mitigation.

Likelihood / Consequence	Very Low	Low	Medium	High	Very High
Catastrophic	P1, S1, S2, S3, S4				
Critical	P2, P6, A1, A7, TT1, C6, E3, E8, TH4	N1, N2, N3, TT3, E1, E2, C3, TH1, S5			
Moderate	P3, A4, A8, TT2, TT4	A5, A6, C1, C2, C4, C5, E7, E9, TH2, TH3, TH5, S6	P4, P5, E4, E5, E6		
Marginal	TT5	A2, A3	TH6		
Negligible					

5.3. N2 Chart

Design N2 Chart by Everyone. Written by J.K. Geijsberts

In chapter 6, the spacecraft subsystems are designed. This design will be achieved through an iterative process. Performing iteration improves the overall design since each part is optimised in parallel. It helps with achieving the requirements, as well as increasing mission success rates. Iterations are a crucial part of the design. In the current design, many iterations are made to come to the best design. Certain subsystems influence others, and through this, design loops can be made. To showcase how different subsystems influence each other, a design N2 chart can be made, which is shown in Table 5.6.

Table 5.6: The N2 chart for the design of the spacecraft.

Structures		Mass, volume, coefficient of radiation satellite		Initial S/C Mass	MMOI, CG uncertainty and thruster misalignment			Shape, mass budget, volume, dimensions, loads
Subsystem mass/volume	***Navigation***	Ephemeris data, required accuracy	Updating frequency, pointing direction (adjustment of orientation), orbital height, the distance between satellites	Maintenance ΔV, orbit maintenance frequency	Antenna accuracy to user/mirror	Orbit characteristics (eclipse time), components power	Orbit characteristics (eclipse time), operational temperatures	Orbit, accuracy, ephemeris data, components
Subsystem mass/volume		***CDH***	Data coding, data rate		Accuracy between satellite links	Computing power used	Operational temperatures	Data rate, encoding system, components
Subsystem mass/volume, antenna position, pointing mechanism			***TT&C***		Pointing accuracy of antenna with relay	Link budget power	Operational temperatures	Link budget, components
Tank pressure, fuel amount, subsystem mass/volume, max loads, positioning of thrusters				***Propulsion***	Thrusters and propellant	Power per manoeuvre	Operational temperatures	Propellant used, thrusters used
Subsystem mass/volume, disturbance torques to determine loads, positioning of elements			Antenna pointing requirements (including gimbals)	Thrust for desaturation and frequency, thruster compatibility	***ADCS***	Component power	Operational temperatures	Type of controller, components, pointing accuracy achieved
Battery, solar panels, power distribution positioning and characteristics						***EPS***	Heat generated	Power budget, solar array size, battery size, components
Subsystem mass/volume, coating, max-min temperatures				Temperature control	Reflectivity of the material radiation	Power used	***TCS***	Temperature range in the spacecraft, components
								Final Design

This N2 chart was used by the team to design the spacecraft iteratively. Individual subsystems could see through the N2 chart what outputs are needed to produce and what inputs they would get from other subsystems. The most influential subsystem in the design is the navigation subsystem, which is in essence the payload subsystem, which makes sense, as the payload should dictate what the other subsystems require to do, and therefore what they must be like. The subsystem with the most inputs is structures, as it needs to know all the components of the other subsystems for sizing the satellite. The final design has been put in the lower right to showcase what parts of the design are included or necessary for the final design.

5.4. Initial Sizing

Performed by M. Vereycken, L.D. van der Peet. Written by M. Vereycken

The initial sizing of the Lunar navigation satellite provides a framework for the spacecraft design. Estimating budgets contribute to an efficient resource allocation and provides initial estimations such that iterations of the spacecraft are possible for a converging and efficient design. First, the mass and power estimation of the Lunar navigation satellite is performed. It is based on historical data which is relevant to the mission, all satellites considered, and their average mass and power can be found in Table 5.7.

Table 5.7: Satellite masses.

Satellite	Mass [kg]	Power [W]
Galileo 5-26 [5]	732.8	1900
GPS IIF [6]	1633	1900
Glonass-M [7]	1480	1600
Beidou 3M [8]	1014	1500
Starlink V2.0 [9]	1250	/
Galileo IOV [10]	640	1420
Average	1125	1664
Standard deviation	400	225

Based on the existing satellites, an average mass of 1125 kg and an average power of 1664 W is estimated. From here, the volume in [m^3] can be predicted as 1% of the total mass [34]. It yields a value of $11.24\,\mathrm{m}^3$, which is too large for the design but provides a reference value to use. The previous values can be further divided for each subsystem. Again, historical data is used based on GPS satellites, namely Block 1, Block 2.1 and Block 2.2 [35]. The respective subsystem masses can be found in Table 5.8.

Table 5.8: Subsystem mass estimation based on GPS satellites [35].

	Propellant [kg]	Dry mass [kg]						
		Payload	Structure	Thermal	Power	TT&C	ADCS	Propulsion
Design	67.9	224.5	248.1	104.3	339.0	49.7	59.5	33.8

Furthermore, an initial power budget can be estimated. This is based on satellites found in [36] [37]. It may be slightly less accurate, as no power budgets on GNSS satellites were found. However, it was deemed sufficiently accurate to perform the first power budget estimation. The first power budget can be found in Table 5.9.

Table 5.9: Initial power budget estimation.

Satellite	Payload	Propulsion	ADCS	TT&C	OBDH	Thermal	Power
SCE [36]	49.8	4.6	9.3	13.2	4.6	4.6	13.9
SC80 [36]	16.8	3.7	7.2	53.9	3.7	3.7	10.9
Magrathea [37]	51.0	2.7	29.9	7.4	2.0	4.0	3.0
Average	39.2	3.7	15.4	24.9	3.4	4.1	9.3
Design	651.9	61.1	257.1	413.5	57.4	68.6	154.5

These values will be used for each of the subsystems described below. However, to keep a consistent spacecraft model, a coordinate system is defined.

5.4.1. Satellite Coordinate System

By I. Maes and N. Ricker

The coordinate system is a body-fixed system. It has its origin in the geometrical centre of the body, with the z-axis pointing towards the Moon, the y-axis in the direction of the solar panels, and the x-axis perpendicular

[5] https://www.esa.int/Applications/Navigation/Galileo/Facts_and_figures
[6] https://spaceflight101.com/spacecraft/gps-block-iif/
[7] https://gssc.esa.int/navipedia/index.php/GLONASS_Space_Segment
[8] https://spaceflight101.com/spacecraft/beidou-3/
[9] https://www.teslarati.com/spacex-elon-musk-next-gen-starlink-satellite-details/
[10] http://www.astronautix.com/g/galileonavsat.html

to both, producing a right-hand axis system. This helps with positioning components as they have a common reference point. It also adds clarity to the analysis of the loads and moments at different areas on the spacecraft. This coordinate system will be used throughout the rest of the subsystem design. The axis system can be seen in Figure 5.1.

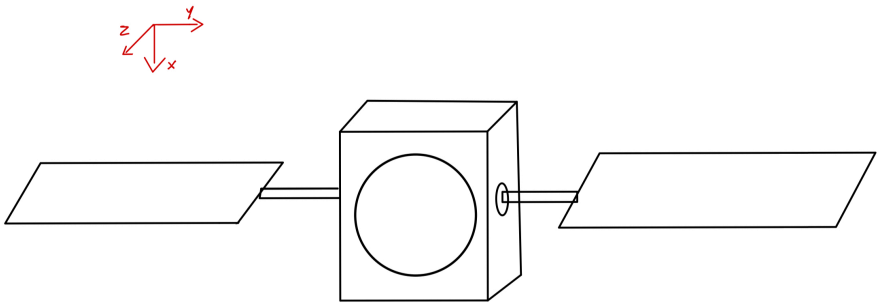

Figure 5.1: Coordinate System definition and antenna and solar array positioning.

6 Subsystem Design

This chapter takes the spacecraft requirements and general overview of the mission and specialises in each subsystem. Each subsystem is designed in an iterative or linear way, depending on the system and interconnections between systems. The subsystems studied are: Navigation (section 6.1), Telemetry, Tracking & Command (section 6.2), Command & Data Handling (section 6.3), Propulsion (section 6.4), Attitude Determination and Control (section 6.5), Electrical Power (section 6.6), Thermal Control (section 6.7), and Structure (section 6.8). Each subsystem concludes with a final design, including components and relevant features, as well as recommendations.

6.1. Navigation Payload

By M. Vereycken

The navigational payload is one of the most important subsystems in the satellite, as it will provide the service to the user. The clock is carefully selected in subsection 4.3.2. However, the clock will not provide the service itself, which means the other payload components should still be considered. As the components are selected based on the requirements, no iteration is done, but rather intelligent components choices are made.

According to the Galileo navigation satellite payload diagram, the selection of a component used for the navigation payload is determined[1]. It consists of the Navigation Signal Generation Unit (NSGU), the Frequency Generator and Upconverter Unit (FGUU), Clock Monitoring and Control Unit (CMCU) and the clocks which are already selected.

6.1.1. Navigation Signal Generation Unit

The NSGU is a critical component responsible for generating the precise navigation signals used by the LNS. With a TRL of 9 and currently operating in the Galileo navigation satellites, the NSGU has undergone extensive testing and validation, ensuring the accuracy and reliability of the generated signals. By selecting the NSGU, the LNS provides highly accurate positioning and timing information. The specification can be found in Table 6.1 and a picture is included in Figure 6.1.

[1] https://www.eoportal.org/satellite-missions/giove-b#spacecraft

Table 6.1: NSGU specifications of the FOC of the Galileo navigation satellite [38].

Parameter	Value
Mass	7.6 kg
Power	22 W
Dimension	270 mm x 280 mm x 116 mm
TRL	9

Figure 6.1: NSGU of the FOC of the Galileo navigation satellite.

6.1.2. Frequency Generator and Upconverter Unit

The FGUU is another crucial component that plays a vital role in the LNS. It is responsible for generating and upconverting the carrier frequencies used for the navigation signals. Having a TRL of 9 and currently operating in the Galileo navigation satellites, the FGUU has proven its capability to operate in space environments. By choosing the FGUU, we can ensure stable and precise frequency generation for the LNS. The specification can be found in Table 6.2 and a visual presentation is included in Figure 6.2.

Table 6.2: FGUU specifications of the FOC of the Galileo navigation satellite [39].

Parameter	Value
Mass	5.2 kg
Power	21 W
Dimension	270 mm x 216 mm x 137 mm
TRL	9

Figure 6.2: FGUU of the FOC of the Galileo navigation satellite.

6.1.3. Clock Monitoring and Control Unit

The CMCU is an essential component that monitors and controls the atomic clocks used for precise timekeeping in the LNS. With a TRL of 9 and currently operating in the Galileo navigation satellites, the CMCU has demonstrated its ability to accurately monitor and control the clocks, ensuring reliable and synchronised timekeeping. By incorporating the CMCU, we can maintain the high accuracy and stability of the atomic clocks throughout the satellite's operational lifespan. The specification can be found in Table 6.3 and a picture is included in Figure 6.3.

Table 6.3: CMCU specifications of the FOC of the Galileo navigation satellite [40].

Parameter	Value
Mass	12 kg
Power	35 W
Dimension	267 mm x 320 mm x 280 mm
TRL	9

Figure 6.3: CMCU of the FOC of the Galileo navigation satellite.

6.2. Telemetry, Tracking & Command System

In any navigation system, communication is crucial, as the user needs to receive the ephemeris data using the transmission of signals through data links to be able to locate itself. Furthermore, to enable the control segment of the mission to operate, the OISL are required. All communication links used throughout the mission are described in this section. Subsection 6.2.1 explains the general requirements and assumptions that were taken during the subsystem design, subsection 6.2.2 explains the design of the Optical Inter-satellite Links,

subsection 6.2.3 explains the ranging using the retroreflector, subsection 6.2.4 explains the communication link with the relay satellite, subsection 6.2.5 explains the communication link with the user and subsection 6.2.6 displays the final design of the TT&C subsystem.

6.2.1. Requirements and Design Assumptions

By A. Van Parys, J.K. Geijsberts.

Requirements and assumptions form the basis of the TT&C design. From the results, the requirements can be updated and made more specific. In Table A.8 in Appendix A the requirements for the final design are displayed.

Furthermore, due to the complexity of the TT&C design, certain assumptions are introduced. Assumptions can lead to simplifications, however, these simplifications will lead to inaccuracies. Thus, they will need to be carefully administered and updated throughout the design process. Some assumptions are listed in Table 6.4. All computations performed for the TT&C subsystem were perfomed using Microsoft Excel and can be found in GitHub-Initial Sizing.

Table 6.4: Assumptions made for TT&C subsystem.

ID	Assumption	Reasoning
TTA-G1	The mass of the transmitter antenna to the user is assumed to be estimated using interpolation with its volume.	As the mass was not mentioned in the source for the antenna, it was interpolated using the mass and volume of similar antennae[2].
TTA-G2	The power received by the user is assumed to be -130 dBm.	The minimum received power for general GNSS signals is around -130 dBm[3].
TTA-G3	The receiver loss in the user communication link budget is assumed to be 0.7.	Data on this loss was not mentioned in the paper on the antenna [41], therefore it had to be assumed. 0.7 is a conservative estimate for any RF losses in general.
TTA-G4	The cable loss in the user communication link budget is assumed to be 0.7.	Data on this loss was not mentioned in the paper on the antenna [42], therefore it had to be assumed. 0.7 is a conservative estimate for any RF losses in general.
TTA-G5	The pointing loss in the user communication link budget is assumed to be 1.	Circularly polarised antennae have very little to no pointing loss.
TTA-G6	The mass of the receiver antenna of the user is assumed to be estimated using interpolation with its volume.	As the mass was not mentioned in the source for the antenna, it was interpolated using the mass and volume of the transmitter antenna for the user communication link.
TTA-G7	Lunar Pathfinder is assumed to be available as a relay satellite throughout the entire mission lifetime.	Lunar Pathfinder is the first element of the Moonlight initiative, so using it would make sense [43]. Another relay satellite could also be used if the communication could happen with the same frequency, losses etc.
TTA-G8	The gains of the transmitter and receiver in the link between the navigation satellite and relay can be assumed to be 10 dB	Values used in [44] are around 20 dB for the spacecraft, and as both the LNS and relay are spacecraft, assuming a gain of 10 for both is conservative.
TTA-G9	The attenuation loss is nonexistent for the link to the relay	There is no atmosphere or rain on the Moon and the link to the relay is in space: Therefore no attenuation loss is present.
TTA-G10	The pointing loss is assumed to be -10 dB for the relay link	Due to the high ADCS precision needed for the lasers, the pointing loss should not be large. Next to that, typical values in [44] are around -0.12 dB. Therefore, a value of -10 dB is conservative
TTA-G11	A system temperature of 135 K can be used for the link budget to the relay	This is a value that can be assumed to be 135 K for 2-4 MHz [35]. The link is in this range.

TTA-G12	The cable losses for the link towards the relay L_l and L_r are both -1.549 dB	These are conservative values similar to those used in [44].

6.2.2. Optical Inter-satellite Links

Performed by A. Van Parys, J.K. Geijsberts. Written by A. Van Parys.

To enable orbit determination & time synchronisation (ODTS) on board the spacecraft, optical inter-satellite links (OISL) are used, as the use of optical cross-links can provide an improved precision to inter-satellite ranging and time synchronisation compared to traditional RF-methods [45]. Although this method is not without challenges, so sufficient investment and engineering will be required. However, the team is confident these challenges can be overcome, as these methods have recently been implemented into operating GNSS constellations such as BeiDou [45] and a budget of 10 Billion Euros is allocated to this mission.

To determine the orbits and synchronise the time of all satellites successfully, both ranging between satellites and synchronisation of the clocks are required. Both actions can be combined in a single system, by making use of dual one-way ranging[4]. As in single one-way ranging, the distance between transmitter and receiver is simply derived from the time of flight of the signal between the two, and only the receiver can calculate the time of flight. This means that any clock reference difference between the transmitter and receiver can lead to time-of-flight calculation errors. To avoid this dual one-way ranging is used, here both satellites can calculate the time of flight as they will both transmit and receive a signal at the same time. Using this method, the clock differences between the two satellites are compensated and time synchronisation between the two is reached. This method is however more complicated as an extra signal is sent between all satellites, thus requiring both a laser transmitter and receiver on each satellite [46, 47]. However, it has already been implemented in a GNSS scenario, as it is currently operational in the BeiDou navigation satellite system (BDS) [48].

After intensive literature research on existing lasers used for similar purposes, only limited options and information were found. Because of this, Dr. Dominic Dirkx, an expert in the field of laser ranging at the Faculty of Aerospace Engineering at the Delft University of Technology, was consulted. He recommended using a laser altimeter, however, he mentioned that a regular altimeter might be an over designed for the mission's application. Therefore, he also recommended using a single photon laser altimeter, as described in the paper by M. Vacek et al. [49]. Using these two options, a link budget calculation was performed for both scenarios. This calculation was done using Equation 6.1, this equation is based upon the equation for the received power for the Optical Inter-Satellite Link Model in the paper by J. Liang et al. [50]. In a second meeting with Dr. Dominic Dirkx, the adaptation of this formula was discussed and deemed valid as the gains and losses are unitless, meaning that neither the unit of the power nor the unit of the energy would be affected.

$$E_R = E_T \cdot \eta_T \cdot \eta_R \cdot G_T \cdot G_R \cdot L_T \cdot L_R \cdot L_{PS} \tag{6.1}$$

In this equation, E_R represents the energy received by the laser receiver on one satellite, E_T represents the energy transmitted by the laser transmitter on another satellite, η_T represents the optics efficiency of the transmitter, η_R represents the optics efficiency of the receiver, G_T represents the transmitter gain, G_R represents the receiver gain, L_T represents the transmitter pointing loss, L_R represents the receiver pointing loss, and L_{PS} represents the free-space path loss for the optical link between satellites. The transmitter gain is here defined as $G_T = 16/(\Theta_T)^2$, with Θ_T representing the full transmitting divergence angle in radians; the receiver gain is defined as $G_R = (D_R \cdot \pi/\lambda)^2$, with D_R representing the receiver's telescope diameter in mm and λ representing the operating wavelength in nm; the transmitter pointing loss is defined as $L_T = exp(-G_T \cdot (\theta_T)^2)$, with θ_T representing the transmitter pointing error in radians; the receiver pointing loss is defined as $L_R = exp(-G_R \cdot (\theta_R)^2)$, with θ_R representing the receiver pointing error in radians; and the free-space path loss is defined as $L_{PS} = (\lambda/(4 \cdot \pi \cdot d_{ss}))^2$, with d_{ss} representing the distance between satellites in km [50].

To be able to determine whether a signal will be detected by the receiver, the amount of photons that are received by the receiver is determined. To achieve this, the energy of a single photon is computed using $E_{photon} = (h \cdot c)/\lambda$, with h representing Planck's constant $h = 6.626 \cdot 10^{-34}\ J \cdot Hz^{-1}$ and c representing the speed of light $c = 299792458$ m/s [51]. The energy received by the laser receiver is then divided by the energy of a single photon, to obtain the total amount of photons that reach the receiver. In the case of the single photon laser altimeter, a single photon reaching the receiver would be sufficient to perform the ranging and

[4] Communication with Dr. Dominic Dirkx, 02/06/2022

time-synchronisation[5]. For regular laser altimeters, however, the number of detected photons can only be as low as 20 to make sure it is distinguishable from the noise and to ensure a low probability of false detection [52].

When performing the link budget calculations for the single photon laser altimeter [49], 8658.062 photons were received, considering the maximum distance between the satellites is 8078.893 km. This distance occurs between two satellites in different orbital planes and is computed using the code in the GitHub-Pointing Accuracy Calculator. When performing the link budget using the regular altimeters that were discussed in the meeting with Dr. Dominic Dirkx, the following values were achieved; for the BepiColombo Laser Altimeter (BELA) 2247223.252 photons were returned and for the Ganymede Laser Altimeter (GALA) $5.093 \cdot 10^{14}$ photons were returned. From these values, it can be concluded that all the laser altimeters are over designed for the purpose of inter-satellite dual one-way ranging, however some more than others. This should be taken into account, as a large over designed would make the satellites unnecessarily mass and power heavy.

Using these values, it was decided that both the BELA and GALA are unsuitable for OISL. Although the single photon laser altimeter is also considered over designed, it is still considered suitable, as smaller space borne laser altimeters are not in existence yet[6]. Thus, a resizing of the single photon laser altimeter, to a smaller, less powerful laser altimeter, is also deemed unrealistic without extreme R&D time and budget. Furthermore, the single photon laser altimeter usage for one-way ranging and time transfer data processing has already been researched before [49, 53], this will aid the implementation of the laser altimeter in the OISL design. The selected single photon laser altimeter and its block diagram can be seen in Figure 6.4a and Figure 6.4b respectively. However, it must be noted that the picture is not entirely accurate as both the laser transmitter and receiver will be installed on a gimbal, this will be further discussed in subsection 6.2.3.

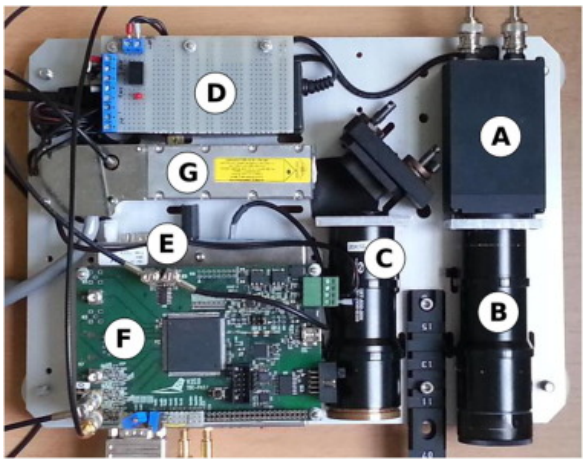

(a) Picture of the single photon laser altimeter without gimbal [49].

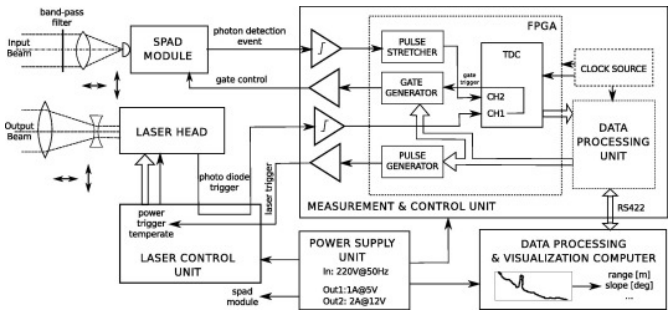

(b) Block diagram of the single photon laser altimeter [49].

Figure 6.4: Single photon laser altimeter.

In Table 6.5 and Table 6.6, all the relevant inputs and outputs for the OISL calculations are listed for all three designs. Where N_P represents the number of photons that are detected by the receiver. All inputs for the single photon laser altimeters were found in the previously mentioned paper by M. Vacek et al. [49], for the BELA however multiple sources were required to obtain all the required inputs [52, 54, 55, 56, 57, 58]. Also, for the GALA multiple sources were consulted [59, 60, 61, 62].

[5]Communication with Dr. Dominic Dirkx, 09/06/2022
[6]Communication with Dr. Dominic Dirkx, 02/06/2022

Table 6.5: Inputs for the OISL calculations.

	Inputs								
	E_T [J]	η_T	η_R	Θ_T [rad]	D_R [mm]	λ [nm]	θ_T [rad]	θ_R [rad]	d_{ss} [km]
Single photon laser altimeter	$3 \cdot 10^{-6}$	0.625	0.04	$8 \cdot 10^{-3}$	40	532	$8 \cdot 10^{-3}$	$8 \cdot 10^{-3}$	8079
BELA	$50 \cdot 10^{-3}$	0.625	0.34	$60 \cdot 10^{-6}$	200	1064	$60 \cdot 10^{-6}$	$50 \cdot 10^{-6}$	8079
GALA	$17 \cdot 10^{-3}$	0.625	0.83	$100 \cdot 10^{-6}$	250	1064.5	$100 \cdot 10^{-6}$	$100 \cdot 10^{-6}$	8079

Table 6.6: Outputs for the OISL calculations.

	Outputs		
	E_R [J]	E_{photon} [J]	N_P
Single photon laser altimeter	$3.233 \cdot 10^{-15}$	$3.734 \cdot 10^{-19}$	8658.031
BELA	$4.195 \cdot 10^{-13}$	$1.866 \cdot 10^{-19}$	2247223.252
GALA	$9.503 \cdot 10^{-5}$	$1.866 \cdot 10^{-19}$	$5.093 \cdot 10^{14}$

6.2.3. Retroreflector Ranging

Performed by A. Van Parys, J.K. Geijsberts. Written by A. Van Parys.

On the Lunar surface, five retroreflectors are located, which were left there by three Apollo crews and two remote Lunokhod rovers [63]. These retroreflectors are used to reflect an optical signal back to its source and can thus be used for Lunar laser ranging. Although these retroreflectors are all located on the near side of the Moon, they can still be used for additional ranging measurements, as long as they are in view of a satellite. Using this additional measurement, the precision of the ODTS for these satellites can further be improved. Furthermore, most of the future Lunar missions will have a retroreflector installed, this will extend the passive ground network and will result in better orbit determination performance [64].

When performing ranging between the satellites and the retroreflectors, no synchronisation of the clocks is required as only the satellites are equipped with a clock and the retroreflectors will just reflect the laser back to the satellite. Therefore, single two-way ranging (or just two-way ranging) can be used for this communication link. The distance between the satellite and the retroreflector is then simply calculated by dividing the time of flight of the signal by two and multiplying the result by the speed of light. The two-way ranging technique has already been performed in a Lunar setting in both the Lunar Laser Ranging experiments [65] and the Lunar Reconnaissance Orbiter [66], however now the laser will be transmitted from a Lunar orbiting satellite instead of from Earth, and it will be reflected by the retroreflectors on the Lunar surface.

For the two-way ranging between the LNS and the Lunar retroreflectors, the same laser altimeters are considered, as discussed in subsection 6.2.2. This decision was made as Dr. Dominic Dirkx recommended these altimeters for both purposes and the number of lasers should be kept to a minimum in any case, as a laser is generally quite heavy on a spacecraft and its other subsystems. Using these options, a link budget calculation was again performed. This calculation was again largely based on Equation 6.1, however some changes with the OISL calculations are present. In the free-space path loss L_{PS}, d_{ss} now represents double the distance between the Lunar retroreflector and the satellite in km, as now two-way ranging is used and thus the signal travels two times the distance before it reaches its receiver. Furthermore, the efficiency of the retroreflectors should be taken into account.

This efficiency is a very significant factor as in over 40 years the lasers have accumulated dust and are now roughly $50\,\%$ covered [67]. In the presence of sunlight shining on this dust deposition, the retroreflectors can become subject to thermal gradients. These thermal gradients will only amount to a few degrees, however, they will diminish the central irradiance by one order of magnitude [68]. Meaning that the intensity of the laser beam that is reflected on the central area of the retroreflector is reduced to one-tenth of its original value. This has two

[5] https://satsearch.co/

[6] https://support.spirent.com/SC_KnowledgeView?id=FAQ18565

clear effects: Firstly, the signal strength returning from the Lunar reflectors is reduced by approximately a factor of ten compared to theoretical expectations, secondly, an additional order-of-magnitude signal reduction will be introduced when the Lunar phase is within approximately 20 degrees of full Moon. Combining both effects results in a returned signal strength that is never greater than around 10 % of the expected values for any Lunar phase, further reducing to 1 % near full Moon conditions [67]. When designing this laser system, the worst-case condition of 1% returned signal strength was considered, as even in full Moon conditions we want to be able to perform ranging with the retroreflectors to enable improved orbit determination precision as much as possible.

To determine whether a signal is detected by the receiver, the same method is used as described in subsection 6.2.2. Considering this, the link budget calculations were performed. For the single photon laser altimeter [49], 18.566 photons were returned to the satellite, considering the maximum distance between a LNS and a Lunar retroreflector is 8723.158 km. This value was achieved by observing the propagation in time of the coordinates of the LNSS satellites, from this the maximum distance from any point on the Moon to any satellite after any time can be computed. These computations are performed using the code in the GitHub-Frozen Orbits. When performing the link budget using the regular altimeters, the following values were achieved; for the BepiColombo Laser Altimeter (BELA) 4818.840 photons were returned and for the Ganymede Laser Altimeter (GALA) $5.093 \cdot 10^{14}$ photons were returned. From these values, it can be concluded that both the BELA and GALA are over designed for the purpose of Lunar retroreflector ranging from the LNSS constellation, whilst the single photon is suited for this application. Again, the over designed design should be avoided as they would make the satellites unnecessarily mass and power heavy.

Thus, the choice is made again for the single photon laser altimeter. It still returns more photons than required for a single photon laser altimeter, however, this is not considered an over designed at all since the noise will be quite significant as the signal needs to travel forth and back. This will increase the travelling distance, thus increasing the probability of noise polluting the signal. To ensure that the signal can still be distinguished from the noise, it can be useful to design for more returned photons to the receiver. Furthermore, the single photon laser altimeter has only been researched for one-way ranging [49, 53], so implementing it for two-way ranging might be slightly more challenging. Therefore, the 18.566 returned photons are justified in this design. Since the selected single photon laser altimeter is the same as in subsection 6.2.2 its picture and block diagram can again be seen in Figure 6.4a and Figure 6.4b respectively. Again, the implementation of the gimbal is still missing in this picture, but this will be elaborated on further in this section.

In Table 6.7 and Table 6.8, all the relevant inputs and outputs for the Lunar retroreflector ranging are listed for all three designs. Where η_{rr} represents the efficiency of the retroreflectors on the Lunar surface as previously discussed in this subsection. Most of the inputs are the same as in subsection 6.2.2, as the same altimeters are considered, therefore the same sources were used to obtain these inputs.

Table 6.7: Inputs for the Lunar retroreflector ranging calculations.

	Inputs									
	E_T **[J]**	η_T	η_R	η_{rr}	Θ_T **[rad]**	D_R **[mm]**	λ **[nm]**	θ_T **[rad]**	θ_R **[rad]**	d_{ss} **[km]**
Single photon laser altimeter	$3 \cdot 10^{-6}$	0.625	0.04	0.01	$8 \cdot 10^{-3}$	40	532	$8 \cdot 10^{-3}$	$8 \cdot 10^{-3}$	8723
BELA	$50 \cdot 10^{-3}$	0.625	0.34	0.01	$60 \cdot 10^{-6}$	200	1064	$60 \cdot 10^{-6}$	$50 \cdot 10^{-6}$	8723
GELA	$17 \cdot 10^{-3}$	0.625	0.83	0.01	$100 \cdot 10^{-6}$	250	1064.5	$100 \cdot 10^{-6}$	$100 \cdot 10^{-6}$	8723

Table 6.8: Outputs for the Lunar retroreflector ranging calculations.

	Outputs		
	E_R **[J]**	E_{photon} **[J]**	N_P
Single photon laser altimeter	$6.932 \cdot 10^{-16}$	$3.734 \cdot 10^{-19}$	18.566
BELA	$8.997 \cdot 10^{-14}$	$1.866 \cdot 10^{-19}$	4818.840
GALA	$2.036 \cdot 10^{-5}$	$1.866 \cdot 10^{-19}$	$1.091 \cdot 10^{12}$

The final element that needs to be addressed about the laser ranging is the implementation within the spacecraft. To make sure that all neighbouring satellites in the constellation can be reached using the optical inter-satellite links, the OISL laser designed in subsection 6.2.2 will be positioned on the side of the spacecraft facing away from the Lunar surface. Both the laser transmitter and receiver will be positioned on a two-dimensional gimbal as described in [69]. In this way, this laser will be able to reach all neighbouring satellites in the constellation that are located in an orbit with the same or larger orbital altitude. Additionally, the laser designed in subsection 6.2.3 will be positioned on the side of the spacecraft facing the Lunar surface. Also, this laser's transmitter and receiver will both be positioned on the same two-dimensional gimbal, as mentioned previously. In this way, this laser will be able to reach both the Lunar retroreflectors on the Lunar surface and all neighbouring satellites in the constellation that are located in an orbit with the same or lower orbital altitude. This means that this laser will perform ranging with both retroreflectors and other satellites, but since the same single photon laser altimeter is chosen as for the OISL this should not form a problem.

To be able to provide the updated ephemeris data, the gimbal should be able to rotate to all neighbouring satellites within a range of 8078.893 km before sending the next updated ephemeris data. Since very little data was available, the worst-case scenario and some margins were taken for the following calculations. A typical satellite gimbal will rotate at around 3.75 degrees per second [70]. Considering this rotation rate is 1 degree per second after applying a margin, it will take the gimbal 180 degrees to rotate over its entire arc. So when a satellite is on the other side of the current laser position, it would take the gimbal 180 seconds to rotate towards it. In a worst-case scenario, it is assumed this would be the case for the rotation to every satellite. Again, in a worst-case scenario, each satellite would be surrounded by six other neighbouring satellites, which means three rotations for each gimbal plus an additional rotation to a Lunar retroreflector for the gimbal pointing down to the Moon. So in a worst-case scenario, a gimbal would need to rotate 180 degrees 4 times, which means 720 seconds or 12 minutes of rotations. With a required updating frequency of 1 hour 36 minutes 11 seconds, which is determined in section 4.3. This means that there is remaining time for the computations done in section 6.3 in order for the satellites to compute their own absolute Kepler coordinates.

6.2.4. LNS to Relay Communication

Performed by J.K. Geijsberts, A. Van Parys. Written by J.K. Geijsberts.

The monitoring of the LNSS is a necessary attribute of the mission, and cannot be left unexplored, as commands to the navigation satellites need to be given in the case of a malfunction. Therefore, a single relay satellite, namely the future Lunar Pathfinder, is used as a relay satellite for monitoring the LNSS.

In the originally chosen design concept, the idea for the relay was such that the relay was a satellite situated at a Lagrange point. However, requirement **NTM-USER-12** only allowed the usage of certain frequencies for the relay satellite towards Earth and from Earth. This meant only antennas with transmitter frequencies to Earth between 7190-7235 MHz could be used, and from Earth to the relay only 8450-8500 MHz could be used. For this, it was found that an already existing planned mission, Lunar Pathfinder, would be the perfect relay satellite for the Moon constellation. This is due to the fact that the Lunar Pathfinder is the preliminary part of the Moonlight project [71]. It is therefore designed for the exact function necessary for the relay satellite. Next to that, other relay satellites like Lunar Gateway can be used for relay purposes as well. What must be noted, is that the relay is used for monitoring purposes, for which no direct requirements are available, except that it must happen, which means it does not necessarily need its link budget to close for the whole part of its orbit period.

The two components of the link budget are in this case the TT&C system on the Lunar Pathfinder [71] and the Endurosat S-band transceiver [72]. All values from these TT&C subsystems were used wherever possible. All other values had to be assumed. All of these assumed values were assumed conservatively as a margin to make sure the link budget closes in the way that is required.

The link budget calculations to the relay as well as the user are done through radio frequencies and methods for establishing the link budget are considered standard, so these are assumed to be common knowledge to the reader.
The parameters used for the link budget calculation to the relay can be seen in Table 6.9. A rationale is given for some parameters if necessary and further detail is given after the table.

Table 6.9: Link budget parameters for the link towards the relay and their respective values.

Parameter	Value [dB]	Rationale (if needed)
SNR_{req}	5	Convolutional coding [71][14], due to regulations. A Commonly used and conservative bit error rate of 10^{-6} was chosen, leading to a required SNR of 5[44].
P_{tr}	3 [72]	TTA-G1
L_l	-1.5	Conservative assumed value, similar to those in [44].
G_t	6.0	Typical values used in [44] are around 20 dB. Therefore, using this value is seen as conservative.
L_a	0	
G_r	0.2[73]	No gain could be found for the current relay antenna, therefore the conservative value of this antenna (phone patch antenna) was used.
$L_{s_{max}}$	-176.9[44]	d = 8055.44 km
$L_{s_{min}}$	-145.0[44]	d = 205.76 km
L_{pr}	-10	Due to high ADCS precision for the lasers, it is assumed the pointing loss is practically non-existent. Next to that, values found in [44] are around -0.12 dB, so using a value of -10 dB is conservative.
L_r	-1.5	Conservative assumed value, similar to those in [44].
R	30	This corresponds to 1000 bit data rate, which is the amount necessary for monitoring for Galileo [74].
k	-228.6	Boltzmann constant.
T_s	21.3[44]	

The most important formula for the link budget is the one for the signal-to-noise ratio margin, which is shown in Equation 6.2.

$$\text{SNR}_{\text{margin}} = \text{SNR}_{\text{act}} - \text{SNR}_{\text{req}} \tag{6.2}$$

The frequency used in the link budget is a frequency of 2066 MHz, which is the centre frequency of the Lunar Pathfinder. The requirements state the system should comply with the FLCA [14] (NTM-LEG-02 and NTM-LEG-03[6]), which this frequency does, as the relay is seen as part of the proximity-link, which allows a conservative frequency range of 2025 – 2110MHz.

Two loss factors are used for the cables, namely L_l and L_r. These are assumed to both be 0.7, which is valid, given that the lowest value in the typical range of values given in [44] is 0.7.

For the space loss, two distances were used, namely the largest distance between the relay and the closest LNSS satellite, as well as the smallest distance from the relay to any LNSS satellite. These distances will determine the range of $\text{SNR}_{\text{margin}}$ values that can exist between satellites and the relay.

Using these parameters, two $\text{SNR}_{\text{margin}}$ values are calculated, which can be seen in Equation 6.3.

$$\text{SNR}_{\text{margin}} = 20.41\,\text{dB} \quad \text{(best case distance, largest distance to closest LNSS satellite.)} \tag{6.3}$$

$$\text{SNR}_{\text{margin}} = -11.45\,\text{dB} \quad \text{(worst case distance, smallest distance to any LNSS satellite.)} \tag{6.4}$$

Noticeable is that the worst-case distance does not meet the 3 dB margin that is necessary for the link budget to function. However, as stated before, this is not necessarily a problem as the link to the relay is only used for monitoring, which does not need to happen continuously. What can be calculated is what the distance is when the link budget fails with these current parameters. Doing this, it can be seen that the link budget fails at around a distance of 2200 km. This is not necessarily too low, and fulfils the requirement that monitoring happens.

Important to know too is that if relatively less conservative (but still conservative generally) values are used for the gains of the transmitter and receiver antenna, the link budget closes for all distances. That is if the gain of the transmitter and receiver are for example both set to 10 dB (assumption TTA-G8), which, looking at values from [44] (they use 20 dB for the spacecraft gain), is still conservative, the link budget closes, for all distances. Then it was noticed that the receiver antenna used was a patch antenna (the assumed antenna with

a gain of 0.2 dB), normally used for users on the ground in GNSS applications, which is not fully applicable in a spacecraft-to-spacecraft link. Therefore, the calculations for the link budget were done again, where the gain of the transmitter was set to 124.7 (which is the same for GPS helical antennas on Earth[75], and the gain of the receiver was set to 100, which is a typical value used in [44]. Doing the calculations again, the following $\text{SNR}_{\text{margin}}$ values occur:

$$\text{SNR}_{\text{margin}} = 58.14\,\text{dB} \quad \text{(best case distance, largest distance to closest LNSS satellite.)} \tag{6.5}$$

$$\text{SNR}_{\text{margin}} = 26.29\,\text{dB} \quad \text{(worst case distance, smallest distance to any LNSS satellite.)} \tag{6.6}$$

Therefore, considering the lack of information on the antennas of both spacecraft, using both these conservative calculations the justification can be made that the link budget will close, and will most likely close for all distances. This does need to however be looked into further.

6.2.5. LNS to User Communication

Performed by A. Van Parys, J.K. Geijsberts. Written by A. Van Parys.

Finally, once all ephemeris data has been computed and updated and possible monitoring has been performed, the user still has to receive the ephemeris data to provide the navigation services. To perform this, a one-way communications link is set up where the LNS will send the ephemeris data every second using circularly polarised antennas[7] to all users on and orbiting the Moon. The communication is one-way as only the LNS will send a signal and no signals are sent back by the user. These transmitted ephemeris signals are updated every **one hour 36 minutes 11 seconds** with newly computed ephemeris data.

When starting any design, it is important to look at the requirements that could restrict the design. This was particularly important in the design of the LNSS antenna, as in the Lunar Communications Architecture Study Report [14] strict requirements are provided for the frequency of the user communication link. There is stated that the proximity link to the Lunar surface has to be within a frequency range of 2483.5 - 2500 MHz. This severely limits the design possibilities as this means that an S-band signal would need to be transmitted, whilst for GNSS application L-band is used almost everywhere. L-band is chosen on Earth as L-band penetrates clouds, fog, rain, storms, and vegetation, this means that GNSS will be able to provide service in all weather conditions, day, or night [76]. However, on the Moon this is not an issue and S-band is chosen to avoid interference with the Earth's GNSS and other missions.

The S-band does limit the antenna choice, as this means that regular L-band antennas that are used on GNSS satellites cannot be used. Therefore, first S-band GNSS were researched, however, they were very limited especially for the small frequency range of 2483.5 - 2500 MHz. Therefore, the search was expanded to patch antennas within the desired frequency range. These are even particularly interesting because of their low mass, volume, and cost. However, whether they could be used to transmit navigation signals to the users was uncertain. Because of this, Dr. Ernst Schrama was consulted. He recommended specifically looking at circularly polarised patch antennas as he also saw the benefit in patch antennas, but to transmit navigation signals a circularly polarised antenna is required.

Using this new information, the search for an off-the-shelf antenna was continued. It was found that there are some Asian countries in ITURegion 3 that already use S-band for navigation. The Chinese Beidou GEO satellites use 2491 MHz as carrier frequency. The Japanese Engineering Test Satellite Number 8 (ETS/8) does this too, and the Indian IRNSS system also sends navigation signals in this band [77]. Furthermore, also Globalstar is also operating at this frequency [78]. Therefore, an intensive literature research was performed to find relevant data about their S-band antennas. However, unfortunately, not a lot of data is publicly made available by the relevant space agencies and companies. Eventually, the decision was made to go with the circularly polarised patch antenna of the Chinese Compass Navigation Satellite System (CNSS), described in the paper by J. Li et al. [42], as from all previously discussed options the most data is available for this antenna. Next, the literature research was also performed to find relevant data about their S-band receivers. However, again, specific data was very hard to find for these space agencies and companies. Eventually, the decision was made to go with the circularly polarised IRNSS receiver antenna, described in [41], as once more this one has the most data available.

After selecting the required components, the link budget can be performed to check whether the antennas are able to provide the communication link required and whether the signal can be clearly distinguished from the

[7] Communication with Dr. Ernst Schrama, 08/06/2022

noise. To perform this link budget Equation 6.7 is used, it is based on Equation 6.1, but it is adapted where necessary. In this equation, P_T represents the power transmitted by the satellite antenna, P_R represents the power received by the user on or orbiting the Moon, L_L represents the line loss or cable loss, L_P represents the antenna pointing loss, L_{PS} represents the free-space path loss for the radio frequency link between the satellite and the user, L_R represents any losses experienced at the user, G_T represents the transmitter gain and G_R represents the receiver gain. The free-space path loss is here defined as $L_{PS} = (c/(4 \cdot \pi \cdot d_{su} \cdot f))^2$, with c representing the speed of light and d_{su} representing the distance between LNS and the user in m.

$$P_T = \frac{P_R}{L_L \cdot L_P \cdot L_{PS} \cdot L_R \cdot G_T \cdot G_R} \tag{6.7}$$

The values that were used to perform this link budget come from various sources. The transmitter gain [42] and receiver gain [41] are specified in the descriptions of these antennae. However, it should be noted that they were given as 8 and 3.05 respectively in the dB scale and thus had to be transformed back to SI units before they could be used in this link budget equation. The typical minimum received power for GNSS users is around -130 dBm[8], also this value had to be transformed to SI units. The frequency is also specified in the description of the transmitter antenna [42]. The distance between LNS and the user is 8723.158 km. This value was achieved by observing the propagation in time of the coordinates of the LNSS satellites, from this the maximum distance from any point on the Moon to any satellite after any time can be computed. This calculation yields a value of $8\,723\,157.9$ m and is computed using the code in the GitHub-Frozen Orbits. The antenna pointing loss is assumed 1 as for circularly polarised antennae the pointing loss is minimal. Finally, the line loss and receiver loss are assumed to be 0.7 as very little data was available on these losses in this use case, thus a very conservative number of 0.7 was chosen for both.

In Table 6.10 all the relevant inputs and output for the LNS with user communication calculations are listed. Here all values are given in SI units and the basic conversion from dB to SI units has already been performed.

Table 6.10: Inputs and output for LNS to user calculations.

Inputs								Output
P_R [W]	L_L	L_P	d_{su} [m]	f [Hz]	L_R	G_T	G_R	P_T [W]
$1 \cdot 10^{-16}$	0.7	1	8723157.9	$2492 \cdot 10^6$	0.7	6.310	2.0184	13.305

An important element about GNSS antennae was noticed during the literature research; almost all the current GNSS satellites have some kind of phased array configuration. So naturally the question was asked why, however not a lot of information was found on this topic. Because of this, Dr. Ernst Schrama was consulted. He explained that these phased arrays are used for two main reasons. Firstly, they are used to be able to transmit a wide range of frequencies, as a single antenna is fixed to the frequency of that specific antenna, however by making use of a phased array the frequency can be varied. However, this is not very useful in this design case, as the frequency range of 2483.5 - 2500 MHz provided by [14] is not very wide in the first place. Secondly, it is used to focus down the GNSS signals more to a specific position on Earth's surface. This could be useful when specific interest is subjected to the Lunar South Pole or any other area more LNSS signals could be (momentarily) focused on that area. Therefore, he recommended the use of a small phased array of three to four antennae, such that the ability to focus down a single area exists if necessary. This phased array was thus implemented in the final design with four transmitter antennae.

Lastly, some requirements were also allocated to the User Terminal Antenna, these should thus be addressed. Looking at the selected design for the receiver antenna as described in [41], it can be observed that the dimensions of the receiver antenna are 28 × 28 × 1.6 mm. Furthermore, the mass is not specified, but assuming the mass varies linearly with the cube root of the volume and comparing it with the transmitter antenna [42], a value of 115.78 grams is achieved. This shows that both the volume and the estimated mass of the receiver antenna are well below the requirements.

6.2.6. Final Design

Performed by A. Van Parys, J.K. Geijsberts. Written by A. Van Parys.

Now that the TT&C subsystem has been completely designed, all final aspects can be summarised. In Table 6.11 both the mass and the power are summarised for every component and the final values for the entire

[8] https://support.spirent.com/SC_KnowledgeView?id=FAQ18565

subsystem are given. It should be noted that the values for the antenna to the user are already summed up for the four antennae on the phased array.

Table 6.11: Summary of all the designed and selected components for the TT&C subsystem.

Component	Mass [kg]	Power [W]
OISL laser	4	20
Retroreflector ranging laser	4	20
Antenna to relay	0.190	1.995
Antenna to user	2.511	53.221
Total	10.702	95.217

Sustainability
Sustainability is an aspect that needs to be considered throughout the entire design of the spacecraft, thus it has also been considered in the TT&C subsystem design. The following aspects of the design are an indication of this. Firstly, whilst designing all communication links, the LunaNet Interoperability Specifications [79] and the Lunar Communications Architecture [14] were always taken into account. The Moonlight initiative was given these constraints to avoid any interference with any other current or future Lunar missions. This means that since they were included in this design, it will experience little to no interference. Secondly, due to the onboard ODTS, which is operative thanks to the OISL, the need for ground stations is reduced. Since the ground stations are only used for monitoring in the design, the amount of resources required for the ground stations is significantly reduced, improving sustainability. Finally, the lasers were designed separately to ensure the best-fitting design was chosen for each use case and as little over-designed as possible was present. Eventually, it resulted in the same laser for both links, however, the design was done with sustainability in mind as the single-photon laser altimeter is significantly more sustainable than a regular laser altimeter, which would have resulted in a severe overdesign.

Verification & Validation
All the computations for both laser links were performed using Microsoft Excel and they were verified by performing the calculations by hand and simply checking whether the result we achieved by the manual calculation matched with the result in Microsoft Excel. On the recommendation of Dr. Dominic Dirkx, a validation of the calculation in Microsoft Excel was performed using the data of the APOLLO experiment [80]. The validation was performed by checking if the same number of photons were returned in the calculation as they received in real life and indeed, taking into account the relevant gains and losses, a similar number of photons was found.

For the calculation of the link budgets between the LNS and the relay and between the LNS and the user, normal link budgets were established in Microsoft Excel and verified and validated, using data from [44], by hand. This means all the calculations were performed again by hand to see if the same values were retrieved, and that this was also done with other data. All of these tests performed in Microsoft Excel passed, meaning that also these two link budgets are verified and validated.

Recommendations
This section is concluded with some recommendations for the TT&C subsystem for future research.

- Look into what angle each retroreflector is exactly pointing at and check where in each orbit ranging with the retroreflectors is possible; to improve the precision of the expected orbit determination accuracy.
- Look into how the Lunar Pathfinder can be replaced when it would go into End of Life before the end of this mission. Possible alternative relay orbiters could be The Lunar Gateway (NASA), Chang'e-4 Queqiao (CNSA), Chandrayaan-2 orbiter (ISRO), and possibly other future planned Lunar orbiters.
- Look into an even smaller, lower pulse energy laser altimeter for the OISL, as the single photon laser altimeter is currently still an over designed for that design. When technology has advanced sufficiently, the use of a smaller laser could be investigated.
- Multiple of the values used for the link between the Lunar Pathfinder and the transceiver on the navigation satellite were assumed. Some of these are the gains of both antennas, as well as pointing losses and cable losses. Further research needs to be performed on getting more accurate values on these variables.
- Multiple of the values used for the link between the navigation satellite and the user were assumed. Some of these are pointing losses and cable losses. Further research needs to be performed on getting more accurate values on these variables.

6.3. Command and Data Handling System

In this section, the central computational part of the LNSS spacecraft is discussed, namely the Command and Data Handling subsystem (CDH). This subsystem is crucial towards the functioning of the spacecraft and can be thought of as the brain of the satellite. First, for the design, requirements and design assumptions are stated in subsection 6.3.1 The design for the CDH is relatively straightforward and includes three iterations. The first iteration, which includes an estimation method to find the mass, power and volume of the CDH subsystem, is shown in subsection 6.3.2. The second iteration, which calculates the same parameters through a different method, can be seen in subsection 6.3.3. The last and third iteration chooses components and can be seen in subsection 6.3.4. Lastly, the verification and validation are explained together with how sustainability was considered in the design and some recommendations are given.

6.3.1. Requirements and Design Assumptions

By J.K. Geijsberts, A. Van Parys.

Requirements and assumptions form the basis of the CDH design. From the results, the requirements can be updated and made more specific. In Table A.9 in Appendix A the requirements for the final design are displayed.

Furthermore, due to the complexity of the CDH design, certain assumptions are introduced. Assumptions can lead to simplifications, however, these simplifications will lead to inaccuracies. Thus, they will need to be carefully administered and updated throughout the design process. Some assumptions are listed in each iteration, in Table 6.12, Table 6.15, and Table 6.18. All computations performed for the CDH subsystem can be found in GitHub-Initial Sizing.

6.3.2. First Iteration

Performed by J.K. Geijsberts, A. Van Parys. Written by J.K. Geijsberts.

In this subsection, the first iteration for the CDH subsystem is shown. The method for calculating the mass, power, and size was taken from literature [81]. This method includes using estimations on, for example, the mass, to then use a specific power to calculate the power needed for the CDH subsystem. Assumptions used in this iteration are shown in Table 6.12.

Table 6.12: Assumptions made for CDH subsystem, first iteration

ID	Assumption	Reasoning
CA-I1	The estimation method used in the reader is accurate for navigation systems.	Method is used for general CDH subsystem budget estimation.

Firstly, a first-level estimation of the power of the CDH was made using literature on GNSS systems, like GPS. The way this is done is shown in section 5.4. Then, using this power, a first-level estimation could be made for the mass and volume of the data handling/acquisition unit using the following data:

$$\text{Mass density: } \sim 0.5 - 1 \text{ kg/liter}$$
$$\text{Specific power: } \sim 1 - 2.5 \text{ W/kg}$$

Using these values, and the power for the data handling/acquisition unit, the mass, and volume can be calculated. These calculated values can be seen in Table 6.13.

Table 6.13: First iteration mass, power, and volume values of the data handling/acquisition unit.

Mass [kg]	32.8
Power [W]	57.4
Volume [L]	43.7

Next to these values, the mass, power, and volume of the other parts in the CDH subsystem must be calculated. These are the command processor unit, data storage, and onboard computer + TM encoders and TC decoders. For the command processor unit, it can be assumed as a first estimate to have the same specifications as the data handling/acquisition unit[81]. This brings the current total to the values presented in Table 6.14.

Table 6.14: Current values in the first estimation of the mass, power, and volume values of the CDH.

Mass [kg]	65.6
Power [W]	114.8
Volume [L]	87.4

Here the mass and power are usual values, however, compared with other existing CDH subsystems, like the Geonardo [38], the volume was deemed too high for the method to be seen as accurate. Later, it was also found that the estimation method should be performed by using the number of TM channels, further intensifying that this estimation method is inaccurate. Therefore, another estimation method was used for the second iteration, which is one that was used for iteration purposes by other subsystems.

6.3.3. Second Iteration

Performed by J.K. Geijsberts, A. Van Parys. Written by J.K. Geijsberts.

General values for a CDH system from SMAD [35] were used as a general starting point for the second iteration. This is useful for a first-level estimation and allows other subsystems to start their iteration process. In the table from SMAD [35], there are standard sizes, weights, and powers given depending on if the system is complex. To allow other subsystems to perform a first iteration, the CDH subsystem used the values in Table 6.16. To be conservative, the CDH subsystem was seen to be a complex subsystem.

Table 6.15: Assumptions made for CDH subsystem, second iteration

ID	Assumption	Reasoning
CA-S1	The estimation method used in the SMAD is accurate for navigation systems.	Method is used for general CDH subsystem budget estimation.

Table 6.16: Shrunk down version of the parametric estimation table in SMAD.

	Complex
Size (cm^3**)**	13,000-15,000
Weight (kg)	9.5-10.5
Power (nominal) (W)	15-25

Therefore, the values for the CDH subsystem mass, power, and size would become as specified in Table 6.17

Table 6.17: Second estimation method values for the mass, power, and volume.

	Complex
Size (cm^3**)**	15,000
Weight (kg)	10.5
Power (nominal) (W)	25

These values align with existing CDH subsystems and were deemed feasible for usage by other subsystems for their first iteration. Note that a third iteration is needed to choose components for the final design of the CDH subsystem.

6.3.4. Third Iteration

Performed by J.K. Geijsberts, A. Van Parys. Written by J.K. Geijsberts.

In this subsection, the third iteration of the CDH subsystem is shown. This iteration is done by finding components that could be used for this specific subsystem.

Table 6.18: Assumptions made for CDH subsystem, third iteration

ID	Assumption	Reasoning
CA-T1	The RINEX file size is at a maximum 300 Mbyte	This is an order of maximum that is given by ESA[9]. More often they will be smaller, thus not always in the order of 300 Mbyte. Therefore, it is taken as a maximum.
CA-T2	The estimation method used in SMAD is accurate, and the assumptions SMAD uses in its estimation method are accurate.	This estimation method is used to calculate the instructions per second. It is a first level estimation method, but it uses general assumptions on the amount of instruction per character and per word to calculate the amount of instructions per second. It is assumed valid because very detailed estimation method is not necessary.
CA-T3	One DMIPS is equal to one MIPS	The Dhrystone benchmark is a test to see how well a computer processes. One DMIPS is how well a one MIPS computer (namely the VAX 11/780) would perform the Dhrystone test. A 100 DMIPS is then definitely better than the 1 DMIPS machine (100 times better in the Dhrystone test), so the assumption is made that one can have 1 MIPS be equal to 1 DMIPS.

The component selected for this subsystem is the on-board computer, which has all necessary features for the CDH subsystem. This computer is the OBC NG [82]. Next to that, in the navigation payload, a navigation signal generator unit is used, which also has parts that can perform CDH functions [38].

There are multiple requirements for the CDH subsystem. Two important requirements are the requirements for the updating of the ephemeris parameters to happen in the allocated updating time (Shown in requirement **NTM-SYS-CDH-PRF-05** and **NTM-SYS-CDH-PRF-07**). The computer chosen can be compared to what is needed for updating the ephemeris parameters.

Ephemeris parameters are usually sent in RINEX format on existing GNSS [83]. RINEX messages can have a size of up to 300 MB[10]. Using a SMAD estimation method [84], the total MIPS that is necessary can be found. The amount of time the spacecraft has to process the data is 5051 sec (which is calculated in subsection 6.2.3). In this time, all the ephemeris parameters from the six satellites that are in view, according to subsection 6.2.3 need to be processed, which is a total that can be calculated and is shown in Equation 6.8. However, there will be a data set from the Moon reflector as well, thus in total, seven data sets are taken into account for each satellites' computations.

$$300 \text{ MByte} \cdot 8 \text{ bits/Byte} \cdot 7 \text{ data sets} = 16800 \text{ Mbits} \tag{6.8}$$

Knowing the amount of time there is to process these amount of bits, one can find the number of bits per second that need to be processed.

$$\frac{1.68 \times 10^{10}}{5051} = 3.33 \times 10^{6} \text{ bits per second}$$

Then, assuming that each character is represented by 8 bits, and that each character needs 10 instructions for processing, the amount of instructions to process the characters can be calculated.

$$3.33 \times 10^{6} \cdot \frac{10}{8} = 4.16 \times 10^{6} \text{ instructions per second (for characters)}$$

Then, it is also known that every 6 characters make up 1 word, where every word needs 100 instructions to be processed. This means that the number of instructions per second that are necessary for the words to be

[9] https://gssc.esa.int/navipedia/index.php/Interfaces_and_Protocols
[10] https://gssc.esa.int/navipedia/index.php/Interfaces_and_Protocols

processed can be calculated.

$$4.16 \times 10^5 \text{ characters per second} \cdot \frac{100}{6} = 6.93 \times 10^6 \text{ instructions per second (for words)}$$

Adding up the two IPS values and converting them to MIPS, the performance needed of the computer can be calculated, and is shown in Equation 6.9.

$$4.16 \times 10^6 + 6.93 \times 10^6 = 1.11 \times 10^7 \text{ IPS} = 11.09 \text{ MIPS}. \tag{6.9}$$

Now it is known that the computer used has a DMIPS of 93, which means the system performs 93 times better than a 1 DMIPS machine, which is around what a 1 MIPS machine (the VAX 11/780) would score on the Dhrystone test[11]. Therefore, if an MIPS of 11.09 is needed, the computer is shown to be powerful enough to process the ephemeris parameters of all the satellites at their highest file size. From this calculation also the total amount of seconds it would take to process the data can be calculated, which is seen to be 602.15 s.

As lasers are used in the TT&C system, GEODYN is used as a method for calculating the ephemeris parameters [49]. An on-board memory is needed for this, and the CDH subsystem must have this memory. GEODYN has been used on other missions like TOPEX/Poseidon [85]. Specifically in the TOPEX/Poseidon mission, a memory of 1152000 bits is required [86]. The OBC NG that is present on the LNS has a memory of 512 MiB for processing [82], which should thus be sufficient for GEODYN.

A couple requirements for the CDH subsystem (**NTM-SYS-CDH-GEN-01** up to and including **NTM-SYS-CDH-GEN-06**), state requirements about security and confidentiality of the system. These have been taken into account in the design of the spacecraft as the OBC NG includes TC AES authentication and decryption with 256-bit keys as well as TM AES encryption with 256-bit keys [82]. These can be used to comply with the requirements specified.

6.3.5. Final Design

Performed by J.K. Geijsberts, A. Van Parys. Written by J.K. Geijsberts.

Now that iterations have been made and components have been checked to comply with the constraints and requirements, the final components can be mentioned, as well as their specifications. They can be seen in Table 6.19.

Table 6.19: Final design parameters of the CDH subsystem.

Component	Mass [kg]	Power [W]	Dimensions [mm]	Storage [Gbit]
OBC NG	9	38	283 x 242 x 278	2 x 374 (with EDAC)
Memory [Mib]	**Performance [DMIPS]**	**Reliability**	**Life Time [years]**	**Security**
512	93 @ 75 MHz	0.99	20	TC AES Authentication and Decryption with 256-bit keys, TM AES Encryption with 256-bit keys

To visualise what the CDH subsystem performs, a data handling block diagram was made, which can be seen in Figure 6.5.

[11] https://www.itwissen.info/en/Dhrystone-MIPS-DMIPS-119059.html#gsc.tab=0

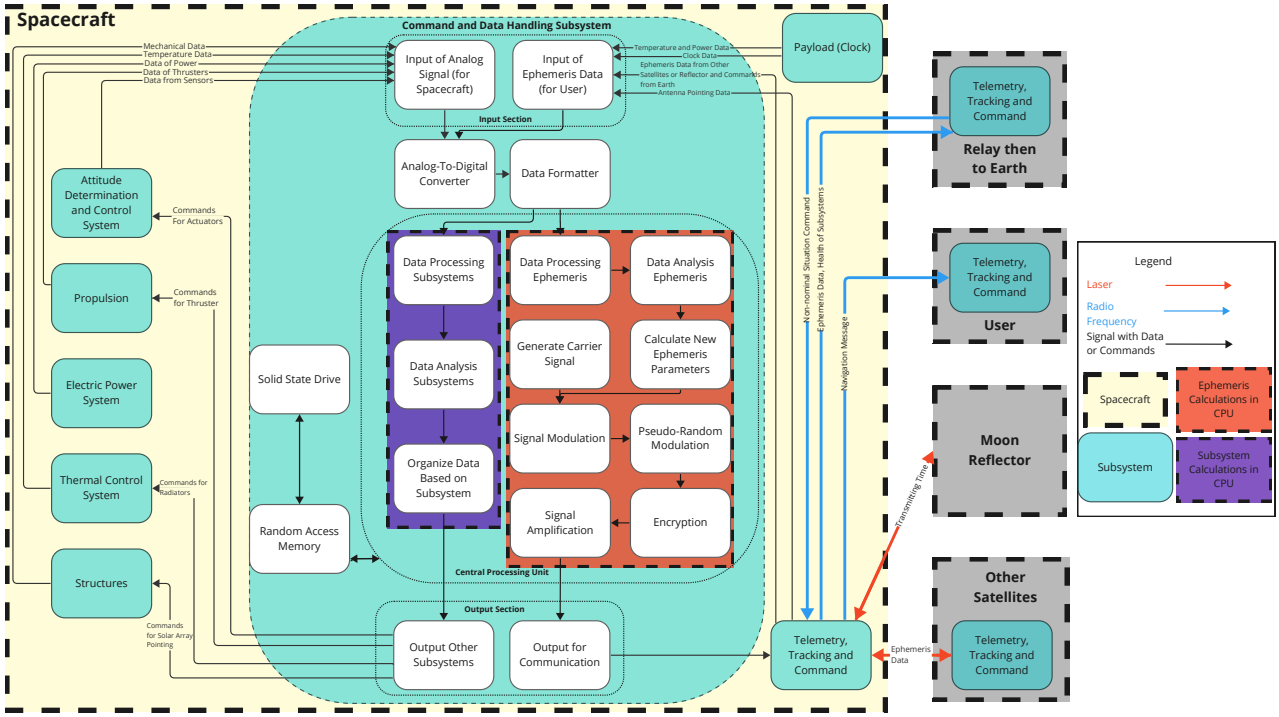

Figure 6.5: Data handling block diagram containing hardware and functions for the CDH subsystem as well as other parts of the missions that need data handling.

Verification and Validation

The calculations for the number of MIPS needed were performed by hand. To verify and validate this, the calculation was performed again with the data used in the SMAD example. The data used there can be found in literature [84]. The verification and validation was therefore done using the data from literature and by redoing the calculation.

Sustainability

The sustainability of the mission is important to be considered throughout the spacecraft, and therefore also the CDH subsystem. First of all, it can be mentioned that the CDH component, the computer is off the shelf, which means no emissions will be present for the development and design of the computer, only for the manufacturing. This is very important, as R&D can be very expensive in terms of carbon footprint. All the testing, iterations and assembly take up a carbon footprint. Having this done already is great for sustainability.

Recommendations

The CDH subsystem has now been fully designed, however, some recommendations are still present. These can be seen in the following list.

- More in-depth analysis can be performed for the processing of the ephemeris data. This has been done through a SMAD estimation method, but should be looked into more through other, more accurate estimation methods.
- More in-depth analysis can be performed on the authentication and encryption method used. It is present, but no specific analysis on its performance is done.

6.4. Propulsion System

By C.A.G.C Spichal.

The propulsion subsystem plays a crucial role when it comes to performing the Lunar insertion orbits as well as the orbit maintenance manoeuvres and end of life procedures. The first step involves the identification of the propulsion requirements that will drive the design of the propulsion system in subsection 6.4.1. The next step, subsection 6.4.2, will entail the trade-off of the type of propellant that will be used. After that, the architecture as well as the exact propellant along with its budget will be analysed in subsection 6.4.3 and subsection 6.4.4.

6.4.1. Requirements and Design Assumptions

The propulsion requirements have been constructed based upon the calculation and documentation that will be detailed in the following sections. The requirements can be found in Table A.3 in Appendix A.
The main assumptions made throughout this subsection are indicated in Table 6.20. In some cases, the assumption is mentioned again in the text, however, the reasoning for it is already provided in the table below.

Table 6.20: Assumptions for the Propulsion system

ID	Assumption	Reasoning
PPA-01	The masses assigned to each phase are burnt sequentially. In other words, for example, at the end of LOI the entire mass assigned to this phase is assumed to be burnt.	This assumption is reasonable provided that most mission phases occur in sequential order. The only exception is the orbit maintenance and ADCS desaturation phase. Assuming they burn one after another does not result in significant variation in the ΔV budget
PPA-02	Thrust is constant when calculating the burn time in Equation 6.11 for the manoeuvres.	Making use of this assumption allows accessing insightful information. If it wasn't assumed to be constant, an integration would have to be performed which would make the study unnecessarily difficult.
PPA-03	The ΔV values found in Table 6.26 fit well with the final orbit configuration	It was decided that the values fit well because the orbits studied in the paper are in the same order of magnitude as the ones selected for the mission.
PPA-04	The positioning only has to be analysed for the low inclination and original constellation orbit planes.	This assumption relies on the fact that the North and South Pole orbits only have two satellites, meaning that they can be transferred into Ballistic Lunar Transfer(BLT) with the necessary time interval for them to be positioned accordingly.

6.4.2. Stage 1 Design

The stage 1 design consists in studying all the available types of propulsion and narrowing them down to one option. When two options will be remaining, a trade-off will be performed.

Preliminary type of propulsion selection
All the types of propellants that can be used for spacecraft are listed below:

- Electric propulsion
- Solid propulsion
- Chemical Mono-propulsion
- Chemical Bi-propulsion
- Cold gas propulsion

Out of all the options above, due to its non re-usability, solid propulsion can be discarded as one wants to be able to use the propellant at different times for different attitude correction manoeuvres. Some preliminary thrust and I_{sp} values have been found in Table 6.21 for all the other types of propulsion:

Table 6.21: Types of propulsion thrust and efficiency

	Thrust $[N]$	**Efficiency** $[s]$
Electric Propulsion	0-356 [87]	123-14000 [87]
Chemichal Monoprop	0.02-572 [34]	200-240 [34]
Chemical Biprop	4.5-27000 [34]	220-350 [34]
Cold gas	1-266 [88]	31-296 [89]

Bi-propulsion presents good thrust and specific impulse that can go up to $350\,$s. The fact that two tanks assigned for the fuel and the oxidiser must be used means that a significant volume of the spacecraft is occupied

by the propulsion system. On top of that, most space missions usually resort to bi-propulsion for the launch phase. The GNSS satellites make use of hydrazine mono-propulsion for their orbit maintenance [12] [13]. The combination of these facts means that bi-propulsion can be neglected for this trade-off.

Cold gas propulsion presents the drawback of having relatively low efficiency combined with a low achievable thrust. These two factors are not advantageous for the LOI which will require some long burns. Therefore, the two remaining types of propulsion that need more thorough research for the trade-off are the electrical and mono-propulsion.

Propulsion system trade-off
Before any of the calculations and documentation are mentioned, it is crucial to remind that one of the requirements from Table A.3 states that no hydrazine, the usual mono-propellant that is implemented in the current satellites, can be used. This means that alternatives, in this case the green mono-propellants, will be found.
The following sections will introduce a more detailed overview of the available electrical and green mono-propulsion systems as well as their performance criteria that will be used to perform the final trade-off.
Two equations will be used to make a comparison between the electrical and mono-propulsion and later on for the propulsion system design. The first equation to introduce is the Tsiolkovsky rocket equation:

$$MR = \frac{M_{full}}{M_{empty}} = e^{\frac{\Delta V}{g_0 \cdot I_{sp}}} \tag{6.10}$$

This equation will prove to be useful when propellant masses need to be compared for each stage and for the types of propulsion.
The second equation to introduce is the burn time for a given thrust and specific impulse, assuming constant thrust during the burn time of the manoeuvre:

$$t_b = \frac{I_{sp} \cdot g_0 \cdot M_{prop}}{F_T} \tag{6.11}$$

This equation is derived from the definition of the specific impulse and will be useful when comparing the performances of electrical and mono-propulsion.
The type of propulsion trade-off is performed while the exact ΔV budget is not fully known yet. A preliminary ΔV of $1\,\mathrm{km/sec}$ is therefore found and extracted from the Lunar Reconnaissance Orbiter mission (LRO) [90]. It has to be mentioned that the LRO final orbit, $50\,\mathrm{km}$, is much lower than the constellation ones'. The first order estimation is also performed without all the mission phases defined.

Electrical propulsion can be broken down into three further categories:

- Electrothermal Propulsion
- Electrostatic Propulsion
- Electromagnetic Propulsion

Resistojets or arcjets make use of electrothermal, Gridded Ion Engines (GIE) make use of electrostatic while Hall Effect Thrusters make use of electromagnetic propulsion.
Out of these types of propulsion, the most notable ones that were or will be used in past or future missions are the Hall Effect Thrusters on the SMART-1 mission, the ion thrusters on some deep space missions (Hayabusa 1 and 2) and Solar Electric Propulsion (SEP) for the Power and Propulsion Element (PPE) that will be launched as the first element of the future Gateway space station [91]. Because deep-space missions differ to what the Navigating the Moon constellation does, ion thrusters are not taken into account in the study. Some data about the thrusters used has therefore been collected and is shown in Table 6.22.

[12] https://spaceflight101.com/spacecraft/gps-block-iif/
[13] https://gssc.esa.int/navipedia/index.php/Galileo_Space_Segment

Table 6.22: Performance of some electrical thrusters

	Type of thruster	Thrust [mN]	I_{sp} [s]	Total Impulse [MN.s]	Power [W]	Status	Mission
PPS-1350-G [92]	HET	88	1630	2.23	1500	Flight-proven	SMART-1
PPS-5000 [92]	HET	200	3000	10	5000	In-development	none
PPE EP String [91]	SEP	338.5	1685	N/A	7000	In-development	PPE

The green mono-propellants can be broken down into three categories:

- Energetic Ionic Liquids (EIL)
- Liquid NOx mono-propellants
- Hydrogen Peroxide Aqueous Solutions (HPAS)

Energetic Ionic Liquids are made out of an ionic liquid, which combined with an ionic fuel result in chemicals with higher specific impulse. The most prevalent green-propellants are the HAN (Hydroxylammonium nitrate) and ADN (Ammonium dinitramide) based propellants. Liquid NOx mono-propellants usually don't require a too complex system and can self-pressurise themselves. Hydrogen peroxide chemicals present good properties for potential multimode systems (systems that make use of one propellant for different types of propulsion, for example electrical and mono-propulsion). Properties of some of these propellants are listed in Table 6.23:

Table 6.23: Green mono-propellants properties [93]

Class	Propellant	Theoretical I_{sp} [s]	Density [g cm^{-3}]	Chamber temperature [K]	Pressure conditions [MPa]
(EIL) HAN based	AF-M315E	266	1.47	2166	2
(EIL) HAN based	HNP225	213	1.16	990	1
(EIL) ADN based	LMP-103S	252	1.24	1903.15	2
(EIL) ADN based	FLP-106	255	1.357	2087.15	2
Liquid Nox propellant	N_2O	206	0.745	1913.15	0.3
Hydrogen Peroxide Aqueous Solution	HTP 98%	186	1.43	1222	1

Most mono-propellants achieve a specific impulse higher than 200 s, most of the time even higher than hydrazine (239 s [93]). The drawback compared to hydrazine is the much higher chamber temperature (1200 K for hydrazine [93]). This means that the propellant tank will have to be designed with different materials. Another feature to keep in mind is that green mono-propellants can still be designed to achieve thrusts going up to 22 N. Further explanations are provided in subsection 6.8.3.

Final type of propulsion selection

Now that both types of propulsion have been presented in more details, some comparisons need to be made. Starting with the burn time, the mass budget originally assumed of $1\,\mathrm{km\,s^{-1}}$ was used to obtain mass ratios using Equation 6.10 and burn times using Equation 6.11.The mass ratios were obtained assuming the I_{sp} ranges from Table 6.22 and Table 6.23. The burn times were taken for the best case scenario propellant mass obtained as well as the most optimal I_{sp} and thrust from Table 6.22 and Table 6.23. The original mass of 1025.1 kg from Table 5.8 was used. The results are shown in Table 6.24.

Table 6.24: First stage mass ratio and burn time comparison

	Mass Ratio	**Best case M_{prop} [kg]**	**Total burn time [hrs]**
Electrical propulsion	1.03-1.06	35	464 (19 days)
Green mono-propulsion	1.45-1.64	481	11

As one can see, EP has the benefit of carrying less propellant mass while mono-propulsion has the advantage of requiring less burn time. The fact that EP systems require such long burn times puts a constraint on the length of the LOI as well as for its potential impulse manoeuvres. In addition to that, the burn time for EP assumes the use of the PPE 338.5 mN thrusters, which are still in development. If the flight proven 88 mN PPS-1350-G thrusters are assumed, then the burn time jumps to 74.5 days.
The next remark to be made questions seriously the use of EP and is related to the power needed to operate the EP system. Assuming the 1500 W of the PPS-1350-G thruster and extracting the estimation made in Table 5.9 that 3.7 % of the total power is assigned to the propulsion system, this means that all the other subsystems' power required would soar to such an extent that the final solar array area needed would add up to $1000\,\text{m}^2$. As a means of comparison, JUICE, the next satellite flying to Jupiter, makes use of $85\,\text{m}^2$ solar arrays [14]. To finish with, the average power of navigation satellites obtained in Table 5.7 amounts to 1664 W, almost the equivalent to what the PPS-1350-G thruster itself needs. The power was therefore used as the main argument as to why EP was not selected.
In addition to the aforementioned arguments, a final remark about the Xenon used for EP systems needs to be made. Xenon is a gas present in Earth's atmosphere that can be easily ionised in the EP system and therefore generate thrust. One constraint that needs to be kept in mind is that only a certain amount of it can be produced every year. Hence, in case of the use of xenon propellant, as little mass as possible should be needed as too much would disrupt the market[94].

6.4.3. Stage 2 design

The stage 2 design primarily focuses on the establishment of a ΔV budget for each mission phase of the Navigating the Moon constellation. The results from the TLI, LOI, satellite positioning, ADCS/orbit maintenance and EOL phases will be provided.

Trans-Lunar Injection

Performing the TLI is an extremely mass demanding manoeuvre. The first type of manoeuvre that was considered was direct Moon transfers. Table 6.25 indicates how much ΔV is needed for both the TLI and the LOI in the case of direct transfers from an Earth orbit at 185 km to a Lunar orbit of 100 km[95]:

Table 6.25: Trans-Lunar Injection and Lunar Orbit Insertion ΔV budgets for different Direct transfer duration

Duration (days)	**ΔV_{TLI}(km/s)**	**ΔV_{LOI}(km/s)**	**Total ΔV(km/s)**
6	3.138	0.829	3.966
4.5	3.134	0.813	3.948
3	3.152	0.893	4.045
2	3.240	1.248	4.488
1	3.831	3.831	6.854

It becomes evident that the TLI requires a significant amount of propellant for direct transfers. It was then looked up whether the launcher used for each satellite, the Falcon Heavy, can bring sufficient payload into a TLI. According to the SpaceX website, Falcon Heavy can bring $26\,700$ kg into geostationary orbit and $16\,800$ kg into Martian orbit [15]. One satellite of the Navigating the Moon constellation will weigh approximately 1000 kg. Assuming from the data provided above that around $20\,000$ kg can be sent into Lunar orbit, the projected six satellites per launch would very easily fit into the launcher. The TLI was therefore neglected.

Lunar Orbit Insertion

Table 6.25 indicates that the ΔV needed to perform the LOI for direct transfers still amounts to a lot. Further research was therefore performed to find a more optimal LOI. A good alternative is the Ballistic Lunar Transfer

[14] https://www.esa.int/Science_Exploration/Space_Science/Juice
[15] https://www.spacex.com/vehicles/falcon-heavy/

(BLT). Such a manoeuvre would take 80 to 130 days without a Lunar fly-by and 110 to 180 days with a Lunar fly-by [96]. The ΔV needed to insert into specific orbits found from the literature are given in Table 6.26.

Table 6.26: ΔV needed for BLT for an elliptical and a high Lunar circular orbit (values extracted from the Ballistic Lunar Transfer Cheat Sheet [96])

		Insertion Manoeuvre (m/s)	Time of flight (days)
Elliptical (100km x 6500km)	Polar	184.2	107.1
	Equatorial	183.8	105.2
High Lunar Orbit Circular (9500 km)	Polar	182.2	94.6
	Equatorial	189.2	106.9

The first notable feature is that insertion into polar or equatorial plane does not require too much variation in ΔV. The final orbits that were selected by the Navigation system in Table 4.2 are four quasi circular orbits with semi-major axis of 5701.2 km, one quasi-circular orbit with semi-major axis of $10\,000$ km and two elliptical orbits with eccentricity 0.6 and semi-major axis of 6541.4 km. The ΔV values found in Table 6.26 were assumed to fit well with the final orbit configuration. Adding an error margin of 5 %, the final Δ V budget was chosen to be $200\,\mathrm{m\,s^{-1}}$ per satellite. A final overview of what could be a BLT with all the Transfer Correction manoeuvres is shown in Figure 6.6.

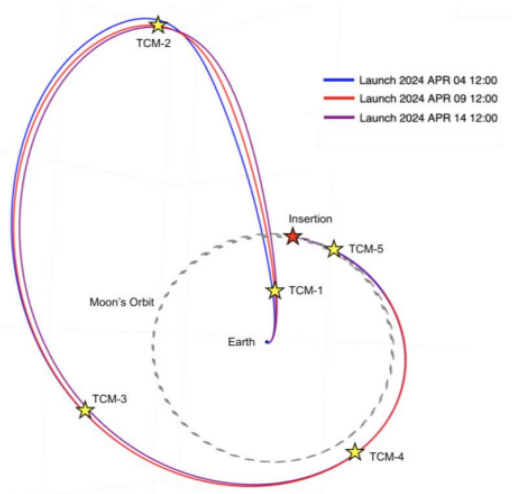

Figure 6.6: Example of Ballistic Lunar Transfer and possible Transfer Correction manoeuvres to perform [96]

Satellite positioning

The next phase that needs to be considered is the positioning of each satellite into their respective position in the orbit. It is assumed that the positioning only has to be analysed for the low inclination and original constellation orbit planes (the reasoning for it can be found in Table 6.20).
The calculations are performed using the amount of change in semi major axis needed to perform the positioning within a certain time range [97].

$$\delta a = \frac{\delta pos_{total} \cdot a}{3\pi} \cdot \frac{T}{T_{total}} \tag{6.12}$$

The satellites that require the most change in semi-major axis are the ones that need the most change in the true anomaly angle. In the case of the original constellation, because of the six satellites in plane for one orbit, the highest change in angle is $180°$. The low inclination orbit only contains 4 satellites, meaning that a 180 degree shift is needed as well. Using a code, the ΔV was obtained for an array of time periods. The results obtained are shown in Figure 6.7a and Figure 6.7b.

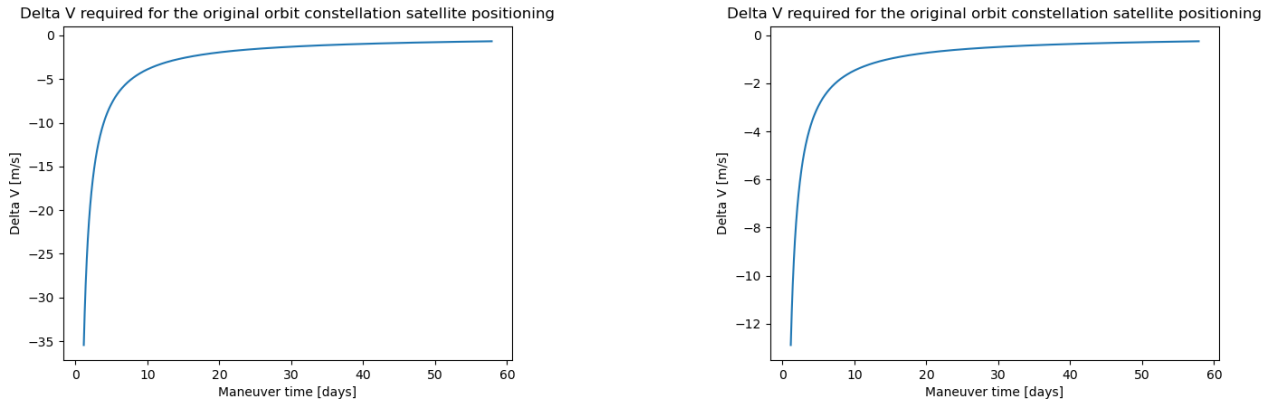

(a) Low inclination positioning ΔV needed

(b) Original orbit positioning ΔV needed

Figure 6.7: Side-by-side plots

By inspection, the point of inflexion approximately occurs at a ΔV of $2\,\mathrm{m\,s^{-1}}$. Adding the $5\,\%$ margin, the final ΔV budget assigned to the satellite positioning for one satellite is $2.1\,\mathrm{m\,s^{-1}}$.

ADCS and orbit maintenance

The ΔV budget for the ADCS system was deduced from the amount of thruster propellant mass needed for the desaturation of the CMG. The calculations for the mass needed can be found in subsection 6.5.6. As for the orbit maintenance, the final ΔV needed per satellite for the entire lifetime was estimated in subsection 4.2.4 to be $63\,\mathrm{m\,s^{-1}}$.

End of life

The last mission phase to be taken into account is the satellite disposal. In this case, two scenarios were considered: crashing on the Moon and removing the satellites out of the Moon's sphere of influence. The reason as to why no graveyard orbit study was included is because no source about it was found. In addition to that, all past Lunar missions that were de-orbited on purpose were crashed onto the Moon. The calculations are performed using the vis-viva equation:

$$\Delta V_{EOL} = V_{orbit} - V_{final} = \sqrt{\mu_{Moon} \cdot \left(\frac{2}{r_{orbit}} - \frac{1}{a_{orbit}}\right)} - \sqrt{\mu_{Moon} \cdot \left(\frac{2}{r_{final}} - \frac{1}{a_{final}}\right)} \tag{6.13}$$

In the case of the Moon crash, r_{orbit} and r_{final} are the apocentre of each orbit as this is how the most efficient manoeuvre can be performed and a_{final} incorporates for the fact that the pericentre becomes the radius of the Moon. In the case of the exit from the Moon's sphere of influence, r_{orbit} and r_{final} are the pericentre of each orbit while a_{final} incorporates for the fact that the apocentre becomes the radius of the Moon's sphere of influence. The results are summarised in Table 6.27.

Table 6.27: ΔV required for both scenarios

EOL procedure	Orbit Constellation	ΔV [m/s]
Crash on the Moon	Original constellation	-292
	Low inclination orbit	-306
	South Pole/North Pole orbit	-67
De-orbit out of Moon	Original constellation	330
	Low inclination orbit	216
	South Pole/North Pole orbit	167

The limiting factors for the crash and de-orbit scenarios respectively come from the low inclination and original constellation orbit. Crashing on the Moon requires slightly less ΔV. Another fact that speaks against the de-orbit from the Moon's sphere of influence is that after it has gone out, it can possibly crash back on Earth or collide with any Earth satellite. The crash on the Moon would occur on a pre-determined location on the Moon and

therefore minimise the chances of colliding with any Lunar user [16]. The crash on the Moon scenario and the $306\,\mathrm{m\,s^{-1}}$ EOL budget were therefore selected for the mission.

6.4.4. Final design

In the final design, all the final parameters and components as well as the green propellant are selected.

Propulsion system selection

Now that green mono-propellants have been selected, the exact chemical needs to be selected. From all the options provided in Table 6.23, the AF-M315E propellant was selected based on the trade-off that can be found in the paper "Modular impulsive green-mono-propellant propulsion system for micro/nano satellites high thrust orbital manoeuvers (MIMPS-G)" [98]:

Propellant	Score per criterion					Overall score (Ranked)
	I_{sp}	ρI_{sp}	T_c	T_F	*Vapor Pressure*	
AF-M315E	10	10	2	10	10	42
HNP225	10	0	20	2	0/Uncertain	32
LMP-103S	10	5	6	3	3.5	27.5
FLP-106	10	7	0	0	9	26

Figure 6.8: Green mono-propellant trade-off

In addition to that, AF-M315E presents the huge asset of having been flight-proven in 2019 during the Green Propellant Infusion Mission (GPIM).

Selected thruster design

As just mentioned above, AF-M315E not only presents the asset of having been flight proven, it also has two thruster designs, GR-1 and GR-22, that were used during the GPIM. As their names indicate, they have an average thrust of respectively $1\,\mathrm{N}$ and $22\,\mathrm{N}$. Their characteristics are found in Table 6.28:

Table 6.28: GR-1 and GR-22 design parameters [99]

	GR-1	**GR-22**
Nozzle Expansion Ratio	100:1	100:1
Valve Power [W]	8.3	15.9
Preheat Power [W]	14.1	37
Feed Pressure (bar)	37.9-6.9	37.9-6.9
Thrust [N]	1.42-0.26	26.9-5.7
Voltage [V]	28	28
Maximum steady-state I_{sp} [s]	231	249

The upper end feed pressure is what was used as the chamber pressure for the tank design iteration in subsection 6.8.3. Another crucial feature to mention is the fact that the I_{sp} does not correspond exactly to the ideal specific impulse of AF-M315E. This is due to losses that occur during the burn. These values were selected for the final ΔV budget iterations. To comply with the redundancies, two GR-22 and twelve GR-1 thrusters were selected. A mass estimation of the valves and filters was also made based on two spacecraft propulsion mass budgets from the "Spacecraft Design and Sizing" reader [34]. Their mass proportion of the total propulsion system mass was found out to be $4.2\,\%$.

Final ΔV budget

The final ΔV and propellant mass budget including the $5\,\%$ margin (see [100]) at each stage is plotted in Table 6.29.

[16] https://lunarresourcesregistry.com/infrastructure/space-debris-graveyard/

Table 6.29: Final mass and ΔV budget.

(a) Final mass budget

Mission phase	Mass [kg]
LOI	82.4
Satellite positioning	0.9
Orbit maintenance	26.4
ADCS desaturation	11.9
EOL	122.5
Fuel mass	244
Propulsion system components	**Mass [kg]**
GR-1 thrusters (12)	3.48
GR-22 thrusters (2)	1.18
Propellant tank	3.5
Valves and Filters	11.1
Total mass	262

(b) Final ΔV budget

Mission phase	ΔV [m/s]
LOI	200
Satellite positioning	2.1
Orbit maintenance	63
ADCS desaturation	30.3
EOL	321.3
Total ΔV	617

Verification & Validation
Only one code was developed for the calculation of the ΔV required for the positioning of the satellites in the orbital plane. Due to the short length of the code, the verification was performed by hand-calculating the ΔV for a given time.

Recommendations
The recommendations provided below include ideas that can be implemented in the short and long term. Out of the four that are given, the two last ones will require more time investment in order for them to be put in practise.

- Compute the exact ΔV that is needed for the LOI into the specified orbits of the constellation.
- Research the possibility of a Lunar graveyard orbit instead of crashing onto the Moon to minimise the risks of colliding with any Lunar user.
- Develop EP such that it requires less power and reduces the size of the batteries and solar arrays.
- Normalise the use of AF-M315E and other green mono-propellants by designing off-the-shelf thrusters that are applicable to a wide range of missions.

6.5. Attitude Determination & Control System

By M. Dinescu

One of the main requirements of the LNSS is to provide full time coverage across the whole Moon. If the spacecrafts are not correctly pointed, the coverage will be heavily affected. Hence, the importance of an effective ADCS arises. This section will deal with the design of the Attitude Determination & Control System (ADCS) ranging from the evaluation of the disturbance environment to the final design and component selection.

6.5.1. Requirements and Design Assumptions

A priori to initiating the ADCS subsystem design, the requirements were determined as a means to guide the design. The majority of them arose as a consequence of the need to counteract the environment or a need to accurately point the laser that will be used for TT&C. All requirements can be seen in Table A.4

Therefore, the most important requirements are the accuracies of attitude determination and attitude control, **NTM-SYS-ADCS-01** and **NTM-SYS-ADCS-02** respectively. Note that the attitude determination is more accurate than the attitude control. This is intentionally chosen to ensure that the determination of the attitude is correct and can comfortably assure that the spacecraft is within the allowable control deviation.

The next subsections will discuss the design of the ADCS. However, in order to do that at this stage, assumptions need to be made. There will be two types of assumptions, ones regarding the disturbance environment and ones regarding the properties of the spacecraft.

Disturbance Environment

In Table 6.30, the assumptions relating to the disturbance torques due to the space environment are stated. One of the natural phenomena that occur in space is omitted due to the fact it will drive the design of the ADCS and hence will be frequently discussed in following sections, namely solar radiation.

Table 6.30: Distubance Environment Assumptions for the ADCS

ID	Assumption	Reasoning
DBA-01	The disturbance torque due to Moon's gravity gradient is negligible and can be considered to be 0.	All spacecraft will be pointed towards the Moon, so the angle between the local vertical and the z-axis of the spacecraft will be 0, meaning the disturbance torque should be zero [101]. Even if the angle is increased by other circumstances, the gravity gradient torque induced will return it to its original attitude.
DBA-02	Disturbance torque due to the magnetic field is negligible and can be considered to be 0.	The Moon lacks a magnetic field, hence the magnetic field strength is equal to 0.[17]
DBA-03	Disturbance torque due to drag is negligible and can be considered to be 0.	The Moon lacks an atmosphere, hence the density is essentially equal to 0.[18]

Preliminary Design Assumptions

These assumptions are made to simplify the design and sizing of the ADCS, but eventually these should be accounted for in future design iterations.

Table 6.31: Distubance Environment Assumptions for the ADCS

ID	Assumption	Reasoning
AA-01	The auxiliary thrusters shall be perfectly placed and that their outputs are all equal.	The effects of thruster misalignment and mismatch will not be computed. This can cause an inaccuracy of 0.1 to 0.5 deg maximum [101]. If the attitude determination requirement lies within this range, then it should be feasible that the LNS can handle the hindrance.
AA-02	The effects of sloshing will not be simulated in this report	This movement of the propellant in the tanks can heavily affect the c.g. and thereby induce internal torques. In the future iterations of propellant tank design, bladders could be added to stabilise the liquid.
AA-03	Rigid appendages shall be assumed. So, oscillations due to equipment on the exterior of the body will not be considered.	The frequency of the oscillations will have to be higher than the natural frequency of the appendages to not cause damage. In addition, magnitudes of thermal shocks due to eclipse emergence will not be designed for yet. This is quite detrimental for a gravity gradient control system, but as will be seen in the following sections this should not be very impacting.
AA-04	Only active control will be considered in the mitigation of disturbance torques.	For a conservative design, active control is implemented in case of failure of gravity gradient control.

With the assumptions clarified, the ADCS design is initialised. As aforementioned, the mission requires the

[17] https://physicalsciences.ucla.edu/ucla-research-discovers-that-full-moon-may-not-be-protected-by-earths-magnetic-field-after-all/#: :text=Earth's%20moon%20has%20no%20atmosphere,encompasses%20the%20full%20moon%20phase.

[18] https://physicalsciences.ucla.edu/ucla-research-discovers-that-full-moon-may-not-be-protected-by-earths-magnetic-field-after-all/#: :text=Earth's%20moon%20has%20no%20atmosphere,encompasses%20the%20full%20moon%20phase.

spacecrafts to be pointing towards the centre of the Moon, indicating that the spacecraft should remain stationary with respect to the body axis and hence no large slew manoeuvres will be performed. However, due to the orientation of some orbits, the solar array will always be parallel to the solar rays from the sun thus not generating any power. In order to account for this, a slow 360° rotation per year of the spacecraft about the z-axis will have to be performed. Additionally, the propulsion subsystem handles the orbit insertion. So the only two control modes are the normal and the acquisition, which occurs right after insertion and in case of emergencies. First, the normal orbit maintenance will be shown.

6.5.2. Quantifying Solar Disturbance Torque

The disturbance from the solar radiation pressure will be the most prominent threat to the stability of the spacecraft and hence will lead the ADCS design and will influence all future calculations. The equation for this can be seen in Equation 6.14 [101]

$$T_s = \frac{F_s}{c} \cdot A_s \cdot (1+q) \cdot \cos(i) \cdot (c_{ps} - c_g) \tag{6.14}$$

Ultimately, the torque depends very highly on the orbit and spacecraft geometry. So to ensure a conservative estimate of the ADCS parameters, the maximum possible solar radiation torque obtained at one point will be assumed to be present during the entire mission. Inspecting Equation 6.14, the solar flux F_s which is approximately $1416\,\mathrm{W\,m^{-2}}$ in the worst case scenario [102], the speed of light, c, and the reflectance factor, q, are all variables that remain unchanged with spacecraft orientation. The other values do change with spacecraft orientation and have to be simulated. From the structures subsystem, it is known that the satellite would be a cuboid or a cylinder, hence the sunlit surface areas, A_s, fell out easily and are used in resultant force and moment calculations in order to uncover the centre of solar pressure, c_{ps}. The reader may ponder why the solar panels are not included in the calculations. The reason is that at every orientation, thanks to the positioning of the solar panels through the centre of mass, the torques from each individual array cancel each other out.

With these values at hand, Equation 6.14 is run through various inclinations to simulate the effect of the orbit on the orientation of the spacecraft with respect to the Sun, of which finally the largest torque is taken. This is reported in a later section, as this value changed multiple times as inputs from other subsystems are iterated.

6.5.3. Pointing Accuracy and Gimbal Effect

It is decided that laser communication will be used between satellites for position determination, in contrast to omnidirectional radio frequency. Hence, the former will become the constraining factor in deciding the pointing accuracy and hence the severity of the mitigation against the disturbance torques.

The satellites will be required to communicate with the nodes adjacent them, both within the orbital plane and out of plane. To distinguish the accuracy requirement, the maximum of the communication distances will be used. The orbits can be seen in Figure 4.4.

The co-planar satellite distances are simple to find. With the Cartesian co-ordinates given from the Navigation subsystem of each spacecraft at each point in time in one orbit, all that is needed is to calculate the Euclidean distance between adjacent nodes. The exception is the elliptical polar orbits as there is a significant amount of time that will be interrupted by the Moon as can be seen. Hence, inter-satellite communication is useless, and they should focus on out of plane communications.

On the other hand, the out of plane distance have an extra layer of complexity deriving from the fact that the orbits are fundamentally different, meaning that their orbital periods also differ. Therefore, two adjacent spacecrafts in separate planes will not remain adjacent. Hence, to account for this, nearly all the distances between each satellite are calculated. By visual inspection of Figure 4.4, it can be seen that the interior satellite constellation will most certainly not hold the largest between plane distance and therefore are not included in the calculations. So, with distances at hand, the minimum distance between a satellite and a plane is taken for each satellite. This guaranteed that each spacecraft is connected only to the closest one in a different plane, which is the goal.

The final step, is to calculate the pointing accuracy. For this, the TT&C subsystem needed to provide laser beam characteristics such as the beam divergence, θ_O, and the transmitter output diameter, D_O. The pointing accuracy is calculated using the following equations[19].

[19] https://www.edmundoptics.eu/knowledge-center/application-notes/lasers/beam-expanders/

$$D_L = D_O + L \cdot \tan(2 \cdot \theta_O) \tag{6.15}$$

$$\theta_P = \pm \arctan\left(\frac{D_L}{2 \cdot L}\right) \tag{6.16}$$

Note that the $\pm$ is used because if the beam direction exceeds the magnitude of this angle, the beam will miss the receiver. The laser the TT&C engineers selected has, by virtue of Equation 6.15 and Equation 6.16, a pointing accuracy of $0.458°$.

Moreover, to remove the need to rotate the spacecraft to each necessary communication point, a gimbal will be installed to the laser. Hence, the spacecraft also needs to counter-act the internal forces from said gimbal. Unfortunately, the full dimensions of the gimbal are not stated in Li et al.[69]. So, as an upper limit approximation, it will be assumed that the gimbal is a cylinder with its diameter equal to its height. Considering only the effect of the gimbal on the spacecraft, conservation of angular momentum can be assumed:

$$H = I_g \cdot \omega_g = I_{s_z} \cdot \omega_s \tag{6.17}$$

Note that the mass moment of inertia around the z-axis of the spacecraft is selected as the structures subsystem placed it on those axes. Leading to the ratio ω_s/ω_g having a value of 0.2×10^{-3}. Adding the further assumption that angular speeds are constant to the fact that they occur in the same time frame means the ratio of rotations is also equal to the aforementioned value. According to the Navigation subsystem, the updating frequency of the laser communication is 1 h 36 min meaning that during that time, the laser communicates with other satellites meaning that as a maximum it will have to rotate $360°$ before returning to the initial satellite communication. So, using the following equation, the amount of momentum storage required to counteract the gimbal manoeuvre can be calculated.

$$h = T \cdot \frac{t}{2} = \frac{4 \cdot \theta \cdot I}{t^2} \cdot \frac{t}{2} \tag{6.18}$$

Here, θ is the spacecraft rotation will be equal to 2 (for the two gimbals) multiplied with $\omega_s/\omega_g \cdot\ 360°$ and I has value of the mass moment of inertia of the spacecraft about the z-axis. In total, for the entire mission, an additional 7.47 mN m s needs to be accounted for each year. When compared to the momentum storage values in the following section is almost negligible and can be easily accounted for in the wheel desaturation process even if several assumptions are taken to reach this conclusion.

6.5.4. Momentum Storage Calculation

The limiting factor of a CMG is its rotational speed and the maximum momentum storage. As previously discussed, there are no large slew manoeuvres much less, ones that need to be performed rapidly. So, the maximum momentum storage will drive the design of the internal actuators.

From the previous sections, it can be seen that the largest threat to the desired zero momentum control method is the continuous solar radiation pressure. So, counteracting the torque is not the satellite's only interest, but ensuring that it remains within the pointing accuracy requirement dictated in subsection 6.5.3. For this, the following approximation is used to calculate the moment storage per orbit needed to sustain the pointing accuracy requirement of the laser [101].

$$h = \frac{T_D}{\theta_a} \cdot \frac{P}{4} \tag{6.19}$$

This approximation assumes that the maximum momentum accumulates in a quarter of the orbit and that it occurs under the worst possible disturbance torque as calculated in a previous section. Plugging in the required values yields a momentum storage of 7.35 N m s per orbit. Using this value for context, the assumptions about previous negligible momentum storage calculations are now justified.

6.5.5. Component Selection

This subsection shall deal with the selection of the ADCS components that will ensure the stability of the satellites during the mission. Firstly, the types of ADCS components will be discussed and which ones are useful for the mission. Next, a trade-off will be performed between off-the-shelf components. Lastly, the final components and their characteristics will be presented.

Types of Sensors and Actuators
The selection of components has always been an intricate process as chosen components must adhere to a certain quality level for the entirety of the mission. Fortunately, using the pointing accuracy requirements and the mission environment, some types of components can be dismissed instantly.

Firstly, on the topic of sensors, many of the sensors do not have the necessary pointing accuracy requirement to fulfil the mission needs. For example, magnetometers have an accuracy range of 0.5° - 3° [101]. This is not even considering the fact the Moon has no magnetic sphere. There exist horizon sensors that do fall in the accuracy range however, they are generally, heavier and more power consumptive than other sensors. That leaves sun sensors, star sensors and gyroscopes. These are all feasible options and considering that the mission is one that requires a very stable and reliable ADCS performance, all shall be included in the final design.

The viable options for actuators are the three internal actuators, reaction wheels, momentum wheels or CMGs and the external actuators propellant thrusters. As a zero momentum control method is selected and proven necessary, combined with the 0.458° the thruster can be dismissed and due to their low accuracy performance. Additionally, it reduces the amount of propellant on board, which benefits sustainability. While both wheels and the CMG can achieve zero momentum, CMG has the advantage of having a gimbal that can rotate the wheel in all directions. Furthermore, seeing as the main opposition to the spacecraft attitude control is the disturbance torque which changes the directional impact with different orbits and with time, it is be wise to make use of the CMG's manoeuvrability. Hence, reaction wheels and momentum wheels are both dismissed. Moreover, the auxiliary thrusters will still be present, but only for the purpose of desaturating the wheel. The design will be discussed in their own section but the actual selection will be done in the propulsion section.

Component Trade-off
Now with the ADCS component categories selected it is time to select the final components. For CMG it is relatively straight forward, as generally the lower the momentum storage the lower the other properties. Hence, the selected CMG, the CMG8 from Blue Canyon Technologies [20]. is one that can fully encapsulate the momentum storage needs while minimising the other properties.

All that remains is the sensor selection. Here the selection process is a bit more intricate as parameters varied for all types of sensors. The method used is very similar to the trade off done in the Midterm report [5]. Weights are assigned to each parameter out of 100 with the most influential receiving the largest cut. Then each sensor will be scored out of 5 on each parameter. The two values are multiplied and summed up to gain the final score. The higher the score the more suitable the sensor is.

The first trade-off will be for the star sensors. The trade-off can be seen below in Table 6.32. It can be seen that the highest rated parameters are accuracy, update frequency and Dimensions. The first two are expectantly highly rated as they are values directed related to a requirement and because star sensor is planned to be main absolute attitude determiner. So, the better the score the larger the margin on satisfying this requirement. Dimensions is highly rated due to the star sensors weakness. If too many solar rays enter the star sensor the images it captures will be blurry and inaccurate. Hence the large the baffle compared to the rest of the star tracker the more optimal the sun exclusion angle is meaning that star tracker is less likely to be affected by the sun [103]. Seeing as this parameter actually improves the design and does not just meet a requirement, it is designated the largest weight. Based on Table 6.32, the selected star sensor is VST-68M but not by a large margin. The details of the selected components will be discussed in the following subsection.

Table 6.32: Trade-off Star sensors

	Accuracy 25	**Update frequency** 25	**FOV** 5	**Power** 5	**Dimensions** 35	**Mass** 5	**Total** 100
Sagitta	5	3	4	3	3	2	70
Cubestar	2	1	4	4	1	4	34
VST-68M	4	3	2	2	5	1	75

The next sensor trade-off is for the sun sensors below in Table 6.33. The trade criteria here can be simply explained. Accuracy is related to its respective requirement. The Field of View(FOV) is important as it means it allows a larger view angle and more sun rays can be taken into account. But no matter the FOV, the sun

[20] https://satsearch.co/products/bluecanyontech-cmg-8

sensors should be able to determine the attitude, thus power and mass are deemed more critical due to their effects on other subsystems and the spacecraft design as a whole. The final selected sun sensor is the mini FSS. The full details will be given later, but it is worth mentioning that while for most of the other sun sensors, the update frequency is not available, for mini FSS it is, and it is higher than the 1 Hz requirement.

Table 6.33: Trade-off Sun sensors

	Accuracy 40	**FOV** 10	**Power** 25	**Mass** 25	**Total** 100
CMOS	3	5	1	4	59
FSS	4	2	1	1	46
SSOC	2	2	3	4	55
Cubesense	3	4	1	4	57
mini FSS	3	4	5	3	72

The final trade-off to be done is for the gyroscopes. As can be seen in Table 6.34, the largest weights are assigned to bias stability, drift, and frequency. Gyroscopes measure relative attitude to a certain reference frame. This measurement over time deviates from the true value. Considering our long mission lifetime of 12 years and perhaps even longer, if the spacecraft would allow it, the bias stability and the drift show how quickly the gyroscope deteriorates. Lastly, the update frequency is important for the same reasons mentioned before. However, this value is larger by a factor of at least 100 than for the other sensors. So, the requirement is no longer limiting, and the weight is just based on performance, hence the lower weight compared to the first two. The selected is sensor here is the ring laser gyroscope GG1320AN.

Table 6.34: Trade-off gyroscopes

	Mass 10	**Bias Stability** 30	**Drift** 30	**Power** 10	**Frequency** 20	**Total** 100
GG1320AN	1	5	4	3	5	82
ADXR2646	2	3	5	3	1	48
GSFOG70A	5	1	1	5	4	60
GSFOG60A	3	2	2	1	2	40

Final Selection

With trade-offs completed, the final components are selected. The properties of the chosen star sensor are shown Table 6.35. As can be seen the accuracy is far better than **NTM-SYS-ADCS-01**. The update frequency also exceeds its requirement, **NTM-SYS-ADCS-03**. The same can be said for the sun sensor in Table 6.36.

Table 6.35: Chosen star sensor.

	Accuracy [○]	**Update frequency [Hz]**	**FOV [○]**	**Power [W]**	**Dimensions [mm]**	**Mass [kg]**
VST-68M [21]	0.00139	5	14x14	3	60x60x138	0.47

Table 6.36: Chosen sun sensor.

	Accuracy [○]	**Update frequency [Hz]**	**FOV [○]**	**Power [W]**	**Dimensions [mm]**	**Mass [kg]**
mini FSS [22]	0.2	2	172x172	0 (passive)	50x46x17	0.05

Table 6.37 shows the chosen ring laser gyroscope for the spacecraft. The most desirable traits are the low bias stability and drift rate along with the very large frequency.

[21] https://www.vectronic-aerospace.com/wp-content/uploads/2020/03/VAS-VST-68M68M-DS2.pdf
[22] https://satsearch.co/products/bradford-mini-fine-sun-sensor

Table 6.37: Chosen gyroscope.

Component	Mass[kg]	Bias Stability[deg/h]	Drift [deg/h$^{1/2}$]	Frequency [Hz]	Power [W]
GG1320AN [23]	0.454	0.0035	0.0035	2000-5000	1.6

Table 6.38 shows the chosen CMG and its characteristics with the most desirable one being the momentum storage which will be further analysed in the next section.

Table 6.38: Chosen CMG.

Component	Mass[kg]	Momentum [Nms]	Torque [Nm]	Power [W]
CMG8 [24]	10	8	8	35

6.5.6. Desaturation

With the maximum storage of 8 N m s and the GR-1 thruster determined, the design of the desaturation phase can be done.

The main occupation of the CMG will be to account for the 7.35 N m s from the disturbance torques. There are other influences, but they are relativily low. Even so, a small margin of 5 % shall be added to account for them. This small margin is added even though approximations are present, but they are also conservative. This raises the momentum storage per orbit to 7.72 N m s which is almost the entire momentum storage capacity of the CMG8, leading to the decision that the wheel will be desaturated every completed orbit. In addition, the GR-1 are to be throttled down to at least 80 %. With this information, the thrust per actuator and pulse time can be iterated over the following equation [101].

$$F_T = \frac{h}{n \cdot t \cdot L} \tag{6.20}$$

There are 12 auxiliary thrusters in total, but not all thrusters will be simultaneously functioning during normal mode. The minimum amount of thrusters fired will be two to ensure that only a pure torque occurs. This leads to a burn times of 5 s per orbit with a thrust of 0.735 N per thruster. If Equation 6.20 is merged with the following equation:

$$F_T = \dot{m} \cdot I_{sp} \cdot g_0 = \frac{\Delta M_p}{\Delta t} \cdot I_{sp} \cdot g_0 \tag{6.21}$$

It is then possible to calculate the propellant used per desaturation cycle. If Δt is let to be the pulse time, t, the following equation is obtained.

$$M_p = \frac{h}{L \cdot I_{sp} \cdot g_0} \tag{6.22}$$

Using information from the propulsion subsystem, the propellant mass per desaturation cycle is 2.82 g. Multiplying this with the number of orbits yield the total propellant mass: 11.88 kg. This value will be further used for ΔV calculations for the propulsion subsystems and for the structures susbsystem.

6.5.7. Acquisition & Slew

So far, only the normal mode is discussed. But in order for this to function as intended, firstly the spacecraft has to be initially orientated correctly and secondly, as mentioned before, the spacecraft solar arrays have to point towards the sun so that no power loss is experienced.

Unfortunately, there is no data regarding the orientation of the satellites when they are ejected from the launcher or when they reach the final orbit. So, once again, the worst case scenario will be assumed. Specifically, the spacecraft will have to perform three $180°$ slews about each axis. The equation to compute the momentum change is the same as Equation 6.18. According to section 6.4, the ballistic trans-lunar injection should have a duration longer than a day, hence there is a large time-frame in which to perform the manoeuvres. However, once again to be conservative, the time taken to perform the slew will accomplish a momentum charge of at

[23] https://aerospace.honeywell.com/us/en/products-and-services/product/hardware-and-systems/sensors/gg1320an-digital-ring-laser-gyroscope

[24] https://www.satnow.com/products/control-moment-gyroscopes/blue-canyon-technologies/43-1186-cmg8

least 0.8 of the wheel's total momentum storage. This results in 2 manoeuvres taking 400 s and the other lasting 120 s. The wheel will also have to be desaturated after each rotation, which leads to an additional 3.84 g.

The spin required to keep the solar arrays oriented correctly is also calculated using Equation 6.18. However, θ is now equal to 360 increasing the moment change, but the time duration is now 1 year. This leads to a momentum change of approximately 0.168 mN m s. In the scope of the 12-year mission lifetime, this is a very insignificant momentum storage, as it only accounts for 0.025 % of the total capability of the CMG.

6.5.8. Iteration Process

Unlike the other subsystems, the ADCS design did not have reiterations in the form of creating an initial design and then developing it further by removing it further and narrowing the detail of design. Rather, the entire ADCS sizing is prepared and then the inputs from other subsystems re-iterated, and changes to the design process are made to meet their needs. For example, to begin with, the dimensions of the spacecraft are assumed to be much larger in altitude, namely 3 x 2 x 1.5 m. This lead to a large disturbance torque leading to an even larger momentum storage, influencing the ADCS design team to select an larger CMG initial, namely the CMG 75-75 S [25]. So, the values for the initial design and the final design can be found below in.

Table 6.39: Initial and Final values.

	Accuracy [∘]	**Momentum [Nms]**	**Disturbance torque[Nm]**	**Dimensions [m]**	**Semi-major axis[km]**
Initial	3.25	72.88	4.805×10^{-6}	2x1.5x3	24500
Final	0.458	7.35	2.520×10^{-6}	1x1x1	10000

6.5.9. Final Design

This subsection presents the final design configuration for the ADCS subsystem. Firstly, all the points that were discussed beforehand will be summarised including an overview of the components. Lastly, the verification and validation done for this subsystsem will be described.

Summary

With all the disturbance torque quantification finished and the components selected. The final design can be summarised. The LNSS satellites will have a pointing accuracy of 0.458° as according to. This leads the ADCS team to selecting a zero momentum control method with a CMG for additional manoeuvrability. In addition, there will be GR-1 auxiliary thrusters will be used for desaturation.

The sensors present will be star sensors, sun sensors and ring laser gyroscopes. The structures subsystem will be communicated that they need to place the sensors in a configuration such that attitude determination is possible and that redundancy is effective. So, for the star sensors, it would be optimal to have them on the side facing away from the Moon such that reflected sunlight is not a problem, and then they should all be facing away from each other looking at different planes. Additionally, they are recommended to be inclined at a small angle to the side (smaller than 30°) in order to ensure that no more than 2 sensors can be blinded by solar arrays. The sun sensors will be placed in a configuration where there are 3 on each side except the side facing the Moon, as it they constantly face away from the sun there, and they are at different orientations to measure different planes. Lastly, the gyroscopes should be placed inside the spacecraft such that their axis of measurements are not parallel to one another.

Table 6.40: Summary of all the designed and selected components

Component	**amount**	**Total Mass [kg]**	**Total Power [W]**
CMG	2	20	70
Star sensor	4	1.88	12
Sun sensor	15	0.75	0
Gyroscopes	4	1.82	1.88

Verification & Validation

There are two codes, one that calculated the pointing accuracy requirement based on orbits provided by Navigation and laser characteristics provided by TT&C, and the other which calculated disturbance torques. For the

[25] https://www.satnow.com/products/control-moment-gyroscopes/airbus/43-1213-cmg-75-75-s

former, large data sets had to be handled so for verification, there are unit tests that checked the size of arrays and ensured the correct size. In addition, the code works with distances meaning, so, a unit test that checks that values are positive is also implemented. This is also implemented for the other code, as the disturbance torque in equations is positive. Lastly, for both codes, verification by comparing to hand calculations is done, and extreme value tests are done for several parameters like dimensions, disturbance torques, etc. For validation, sensitivity analysis are done for several parameters. Additionally, many equations were incorporated from the SMAD [101]. So, hand calculations were done and compared to the results of the code. Lastly, the SMAD has some example calculations for other spacecrafts, so the disturbance torques were compared in order to gage whether the orde of magnitude was correct. All tests are passed.

6.5.10. Recommendations

The scope of the design of this section is to ensure that the satellite could endure the harsh space environment while meeting high level requirements, which has been achieved through a conservative design process. However, for future iterations of the design, improvements can be made.

- A functional control algorithm containing all the sensor, actuator, and disturbance dynamics should be created and simulated to see if the pointing accuracy can still be sustained.
- A vibrational analysis should be performed. While the sensors are selected to ensure pointing accuracy requirements, vibrations can alter the quality of the detection and hence should be assessed.
- While the torque from gravity gradient is zero, there is a possibility that slow oscillation occurs about the local vertical. So, this needs to be checked for component performance.
- The assumptions relating to internal disturbance torques (sloshing etc.) should be analysed in higher depth to quantifying their effect on the stability of the spacecraft.
- While the design was conservative and margins were included, it did not greatly account for the emergency mode of the ADCS. In some cases, acquisition mode and safe mode can be considered to be the same[101]. But given the zero momentum state of the satellite, the ADCS team recommends extra research is done in developing the safe mode further.

6.6. Electrical Power System

Performed by L.D. van der Peet, M. Vereycken. Written by L.D. van der Peet

The EPS is an intricate part of a spacecraft, with nearly all components of the system requiring power. It serves the role of generating, distributing and managing the power. To ensure sufficient power is supplied for nominal operations of the components, the solar array and battery shall be sized according to the system needs. Sizing is an iterative process, starting from requirements and assumptions which will lead to a more specific design.

6.6.1. Requirements and Design Assumptions

Requirements and assumptions form the basis of the EPS design. From results, requirements can be updated to be more specific. In Appendix A Table A.5, the requirements set for the final design are presented.

Due to interdependencies, design of the EPS is a complex process. To reduce complexity, assumptions are used. Assumptions may lead to a simplified approach, but will thereby introduce inaccuracies. Therefore, they shall be carefully considered and updated where necessary. Some assumptions that hold for the final design are listed in Table 6.41 below. All the computations performed for the EPS can be found in GitHub-EPS.

Table 6.41: Assumptions for the EPS

ID	Assumption	Reasoning
PA-01	Umbra and penumbra are modelled as full eclipse, meaning that no power is generated by solar arrays in these regions.	A worse scenario is considered, where the solar arrays can not provide any power. Thus, the spacecraft is relying on batteries. thereby taking a conservative approach in sizing the batteries.
PA-02	Solar arrays are constantly oriented perpendicular to incoming solar rays.	The solar array can be rotated towards the incoming solar rays.
PA-03	Yearly degradation of the solar cells is $3\,\%$.	Lithium-ion cells have a degradation between 2 and $3\,\%$ [104]. The worst case is considered.
PA-04	The substrate has an $85\,\%$ fill ratio.	SpaceTech has exceptional fill ratio performance[26].
PA-05	The longest eclipse is the sum of Earth-caused and Moon-caused eclipse.	The orbital periods of satellites is shorter than the eclipse time, thus only two eclipses may occur consecutively.
PA-06	The solar flux is constant, at worst case (furthest from the Moon).	This is a conservative approach, ensuring that the power demand is always met.
PA-07	Radiation does not influence the EPS.	Protective films will nullify the effect of space radiation.
PA-09	A margin of $20\,\%$ must be added to the power budget.	Following from ESA [100], a margin is applied to the total power budget.
PA-10	Orbits with an eccentricity <0.1 are modelled as circular.	The difference between elliptical and circular are minor in this case, and circular is a conservative approach.

6.6.2. Stage 1 Design

In the first stage, not all components have been selected. Therefore, sizing of the solar array and battery are based on the initial estimates obtained in section 5.4. The required power at EOL equals $1664\,\text{W}$, which translates to a Begin of Life (BOL) power of $2398.2\,\text{W}$. This power must be provided to the system at any point of the orbit. Since, solar arrays will be used, batteries must be sized corresponding to the power requirement. First, the eclipse time shall be computed, after which an estimate is made for the battery capacity. Finally, the solar array has a required size to provide the power during non eclipse time is computed.

Eclipse Time

Eclipse time is the time spent in the umbra or penumbra of the orbit, also known as the shadow part. During this time, power generation by solar arrays is hindered, hence relying on other power sources. Lunar missions have the downside of having two occulting bodies, Earth, and the Moon, as seen in Figure 6.9. This will influence the length of the eclipse time. When considering the worst case scenario, the satellite exits the eclipse caused by the Moon, and immediately enters the eclipse caused by Earth. Fortunately, due to the long orbital period, the Moon is only in Earth's umbra 2 to 5 times per year[27]. Thus, the worst case eclipse does not occur frequently.

[27] https://eclipse.gsfc.nasa.gov/LEdecade/LEdecade2031.html

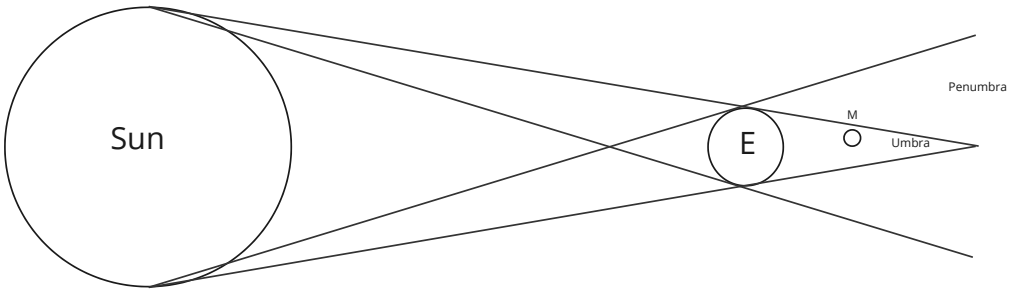

Figure 6.9: Eclipse of the Moon due to Earth

Even though most orbits are assumed to be circular, the satellite around the Moon with a semi-major axis of 6541.4 km, which has an eccentricity of 0.6. This eclipse time must be computed with a different method. NASA developed Equation 6.23 to calculate the eclipse factor (μ_0) of an elliptical orbit [105].

$$\mu_0 = \frac{e \cdot (1-e^2)^{\frac{1}{2}}}{2\pi} \cdot \left[\frac{\sin(\theta_1)}{1 + e \cdot \cos(\theta_1)} - \frac{\sin(\theta_2}{1 + e \cdot \cos(\theta_2)} \right] + \frac{1}{\pi} \cdot \left[\arctan\left(\frac{(1-e) \cdot \tan(\frac{\theta_2}{2})}{(1-e^2)(\frac{1}{2})} \right) - \arctan\left(\frac{(1-e) \cdot \tan(\frac{\theta_1}{2})}{(1-e^2)(\frac{1}{2})} \right) \right] \tag{6.23}$$

The two angles in Equation 6.23 represent the angles from semi-major axis to the point where the orbit enters and leaves the eclipse (θ_2 and θ_1 respectively). The eclipse factor is then multiplied with the orbital period, to arrive at the total eclipse time for an elliptical orbit. This is shown in Figure 6.10

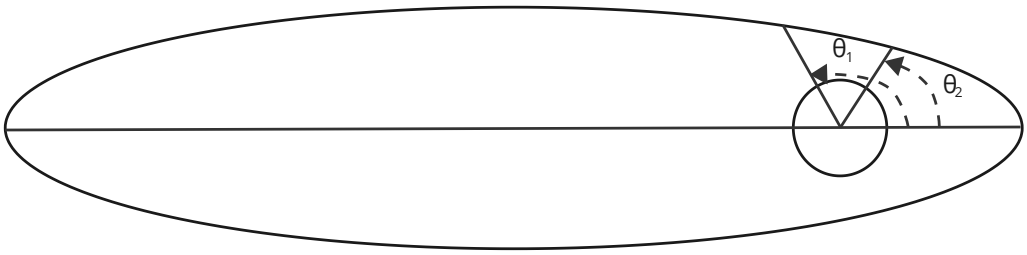

Figure 6.10: Sketch showing the angles θ_1 and θ_2

To go from eclipse parameter to eclipse time, it is multiplied by the orbital period. To compute the eclipse time of orbits with an eccentricity <0.1, a circular orbit is assumed. The results for each individual orbit and their parameters can be found in Table 6.42.

Table 6.42: Orbital parameters and eclipse time of the Moon and its constellation

Orbit	Semi-Major Axis [km]	Eccentricity	Orbital Period [h]	Orbital Cycles in 12 years	Eclipse Time [h]
Moon around Earth	384400	0.0549	658.85	160	4.082
Satellite around Moon	5701.2	0.002	10.73	9797	0.956
Satellite around Moon	10000	0.038	24.93	4218	1.271
Satellite around Moon	6541.4	0.6	13.19	7972	0.927

The eclipse time of the Moon due to the Earth is first computed using its orbital parameters, and leads to a Moon-Earth eclipse time of $14\,695$ s or 4.082 h. This can also be repeated for the Satellite-Moon eclipse. Using the orbital parameters from Table 6.42, the longest eclipse time equals 1.927×10^4 s or 5.353 h.

Battery Sizing

During deployment phase, the solar arrays will be folded inwards. When in folded configuration, no power is generated. The power for start-up procedures must therefore come from a different source. Additionally, an inherent flaw of solar arrays is the inability to generate power without direct exposure to sunlight. When in eclipse, the solar arrays can therefore not provide power to the spacecraft. Both limitations are resolved with batteries. Hence, the two important functions can be identified for the battery during operation of the mission are: the battery shall provide the power required to deploy the spacecraft after launch, and the battery shall provide power to the components of the spacecraft during eclipse.

To start up the system, solar arrays must first be deployed. After solar array deployment, power is provided by the solar arrays and the start-up procedure can continue without batteries. This initial energy is insignificant compared to energy during eclipse. Thus, sizing of the battery shall solely be focused on the capacity needed to provide power to the system during eclipse. The capacity is based on the initial power estimate from section 5.4, and is multiplied with the estimated worst case eclipse time. However, there is a difference between power in and out of eclipse, which is charging the batteries and generating or providing heat. Thus, after sizing the batteries, the solar array requirements must be updated in order to charge the battery.

M. Patel [106] proposed Equation 6.24 to compute the capacity of a battery cell. This equation considers several aspects affecting the capacity of the battery, and is therefore used for a detailed battery design. Additionally, Equation 6.24 is redundant for single cell failure, thus introducing a safety margin.

$$Ah_b = \frac{P_e \cdot t_e}{N_b \cdot \eta_{dis} \cdot \{(N_c - 1) \cdot V_{cdis} - V_d - V_{hdis}\} \cdot DOD} \tag{6.24}$$

In Equation 6.24 above, the result is the capacity per cell in A h. The parameters are: P_e; the eclipse power in W, t_e; the eclipse time in h, N_b; the number of batteries in parallel, η_{dis}; the discharge efficiency, N_c; the number of cells in series in the battery, V_{cdis}; the voltage per cell in discharge, V_d; the voltage drop when a cell fails, V_{hdis}; voltage drop in harness from battery to PRU, and DOD; the depth of discharge.

The capacity of the battery for initial sizing is based on power needs. With an eclipse time of 5.036 h and initial power budget of 2266.8 W, the minimum capacity shall be above 11 kW h. Based on this need, a preliminary battery is selected. The battery used is the Saft VL51ES[28], and its properties are listed in Table 6.43 below.

Table 6.43: Properties of Saft VL51ES battery cells

Parameters	Height	Diameter	Capacity	Mass	V_{cdis}
Value	222 mm	54 mm	51 A h	1.08 kg	3.5 V

Yet, some values to perform Equation 6.24 are unknown. These remaining variables are extracted from research. For the depth of discharge, with the largest number of cycles being approximately $10\,000$ (from Table 6.42), a DOD of 42 % shall be used [107]. To obtain a value for V_d, the assumption to use Schottky diodes[29] is made. These have a V_d ranging from 0.15 V to 0.45 V.

The goal of battery sizing is to design the lowest possible mass and volume, while still adhering to the capacity requirement. To achieve this goal, the lowest number of cells shall be used. The first stage design results in a battery with parameters as listed in Table 6.44.

Table 6.44: Parameters for the battery in first stage design

Parameters	Capacity	Number of cells	Mass	Volume
Value	2.876×10^4 W h	162	169.55 kg	95.23 L

The mass of the battery is more than 10 % of the estimated spacecraft mass. This is more than budgeted, leading to a snowball effect in the design. To reduce this mass, other configurations shall be considered in the optimisation process.

[28] https://www.saft.com/products-solutions/products/vl51es-battery

[29] https://www.electronicshub.org/schottky-diode-working-characteristics-applications/

Solar Array Sizing
For a spacecraft to operate over an extended period of time, power must be generated. There are two widely used options to generate power; either solar arrays or Radioisotope Thermoelectric Generators (RTGs).

Solar arrays convert the solar flux to useful electrical energy via photovoltaic cells. RTGs on the other hand convert heat generated by the radioactive decay of a radioisotope into useful electrical energy. The advantage of using RTGs is that eclipse does not impact the generation of power, which is the case for solar arrays (see eclipse time in subsection 6.6.2). However, the radioactive nature of the isotopes are not in line with the environmental sustainability considerations of the mission in anticipation of human Lunar missions[30]. Thus, the use of RTGs is not desirable for the mission and solar arrays shall be used.

As aforementioned, batteries shall be used to cover the power needs of the spacecraft during eclipse. In addition to the power needs of the system in operation, the battery must also be charged. Charging of the battery can only be done during eclipse time, meaning that during daytime the generated power must be higher compared to eclipse.

Since the power required at EOL is known, the solar arrays can be designed accordingly. However, due to degradation of the solar arrays, the EOL power must first be converted to Begin of Life (BOL). For this, a yearly degradation of $3\,\%$ is assumed [104], by which a BOL power of $2266.8\,\mathrm{W}$ is computed.

The solar cells initially used for the design are Inverted Metamorphic Multi-junction (IMM-α) solar cells. This type of solar cell, developed by SolAero[31], has a BOL efficiency of $32\,\%$ and offers a less costly and more efficient solution than most other solar cells on the market [108]. Moreover, the technology has been validated in missions, leading to a Technology Readiness Level (TRL) of 9.

Another aspect considered in the sizing of the solar array area is the solar flux received perpendicular to the solar array. Around the Moon, the solar flux is approximately $1360\,\mathrm{W\,m^{-2}}$ [102]. In reality, this can vary with $\pm$ $50\,\mathrm{W\,m^{-2}}$, thus the worst case scenario entails a solar flux of $1310\,\mathrm{W\,m^{-2}}$. Additionally, the Power Conditioning and Distribution Unit (PCDU), which converts raw generated power into regulated stable power and distributes the power to components of the system, has losses, which will be covered by a margin of $20\,\%$.

The combination of all these characteristics are taken into account when sizing the solar array, resulting in a first solar array size of $7.1\,\mathrm{m^2}$. Taking an area density of $2\,\mathrm{kg\,m^{-2}}$ of the cells and $3\,\mathrm{kg\,m^{-2}}$ for the solar array substrate[32] for a total of $5\,\mathrm{kg\,m^{-2}}$. The total mass of the solar arrays then equals $35.5\,\mathrm{kg}$.

6.6.3. Iterations
After performing the first stage design for each subsystem and selecting components, a new power budget is produced. This budget contains more representative values and allow for optimisation. After sizing the battery and solar array, final components are selected for distributing power to the system.

Revised Power Budget
After the selection of suited components in the first stage design, revised power budgets can be generated. The power budget is split up into two different budgets. Table 6.45 shows the EOL power required during daytime, which is used to size the solar arrays, whereas Table 6.46 depicts the EOL power required during eclipse, which is used to size the batteries.

[30] https://ntrs.nasa.gov/api/citations/20205004953/downloads/IAPG%20RECWG%20NASA%20July%202020.pdf
[31] https://www.rocketlabusa.com/assets/Uploads/RL-SolAero-Data-Sheet-IMM-Alpha.pdf
[32] https://spacetech-i.com/fileadmin/user_upload/Equipment/Solar_Arrays/STI-DS-03-20229-191_Datasheet_SolarArrays_2022-9-28_final_web.pdf

Table 6.45: Final power budget for non-eclipse EOL

Subsystem	Power [W]	Percentage
ADCS	83.88	6.27 %
CDH	38	2.84 %
Navigation	210	15.69 %
Propulsion	304.6	22.75 %
TT&C	95.2	7.11 %
TCS	330	24.65 %
EPS	277	20.69 %
Total	1338.68	

Table 6.46: Final power budget during eclipse EOL

Subsystem	Power [W]	Percentage
ADCS	83.88	7.90 %
CDH	38	3.58 %
Navigation	210	19.78 %
Propulsion	304.6	28.69 %
TT&C	95.2	8.97 %
TCS	30	2.83 %
Total	761.68	

The differences between day-time and eclipse originate in the EPS and TCS. During day-time, the solar array shall charge the batteries such that power is provided during eclipse. Moreover, at EOL, the surplus of power generated has drastically decreased due to the 3 % degradation per year. Consequently, the power dissipated decreases, leading to a colder spacecraft. Heaters are used to achieve the operating temperature range.

The margin of 20 % is yet to be added to Table 6.45 and Table 6.46. Therefore, final values of 1605.6 W for day-time and 914 W during eclipse are used to size the batteries and solar array.

Battery Sizing

The first design stage only considered one battery. However, the frequency of the eclipse due to the Moon and due to the Earth differ significantly. The number of discharge cycles influences the DOD. The more cycles, the lower the DOD. Therefore, by splitting the batteries may lead to a lighter and smaller design. The first battery is used for Moon eclipses, meaning that it shall endure around 10 000 cycles, which in turn results in a DOD of 40 %. The second battery is used for Earth eclipses, which have a longer duration, but have a lower frequency. The DOD may in this case be increased to 80 %. The concept of two batteries is evaluated and compared to the results of a singular battery, taking mass and volume as deciding factors.

Taking the power from Table 6.46, the results for the dual battery configuration can be found in Table 6.47 and Table 6.48.

Table 6.47: Size of the first battery, with a 40 % DOD

Battery 1	Values
Cells	14
Total capacity	2366.1 W h
Battery mass	29.64 kg
Battery volume	7.67 L

Table 6.48: Size of the second battery with an 80 % DOD

Battery 2	Value
Cells	31
Total capacity	4832.5 W h
Battery mass	48 kg
Battery volume	16.3 L

Notice that the mass has already decreased significantly as compared to Table 6.44. The total mass reduced from 169.55 kg to 77.64 kg. The results of using a singular battery can be seen in Table 6.49.

Table 6.49: Size of using a singular battery with a 40 % DOD

Singular Battery	Value
Cells	66
Total capacity	11 701.7 W h
Battery mass	85.8 kg
Battery volume	34.1 L

The singular battery mass and volume are higher than using the dual batteries. With the increase in specific performance, the dual battery configuration is preferred. Thus, two batteries are used in the final design.

Solar Array Sizing

Due to the high temperature differences in space, the IMM-α solar cells are no longer sufficient. New solar cells are selected, which can operate in the environment around the Moon. Recently, ESA has developed new solar cells, called Quadruple Junction Solar Cell 4G32C[33], for their JUICE mission[34]. These solar cells shall survive

[33] https://www.azurspace.com/images/0005979-01-01_DB_4G32C_Advanced.pdf

[34] https://www.esa.int/Science_Exploration/Space_Science/Juice

the rough environments and rapid temperature changes it is subjected to. Its efficiency is similar to IMM-α at $32\,\%$ for BOL, and it offers the best performance in its class. Since the launch of JUICE, the corresponding TRL is 9. Thus, no additional validation is required before implementation.

The only parameter that changes is the specific mass. It goes from $2.09\,\mathrm{kg\,m^{-2}}$ to $0.89\,\mathrm{kg\,m^{-2}}$ for the solar cells. Together with the substrate, the total specific mass shall be around $4\,\mathrm{kg\,m^{-2}}$ [35]. The day-time power requirement is $1338.68\,\mathrm{W}$, which equates to a BOL power of $1929\,\mathrm{W}$. The final solar array area is computed to be $6.8\,\mathrm{m^2}$, and has a mass of $27.2\,\mathrm{kg}$.

6.6.4. Final Design

With the final sizing of the solar array and batteries, integral components of the EPS can be selected. These components are selected based on the mass added and required performance.

Power Conditioning and Distribution Unit (PCDU)

Before the power is distributed to the system, it is first converted to appropriate voltage levels, usually by a DC-DC converter. After conversion, the power is directed to the components. This process is regulated by the PCDU. The PCDU is selected based on the power to be distributed and the possibility to dissipate additional power via shunts. Out of the available PCDUs, one from Terma is selected. Their collaboration with ESA for Galileo[36], and in orbit validation of their PCDU, leads to a desirable status. Their Galileo OIV model can handle up to $2000\,\mathrm{W}$, and has a mass of $18.2\,\mathrm{kg}$.

Cable Harness

The cable harness is the physical connection between the PCDU and the individual components. It serves the purpose of establishing electrical connections and can thereby be considered the veins of the system [109]. The cable harness is highly dependent on the system design. Voltages delivered to components are classified into four groups. The lowest voltage is $5\,\mathrm{V}$, which is for sensors. A higher voltage of $12\,\mathrm{V}$ is required for larger components such as the radiator and transceivers. $28\,\mathrm{V}$ is the high range for the spacecraft components and is required for heaters and computations. Finally, the 'HV' cables indicate high voltage, for power delivering components. The voltage ratings for components and their connection to the power grid are shown in Figure 6.11. Without knowing the lengths, thicknesses, and materials of the connections, the mass can not be determined. That is why a mass of $100\,\mathrm{kg}$ is taken as a conservative estimate, following from literature [109].

[35] https://spacetech-i.com/fileadmin/user_upload/Equipment/Solar_Arrays/STI-DS-03-20229-191_Datasheet_SolarArrays_2022-9-28_final_web.pdf

[36] https://www.terma.com/markets/space/space-segment/

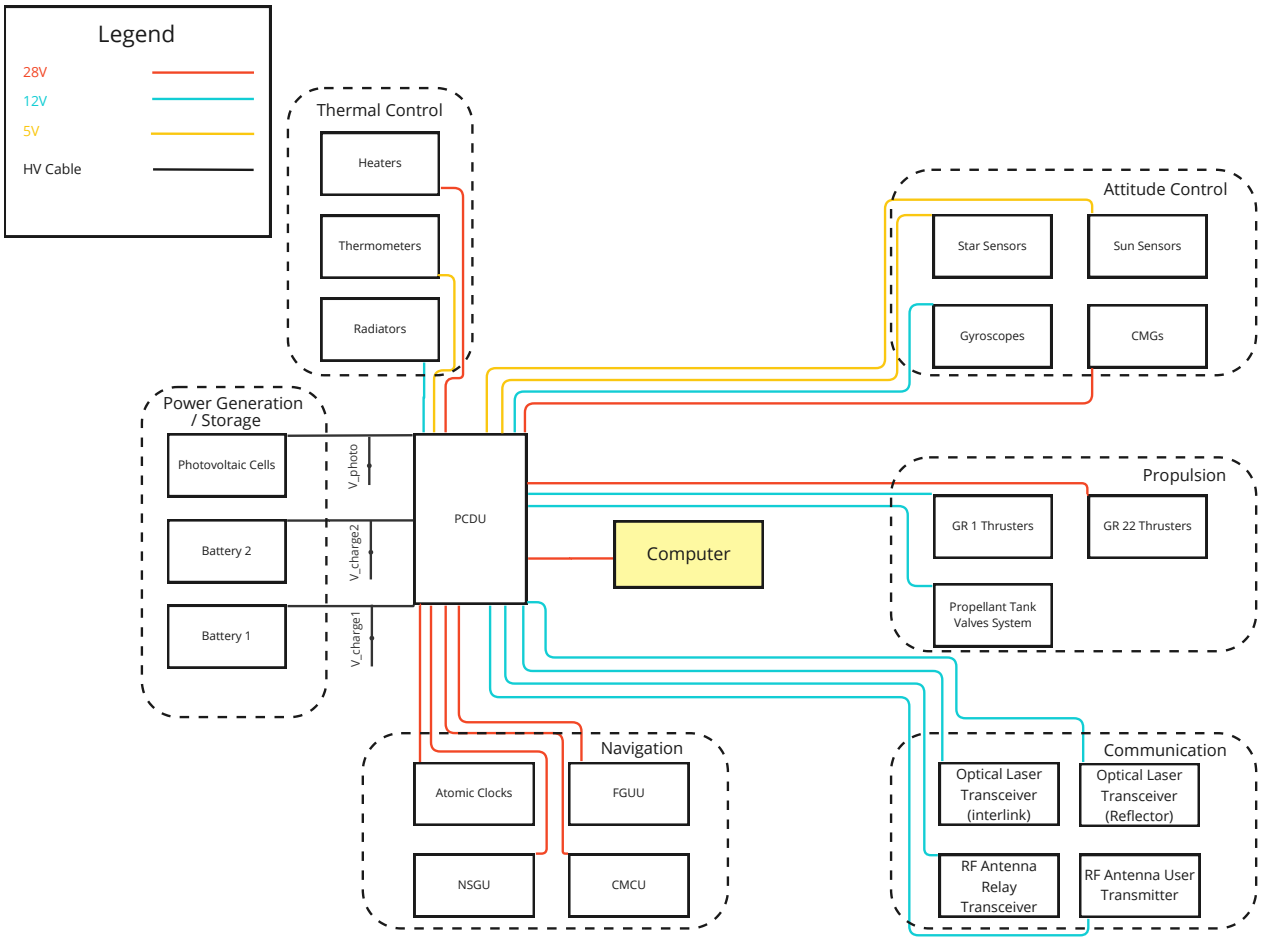

Figure 6.11: Electrical Block Diagram of the EPS

Summary

All primary components are now designed or selected for the current design stage. In Table 6.50, important characteristics such as the mass and volume are listed.

Table 6.50: Summary of all the designed and selected components

Component	Mass [kg]	Volume [L]	Other
Solar array	27.2	-	Area = $6.8\,\mathrm{m}^2$
Battery 1	29.64	7.67	Capacity = $2366.1\,\mathrm{W\,h}$
Battery 2	48	16.3	Capacity = $4832.5\,\mathrm{W\,h}$
PCDU	18.2	0.045	
Cable harness	100	-	

Verification and Validation

The general V&V procedure follows unit tests for all individual scripts and system tests for the entire block. This entails that not only equations are tested, but also the whole flow of the script.

Verification is performed throughout the design. Other than input parameters, no changes are made to the scripts written. Therefore, verification consists of checking inputs and outputs of the model. These outputs are then compared to calculations by hand. The eclipse time considers two scenarios: elliptical and circular orbits. Calculations for circular orbits are readily available and can easily be implemented. Elliptical orbits on the other hand require more attention. Extreme value tests are deemed most useful, as an orbit with eccentricity of 0 is a circular orbit. This can then be compared to the outcome of the other script. Battery sizing is checked for zero input power and large input power.Solar arrays are tested over a range of incident angles. With the angle deviating from the norm ($90°$), the solar arrays are expected to grow larger, as they do not receive the same amount of solar flux. Moreover, it is tested that when the power requirement increases, the solar array area

increases accordingly.

Validation is performed by comparing outcomes from input parameters compared to literature. Circular orbits are widely used, thus comparison with existing orbits is relatively simple. This is more difficult for elliptical orbits, but by evaluating the source of the equation used, relative confidence in the validity is achieved. Battery and solar array sizing are compared to the specifications sheet of the manufacturer.

To test the accuracy of the computations performed, all results are being tested for sensitivity. If a minor change in the input value has a drastic impact on the outcome, the effect must be studied, in order to be effectively accounted for. This is done for the entire system, thus all inputs are analysed. This is done by changing the input power at EOL. A change in power leads to an increase in solar array area. This is a linear relation, thus no anomalies are found in the solar array sizing. The batteries have a similar behaviour.

Recommendations
The following recommendations are given to develop the next design stage:

- Investigate effects of occulting bodies in the simulation. This will greatly improve the accuracy for the eclipse the orbits, and allows for a more efficient design.
- Investigate solar flux variations during orbit. This could show higher average solar flux, thus a decrease in solar array area can be achieved.
- Investigate the option of custom batteries with more efficient cells. Battery capacities may be reduced, leading to a lower mass.
- Investigate cable current ratings. This is directly proportional to cable mass, and thus more accurate numbers on mass can be obtained.

6.7. Thermal Control System

Performed by M. Vereycken, L.D. van der Peet. Written by M. Vereycken
The thermal control system (TCS) is an essential subsystem of the LNS, ensuring reliability during the operational lifetime of its subsystems and instrument in the harsh Lunar environment. The extreme temperature fluctuations experienced in Lunar orbit poses significant challenges to the spacecraft's functionality, making effective thermal control crucial during the mission.

First, the requirements will be established and the design assumptions will be explained. Afterwards, the stage 1 design of the TCS will be performed, which includes the choices of different thermal control systems. Later, an iterative process is carried out with the inputs of other subsystems such as efficiency and operating temperature range. The iterations will lead to a final design with a detailed outline and existing component selection. Lastly, the V&V is performed to ensure a high confidence level of the design and recommendations are stated.

6.7.1. Requirements and Design Assumptions

The first step in designing the TCS is deriving the requirements. The thermal environment around the Moon is heavily subjected to temperature changes due to the absence of an atmosphere. Surface temperature can range from 18 K to 439 K [37]. This will strongly influence the intensity of the infrared radiation, which the spacecraft experiences during orbit. By understanding these thermal characteristics of the Lunar environment, valuable information is considered for determining the requirements of the TCS.

Furthermore, the constraints of the different subsystems, and more specific components should be carefully considered when setting up the requirements. Taking everything mentioned above into account, the requirements table for the TCS can be found in Table A.6. The most driving requirement for the TCS is the operative temperature range inside the spacecraft which shall be between $0\,^{\circ}$C and $40\,^{\circ}$C. This is due to the temperature range of the battery and navigation signal generation unit, where the battery experience a drop-off in performance when the temperature reaches below $0\,^{\circ}$C [110] and the navigation signal generation unit is constraint at an operative temperate of $40\,^{\circ}$C due to the manufacturer [38].

When designing the TCS system multiple assumptions are made which are partly due to resource and time constraints. All assumptions that are applied during the whole design process can be found in Table 6.51.

[37] https://www.nasa.gov/sites/default/files/atoms/files/ericstalcup_lunar_thermal_environment_v2.pdf
[38] https://www.thalesgroup.com/sites/default/files/database/d7/asset/document/TRIS_NSGU-092012.pdf

Table 6.51: Assumptions made for TCS.

ID	Assumption	Reasoning
TA1	The temperature inside the spacecraft is the same at every point, excluding the radiators, solar arrays and their attachments.	The material used as the basis for the spacecraft is Al7075 alloy, which is highly thermal conductive. This will minimise temperature differences inside the spacecraft. This assumption is not conservative, thus margins will be taken.
TA2	The equilibrium temperature of the spacecraft's body and the solar arrays are different, and no heat is exchanged between them.	The attachment between the spacecraft body and solar array can only transfer $0.3\,\mathrm{W/K}$, which is extremely low.
TA3	The equilibrium temperature is calculated based on the hottest and coldest case. It does not include the heat absorbed or dissipated when material is heating up or cooling down respectively.	This is a conservative but valid approach, as the orbital period and eclipse time are relatively long.
TA4	The longest eclipse time is the sum of Earth-caused and longest Moon-caused eclipse.	This is a conservative approach, ensuring thermal control is always met.
TA5	During the entire eclipse time, full eclipse is considered, even if the satellite is located in the penumbra of the eclipse.	This is a conservative approach as the satellite experience solar flux, thus heat, in the penumbra of the eclipse.
TA6	Assume a maximum and minimum solar flux of $1420\,\mathrm{W}$ and $1360\,\mathrm{watt}$ respectively [35].	This is conservative as it considers the two most extreme cases.
TA7	Assume the smallest and largest orbital distance to the Moon for the hottest and coldest case respectively, as this will influence the infrared radiation from the Moon.	This is conservative, as infrared radiation is dependent on the distance to the surface of the Moon.
TA8	The coating covers all of the spacecraft's body surface and heat exchanged due to equipment on the outside of the spacecraft's body is not considered. Thus, absorption and emission is only calculated with the coating properties.	As the main surface area exposed to space is covered with the coating, only a limited error is introduced. However, the assumption is not conservative.
TA9	The heat absorbed due to infrared radiation is absorbed by the emissivity constant of the spacecraft	The emissivity constant of the spacecraft is based on the infrared radiation emitted by the spacecraft itself, thus it is more accurate.
TA10	The spacecraft's power efficiency η range is 0.7 to 0.95 for the hot and cold case respectively [35].	This is a conservative approach, as it was impossible to obtain the power efficiency of all components in the limited time.

6.7.2. Stage 1 Design

In the first design stage, components are yet to be selected, thus the TCS is designed based on the values found in section 5.4 and subsection 6.8.2. The most important values taken are the spacecraft's power P of $1664\,\mathrm{W}$ and the spacecraft's volume of $1\,\mathrm{m}^3$. The spacecraft is considered a cube, thus the emissivity Area A_ϵ of the spacecraft is $6\,\mathrm{m}^2$ and the absorptivity Area A_α of the spacecraft is $1.5\,\mathrm{m}^2$ and $1.0\,\mathrm{m}^2$ for the hot and cold case respectively. This design stage excludes the effects due to the solar arrays. Furthermore, the spacecraft's temperature range considered for the initial design will be between $0\,^\circ\mathrm{C}$ and $25\,^\circ\mathrm{C}$ [35].

The first step in designing the TCS is optimising the coating for passive control. From Table 6.51, the maximum and minimum solar flux J_s is used for the hottest and coldest case respectively. During the eclipse, no solar flux is experienced, as well as no solar flux due to the albedo factor of the Moon J_a. Furthermore, the infrared radiation J_{IR} is also different for the hot and cold case. All input values for the three different cases are given in Table 6.52. The warm eclipse case is not considered as it is redundant because of the cold eclipse case.

Table 6.52: Input variables used for the initial estimation of the thermal control system for the 3 different cases.

Variable	Hot Day	Cold Day	Cold Eclipse
$P\ [W]$	1664	1664	1644
η	0.7	0.95	0.95
$J_s\ [W/m^2]$	1420	1360	0
$J_a\ [W/m^2]$	99.4	95.2	0
$J_I R\ [W/m^2]$	521	0.3	0.3
$A_\epsilon\ [m^2]$	6	6	6
$A_\alpha\ [m^2]$	1.5	1.0	1.0

Here, the infrared radiation is dependent on the orbit height and surface temperature. Equation 6.25 gives the correction factor for infrared radiation based on the orbit radius R and radius of the planet R_0.

$$IR_{correction} = \left(\frac{R}{R_0}\right)^2 \tag{6.25}$$

Putting in the input variables of Table 6.52 in Equation 6.26 while considering an array of values for α/ϵ and some values for ϵ will give an array of the equilibrium temperature (T_{eq}).

$$T_{eq} = \left(\frac{((J_s + J_a) \cdot \alpha_{SC} + J_{IR} \cdot \epsilon_{SC}) \cdot A_\alpha + P \cdot (1 - \eta)}{\sigma * \epsilon \cdot A_\epsilon}\right)^{\frac{1}{4}} \tag{6.26}$$

Plotting the values for the 3 different cases will lead to an efficient absorptivity and emissivity selection of the coating. The plots can be seen in Figure 6.12.

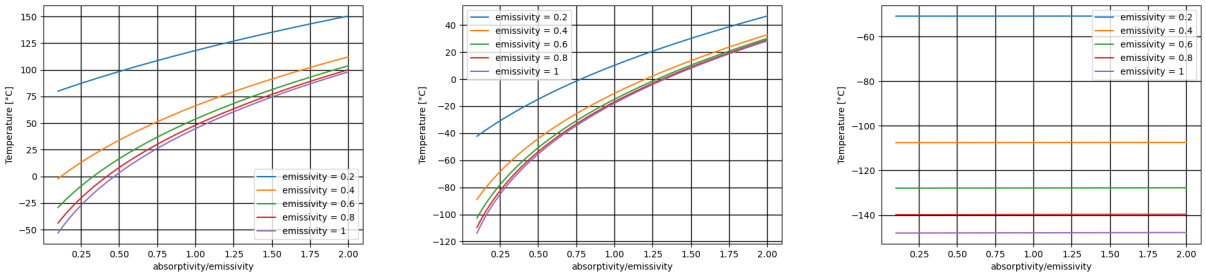

(a) **(b)** **(c)**

Figure 6.12: Equilibrium temperature in function of α/ϵ for different ϵ values where only passive (coating) control is considered for **(a)** hottest case during the day, **(b)** coldest case during the day, **(c)** coldest case during eclipse.

No coating remains within the operating temperature range, thereby showing that only passive control due to coating will not work. The constraint of $25\,^\circ$C temperature range can not be met for any combination of absorptivity and emissivity. Thus, heat dissipation/absorption done by the TCS system should be considered. Equation 6.27 will calculate the absorbed or dissipated heat for a set temperature. Again, an array of values for α and some values for ϵ are considered.

$$Q = T^4 \cdot \sigma \cdot \epsilon \cdot A_\epsilon - ((J_s + J_a) \cdot \alpha_{SC} + J_{IR} \cdot \epsilon_{SC}) \cdot A_\alpha - P \cdot (1 - \eta) \tag{6.27}$$

Plotting the values for the 3 different cases will give a clear view of the most efficient coating coefficient such that active control can be minimised. The plots can be seen in Figure 6.13.

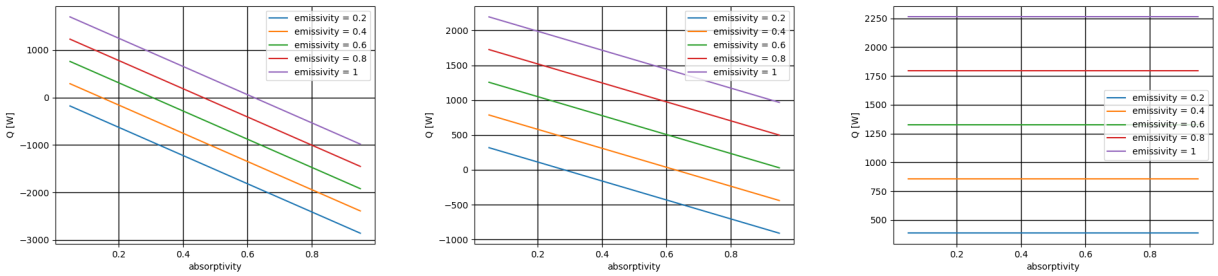

Figure 6.13: Heat absorbed or dissipated in function of α for different ϵ values where only passive (coating) control is considered to have an equilibrium temperature of $15\,^{\circ}$C for **(a)** hottest case during the day, **(b)** coldest case during the day, **(c)** coldest case during eclipse.

By combining the information of all plots, the results show that the most optimal coating should have a low emissivity as well as absorptivity. However, no final, clear result can be extracted. By taking the absolute value for every Q for every absorptivity and emissivity combination, a final plot can show the most optimal coating characteristics. However, heating up the spacecraft during eclipse time introduces more challenges as no solar array power is available. Thus, the Q value during eclipse time is multiplied by 2. The final plot can be seen in Figure 6.14.

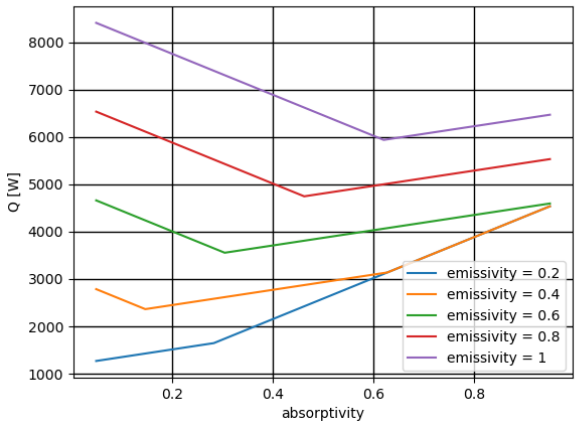

Figure 6.14: Total weighted heat for the combined 3 cases in function of α for different ϵ to have and equilibrium temperature of $15\,^{\circ}$C.

The results indicate that a emissivity around 0.2 is preferred with a low absorptivity. However, the slope of the blue curve is small when the absorptivity reaches 0.3 or less. Thus, the range of the absorptivity should be between 0 and 0.3, while the emissivity should be around 0.2. Taking this into account, multiple coatings are considered.

Apart from the coating absorption and emission characteristic, degradation should also be taken into account. A common aerospace coating to prevent degradation uses hexavalent chromium [39]. However, resent studies shows its toxicity [111]. It is hazardous to human health. Due to this reason, chromium is banned as an option for the spacecraft's coating.

Furthermore, the basis material should be considered for the coating selection. From subsection 6.8.2, Aluminium is chosen as base material for the spacecraft, thus a coating that is complementary with the base material is preferred. Due to all these reasons, the Kapton film (Aluminium-Silicon Oxide Overcoating) is chosen with an α of 0.12 and an ϵ of 0.18 [112]. Apart from the right absorptivity and emissivity characteristics, it has decent surface resistivity, a width operative temperature range and a small coating thickness for minimising the mass [40].

[39] Communication with Jingjing Zhao, dd. 12/06/2023

[40] `https://www.dunmore.com/products/ito-sio2-aluminized-polyimide-film.html`

Lastly, the degradation of the coating should be taken into account. As no specific degradation information on the coating could be found, a more general coating degradation is considered. A margin of $15\,\%$ and $5\,\%$ is taken on the absorptivity and emissivity constant respectively during the design life of the satellite [113]. This will later be applied such that the most conservative case will be considered.

Even with an optimal coating, the three cases all need extra thermal control. For the hot day case, heat should be dissipated. Therefore, a radiator with a mechanical pumped fluid loops should be implemented. For the cold day case, heaters are implemented as no battery storage is required. This only requires extra power from the solar arrays. For the cold eclipse case, a Thermal Storage Unit (TSU) is chosen which uses phase changing materials. These materials can be heated to liquid during the day by heaters which uses the power of the solar arrays or from external heat sources like the Sun itself. Doing this, no extra battery capacity is needed and in case of battery failure, the temperature range will still be in the operative temperature range. These choices are all carefully considered based on information found in [114].

6.7.3. Iteration Process

During the iteration process, detailed information for all subsystems became available. This leads to new power and volume updates which directly effect thermal control. Because of clear communication within the team, the iterations followed a natural process and multiple iterations were performed. Especially, the communication between the EPS and TCS was outstanding to converge to an optimal design.

Due to the **NTM-SYS-TCS-06** requirement found in Table A.6, temperature sensors should be selected. There were 26 critical components identified within the satellite, thus 26 temperature sensors should be selected, one for each component. The primary goal for the sensor is to be lightweight and minimise power consumption, while meeting the requirement. Therefore, the thin film platinum sensor (46D) is selected. It has a power consumption of $0.2\,\text{mW}$, an operative temperature range of $-271.66\,^\circ\text{C}$ to $126.85\,^\circ\text{C}$ with an accuracy of $0.5\,^\circ\text{C}$ and an estimated mass of $10\,\text{g}$ [41] [42].

During the iteration process, the solar arrays were also considered. The first solar array cells chosen by the EPS were the IMM-α cells, who showed excellent efficiency. However, due to the operative temperature range of $-40\,^\circ\text{C}$ to $85\,^\circ\text{C}$ and the harsh Lunar environment, the cells were eliminated [114]. The new selected solar cells showed an operative temperature range of $-230\,^\circ\text{C}$ to $110\,^\circ\text{C}$ [43]. The calculated equilibrium temperature for the two most extreme cases showed a minimum temperature of $-163\,^\circ\text{C}$ and a maximum temperature of $78.9\,^\circ\text{C}$. For these calculations, a degradation factor of $3\,\%$ on the solar cell efficiency obtained by the EPS was taken into account. Furthermore, an emissivity factor of 0.8 is assumed [115]. Lastly, for the coldest case, assumption TA2 from Table 6.51 is not valid, as the temperature difference between the solar panels and the spacecraft's body is significant. Therefore, a heat transfer of $43\,\text{W}$ per solar panel attachment is calculated and integrated.

The first step in the iteration process of the spacecraft's body was selecting the phase change material. As the operative temperature range of $0\,^\circ\text{C}$ to $40\,^\circ\text{C}$ due to component selection was established, the phase change material was selected. It is hexadecane with a fusion heat capacity of $237\,\text{kJ/kg}$ and a phase change temperature of $16.7\,^\circ\text{C}$ [44]. This material influences the equilibrium temperature during the cold day case and the cold eclipse case. For the cold day case, an equilibrium temperature of $290.0\,\text{K}$ was chosen, as this is $0.15\,^\circ\text{C}$ higher than the phase change temperature of the material. This is done such that no heat is absorbed from the phase change material during the day. For the cold eclipse case, an equilibrium temperature of $299.85\,\text{K}$ was chosen, as this is the phase change temperature of the material. Again, Equation 6.27 can be used to calculate the required heat. The same is done for the hot day case, where an equilibrium temperature of $308.15\,\text{K}$ is chosen. This is $5\,\text{K}$ under the maximum operative temperature to have a margin. All final results based on the final BOL power, EOL power and eclipse power can be found in Table 6.53, Table 6.53 and Table 6.55.

[41] https://www.scientificinstruments.com/wp-content/uploads/2019/09/020-134E.pdf
[42] https://www.scientificinstruments.com/wp-content/uploads/2023/06/Aerospace-Datasheet-2023.pdf
[43] https://www.esa.int/ESA_Multimedia/Images/2020/10/Juice_solar_panels_ready_to_turn_into_wings
[44] https://satsearch.co/products/thermal-management-technologies-thermal-storage-units

Table 6.53: Final TCS inputs and outputs for BOL of the spacecraft's body at hottest case during day.

Inputs	Value
T_{eq}	$308.15\,\mathrm{K}$
P_{BOL}	$2149\,\mathrm{W}$
η	0.7
J_{sun}	$1420\,\mathrm{W/m^2}$
J_a	$99.4\,\mathrm{W/m^2}$
J_{IR}	$521\,\mathrm{W/m^2}$
α_{SC}	$1.15 * 0.12$
ϵ_{SC}	$0.95 * 0.18$
R_{SC}	$2616\,\mathrm{km}$
A_ϵ	$6\,\mathrm{m^2}$
A_α	$1.5\,\mathrm{m^2}$
Outputs	**Value**
$P_{dissapted}$	$586\,\mathrm{W}$

Table 6.54: Final TCS inputs and outputs for EOL of the spacecraft's body at coldest case during day.

Inputs	Value
T_{eq}	$290.0\,\mathrm{K}$
P_{EOL}	$1419\,\mathrm{W}$
η	0.95
J_{sun}	$1360\,\mathrm{W/m^2}$
J_a	$95.2\,\mathrm{W/m^2}$
J_{IR}	$0.3\,\mathrm{W/m^2}$
α_{SC}	$0.85 * 0.12$
ϵ_{SC}	$1.05 * 0.18$
R_{SC}	$10\,466\,\mathrm{km}$
A_ϵ	$6\,\mathrm{m^2}$
A_α	$1\,\mathrm{m^2}$
Outputs	**Value**
$P_{heaters}$	$232\,\mathrm{W}$

Table 6.55: Final TCS inputs and outputs for EOL of the spacecraft's body at coldest case during eclipse.

Inputs	Value
T_{eq}	$289.9\,\mathrm{K}$
$P_{battery}$	$761.6\,\mathrm{W}$
η	0.95
J_{sun}	$0\,\mathrm{W/m^2}$
J_a	$0\,\mathrm{W/m^2}$
J_{IR}	$0.3\,\mathrm{W/m^2}$
α_{SC}	$0.85 * 0.12$
ϵ_{SC}	$1.05 * 0.18$
R_{SC}	$10\,466\,\mathrm{km}$
A_ϵ	$6\,\mathrm{m^2}$
A_α	$1\,\mathrm{m^2}$
Outputs	**Value**
P_{TSU}	$410\,\mathrm{W}$

With these results a radiator and heaters can be selected for the hot and cold day case respectively. The chosen radiator has an original heat-rejection capacity of $1250\,\mathrm{W}$ and already includes a mechanical fluid pump system [45]. However, less than $600\,\mathrm{W}$ heat rejection capacity is needed, therefore the deployable radiator area, the mechanical fluid pump system and mechanism are divided by two, which is still capable of rejecting $625\,\mathrm{W}$. For the cold day case, multiple flexible polyimide heaters are chosen which are ESA-qualified, with an optimal heat transfer and lightweight characteristics [46]. The specific heater chosen is the SC050075Q, which has a heating power of $15\,\mathrm{W}$. To calculate what amount of heaters are necessary, the power needed to heat up the phase change material should also be considered. With a $5\,\%$ margin on the P_{TSU}, and considering the longest eclipse time caused by the Moon, plus the Earth eclipse time, a TSU mass of $35\,\mathrm{kg}$ is found. To calculate the power needed to heat up the phase change material, the worst eclipse time over orbital period should be taken. Again the margin of $5\,\%$ is applied. Equation 6.28 shows the minimum average power (Q_{charge}) to heat up the phase change material.

$$Q_{charge} = \frac{T_{e_M} \cdot P_{TSU} \cdot 1.05}{T_M - T_{e_M}} + \frac{T_{e_E} \cdot P_{TSU} \cdot 1.05}{T_E - T_{e_E} - \frac{T_E}{T_M} \cdot T_{e_M}} \tag{6.28}$$

where T_{e_M} is the Moon caused eclipse time, T_{e_E} is the Earth caused eclipse time, T_M is the orbital period of the satellite around the Moon and T_E is the orbital period of the Moon around the Earth. This results in a charging power of $45\,\mathrm{W}$. Thus a minimum of 19 heaters are necessary, including the heating power for the cold day case. To have enough redundancy a last margin of $5\,\%$ will be taken on the heaters, thus the spacecraft shall be able to operate 20 heaters simultaneously. Furthermore, there will be 2 extra heaters included for heater failure.

6.7.4. Final Design

With all components carefully chosen, the final design for the TCS system can be seen in Table 6.56.

Table 6.56: Final components for the TCS where the radiator includes the Mechanical Fluid Pump, Deployable Radiator and the Mechanism.

Component	Mass [kg]	Power [W]
Radiator	10.85	30
Mechanical Fluid Pump	4.75	30
Deployable Radiator	5.1	0
Mechanism	1.0	0
Heaters	1.1	300
TSU	35	0
Coating	1.0	0
Thermometers	0.26	0.0052

[45] http://matthewwturner.com/uah/IPT2008_summer/baselines/LOW%20Files/Thermal/Spacecraft%20Thermal%20Control%20Handbook/06.pdf

[46] https://satsearch.co/products/zoppas-industries-space-stock-polyimide-flexible-heating-element

Verification and Validation
All calculations used for in section 6.7 were performed in Python. To verify all formulas used to obtain the results, unit test were performed with the help of the unittest packages. Here, dummy values were used, and the outcome was calculated by hand and afterwards compared to the obtained value in python. Module test and sensitivity analyses are performed with the use of the graphs, which can be seen in subsection 6.7.3. Furthermore, validation is done by comparing literature values with our results [116]. Lastly, all TCS requirements were verified and checked.

Recommendations
Apart from the more accurate determination of the eclipse time, discussed in subsection 6.6.4, multiple recommendation for the TCS can be given:

- Account for temperature differences inside the spacecraft's body or solar arrays such that a more accurate thermal analysis can be obtained.
- Consider the specific heat and exact efficiencies of all components. The satellite would gradually undergo temperature changes and it may not come to an equilibrium.
- Consider heat exchange due to equipment on the outside of the spacecraft's body, this will influence the equilibrium temperature of the satellite.
- Consider solar flux based on the position of the satellite inside the penumbra of the eclipse.

6.8. Structure System

By I. Maes and N. Ricker
The structure system is focused on the load-carrying components of the spacecraft and keeps the other subsystems safe in the hazardous environment. This section focuses on its design, combining requirements and assumptions in subsection 6.8.1, initial design in subsection 6.8.2, performing iterations and increasing accuracy in subsection 6.8.3, to finally select a design and perform V&V in subsection 6.8.4.

6.8.1. Requirements and Design Assumptions

Before brainstorming designs and doing trade-offs, the requirements are derived from the environment in which the spacecraft is. The requirements are obtained mainly from the launch and nominal operations. Sustainability is also taken into account at every stage of the design. Most requirements are related to the dimensions allowed (**NTM-SYS-STR**), loads and behaviour under certain scenarios (**NTM-SYS-STR-PERF**), along with integration between subsystems (**NTM-SYS-STR-INT**).

All requirements, along with their respective rationale, can be found in Appendix A. Nonetheless, some key values were obtained from the literature to develop proper requirements. With respect to the launcher, the maximum loads are 8.5g axially and 3g laterally, which must be withstood without yielding. The natural frequencies are 25 Hz axially and 10 Hz laterally. [47] Other values used in the requirements emerged from the mission design, objectives set by the team, or other subsystems. These will provide useful to set guidelines in the final outcome of the design.

In the next subsections, there are three main aspects to develop: the satellite's skeleton, propellant tank, and mechanisms/integration elements. In order to compute these values, some general assumptions were made. These were studied to be accurate enough for the stage of the design, and appropriate margins are also included. The following assumptions apply to the whole design process:

[47] https://www.spacex.com/media/falcon-users-guide-2021-09.pdf

Table 6.57: Assumptions made for structures subsystem

ID	Assumption	Reasoning
SA-G1	The system is modelled as an assembly of rigid bodies and idealised joints.	Simplification when performing models, valid when deflections are small and stresses are distributed.
SA-G2	The inside of the spacecraft does not include supports for components.	No final positioning is set, given the early stage in the design and unknowns in the exact connections between components. A mass and volume margin are included to account for it.
SA-G3	The spacecraft has a constant centre of mass.	Most loads occur at launch when the total mass is constant and components are fixed.
SA-G4	Material properties are uniform and constant throughout the whole system.	The materials have small variations and are well-characterised.
SA-G5	The materials respond elastically and linearly to loads.	The stresses must be under the yield limit to stay in the linear range.
SA-G6	The loads at launch are constant and equally distributed.	The integration with the launcher must be capable of translating the loads uniformly.
SA-G7	Stresses are independent of each other and cannot be modelled together.	Launch and temperature stresses are usually decoupled. Axial and lateral loads are considered together to comply with the worst-case scenario.
SA-G8	The spacecraft is clamped when stresses are calculated.	Conservative approach increasing stresses, it can be reassessed in future stages to reduce mass.
SA-G9	The spacecraft does not experience random vibrations.	The sources of random vibrations are small and apply mainly for launch, which can be reduced by an appropriate adapter.
SA-G10	Natural frequencies are calculated using a uniform beam.	The shape of the structure resembles a beam, and mass is distributed almost equally throughout the whole skeleton.
SA-G11	Only the first natural frequency for each axis is considered in the design.	The effect by multiples of eigenfrequencies is negligible. A sufficient margin should be considered for a conservative approach.
SA-G12	The zero stress temperature of the structure is $20\,^{\circ}$C.	Conservative approach where materials are designed for nominal Earth temperatures.

These assumptions present idealisations, simplifying the computational process. They are not conservative scenarios, but enough margins are considered to account for a real environment. The standard margins added are a factor of 1.1 to yield stress, 1.25 to ultimate stress, 1.5 to natural frequencies, 1.5 to propellant pressure, a 10% added volume to the propellant tank, and a 20% increase in the dry mass, as specified by ESA [100]. In the following subsections, specific assumptions for a design stage are stated.

6.8.2. Stage 1 Design

In the first stage of the design, the focus is on studying shapes, materials and limiting factors. It takes values from section 5.4, and uses them to obtain a preliminary estimation of the size, and the behaviour of completely different study cases. This subsection concludes with a trade-off, guiding the design in a specific direction.

Computational Model

A simplified model of the spacecraft is developed to test two shapes and various structural materials. This model receives initial mass, structure dimensions and panel size as inputs. It computes stresses, limiting thickness and an updated mass. It can be accessed in GitHub-Stage 1 Structure. The model has the following assumptions:

Table 6.58: Assumptions for Stage 1 Design

ID	Assumption	Reasoning
SA-I1	The spacecraft is a rectangular prism or cylinder.	Most common spacecraft shapes, reducing the complexity of the model while providing good features.
SA-I2	The spacecraft is a solid body of homogeneous distributed mass, except for the solar panels.	The lack of components at the current stage allows for an accurate prediction. Components must be distributed evenly in the next stages.
SA-I3	Solar panels are thin plates without an arm connecting them to the skeleton.	It allows computations of preliminary behaviour without much information, a detailed design is required to ensure compliance.
SA-I3	Solar panels have the same width as the satellite and length is obtained from the surface area required.	At the early stage of the design, there is no precise information on the stresses each component introduces, and no specific ratio is set. It must be reassessed in the next iteration.
SA-I4	The spacecraft only experiences tensile, compressive, and thermal stresses.	The main stresses at launch and operations are considered. Other stresses are studied in the next stages.
SA-I5	Buckling calculations are performed assuming a cylindrical shape.	Simplification for rectangular prism, using established formulas. It does not capture all features and must be updated in the future.
SA-I6	No thermal system is considered when studying thermal stresses.	Larger stresses are achieved following a conservative approach, useful at a preliminary stage.

As introduced in the assumptions, there are two main shapes with varying dimensions: rectangular prism and cylinder. These are both valid shapes, but in order to make a decision, an optimisation process is performed. It assumes the mass and volume calculated in section 5.4 of $1125\,\text{kg}$ and $11.25\,\text{m}^3$. Finally, for the calculations, the structure material is assumed to be Aluminium 7075. The following results were obtained:

Table 6.59: Comparison Satellite Shapes

Shape	Dim. Ratio	Structure Mass [kg]	Tens. Stress [MPa]	Comp. Stress [MPa]	Thickness [mm]	Axial Freq. [Hz]	Lateral Freq. [Hz]
Cube	1x1x1	176.9	7.32	10.26	2.1	183	167.7
Rectangular prism	1x1x2	154.4	1.96	23.55	1.7	118	54.0
Cylinder	1x2	77.8	23.10	29.60	1	112	88.9

Table 6.59 shows the results of the computations. ”Dim. Ratio” represents the proportions between length, width, and height for cuboids, or radius and length for the cylinder. For all cases, the limiting characteristic for thickness dimensioning is buckling stress. Other stresses are much smaller and do not pose a risk. Cylinders use mass more efficiently, requiring a smaller thickness to carry all loads. On the other hand, cuboids have larger margins for all relevant loads and vibrations. Furthermore, fitting all components and characterising the spacecraft’s motion is simpler. The final choice was a **rectangular prism/cube**, it presents the best results and is convenient for all subsystems to work with. It also provides a large surface area which is required to fit all the antennas for the navigation system.

Material Selection

The material selection introduces a complex decision, where several aspects must be considered. First, all performance requirements (**NTM-SYS-STR-PERF**) must be complied with, while also considering manufacturability (**NTM-SYS-STR-MAN**) and sustainability (**NTM-SYS-STR-SUS**) in mind. The skeleton material is selected in this subsection, while the propellant tank is left for later stages when more information is available about the requirements of the propulsion system. The following are the criteria to consider for each material:

- Thermal Expansion Coefficient. A higher value increases the stresses of the structure, putting the system at risk and depending on the thermal system for nominal operation. Complies with requirement **NTM-SYS-STR-PERF-07**.
- Specific Strength. A higher value reflects more efficient use of material for load-carrying structures. Complies with requirements **NTM-SYS-STR-PERF-01** and **NTM-SYS-STR-PERF-02**.
- Mass. Achieving a low mass reduces costs and environmental impact. It also reduces the complexity of the system and allows for further optimisation. Complies with requirement **NTM-SYS-GEN-01**.
- Cost. Material cost is relevant as it reflects how effectively the budget is being used, and given the large production required, reducing this criterion yields more optimal results. Complies with requirements **NTM-SYS-GEN-03**.
- Manufacturability. Choosing readily manufacturable materials simplifies the production stage of the mission, further reducing costs. It complies with requirement **NTM-SYS-STR-02**.
- Sustainability. As a pillar in the design, the material used must not be toxic or damage its environment. It should also aid in reducing pollution as much as possible. It complies with requirement **NTM-SYS-STR-SUS-02**.

The materials considered were obtained from SMAD [35]. Some materials were immediately rejected after performing a quick search, others were taken further for a more complete study. The rejected materials and reasoning are the following:

- Magnesium. It is not a popular material for designing the load-carrying structure of the satellite. It has a relatively low specific strength of $0.12\,\text{Pa}\,\text{m}^3\,\text{kg}^{-1}$, and the highest thermal coefficient [48].
- Beryllium. A material with very good properties, but it is toxic on the skin and inhaled. There are government regulations arising, limiting exposure [49].
- Heat-res alloys. These alloys have great material properties, but are generally very heavy and only used for specific components or sections [50].
- Steel 17-4PH. Similarly to heat-res alloys, steel is heavy and does not provide a high specific strength ($0.11\,\text{Pa}\,\text{m}^3\,\text{kg}^{-1}$) [51].

The final materials are various aluminium alloys (6061-T6, 7075-T73, 2219-T851) and titanium (Ti-6AL-4V). They all present good properties, and even though titanium performs better, there is a limitation in its manufacturability. It is "one of the most difficult materials to machine" [52]. Furthermore, aluminium is a common material. It has well-established methods for manufacturability, along with innovations for more sustainable production [53]. It is commonly used in the space industry and permits more flexibility in the design. The specific aluminium alloy is selected based on the best performance among them. The chosen alloy and properties are:

Table 6.60: Selected structure material

Material	**Ultimate Stress** [MPa]	**Yield Stress [MPa]**	**Young's Modulus [GPa]**	**Thermal Coefficient [μm/m]**	**Specific Strength [Pa m^3 / kg]**	**Shear Strength [MPa]**	**Fatigue Strength 500M cycles [MPa]**
Aluminium 7075-T73	505	435	72	23.6	0.155	300	150

After making all necessary selections, a preliminary set of dimensions is chosen to consider the previously mentioned parameters. After the first stage design, the result is a satellite of dimensions 2.1x2.1x2.7 m, a thickness of 1.9 mm, mass moments of inertia (MMOI) range of 1096-1528 kgm^2, buckling stress as limiting factor, and natural frequencies range of 109-155 Hz. These are values used for the next iterations and as first-order estimates in other subsystems.

[48] https://www.matweb.com/search/datasheet.aspx?matguid=d1e286e1ac0742358544b953bbf3c2e9&ckck=1

[49] https://www.ncbi.nlm.nih.gov/books/NBK585042/#:~:text=Beryllium%20is%20toxic%20as%20both,pain%2C%20or%20shortness%20of%20breath.

[50] https://www.specialmetals.com/documents/technical-bulletins/inconel/inconel-alloy-718.pdf

[51] https://www.pennstainless.com/resources/product-information/stainless-grades/precipitation-hardening-grades/17-4ph-h1150/

[52] https://kingsburyuk.com/machining-titanium-is-it-really-that-hard/#:~:text=Despite%20its%20popularity%2C%20titanium%20is,and%20ruined%20workpieces%20are%20abundant.

[53] https://www.comhan.com/en/blog/news/how-sustainable-aluminium#:~:text=Aluminium%20can%20be%20recycled%20without,very%20durable%20type%20of%20metal.

6.8.3. Detailed Design

Once the initial values have been set, a more detailed design can be produced. In this subsection, components are placed in provisional locations, focusing on limiting dimensions. The solar panel support and dimensions are also studied, along with a propellant tank sizing. Support structures are considered for the layout and the thickness is resized taking into account the new data acquired.

Computational Model

The detailed design is performed by using a Computer Aided Design (CAD) model and programming script. The CAD is mainly used for positioning elements, while the script computes all relevant features and performs mass optimisation. There are four main elements that can be given as input to the program.

- Point Mass. Individual components with a mass and position with respect to the coordinate system.
- Structure. Rectangular prism with length, width, height, and thickness. Centred at the origin.
- Propellant Tank. Sphere or cylinder with spherical caps with radius and length. Has propellant and structure mass, along with a position in the system.
- Solar Panels. Panels with length and width, along with the total mass.

The last three elements have more complex shapes and have unique MMOI. Once all elements are inserted into the program, a stress, and vibration analysis is run, followed by a compliance check and a calculation of the total system mass and MMOI. The assumptions considered in this model are introduced in Table 6.61.

Table 6.61: Assumptions for Detailed Design

ID	Assumption	Reasoning
SA-D1	Small sized components are modelled as point mass elements	Most components are considered to have a concentrated mass, giving a short distance from the centre of gravity. Large-sized components are modelled in more detail, such as solar panels or the propellant tank.
SA-D2	The MMOI are taken from the origin of the coordinate system instead of the centre of gravity of the satellite.	The satellite is designed to keep both points as close as possible, for which differences are negligible.
SA-D3	Buckling is modelled by a set of four clamped thin panels, ignoring corners and crippling.	Simplified approach to modelling buckling. Presents similar results. Crippling should not occur given the small loads introduced. A sufficient margin is required.
SA-D4	For MMOI calculations of the skeleton, the total mass is distributed equally among all panels.	Simplification of the model. It is valid while the dimensions are similar.
SA-D5	The satellite is clamped on one side for launch stress/vibration calculations	During the launch, the satellites are connected to a central column, keeping them fixed on one side. Valid while the adapter distributes loads equally.
SA-D6	Bodies without a clear position or uniformly distributed are positioned as point masses in the origin.	Given their small contribution to the total MMOI, they are only considered for total mass calculations. It produces a slightly smaller MMOI.
SA-D7	Maximum shear stress is computed assuming thin walls and a point load at the centre of gravity.	The satellite has a ratio of 1:100 for the wall thickness, making it a valid scenario. Furthermore, the maximum shear stress occurs at the clamped side and is independent.
SA-G13	The spacecraft undergoes a temperature range between 0 and 40 °C.	Values obtained from previous sections, allows for a more precise analysis of the structure.

Furthermore, there are other specific requirements for the propellant and solar panel design. The corresponding script for the introduced model can be found in GitHub-Detailed Structure.

Propellant Tank Design
The propellant tank is designed based on the volume, pressure, temperature, and some ratio between dimensions. It is updated multiple times, as there is a close relation between the fuel required and the dry mass of the system. Some specific assumptions are considered in Table 6.62.

Table 6.62: Assumptions for Propellant Tank

ID	Assumption	Reasoning
SA-P1	Only hoop and axial stresses are calculated.	These are generally the limiting stresses, with radial stresses being negligible. Thermal stresses are considered when selecting the material.
SA-P2	No support structure for the tank is designed.	Given the early stage of the design, there is no clear support, but a 10 kg margin is considered for it.

There were two stages in the design: choosing a shape and selecting a material. The most common shapes are a sphere and a cylinder with spherical caps. Most small satellites work with spherical tanks, but given some large manoeuvres required, the propellant volume is ($0.185\,\mathrm{m}^3$). To have more efficient use of the space inside the skeleton, a **cylindrical shape** has been chosen. The specific dimensions were chosen in parallel with setting the layout of the components, explained further in the report.

The material is chosen based on the propellant from the propulsion section. The structural material used for these tanks is generally Grade 5 titanium (AM Ti-AL6-V4). It has high-strength properties for pressure and launch loads while resisting the required temperatures[54]. By combining them, and after performing the required iterations, the propellant tank has the following features:

Table 6.63: Propellant Tank Characteristics.

Shape	Material	Radius [m]	Total Length [m]	Thickness [mm]
Cylinder with Spherical Caps	Ti-6AL-4V	0.27	0.987	2.0

Solar Panel Design
The largest structures attached to the outside of the spacecraft are the solar panels. These will be attached to the sides of the spacecraft. The solar panels are attached along the y-axis of the spacecraft, as can be seen in Figure 5.1. For the spacecraft to not block the view of the solar panels, the solar panels are attached using arms. The solar panels will be able to rotate around the y-axis for ideal positioning towards the Sun.

The solar panels have a surface area of $3.4\,\mathrm{m}^2$ each. The solar panels have been designed to have a 4 to 1 aspect ratio. This aspect ratio is chosen to make the solar panels not stick out along the z-axis, to avoid colliding with the central support structure during launch. This gives the solar panel a width of $0.925\,\mathrm{m}$ and a length of $3.73\,\mathrm{m}$. The length of the solar panels is divided into 4 squares. These can fold inwards to make the spacecraft fit in the launcher.

The solar panel support is included to have the solar panels' view of the Sun not be obstructed by the spacecraft. The support structure of the solar panels has been chosen to be $0.4625\,\mathrm{m}$. This is half the width of the solar panels and should provide enough margin for the solar panels.

The design of the support of the solar panel is crucial. Since this support arm will not be able to rotate inwards during the launch, it will need to carry the full load of the solar panels during the launch. As described by **NTM-SYS-STR-INT-07**, individual elements of the spacecraft structure will not deform more than $2\,\%$ additionally, according to **NTM-SYS-STR-PERF-01**, the structure shall not yield. Therefore, the arms will be analysed and designed for the two failure modes. First, the arm will be designed for the displacement requirement. Afterwards, the maximum stress within the arm is analysed to check whether the support yields. Some additional assumptions are made during this design process, including:

[54] https://plasmapros.com/wp-content/uploads/S3VI-Webinar-Presentation-Emerging-Green-Prop-Technology_UPDATED_02.10.21-1-1.pdf

Table 6.64: Assumptions made for the solar panel support design.

ID	Assumption	Reasoning
SA-S1	The solar panel support structure acts as a cantilever beam under bending.	Due to solar panel support being slender and only axial loads being considered, the cantilever beam approximations are sufficient for this analysis.
SA-S2	Superposition of deflections in the axial direction of the support.	The deflections in different directions can be considered independent when deflections are small.

Since the solar panel support is loaded in 2 axial directions, a thin-walled rectangular cross-section is used. The loads are as shown in Figure 6.15. These loads are the combination of accelerations at launch and solar panels mass (13.68 kg per panel).

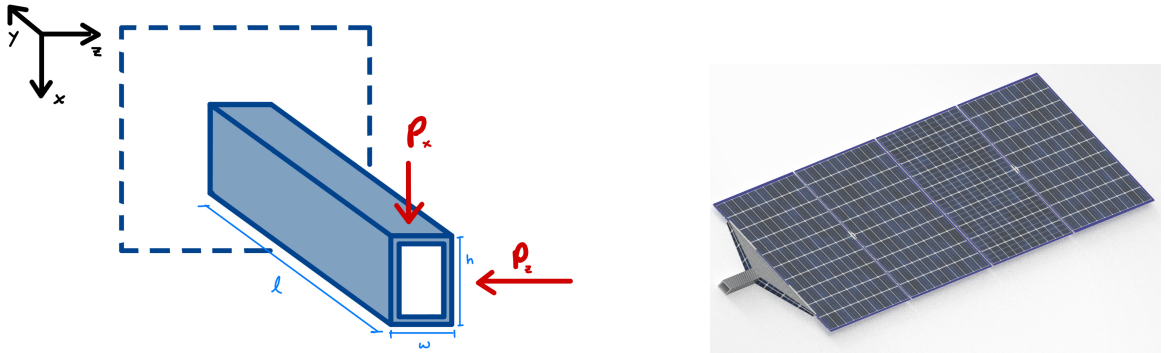

(a) The axial loads on the solar panel support.

(b) Solar panel render.

Figure 6.15: Solar panel arm

Using the cantilever beam deflection due to the bending equation, the deflection along the z-axis and x-axis can be calculated for different rectangular cross-sections and thicknesses. A set of ranges is used to optimise for the mass, leading to the final parameters seen in Table 6.65.
Using this equation, the dimensions of the cross-section can be optimised for the mass of the support structure. This was done by checking a range of heights from 0.06 - 0.14 m, a range of widths of 0.04 - 0.13 m and a range of thickness from 0.001 - 0.006 m. This led to the final parameters of the support structure as seen in Table 6.65.

Table 6.65: Solar panel support structure characteristics

Height [m]	Width[m]	Thickness[m]	δ_x	δ_z	δ_{total}	Max stress[MPa]
0.068	0.048	0.005	0.75 %	1.7 %	1.86 %	27.0 MPa

As a validation technique, the solar support structure was modelled in CATIA. This model is used in a FEM analysis. The outputs gave differences of 5 % between both scenarios. The results provide confidence in the model.

Components Positioning

Once all structural components have been designed, a preliminary positioning is required to analyse the skeleton's behaviour. This allows for a design of the satellite's thickness. As well, it will limit the dimensions.

The main elements to position are the solar panels, user antenna, propellant tank, and control moment gyros. The solar panels must be facing the Sun as much as possible, without interfering with the antenna pointing towards the Moon. They are positioned as shown in the coordinate system from section 5.4. The propellant tank should be in the direction of the x-axis, in order to affect the centre of gravity(CoG) the least possible. Finally, the control moment gyros (CMG) should be in any of the axis aligned with the CoG to counter the torques in the most efficient way.

From the positioning of these elements, there are two limits on the dimensions of the solar panel, mainly the longitudinal dimension of the propellant tank, and the total distance between the two CMGs and the propellant

diameter. A diagram showing the dimensions is introduced in Figure 6.16. Similar dimensions arise from a desire for a symmetrical satellite, which reduces the need for control manoeuvres and optimises the area.

Furthermore, from the analysis of the components performed in previous sections, the total volume + $20\,\%$ margin is $0.56\,\mathrm{m}^3$ is required. It is relevant to emphasise that these elements cannot be perfectly positioned. To account for this, each component should have a margin of 10% for each length. This would give a necessary volume of $0.74\,\mathrm{m}^3$. Two dimensions were previously defined by the positioning of large components, such that the x and y lengths are $1\,\mathrm{m}$. The z length should be at least $0.74\,\mathrm{m}$. The team opted for a **cube satellite with** $1\,\mathrm{m}$ **dimensions**. This simplifies calculations, while also giving larger margins for components. Furthermore, a larger satellite surface proved useful when positioning elements in the exterior, such as solar panels, antennas, and radiators. The increase is not very large, and it has minimal consequences for the overall mission. This fulfils requirement **NTM-SYS-GEN-02**.

Multiple load-carrying structures were considered. One interesting concept is to use the fuel tank in the centre of the satellite as a load column. Increasing the moment of inertia would provide sufficient stiffness while reducing the total mass and thickness of the wall. However, during the thickness iteration, some constraints of the wall due to bending stresses were imposed. This concluded with discarding the cylinder since it added mass to an already proven concept.

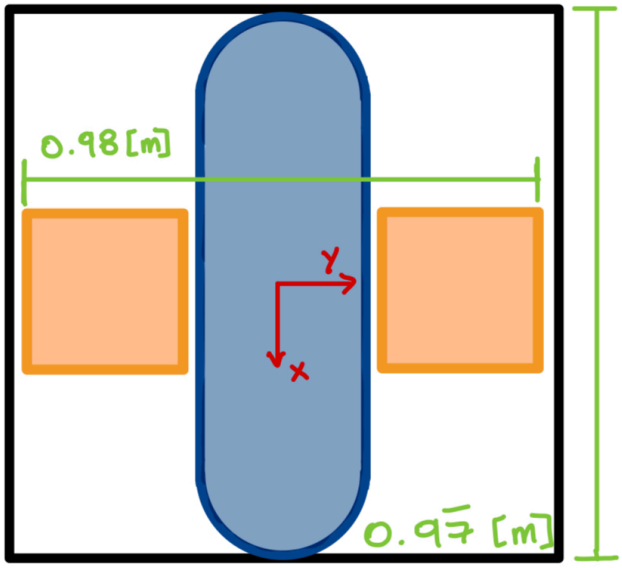

Figure 6.16: Structure and propellant tank dimensions

Payload Integration in Launcher
By I.Maes and N. Ricker

Each Falcon Heavy launcher can fit 6 spacecraft. These spacecraft are put in a triangular configuration around a triangular support structure, as can be seen Figure 6.17. This triangular support structure uses the least amount of area for 3 spacecraft in this configuration. 2 sets of this configuration are put on top of one another to reach the maximum capacity of the launcher. Between the support structure and the spacecraft, a $30\,\mathrm{cm}$ interface mechanism holds the spacecraft. This $30\,\mathrm{cm}$ is necessary for the clearance of components on the back side of the spacecraft, as can be seen in Figure 6.17b. The x-axis of the spacecraft is oriented downwards. This is because the spacecraft has been designed to withstand the launch loads in this direction.

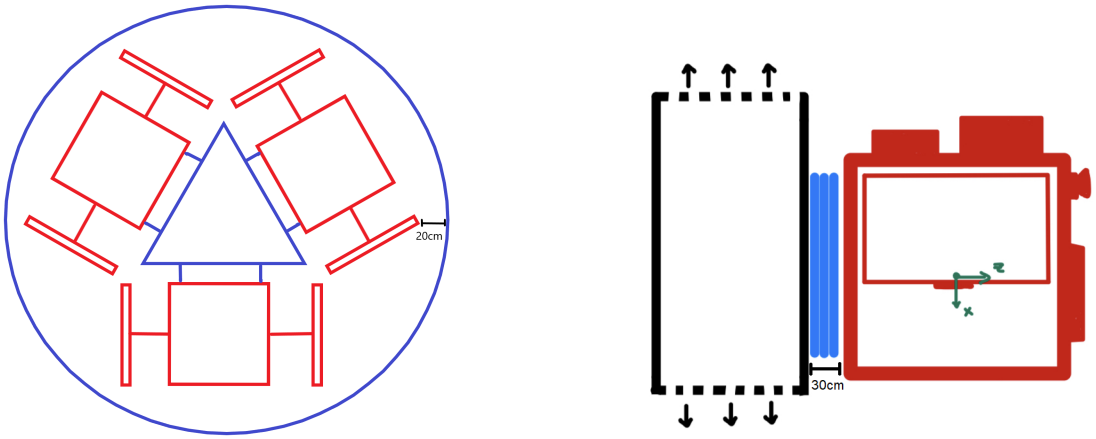

(a) Launcher payload integration triangular configuration.

(b) Detailed View at the payload integration.

Figure 6.17: Payload integration in the launcher

With all components in place, a final analysis of the stresses can be performed to find the limiting thickness and optimise for the lowest mass.

Thickness Iteration

Similarly to the previous stage, the thickness is calculated based on the limiting stresses. There are several stresses considered: tensile, compressive, thermal, buckling, shear, and solar panel bending. All these stresses are checked to not exceed the limits. Fatigue strength is also studied when applicable. All stresses were computed in the script GitHub - Detailed Design, except for the solar panel bending.

During launch, the solar panels are experiencing the same accelerations as the rest of the spacecraft. These solar panels are folded, but are still at the solar support structure's length from the spacecraft panel. This will cause a bending moment at the locations the solar panels are attached. Therefore, the thickness of the structure needs to be designed for this loading mode. To model this load, several assumptions are made:

Table 6.66: Assumptions made for the spacecraft panel thickness iteration.

ID	Assumption	Reasoning
SA-T1	The force of the solar panels due to the launch acceleration is applied at the end of the arm.	Since the solar panels are located at the end of the arm, the force will be concentrated here, the effect of this assumption is minimal.
SA-T2	The spacecraft panel is clamped on all four sides.	This should present similar results, crippling should not occur given the small loads introduced. A sufficient margin is required.
SA-T3	The attachment of the solar panels to the spacecraft panel is a solid connection.	This is assumed as the connections would be designed afterwards and be tailored to the requirements set by the spacecraft panels.

These assumptions are used when doing a Finite Element Methods (FEM) analysis. The FEM will be used to find the limiting thickness of the structural panels. The requirements taken into account during this optimisation are **NTM-SYS-STR-INT-07** and **NTM-SYS-STR-PERF-01**. In this case, **NTM-SYS-STR-INT-07** means that any point on the structural panel should not displace more than $2\,\%$ of the panel's thickness. For the FEM analysis, the solar support structure is attached to the spacecraft panel using an attachment piece. This piece resembles the mechanism that would rotate the spacecraft. The dimensions are different on the x-axis and z-axis to distribute loads better.

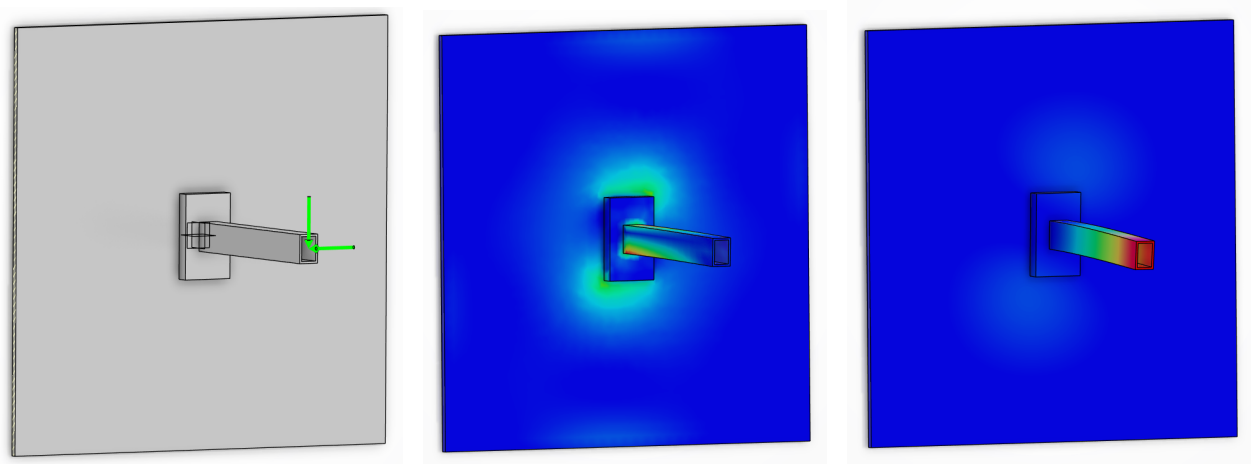

(a) Setup for the FEM analysis solar panel load. **(b)** Results of the stress analysis using FEM **(c)** Results of the displacement analysis using FEM

As seen in Figure 6.18a, both the forces also seen in Figure 6.15 are now applied on the larger system. Now different thicknesses were investigated for the structural panel, ranging from 10 mm to 20 mm. This investigation yields Figure 6.19, where the thickness is plotted vs its deformation when applying the loads.

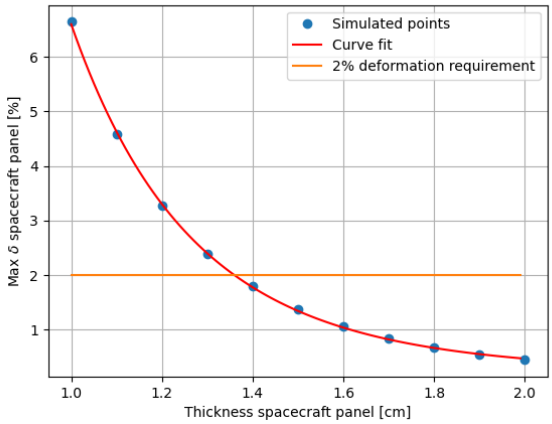

Figure 6.19: Thickness of the structural panel vs. the deflection percentage.

Now that all stress calculations are included in the model, an iteration stage starts. In this, a high dry mass is considered to compute the propellant required. The fuel mass is combined with the components' mass to compute a limiting thickness based on the stresses stated. A new dry mass is obtained, and the process is repeated until convergence is achieved. The limiting thickness is obtained from the maximum deformation allowed by bending due to solar panels. This thickness is 1.4 cm. The other relevant stresses are introduced in Table 6.67.

Table 6.67: Maximum structural loads.

σ_{max} **Tensile Launch [MPa]**	σ_{max} **Compressive Launch [MPa]**	σ_{max} **Tensile Thermal [MPa]**	σ_{max} **Compressive Thermal [MPa]**	τ_{max} **Shear Launch [MPa]**
4.62	-4.62	34.0	-34.0	6.2

From the material properties, the fatigue strength is 150 MPa for 5e8 cycles. Only thermal loads are cyclic stresses. For the designed lifetime of a satellite, it will experience around 10000 cycles, deeming fatigue as negligible for the structure's design.

6.8.4. Final Design

Now that the structural subsystem has been completely designed, all final characteristics can be summed up. The first characteristic to study is the total mass. A mass budget is introduced in Table 6.68, where each subsystem's mass is considered. From it, requirement **NTM-SYS-GEN-01** about mass limit is fulfilled.

Table 6.68: Mass budget spacecraft

Subsystem	Mass[kg]	Percentage
ADCS	24.45	3.6%
CDH	9	1.3%
Navigation	72.5	10.8%
Propulsion	23.93	3.6%
TT&C	10.7	1.6%
TCS	47.95	7.2%
EPS	223.2	33.3%
Structure	273.1	38.6%
Total Dry Mass	669.9	
Total Dry Mass with 20% Margin	803.9	
Propellant	244	
Total Wet Mass	1047.9	

The heaviest subsystems are the EPS subsystem and Structures subsystem. The EPS subsystem's mass comes mainly from the batteries. Due to the many communication and navigation instruments the spacecraft has, the batteries needed are large and heavy. The structure subsystem contains all supports, mechanisms and primary structure. The large bending loads contributed to a heavier skeleton. The total wet mass of 1047.9 kg is consistent with the values obtained in the Initial Sizing, giving confidence in the design. The mass distribution for the subsystems is a bit higher for structure, while the other subsystems have smaller values.

All requirements stated in Table A.7 were fulfilled. The final structural characteristics to include are MMOI and eigenfrequencies. For an unstowed mode of both solar panels and radiators, the MMOI are [365, 132, 375] kgm^2. The natural frequencies during launch are 522 Hz axially and 477 Hz laterally.

Verification & Validation

The verification and validation procedures are performed both on the models developed and on the underlying equations considered. Several assumptions are also validated with more complex methods to ensure they could be used for the current design. Specifically referring to the verification of the computational models, both are tested through unit, module, and sensitivity analysis tests.

The initial design model has verification codes for the Cylinder, Rectangular Prism, and Structure objects. In all three, correct inputs are ensured, followed by tests on the correct output of geometrical features, such as MMOI or cross-sectional areas. The structure object encompasses the first two, and the correct numerical results for limiting thicknesses are tested against hand-calculated values. The addition of solar panels is also studied. No extensive testing was performed on this model since it only provided initial estimates and values obtained are not used further in the report.

On the other hand, the detailed design had more tests, since it is the backbone of the structural design. It tested the Propellant Tank and Structure objects. In the first one, inputs are checked, followed by a correct calculation of the thicknesses for both cylinder and sphere. The sensitivity analysis studies the relation between the thickness and mass of the propellant. The structure initialisation is tested followed by the correct addition of elements. The skeleton, tank, and panel are studied separately. The stresses and vibrations are also verified by hand, and a full system is modelled and compared to handwritten values. Two sensitivity analyses are performed on the MMOI due to distance, as well as changes in the solar panels' area. All tests were successful for both models.

Validation of the structural subsystem is mainly done by checking whether formulas and methods used in the design process are common in spacecraft design. SMAD [101] was primarily used for the design stages up to the solar panel design and thickness iterations. For the solar panel support design, the CATIA linear structural validation tool was used to validate the results. A 5% difference was found in the deflection results received

in the CATIA when compared to the analysis. The deflection received from the linear structural validation was lower than the analysis. For the thickness iteration, linear structural validation was used as a tool for the design. This was mainly due to the very complex system. However, the tool was used for one variable which needed to be checked for the new solar panel bending load only. And was changed in the function of that load. Other loads were checked afterwards using analysis methods from SMAD [101] to validate the final design of this component.

Recommendations
Several recommendations can be given after the design stage of the structure subsystem. These recommendations arise from optimisation opportunities found, lack of time for the design, or more complex scenarios:

- Investigate inwards rotating solar panel supports. This greatly decreases the moment arm of the launch forces on the spacecraft support structure due to the solar panels.
- Investigate the connection joints between structural elements for the solar panels to check whether loads are acceptable.
- Investigate the mechanisms between the rotating elements. These could be major failure points and can change structural characteristics severely.
- Optimise the positioning of elements inside the spacecraft to reduce the total volume, further optimising the mass.
- Study launch load effects on the propellant tank, as well as reassessing the possibility of using it as a support structure.
- Investigate stress concentrations due to holes required by components. This could potentially require reinforcements in certain areas, as well as having an effect on other subsystems.
- Compute stresses and vibrations through more numerical methods, increasing the accuracy by studying the specific test case.

6.9. Conclusion

Written by J.K. Geijsberts.
In this chapter, the design of the navigation satellites was performed and discussed. The satellite was divided into multiple subsystems, which were all designed in their own respect. The subsystems use data from each other to design their respective subsystem. Then, iterations are performed to narrow in on the optimal design. In the final iterations, components are chosen, and these are shown in the respective concluding subsections. There, the respective verification and validation are explained and recommendations are given. This concludes the specific preliminary design. The next chapter summarises them and studies the subsystems' integration.

7

Final Overview

All chapters before focused on performing the design. Now, the design of the LNS and constellation are fixed. In order to comply with requirements considering launch dates and operational status, a plan for logistics must be devised. Additionally, the economic and environmental cost associated with development and deployment of both the LNS and mission. First, section 7.1 describes the timeline of the mission. Then, section 7.2 provides the final parameters of the mission and shows the communications flow. After that, the spacecraft characteristics are summarised in section 7.3, showing the final spacecraft design and the functions of the subsystems. Next, in section 7.4, the RAMS characteristics are evaluated for the mission. All above characteristics lead to the evaluation of the compliance with the compliance matrix in section 7.5. section 7.6 discusses the sustainable development strategy of both the mission and satellite in design and deployment. Finally, the section 7.7 lays out a plan for R&D, testing and manufacturing of the satellites.

7.1. Mission Timeline

Mission Timeline by N. Ricker. Gantt Chart by A. Van Parys. Written by N. Ricker.

The timeline introduces a plan for the team to go from a feasibility design to a fully operational mission. It has a set of phases commonly defined, milestones, and various relevant processes, as seen in Figure 7.1.

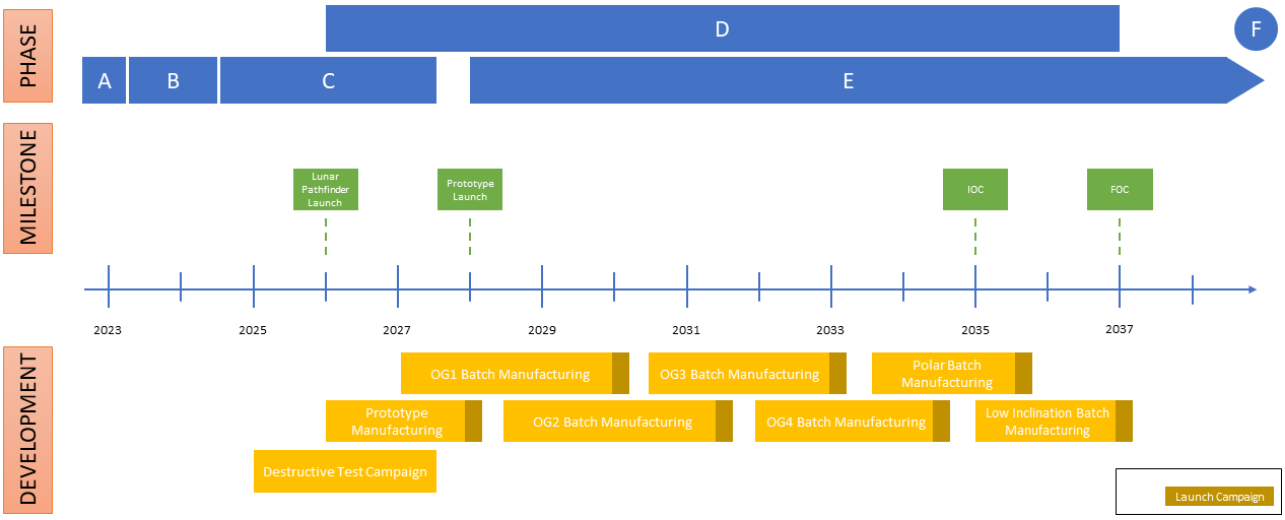

Figure 7.1: Navigating the Moon Timeline

The mission development is planned as a 14-year process, with one year as buffer in case any delays occur. It is divided into different phases, each referring to certain procedures. The phases go from A to F as introduced by ESA [1].

- Phase A - Feasibility. In the first stage of the mission design, some concepts are tested to ensure that the product is reproducible.
- Phase B - Preliminary Definition. The system requirements and interfaces are selected. Subsystems are designed, along with general mission aspects.
- Phase C - Detailed Definition. Two models are developed: Structural and Thermal Model (STM) and Engineering Model (EM). These are subject to tests to prove them beyond doubt.
- Phase D - Qualification and Production. The Flight Model (FM) goes into production, and qualification is performed through the Flight Acceptance Review.
- Phase E - Utilisation. Nominal Operations Phase, where the satellites fulfil their objective.
- Phase F - Disposal. End of Life (EOL) of the satellite or mission, along with corresponding deorbiting procedures.

Phase A corresponds to the first draft performed by the team for the midterm, together with the mission layout set by the tutor. Several concepts were compared and critically analysed. Phase B1 is the state of the project performed in this report. Some initial layout has been set, with preliminary calculations on all subsystems. In the next steps, a more detailed conceptual design is required (B2). For the entire phase, a full calendar year has been assigned. Once the design has been set, a physical testing phase shall take place between 2024 and 2027.

Production is planned to start in 2026, with the earliest launch by 2028. The first satellite is a flight-proven prototype, used as a proof of concept and technology for the constellation. It has a two-year testing window, where necessary modifications can be implemented before sending the first batch to space. Some new technologies, such as self-control and communication through the Lunar Pathfinder shall be tested out. It follows a similar approach to procedures followed by the Galileo navigation system[2].

The year 2030 marks the start of launches for the nominal constellation. Each batch consists of 4-6 satellites manufactured and tested throughout a 2-3 year period, depending on the production learning curve and reliability of the system. After testing, a 3-month period is set for an optimal launch window opportunity. To enable

[1] https://www.esa.int/Science_Exploration/Space_Science/Building_and_testing_spacecraft
[2] https://www.eoportal.org/satellite-missions/giove-a#spacecraft

Initial Operational Capabilities (IOC), a specific launch sequence is set. All launches are chosen to carry all satellites for one orbital plane, reducing the manoeuvres required. The order is introduced below:

- Original Orbit Constellation (OG)
- Polar Orbits
- Low Inclination Orbit

The first constellation has four orbital planes and offers four-fold coverage to the entire Lunar surface. It does not meet requirements regarding DOP, giving a low accuracy. Nonetheless, by sending these elements first, there should be IOC in place by 2035. The next launch is relevant to reduce errors at the poles, given the high scientific relevance they have. Finally, to meet all requirements, the last launch provides better coverage of the Equator. This final launch is planned for 2037. After it has been set in place, FOC are achieved and the service is completely functional. Given the uncertainty in the duration of the service, the final phase (F) does not have a fixed date. As well, further satellite batches might be required given the expected 12-year lifetime per satellite.

The timeline provides a general overview of the mission, now specifics are summarised in further sections of the chapter. A future action plan has been provided in the form of a Gantt Chart in section B.2.

7.2. Mission Characteristics

A navigation system for the Moon must be provided and requirements for this mission must be complied with. These needs are met by designing a navigation mission with the goal to comply with the position, velocity, and time accuracy requirements of the user on the Moon surface, landing on the Moon or orbiting it. These requirements are shown in Appendix A in Table A.2. In order to choose a design, iterations computations including spatial and temporal simulations are done and explained in chapter 4. This part has a structure as follows: first, the general final values for the mission design are presented and discussed. Then, the communication diagram is shown and described. This part also includes considerations about the self-control part of the satellites.

7.2.1. Final Parameters and Discussion

Performed by S. Nedelcu, K. Scherpenzeel; Written by S. Nedelcu

The most important orbital and navigation parameters found in this design are found in Table 7.1.

Table 7.1: Mission Final Design Parameters

Type	Characteristic	Value	Unit
All Orbits	Total Orbit Plane Number	6	[-]
	Total Satellite Number	34	[-]
	Allowable Ephemeris Position Error	0.9494	[m]
	Allowable Ephemeris Velocity Error	0.07841	[m/s]
	Updating Frequency	1.603	[hr]
Navigation Message Content and Size	Satellite ID	6	[bits]
	Satellite Health, Quality and Availability	6	[bits]
	Kepler coordinates in Selenocentric frame	192	[bits]
	Time of Signal Transmission	16	[bits]
	Errors' Correction	104	[bits]
	DSAC-UTC conversion	99	[bits]
	Ephemeris Accuracy	8	[bits]
Relay	Lunar Pathfinder	-	-

Some final comments can be made about these values. The three different types of orbits : original constellation, low inclination and polar, were taken from literature included in Table 7.1. The original constellation did not perform according to the requirements, thus the Moon surface plots were inspected and the addition of the low inclination and the polar orbits was decided. These together perform well enough to meet all accuracy requirements. Moreover, redundancy was also taken into account: if any combination of two satellites fail, all requirements are still met and the navigation system is still full operational. For this, only three satellites have been added in strategic points of the constellation such that no manoeuvres using ΔV are required to compensate for those failures. Then, what is added to the literature are all the DOP calculations which are done for a full period of the furthest satellite from the Moon and all 10000 discretised Moon points. These lead to allowable LNSS satellite errors which when reached, the update period is complete, and they have to

recompute their position with the Moon reflectors and through self-control by inter-satellite linking and send the new updated ephemeris data to the user. This self-control part is also something that has been added to the literature, and it takes 12 minutes as found in subsection 6.2.3 for the satellites to point towards the other satellites and the Moon reflectors to obtain data about their coordinates. Furthermore, computation of those Kepler coordinates from the data done by the CDH subsystem takes 10 minutes and 3 seconds, as found in subsection 6.3.4. Since this number is smaller than half the update period, the system can be functional and provide the navigation service to the user with the required accuracy. Finally, about the Navigation message content, the errors' correction refer to the clock and broadcast group delay ones as stated in Table 4.6 in subsection 4.3.2.

7.2.2. Communication Flow Diagram

Performed by S. Nedelcu, I. Maes

The communication flow is essential to be properly described for an LNSS system. The main interactions between the subsystems for their own Kepler coordinates determination are shown with an emphasis on the process to determine the user's position, velocity, and time. Figure 7.2 gives an overview of the communication within the system.

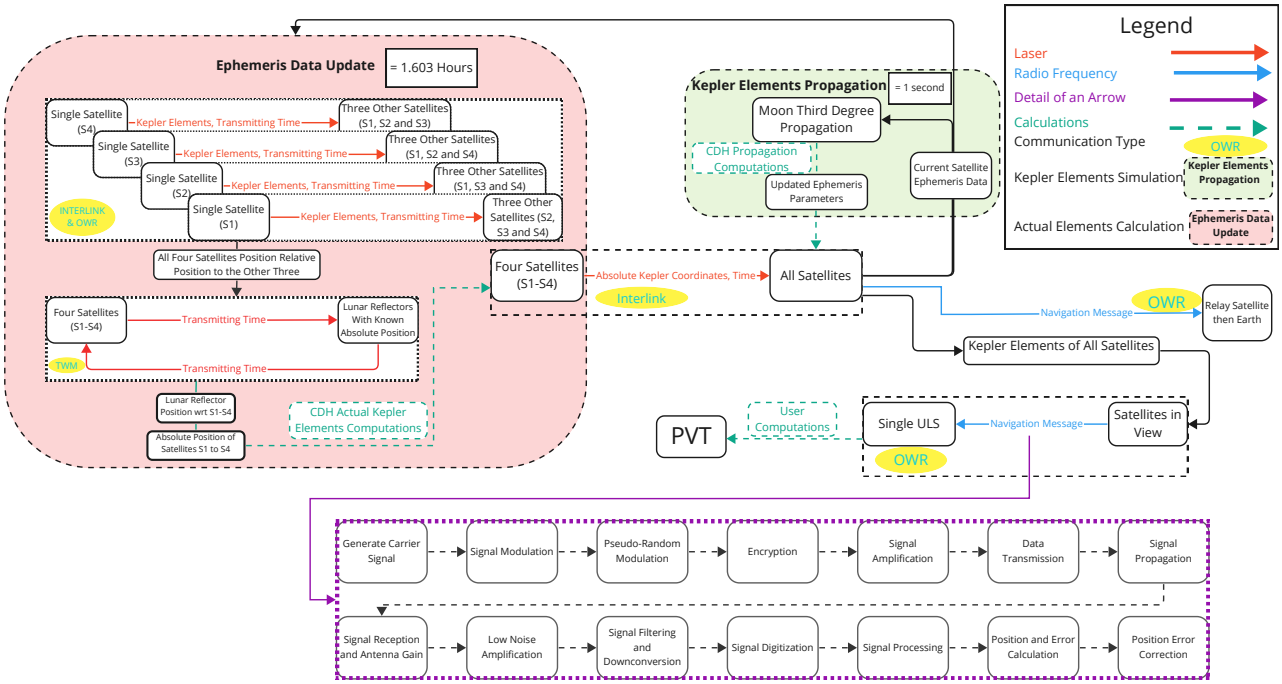

Figure 7.2: Communication Flow Diagram

The main blocks in this diagram consist of the satellites acquiring and computing their own actual position once every update period which is 1h36min11sec (=1.603 hours as seen in the diagram) by communicating between themselves and sending signals to the Moon reflectors, and then between themselves again so that all the satellites know their position. The pointing of the lasers, and the start of the calculations have to begin at least 22 minutes and 3 seconds before the updating frequency, as the updated position should arrive before the end of the ephemeris error window. This is all seen in the red block on the top left in Figure 7.2. Then the satellites in view send the Navigation Message with the actual real Kepler coordinates to the user or to the relay satellite, the Lunar Pathfinder, which will transmit it further to Earth for monitoring. At the same time, as seen in the green block, the satellites propagate their coordinates in time with the third degree Moon gravity field every second starting with the actual Kepler coordinates. These are sent to the user every second using a radio frequency AFS, so that it doesn't have to perform the simulation calculations itself. The user can thus compute its PVT at least once per second to comply with **NTM-SYS-NAV-PVT-01**. However, after 1.603 hours, the deviation from the real coordinates to the propagated ones is too high for the accuracy requirements to be met, consequently, the result of red block (real Kepler coordinates) must be sent to the user again. The satellites find their coordinates and communicate them to the user, the propagation can start again while the satellites recompute their position during the update period of 1.603h. The purple arrow and blocks show a detail on how the signal from satellite to user is built and sent.

7.3. Spacecraft Characteristics

By Everyone. Written by I. Maes

From the general mission description in section 7.2, there are 34 satellites which are orbiting the Moon. To zoom in on the mission design, the spacecraft design including all subsystems parameters and links will be presented in this part. This subsection will discuss first general parameters, followed by the spacecraft layout, internal and external. Following this, the hardware and software diagrams will be discussed. Then, payload integration in the launcher will have a subsubsection. Finally, the spacecrafts' functions and links will be described using an N2 chart in Table 7.3.

7.3.1. Final Parameters and Discussion

These spacecrafts' main performance characteristics can be seen in Table 7.2. These characteristics contain the most important performance aspects for the spacecraft's mission. Some general characteristics are included like the lifetime, ΔV, launch mass, dimensions and power performance. Some more specific characteristics related to the spacecraft's mission are given as well, including its attitude, accuracy, and data performance.

Table 7.2: Spacecraft Main characteristics

Lifetime	12 years
Max ΔV	$617\,\mathrm{m\,s^{-1}}$
Initial Mass	$1047.9\,\mathrm{kg}$
Dimensions (unstowed)	9737.5 x 3060 x $1576.1\,\mathrm{mm}$
Dimensions (stowed)	2347.75 x 1560.27 x $1576.1\,\mathrm{mm}$
Clock Drift	$1\,\mathrm{s}$ in 10 million years
EOL Solar Array Average Power	$1338.7\,\mathrm{W}$
Batteries Capacity	$2366.1\,\mathrm{W\,h}$, $4832.5\,\mathrm{W\,h}$
Nominal Operating Temperature	[289.9-308.2] K
Attitude Control Accuracy	$0.46°$
Computation Time	$10\,\mathrm{min}\ 3\,\mathrm{s}$
Laser Pointing Time	$12\,\mathrm{min}$
Power Transmitted to User	$13.3\,\mathrm{W}$
SNR Relay	$26.29\,\mathrm{dB}$
#Photons Received OISL	8658.031
#Photons Received Retroreflector Ranging	18.566

7.3.2. Function N2 Chart

By J.K. Geijsberts

For the functioning of the spacecraft to be shown, an N2 chart can be made. Here, the subsystems are shown on the diagonal, and their inputs and outputs to and from other subsystems are shown in the cells other than the diagonal. The N2 chart can be seen in Table 7.3

Table 7.3: N2 chart for the functions within the spacecraft. The subsystems on the diagonal receive or send inputs and outputs to the other subsystems which makes use of them.

Structures				Propellant tank		Controlling Solar Panels	
	Navigation	RINEX data, clock data					
Commands for moving the solar panel	Commands for controlling the NSGU, FFGU, and CMCU	***CDH***	Commands for creating the signal, moving antennas, data for antennas and lasers	Commands for starting the engine	Commands for controlling the CMGs		Commands for controlling the radiators
		Received data for analysis and computations	***TT&C***				
		Operational data of the engine		***Propulsion***	Desaturation		
		Operational data, Attitude data	Provide attitude for pointing the lasers and the antennas	Provide attitude for accurate positioning of engine	***ADCS***	Provide attitude s.t. the solar panels function as required	Provide attitude s.t. the spacecraft is in the temperature range as required
Power for controlling solar panels	Power for the clocks, NSGU, FFGU, and CMCU	Power data of other subsystems, power for the computer	Power for the antennas and lasers	Power for the pumps and valves in the engine and for the RCS valves	Power for activating the CMGs	***EPS***	Power for the radiators
Regulating temperature of the structure of the spacecraft	Regulating temperatures of the clocks, NSGU, FFGU, and CMCU	Temperature and operational data of other subsystems, regulating temperature of the computer	Regulating temperatures of the antennas and lasers	Regulating the engine temperature	Regulating CMG, gyroscope, and sensor temperatures	Regulate solar panel temperature	***TCS***

As can be seen in Table 7.3, the most important part in the functioning of the spacecraft is the CDH, which commands all the other subsystems. All data is first sent to the CDH subsystem, after which it is processed to then be sent to the other subsystem that needs that processed data. Two other important subsystems are the TCS and EPS subsystems, which determine the temperature of other subsystems as well as the power that they receive. The ADCS subsystem allows for the attitude to be changed depending on the requirements of the other subsystems.

7.3.3. Spacecraft Layout

Internal

Written by I. Maes. Designed by N. Ricker and I. Maes

The largest and most massive internal components are positioned in the CATIA. These are modelled like cuboids that represent their 3D dimensions. The layout has been optimised to provide limited distance between the components that are most interconnected. This is also the case for the external components of the spacecraft. As can be seen, the NSGU and FGUU are located near the antenna and lasers where signal generation is needed. The atomic clocks are located close to these, since information exchange is constant between these components. The propellant tank is kept in the middle of the spacecraft. The propellant tank with its fuel is the most massive component in the spacecraft. To keep its effect on increasing the MMOI low and the displacement of the C.G. minimal, it is placed at the centre of the spacecraft. The CMG's need to be close to the C.G. for maximal effect and are therefore located nearest to the C.G. still possible. The gyroscopes' axis needs

to cross the C.G, they are spaced around the propellant tank for this purpose. The PCDU, batteries, Phase CMCU are positioned on the opposite side of the NSGU, FGUU, computer and atomic clocks. The reasoning behind this is mainly to keep the C.G. central, since all these components are relatively heavy. The PCDU and batteries are located closely for simple integration between these components. Figure 7.3, Figure 7.4 and Figure 7.5 show a preliminary visualisation of this positioning.

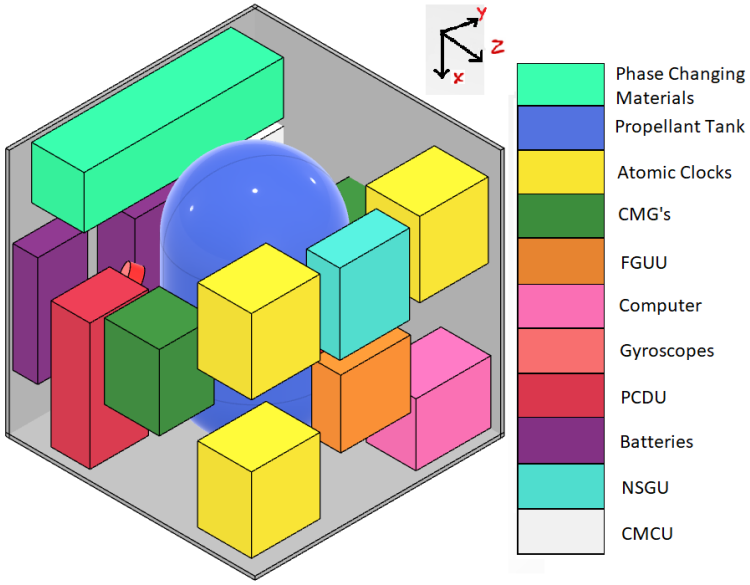

Figure 7.3: Satellite inner components isometric view

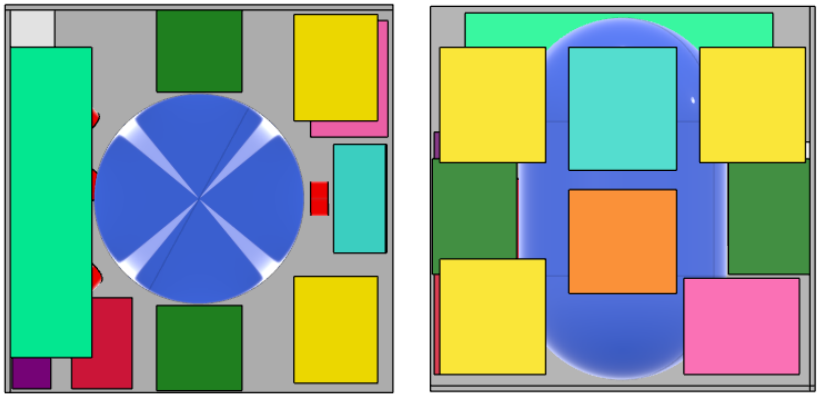

(a) Satellite inner components top view **(b)** Satellite inner components front view

Figure 7.4: Various views of the spacecraft inner layout.

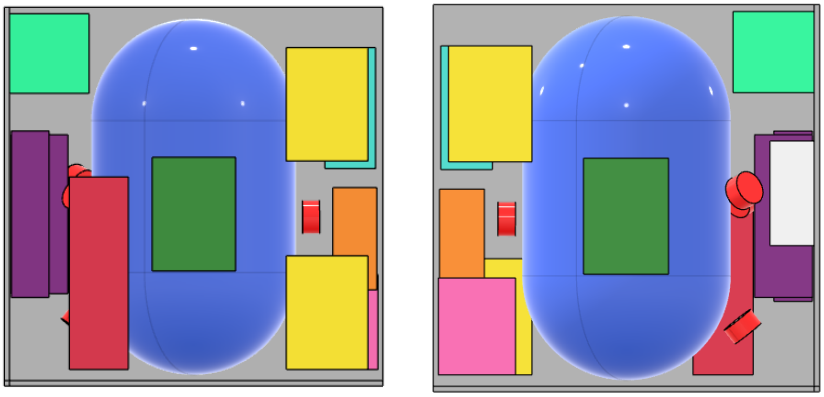

(a) Satellite inner components left view **(b)** Satellite inner components right view

Figure 7.5: Various views of the spacecraft inner layout.

Several areas within the spacecraft do not contain any components in the visualisations. These areas would serve as space for support structures for the internal components, the cable harness for the connections between components, filters and valves for the ADCS and propulsion system and for structural mechanisms.

External

By I.Maes

The spacecraft's main external components are shown in Figure 7.6. A more detailed look is provided in the technical drawing seen in section B.1. The exterior design of the spacecraft is optimised to provide good viewing angles to the critical instruments of the spacecraft. The optical lasers and the S-Band antenna are located at the Moon facing side of the spacecraft. The optical lasers use a gimbal to be able to accurately point towards the Lunar reflectors and other satellites for interlink communication. Both solar panels and the radiators are located as such to not block their view. The solar panels and the radiators are the largest structures attached to the spacecraft. The radiators are located where most heat is generated by internal components. These being the clocks, NSGU for the top radiator and the thrusters for the bottom radiator. The solar panels are situated to provide the least amount of movement needed for sun pointing. The GR 22 thrusters of the spacecraft are located in the direction of velocity of the spacecraft and the GR 1 thruster are located in various locations to provide 3-dimensional manoeuvre capabilities. Finally, the star sensors are situated on 4 different sides of the spacecraft to provide different reference points for attitude determination.

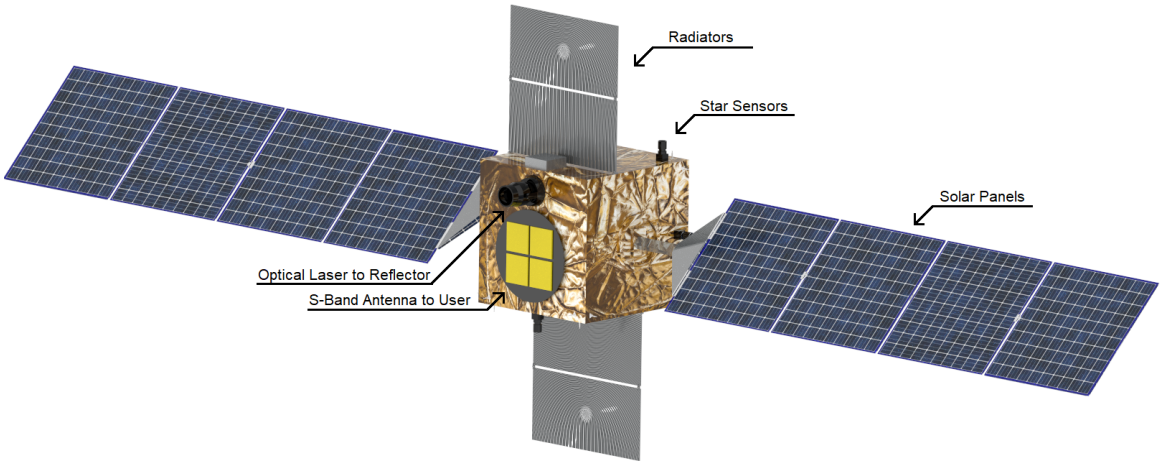

Figure 7.6: External layout of the spacecraft.

Overall, the spacecraft is configured in function of the payload, meaning the antennas take centre stage in the design philosophy, together with the layout of the internal components, the design is optimised for delivering the navigation service.

7.3.4. Hardware/Software Diagrams

Hardware

By I. Maes, S. Nedelcu

The hardware diagram provides a visual representation of the essential components and their interconnection in the mission network. It shows the physical elements involved in receiving and processing signals. The main subsystems in the design are the Earth ground station for monitoring, the satellite constellation around the Moon providing navigation services and the relay satellite enabling communication between the Earth GS and the Lunar satellite constellation. Figure 7.7 shows the hardware diagram. Note that in the Central Processing Unit (CPU), the Power Generation Unit provides power to the whole CPU, and therefore the Electrical Power Cables are only necessary for the Transceivers, which are positioned outside the CPU.

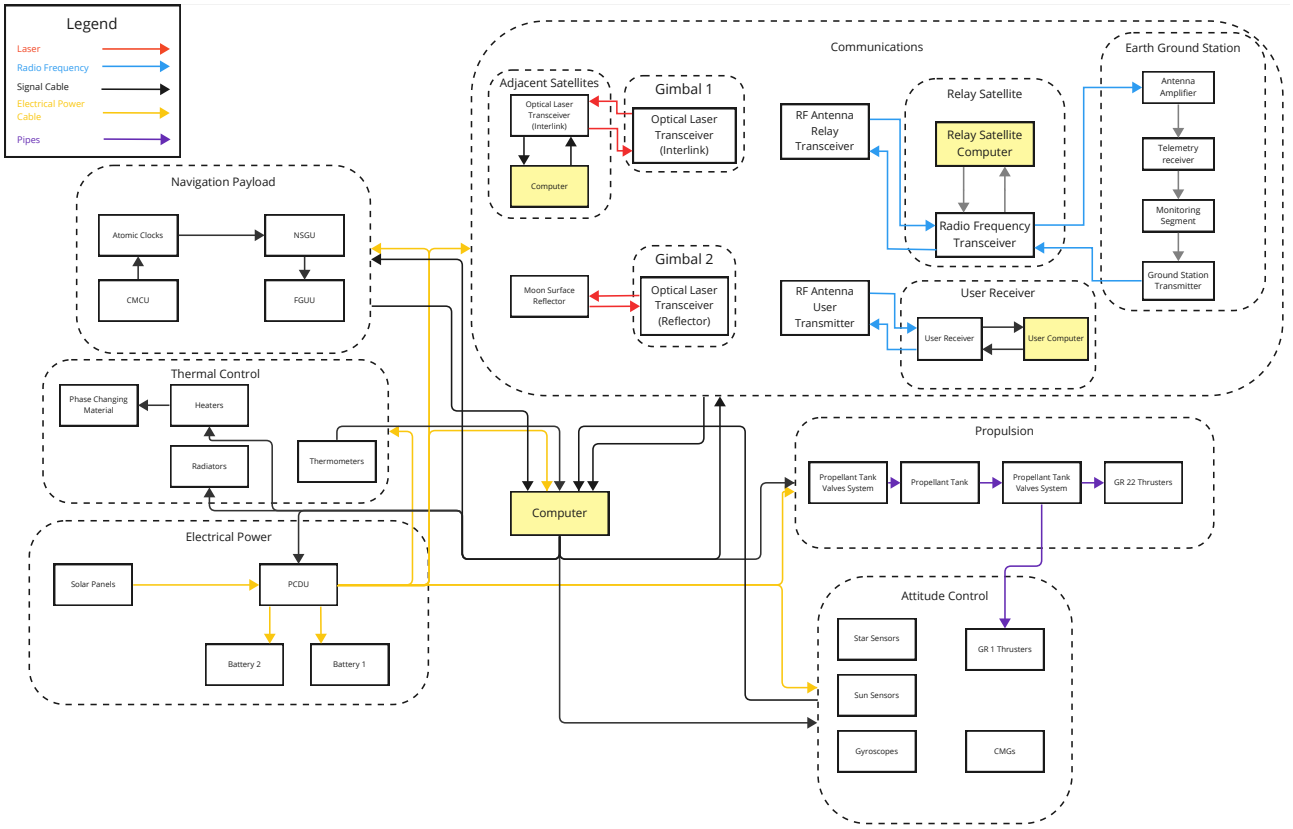

Figure 7.7: Hardware block diagram

Software

By M. Vereycken, S. Nedelcu

The diagram in Figure 7.8 represents all essential software processes. It shows what information needs to be extracted and how it will be transferred.

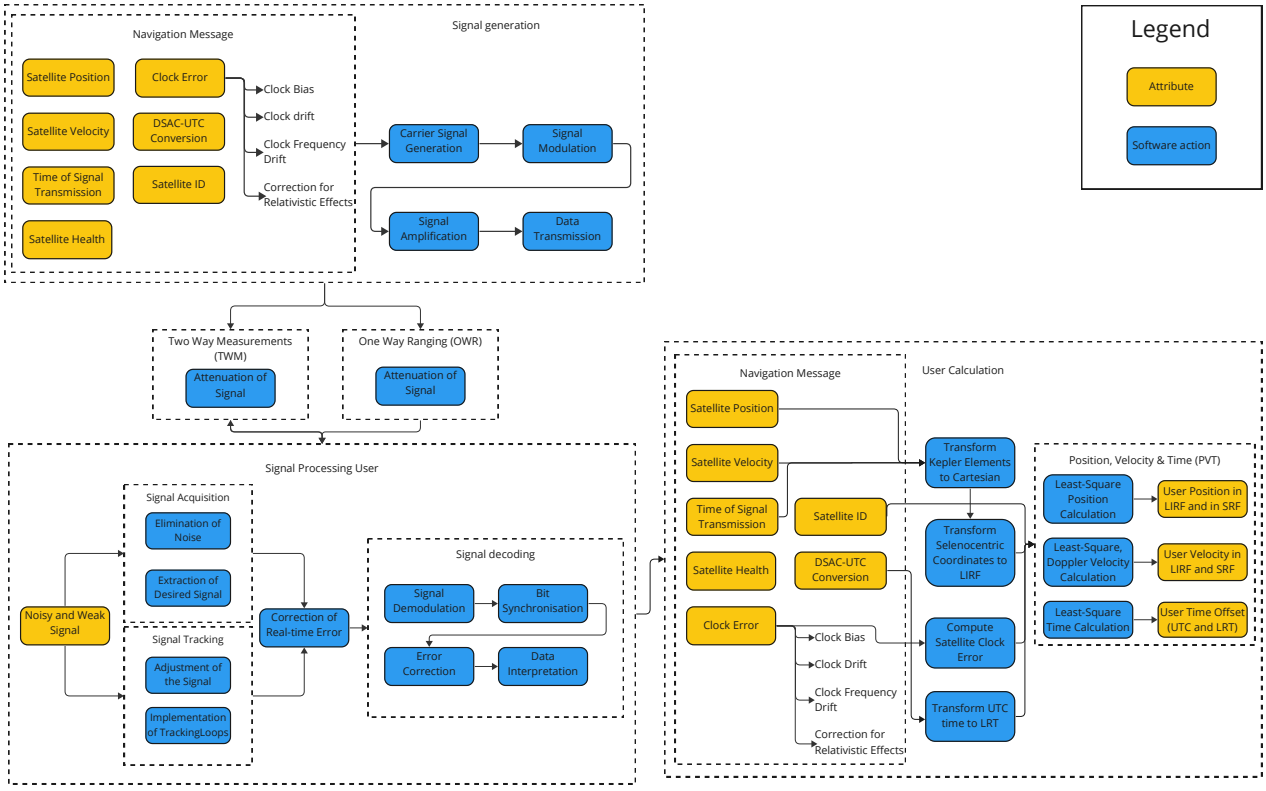

Figure 7.8: Software block diagram

The message signal is modified to account for the attenuation that would occur during the TWM and OWR services. This is achieved through signal modulation and amplification to obtain the modulated signal that will carry the satellite's ephemeris data to the receiver. When it reaches the receiver, the signal will be noisy and weakened due to the environment and distance travelled. Hence, the software will have to be able to eliminate the noise from the acquired noise and also eliminate any other effects due to disturbances. The software will also have to accurately retrieve the original data signal from the now distorted modulated one. The Navigation Message does not include everything that was previously discussed, only the relevant parts for the user to compute its PVT. Clock corrections are described according to [117] and are included in the message so that the user can use them to mitigate the error as much as possible.

Lastly, SRF means Selenocentric Reference Frame and LIRF stands for Lunar Inertial Reference Frame. The calculations the user must perform in order to comply with most requirements include transforming from SRF Kepler to Cartesian coordinates, which will give the Cartesian position and velocity of the satellites. After this, frames can be transformed from the SRF to LIRF in order to comply with both **NTM-SYS-NAV-03** and **NTM-SYS-NAV-04**. Finally, UTC to LRT can be done as well in order to comply with both **NTM-SYS-NAV-05** and **NTM-SYS-NAV-TS-02**. Finally, the least squares estimations can be performed in order for the user to compute its position, velocity, and time within the 2-sigma accuracy requirements, which are all met.

7.4. Reliability, Availability, Maintainability & Safety

The designed Lunar navigation satellite constellation is a vital component in providing critical positioning, velocity and time services for users operating in the Lunar environment. Ensuring the reliability, availability, maintainability, and safety of such a constellation is of most importance. This section explains the key RAMS characteristics of the LNSS, ensuring the operational success, longevity, and safety.

7.4.1. Reliability

By I. Maes

The reliability of the navigation services is a crucial aspect of the Lunar navigation satellite constellation. Reliability refers to the constellation's ability to provide navigation services without degradation or failure. On a more detailed level, it also refers to the capability of the satellite to perform its functions without degradation. On a satellite level, **NTM-SYS-STR-PERF-10** is an example of a reliability requirement needed for the functioning of the satellite for a prolonged period of time. The reliability of the satellites in the constellation is tested

by extensive testing campaigns during the production phase. These tests provide insight into the reliability of subsystems and the complete system. Reliability is also introduced in the constellation design by using several backup satellites. These satellites make sure there is little to no reduction in navigation service quality after satellite failures.

7.4.2. Availability
By M. Vereycken

Maximising availability is crucial for a Lunar navigation satellite constellation to provide continuous and reliable navigation services. Availability refers to the percentage of time the constellation is operational and able to deliver its intended service. Hence, clear requirements should be set up which include constraints on the minimum availability of the service. One of the requirements extracted from this philosophy is **NTM-SYS-NAV-TS-04:** which can be found in Table A.2. Minimising downtime due to failures, maintenance activities, or other factors is essential. Therefore, redundancies and fault management strategies should be implemented during the design. Components that are prompt to have a high failure rate, like the orbital maintenance thrusters, need redundancy incorporated to ensure a high-quality service. Additionally, efficient maintenance such as software updates should be created while still providing the service. This can be done by updating the satellites' software one by one such that the required availability is always met.

7.4.3. Maintainability
By I.Maes, M. Vereycken

Maintainability focuses on the service needed to keep the navigation system operational. Before the deployment of each satellite, the structure of the satellite is designed to be easily accessible. This makes upgrading or repairing components straightforward. After deployment, repairing and upgrading the satellites is not possible. However, software updates should be considered to increase service quality and satellite performance. By clear communication between the LNSS, relay satellite and Earth ground station, LNSS downtime can be minimised. Furthermore, by implementing intelligent updating of the satellites, which is explained in subsection 7.4.2, coverage and accuracy requirements can still be met. Later, new satellites with better navigation components can be launched, which can improve the constellation's performance and replace older satellites. A self-control system does regular orbit maintenance. Self-control is a design choice that makes maintainability of the constellation significantly more efficient. No resources have to be spent on the computation and propagation of the satellite's state and position. To make sure the constellation and satellites are performing well, remote monitoring is introduced. Satellites send ephemeris data, which includes satellite health data, to the Earth ground station.

7.4.4. Safety
By I. Maes, M. Vereycken

Safety concerns the constellation's risks to other missions and people. **NTM-USER-08** is a major requirement related to safety. In the constellation's case, this is mostly related to EOL protocols. To prevent failing satellites to be a danger to users on the Moon, the satellites will perform an EOL burn, which makes them crash in a graveyard crater. Collision avoidance protocols play a critical role in ensuring mission safety. These collisions can critically damage satellites, making them inoperative. This could even prevent its EOL protocols to be performed. The Earth ground station will monitor large debris. If a collision course is detected, the Earth ground station will command the satellites to perform a manoeuvre to avoid the collision, ensuring the mission's safety.

7.5. Compliance Matrix and Feasibility Analysis
By J.K. Geijsberts

In this section, the compliance matrix, which shows the user requirements and whether they are met, is shown in Table 7.4. Next to that, a feasibility analysis is performed which states modifications needed to make the design comply with the user requirements as well as a rationale why parts of the current design do not comply with the user requirements.

7.5.1. Compliance Table
In this subsection, the compliance matrix showcasing the compliance to the user requirements is shown in Table 7.4. If a requirement is not complied with, no checkmark is present in the compliance matrix and an explanation is given in subsection 7.5.2.

Table 7.4: The compliance matrix showing the user requirements and if they are complied with.

ID	Requirement	Compliance
NTM-USER-01	The position of orbiters shall be determined with an accuracy of at least 100 m within two-sigma standard deviation.	✓
NTM-USER-02	The position during landing shall be determined with an accuracy of at least 50 m within two-sigma standard deviation.	✓
NTM-USER-03	The position on the surface shall be determined with an accuracy of at least 10 m within two-sigma standard deviation.	✓
NTM-USER-04	The velocity during landing and on the surface shall be determined with an accuracy of at least $1\,\mathrm{m\,s^{-1}}$ within two-sigma standard deviation.	✓
NTM-USER-05	The time dissemination on the Moon shall have an accuracy of less than 1 microsecond.	✓
NTM-USER-06	The system shall be failure-proof up to 2 provider nodes.	✓
NTM-USER-07	Costs shall include costs of offsetting or paying for atmospheric pollution through greenhouse gases or substances for the ozone layer.	✓
NTM-USER-08	The system shall not pose a risk to humans or user's equipment on the Moon at the end of life.	Intend to comply with
NTM-USER-09	The total development cost shall be below 10 billion euro.	✓
NTM-USER-10	The first deployment of the network shall take place at latest in 2028.	✓
NTM-USER-11	The navigation system shall include coverage of the South Pole and back side of the Moon.	✓
NTM-USER-12	The system shall be compliant with the legal specifications.	Intend to comply with

7.5.2. Feasibility Analysis

In this subsection, the feasibility analysis, which includes a rationale for requirements that were not met, and modifications to the design to make it comply with these requirements, is shown. Only user requirements that need analysis are shown.

Non-compliance with NTM-USER-08

Although an assigned area to crash each of the satellites has been found, the risk still exists. The requirement has therefore not been fully complied with. A modification that could be made is to perform research on finding a graveyard orbit around the Moon.

Non-compliance with NTM-USER-12

Two of the three link budgets are fully compliant with the legal specifications: The one to the relay and the one to the user. The laser links are not compliant in the sense that the cross-link should have used a wavelength of 1550 nm, and the wavelength that was actually used was not this wavelength (but instead a wavelength of 532 nm). This is because existing, but slightly modified lasers, which do not use the wavelength of 1550 nm, are used in the ODTS system. The lasers are used for ranging instead of communications, which is why this choice was justified. However, modifications to the laser or new designs can be made, changing the wavelength to 1550 nm. Other than that, the laser link is fully compliant.

7.6. Sustainability Strategy

Performed by A. Van Parys and N. Ricker. Written by A. Van Parys.

This section is based upon the Sustainability Strategy from the Baseline Report [6] and upon the elaboration in the Midterm Report [5]. In this final report, this strategy is further elaborated upon in both subsystem design and in this section. Since sustainability is a crucial element that is considered during the design of every single subsystem separately, as it is fundamental in every step of the design phase. Therefore, it requires contribution of every single subsystem. This section focuses on the sustainability effects from the technical aspect throughout the entire mission, which is crucial to include as it is an intrinsic component in the requirements and constraints, as well as the design of the mission. The section studies environmental and social/economic sustainability. It is divided into sustainability during the design of the mission in subsection 7.6.1 and sustainability during the mission in subsection 7.6.2. This section thus mainly focuses on the entire mission, however further detailed sustainability analysis can be found in the relevant subsystem designs.

7.6.1. Sustainability on Design

The design of the mission is vital for sustainability. It gives the path the mission will follow throughout its life. Two main components are considered: Research and Development, and Manufacturing.

Research & Development

Research and Development (R&D) is an integral part of the whole mission. In this phase, the steps to follow are defined as the objectives, requirements, and constraints. Even though the direct environmental and social impact of a poor R&D plan is not severe, the chain effect flowing down onto the next steps could lead to the success or failure of the mission.

The first component to consider is the mission design. In the early stages of the mission, there were multiple viable options and the best one has been chosen. The best option is generally a trade-off between technical, economic, social, and sustainable parts. As composites and toxic materials are often used in the space industry, innovative alternatives must be considered which can be recycled energy-efficient and emission friendly. First, the design was made as simple as possible and flexible. Given the large variation in the first stages, the design was made adaptable to changes, to avoid time and money being wasted. Moreover, the design was made as simple as possible, to avoid confusion, extra time, and miscommunication. To accomplish this, the design has been encapsulated in smaller subsystems, for which clearly defined requirements were set, allowing for the creation of products that perform no better than required, without spending extra effort on unnecessary features.

Referring specifically to satellite design, there are certain design choices affecting environmental sustainability. In line with this, the project focused on optimising the number of satellites. Optimising does not necessarily imply minimising the number of satellites, but rather performing a trade-off between complexity, propellant needed, waste produced, and risk. Furthermore, the system has been adapted from and uses GNSS systems as much as possible. Recycling as much knowledge and reallocating resources to other components. Finally, there has been a constant analysis on the total failure risk, such that it can be minimised. This can be achieved through the implementation of redundancy of subsystem elements.

Responsible management minimises the chance of inappropriate use of resources. This is done by carefully planning and setting up an efficient design and manufacturing plan. During the development stage the relevant resources consist of energy, computational power, time, and money. The system design also uses a reusable energy system; solar arrays, along with passive thermal control systems, were possible. This allows for less resource allocation.

There is also a social sustainability component to be considered while performing R&D. First, all employees shall work to the maximum of their capacity, but without overworking themselves. It promotes an efficient work scheme and reduces waste. A proper study of the stakeholders and the risks related to them is relevant to keep a positive atmosphere around the mission. Along the same lines, people involved in the project shall not be discriminated against, promoting diversity and inclusion in all areas of the mission. In such an environment, all workers will be able to contribute and open up about both technical and non-technical aspects of the job. Finally, the mission must follow an ethical approach. It is vital for a mission with such complex systems to be transparent and open in the development. Furthermore, the sustainable development strategies should make it to the work floor. Both can be checked by external partners like ESA. This will generate trust with potential customers. Finally, all regulations must be checked to meet political requests.

Manufacturing
Manufacturing is a crucial aspect to consider in the sustainability analysis of the mission, as it is the process were relatively the largest amount of waste is generated. Wastes can be grouped into waste of energy, workforce, potential as well as waste in material resources. These wastes and sustainability aspects are considered for both the environmental and social aspects during the manufacturing phase.

In the manufacturing process, there are a multitude of aspects that have an influence on the environmental sustainability. A large contribution is delivered by the choice of materials used in the spacecraft and infrastructure. First of all, when looking into the possible materials, specific attention should be given to green or biological materials. Biological based composites are a great example of this, although further research on utilisation in space application is required. Self-healing materials are another promising option to prevent possible repairs necessary due to the failure of certain systems or to prevent the failure of the entire spacecraft. The selected materials should also be recyclable where possible, especially after decommissioning where a spacecraft may crash on the Lunar surface. As there are already plans for a Lunar space debris landing zone, recycling of crashed spacecraft can be feasible[3]. Metals or thermoplastic composites are both viable options for recycling, due to their ability to be reformed and repurposed. Finally, the materials should be processed sustainably, processes that are polluting should be limited, and alternative materials should be considered if production of a material is not possible without such a process. Because of these reasons, Aluminium 7075-T73 was chosen as the material of the main structure. Its manufacturing methods are well-established, and innovations are being made for more sustainable production[4]. It is also commonly used in the space industry and permits flexibility in the design.

Within the manufacturing process, the part production also needs to be considered. This can be done in an environmentally sustainable way by minimising the overall production of waste. Additive manufacturing comfortably enables the production of parts with zero or highly limited waste, so this technology should definitely be considered, however, this also depends on the materials used. Furthermore, it is beneficial in general to use the Lean Manufacturing principles to minimise waste, whilst maximising value added to each process. Part production can also be done by external companies. To ensure ethical work circumstances, surprise visits are considered as well as talking to employees. Additionally, the external companies should provide their V&V plan to ensure good quality of the product.

Furthermore, in the assembly process, environmental sustainability needs to be considered. Again, the main goal here is to minimise the overall waste production. It might be beneficial to perform the assembly using a dock configuration, as this is generally the most efficient assembly method for spacecraft [10]. However, the use of batch manufacturing could also be further investigated, although the waste will most likely be higher. Waste can also be minimised by implementing a Just-In-Time principle, as less time, storage space and thus cost is wasted during the assembly. Furthermore, waste is avoided by assembling the spacecraft for each launch in a separate batch, this way the benefits of very similar parallel production can be used, but also improvements learned from the previous batch can be implemented in the next batch, such that waste is consistently minimised.

Transportation is another element of the manufacturing process where environmental sustainability should be taken into account. The transportation of the spacecraft should be aimed to be performed using a transportation method which has the lowest emissions, such that the impact on the environment is minimised. Transportation using trains would be a good option, that is preferred over trucks or planes.

A crucial element of the manufacturing process is the energy provided to enable each manufacturing step. This energy should be from environmentally sustainable sources, such as solar, wind, hydropowered or nuclear sources. The last option could be argued to be less sustainable, however considering the huge amount of energy that will be needed during the manufacturing process, it is definitely an option that should be considered as probably not all energy will be able to come from the other 3 sources.

Even after making each manufacturing step as environmentally sustainable as possible, during the entire manufacturing process there will still be atmospheric pollution through greenhouse gases and through ozone layer damaging substances. However, all of this pollution should still be offset by funding several carbon offset

[3] https://lunarresourcesregistry.com/infrastructure/space-debris-graveyard/

[4] https://www.comhan.com/en/blog/news/how-sustainable-aluminium#:~:text=Aluminium%20can%20be%20recycled%20without,very%20durable%20type%20of%20metal.

projects such that our design will be carbon-neutral and does not contribute to climate change. The costs of this will need to be included in the cost budget. Not only the pollution but also the water usage shall be kept to a minimum during the entire manufacturing process. Especially during material processing and part manufacturing a lot of water is used, so by focusing on these the overall water usage can be significantly decreased. A serious effort should be made to look into alternative manufacturing techniques and into ways how to minimise the overall water use in existing processes.

Next to environmental sustainability, also social sustainability during the manufacturing processes should be considered. First of all the workforce in every manufacturing step should be used in the most efficient manner, they should also be treated in a humane manner, a motivating work environment should be in place and each worker should be compensated fairly for their labour. Most of these concepts can be achieved by again introducing a lean system in the manufacturing process. Finally, the source of the materials used is also crucial for social sustainability. The materials shouldn't be produced or extracted in environments where the workforce is exploited to obtain these materials. In general, ethical manufacturing is desired for the entire manufacturing process from raw material to end product.

7.6.2. Sustainability during Mission

Next to sustainability during design, also the sustainability during the mission shall be considered. As all aspects of the mission shall be considered during a sustainability analysis, the following parts are covered: the launch, the mission operation, the end of life of a single spacecraft, and the end of the entire mission.

Launch

During launch, there are large risks, both for the mission and the environment. These should be minimised to achieve a sustainable outcome. First, there needs to be a proper analysis on the launcher and how it affects its surroundings. In order to reduce waste and comply with environmental sustainability measures, aim to use reusable launcher. As well, the fuel must be as clean as possible, and the budget should account for pollution offset. Pollution offset will work as a countermeasure for damaging effects on the Earth. Looking into sustainable launching companies is also a good alternative. Since the mission considers acquiring a travel pass to the Moon instead of designing one, the options to limit its effects are not broad.

On the other hand, the team does have certain control on the number of launches and trajectories followed. Minimising the amount of launches could provide significant improvements both on economic and environmental sustainability. The mission design has a relevance in how many launches are needed, given the orbiting paths of the satellites. The trajectory taken by a rocket shall be efficient and traded off with the consequences left behind. Some areas must be spared, such as cities, military zones or protected natural areas. This permits a healthier relation with regulatory bodies and communities. As well, time needed for launching each satellite shall be considered and reduced, since it allows for a faster transition into a navigable Moon surface. It provides an increase in interest and revenue.

The spacecraft will be compliant with all safety regulations to reduce the risk of failure. A clear case is the launch requirements, such as loads and vibrations. They have been examined in detail in order to reduce risks. In case of failure, there will be a loss in time, money, and effort. It would produce an effect on various stakeholders, hurting motivation and scaring potential clients. The use of a Radioisotope Thermoelectric Generator (RTG) was looked at, but it has been neglected, so it will not have an influence on the launch.

Some specific stakeholders have an important role during launch, mainly the staff involved in the launch and the population surrounding the launching site. The amplified consequences of a launch must be considered when building the site and how they might exert an effect on its surroundings. The noise, pollution, and water usage are enormous and must be dealt with. As a customer for the launching company, the team shall choose a business that takes all these elements into consideration. A competitive process can be performed to achieve this goal, comparing all competitors and finding one that complies with all requirements.

The workers in the launching company are also relevant when referring to social sustainability. There must be proved safety protocols throughout the launching procedure. It confirms people are safe and there are fewer risks. As well, given a large segment of the company participates in the success of a launch, involving them during launching phases increases motivation and should be promoted. Once again, ethics should be involved in the launching process, along with following regulations and being transparent.

Taking all of this into account, the Falcon Heavy will be used to launch the batches of satellites to TLI and the polar satellites. The propellant used by the vehicle is RP-1 and O_2(l). Both propellants are accepted by ESA [5] and can be used for future launches. However, due to the use of RP-1, 467.4×10^3 kg of CO_2 is emitted per launch, as calculated in [5]. Five launches are necessary, which will produce 2337×10^3 kg CO_2, or 6.3×10^{-8} % of total CO_2 produced in 2021 [6]. Additionally, O_2(l) is one of the greenest propellants out there. Furthermore, The boosters and main stage are partially reusable because they land back on Earth after launch. Combining all this, the Falcon Heavy is one of the greenest launchers on the current market.

Next to the Falcon Heavy, the Falcon 9 will be used to launch the prototype and the low inclination satellites. The propellants used by Falcon 9 are also RP-1 and O_2(l). Due to the use of RP-1, 336.552×10^3 kg of CO_2 is emitted per Falcon 9 launch[7]. Two launches are necessary, which will produce 673×10^3 kg CO_2, or 1.8×10^{-8} % of total CO_2 produced in 2021. The rocket is partially reusable, as the first stage lands back on Earth's surface after launch and can be reused in a next launch. Combining all this, the Falcon 9 is also one of the more sustainable launchers on the current market.

Operation

The operation is another process of the mission where sustainability should be considered. The operation is seen as the most important part of the mission as this is the part where the actual mission objective will be achieved, making this part sustainable is thus significant to make the entire mission more sustainable. Furthermore, the operation spans a long period of time, which means that bad sustainability can have a large influence over time.

During the entire operation of the mission, there are several aspects that have an influence on environmental sustainability. First of all space debris and other spacecraft have been considered when determining both the transfer orbit and the trajectory around the Moon as a collision with any form of space debris or other spacecraft could be catastrophic for the mission and would have a detrimental effect on the Lunar-Earth space environment. Furthermore, when determining the trajectory, the most efficient trajectory option has been chosen, in the form of frozen orbits, such that the propellant usage can be minimised and the overall emissions of the mission are kept to a minimum. The station-keeping manoeuvres are also minimised thanks to the frozen orbits. This will further reduce the propellant usage and thus the overall emissions are also reduced again. Next to that, during trajectory determination gravity assist is being used where possible to minimise the required ΔV and this again reduces propellant usage and emissions to the environment.

Environmental sustainability has also been implemented in the ADCS. It has been designed to achieve the required Attitude and Control, using natural forces as much as possible, this will reduce the required propellant or power depending on the specific ADCS component. This will again reduce the overall emissions of the mission. Power will also be saved by using different possible modes in the spacecraft operation, to minimise the power usage in each scenario, by shutting off unnecessary systems in each scenario. For example, a dark mode could be used when the satellite is in eclipse, as no power can be provided by the solar arrays. This reduces the required power of the satellite enabling either smaller batteries to be installed on the spacecraft, reducing the overall mass, and thus also the required propellant for the manoeuvres and launch, thus reducing the emissions.

The choice of propellant will obviously have a significant impact on the environmental sustainability as well. The propellant used during the operation was designed to be sustainable according to the REACH regulations [118]. The high-performing, but highly toxic propellant hydrazine thus had to be avoided at all costs and research has been done to find suitable alternatives. For the design of the navigational satellites, green propellants have been considered for orbital maintenance, as they benefit the protection of celestial bodies and their environment. After careful consideration of both green-monopropellants and electrical propulsion, which are both sustainable options, the choice was made to go for the AF-M315E monopropellant based on performance numbers.

Throughout the operation of the mission, there are also several aspects that will influence the social sustainability of the mission. First of all collisions with other missions were avoided at all costs when determining both the transfer orbit and the trajectory around the Moon as such a collision would not only be catastrophic for this mission, but it would also ruin the other mission, meaning that all the hard work of both mission teams is lost. Social sustainability during operation has further been implemented by avoiding interference of signals, send

[5] https://eurospace.org/working-bodies/reach/

[6] https://www.statista.com/statistics/276629/global-co2-emissions/

[7] https://8billiontrees.com/carbon-offsets-credits/carbon-footprint-of-space-travel/#ref-4

between different elements in our mission, with other missions. This has been achieved by complying with a specific, unique bandwidth for the communications within the navigation system, that has been determined by legislation [14].

Overall redundancy during operation is also crucial for the social sustainability, as it must be avoided that the failure of a single element could lead to the end of the entire mission. Even the failure of an entire satellite is not detrimental to the entire mission. By implementing sufficient redundancy throughout the entire operation, the customers will always be able to rely on the provided navigation services. The stakeholders will also rely on the accuracy of the navigation system, to ensure social sustainability in this case, it is ensured that the accuracy does not decrease significantly throughout the operation of the mission. The accuracy should also remain competitive, compared to possible alternative Lunar navigation systems, such that the customers will not find the need to look at competitors.

A successful operation of the mission would provide an ideal marketing opportunity to promote the entire space industry and Lunar missions in specific, as once the infrastructure is in place, a lot of mission designs will follow. Resulting not only in more customers, but also in an increased interest in the space industry, meaning that more investments will be made. This will also benefit relevant education for example by funding of STEM camps, which can ensure the future of the industry. This all contributes to increased social sustainability surrounding the space industry. To enable a successful operation, a ground control system with a ground control crew is required though. This ground control crew should be treated in a humane manner, a motivating work environment should be in place, and each worker should be compensated fairly for their labour.

End of Life of Spacecraft

The mission has a long-term objective. To achieve this purpose, individual satellites will be designed to be reliable. Nonetheless, there might be times when they are decommissioned either by failure, age, among others. To comply with the sustainable measure set above, a corresponding End of Life (EOL) procedure has been set. This should attempt to produce the least effect on the space environment and customers.

In terms of environmental sustainability, space debris is the main scenario to study. After the satellite is decommissioned, the team studied both sending the satellite further away or crashing it to the Moon, as there are already plans for a space debris Lunar landing zone [8]. In these cases, there are both positive and negative consequences. They are traded off to choose the one that maximises positive outcomes. In subsection 6.4.3 the option of crashing the satellite on the Moon has been chosen. Nonetheless, the operation must still be carefully handled to avoid other issues. Given the Moon is a giant lab space, the damage caused to it must be minimised. The mission shall comply with the corresponding regulatory bodies to have a successful EOL procedure. However, as of now, the regulations are very limited and new regulations should be pushed for a more sustainable space environment [9]

In subsection 6.4.3 the final manoeuvres that are required are quantified, these are necessary given the lack of atmosphere on the Moon. This final action will require a certain propellant. The manoeuvre has been optimised to minimise the fuel needed, along with finding the right trajectory depending on the final destination. All subsystems must be managed appropriately as well. When the satellite is sent to the surface, some materials might be hazardous and have to be safely disposed.

Even though not studied in this report, other EOL possibilities can be considered. These are mainly recycling and repairing. Both solutions could potentially have a positive effect on the environmental sustainability, but tend to have higher costs, making them non-profitable. However, they are still valid. Providing a cleaner landing on the Moon of the satellite could allow for more recycling of elements. Given the large extent of the satellites used, this could potentially be used for reusing in new versions of the same mission. A second option is repairing the faulty satellite. It would not be applicable in all cases, but give an alternative to reducing waste. The required technology and fuel must still be studied before considering it a viable option.

The most important part of sustainability for EOL relates to the social aspect. A hard requirement states that no part of the space component should pose a risk for humans or users' equipment on the Moon at the end of life. It involves two parts, not affecting orbiting missions, nor damaging elements on the surface. To accomplish it, a proper trajectory has been planned to a pre-determined location on the Lunar surface and the risk of

[8] https://lunarresourcesregistry.com/infrastructure/space-debris-graveyard/

[9] https://www.space.com/national-space-council-moon-bases-space-junk-regulation

losing control of a satellite is minimised. Failing to achieve this could cause extreme consequences on budget, science, and space.

A final aspect to consider is the consequence EOL has on the customers and how the mission will be sustainable about it. This can be achieved through redundancy of the system and appropriate planning. The customers need to have a reliable system for the entirety of the mission, so ensuring the performance loss is minimum during this stage is vital. Therefore, three extra satellites are implemented in strategic orbits, such that up to two satellites can fail without any reduction in performance of LNSS system. Following these steps, even after a satellite is decommissioned, both environmental and social sustainability are achieved.

End of Mission
As earlier stated the mission has a long-term objective, however, the mission could eventually come to an end due to a catastrophic failure of the entire mission, technological obsolescence, technical limitations or issues etc. In case the mission needs to be discontinued entirely, suitable procedures for this should be in place. These procedures should of course be sustainable, causing the least effect on the space environment and all stakeholders.

The decommissioning of all satellites part of the mission should be done whilst ensuring environmental sustainability. The same methods are considered here as for the decommissioning of a single satellite, as discussed in 'End of Life of Spacecraft'. However, at the end of the entire mission, a significant amount of time might have passed, meaning that 'cleaner' technology might be available for the decommissioning of a spacecraft. Possible options could be a controlled landing on the Lunar surface or a purpose-built space debris remover which could rendezvous with the satellite and move it to a desired location (Earth, Moon, burn up in the atmosphere etc.). The first space debris removal mission is planned to launch in 2025 [10]. Using these 'cleaner' technologies might enable for re-use of certain parts or enable a more complete recycling of the satellites, which improves the overall environmental sustainability.

The end of the entire mission would also mean that the ground control facilities will be abandoned by the ground control crew. To ensure environmental sustainability, these facilities should be put to other use where possible and demolition of the facilities should be avoided at all costs. Next to that general waste of resources (paper, computers, instruments etc.) should be avoided when abandoning the facilities, the resources should be re-used or recycled where possible.

In case of an End Of Mission, all customers will need to look for a suitable alternative. This means that if the demand for a Lunar navigation system is still there when this mission is ended, a suitable alternative should be in place to ensure social sustainability with regard to the customers. At the End of the Mission, all staff involved in the mission will need to look for other opportunities of employment, this should preferably be within the same company on a different mission possibly. If this is not possible, they should be treated correctly when being fired and alternative job opportunities could be presented to them. These actions will ensure social sustainability with the staff.

In general, regulations regarding the discontinuance of a mission should be followed precisely. Next to that, documents and research of the entire mission could be made public to help further research, innovation, and development. This will benefit the space industry as a whole, ensuring social sustainability towards the entire industry.

7.6.3. Concluding Remarks on Sustainability
Navigating the Moon considers sustainability throughout the entire life cycle of the mission, from conceptional phases all the way to (beyond) the end of mission. By considering sustainability in all phases, Navigating the Moon aims to perform its mission, whilst simultaneously limiting its (negative) environmental impact. This starts, during R&D, by evaluating the consequences of initial design choices. The R&D phase may not look like a big contributor to the sustainability, but by laying the ground of the project, a snowball effect can occur. Optimisation during this phase will lead to the least amount of wasted resources whilst still adhering to the mission requirements. Sustainability in the R&D phase leads to conceptual sustainability throughout the manufacturing, launch, operation, EOL and End of Mission phases.

[10] https://www.esa.int/Space_Safety/Clean_Space/ESA_commissions_world_s_first_space_debris_removal

7.7. Production Plan

By C.A.G.C. Spichal.

The production plan aims to implement a detailed timeline and activities for the manufacturing, assembly and integration phases of the spacecraft. In order to gain a better overview of the manufacturing, assembling and integration timeline, a production plan diagram has been made and can be found in section B.2. The diagram assumes the simultaneous production of six satellites, given each launch will send up to six satellites at a time. In the following section, first, subsection 7.7.1 will explore the manufacturing techniques for the components of the spacecraft that will be built 'internally' and comment on the ones that are built 'externally'. Finally, subsection 7.7.3 will explain the details of the testing campaigns.

7.7.1. Manufacturing

This section focuses on the manufacturing of the primary structure and propellant tank. It is a relevant stage in the mission as it converts the raw material into finished products capable of fulfilling a purpose.

Primary Structure

The primary structure is usually manufactured using forming and machining processes. In recent years, the development of additive manufacturing has allowed to design more complex parts in a time-efficient way. Provided that most of the structure is made out of Aluminium, SLM (Selective Laser Melting) can be used for some parts of the primary or secondary structure. Nevertheless, due to the relatively larger size of the mission's satellites compared to CubeSats, some classical techniques might still have to be applied to some parts. A combination of both techniques is therefore the most probable process to select. After manufacturing, tensile tests need to be performed on the parts and later on thermal and vibration tests on the primary structure.

Propellant Tanks

After the primary structure, the propellant tank also needs to be studied. The tank will be made out of the Titanium alloy Ti-6AL-4V. Its shape is a cylinder with spherical caps. Two manufacturing approaches can be chosen in that case: The more classic one consists in forging Titanium sheets into the desired shape and then welding them together using an electron beam to either form the cylindrical or spherical part of the tank. The second option is less conventional but faster. It consists in building a mould of the tank's shape and then casting the tank in it [119]. After this, the holes to connect the tank to the tubes need to be cut. Given the gains in time, the casting procedure is therefore the best option. Similarly to the primary structure, tests will also have to be performed. The most important tests for the tank are the tensile and fracture tests to avoid any type of leaking during the mission.

Rest of the Components

All the other components are manufactured by external companies. Some of them are assumed to be off-the-shelf (OTS in the diagram), their allocated time range in the production plan diagram (section B.2) remains however at two months at least to make a conservative approach. The manufacturing is then followed by the shipping of the components. After that comes the testing performed on the individual components. Although one testing on its own might just take a couple of days, the accumulation of the components, the logistics as well as the documentation that must be provided is also taken into account.

7.7.2. Assembly and Integration

After that comes the assembly of the subsystems (only for the ones for which it is relevant). For example, the assembly of the propulsion system should be made before it is integrated with the components, while each individual element from the ADCS subsystem is individually implemented on the satellite. Ideally, electrical connections should be made as much as possible to reduce the complexity of the wire integration.

The next step to be considered involves the order of integration of each component or subsystem. The process must be performed in the most logical order possible. First, the primary structure is set up with the propellant tank, tubes, and valves that come with it. After that, individual or assembled components are integrated in such a way that the ones located internally come first. While all of this is done, all the electric connections need to be established. The final components are the ones that are located outside the spacecraft, in this case the radiators, the sensors, and most importantly the solar arrays.

The buffer time accounts for the uncertainties as well as the time that will be gained thanks to the learning curve. It is assumed that the following batch productions can be reduced to 2.5 and then 2 years. The time gained will come mostly from the more efficient test campaigns and the know-how gained on the integration process.

7.7.3. Testing Campaigns

Now that the production plan diagram has been provided, the testing phase can be elaborated a bit more. This section provides more details about the first and second testing campaigns.

First Testing Campaign

The first crucial testing campaign that must be performed is for each of the selected components. This allows to check whether the specifications provided by the manufacturer comply with the limit loads applied during the various tests. For each test that can be performed for the different components, a test location was identified. Most of the tests can be done at ESTEC (European Space research and TEchnology Centre) in Noordwijk (the Netherlands), the rest is performed at the NSPTF (National Space Propulsion Test Facility) in the United Kingdom, Airbus Defence & Space test facilities in France and at the CEA (French Atomic Energy Commission) in France. All the results from this research are provided in Table 7.5:

Table 7.5: Component Testing Plan

Components	Test to perform	Rationale	Testing facility	Estimated time [days]
Thrusters	Vibration test	Verify that the thruster performs accordingly when subjected to important vibration loads.	NSPTF Westcott, UK	2
Propulsion system	Static fire test	Verify that all the valves and filters function properly during the burn and storage phases.	NSPTF [11] Westcott, UK	3
Clock	Ground-based accuracy test	Verify that the accuracy provided by the clock manufacturer corresponds to what is the case.	ESTEC Noordwijk, Netherlands	1
Batteries	Heat test	Verify whether the batteries still work properly beyond their provided maximal operational temperature.	CEA (Atomic Energy Commission) France [12]	2
	Charge test	Verify that the battery does not explode and permanently damages the entire satellite in the case it charges too much.	CEA (Atomic Energy Commission) France	2
PCDU	Electromagnetic test	Verify that no electromagnetic signal is generated that could make the signal sent to a component become unusable.	Electromagnetic Compatibility Laboratory ESTEC Noordwijk, Netherlands [13]	1
	Power distribution test	Verify that the PCDU can properly distribute the power to different components at once.	Electromagnetic Compatibility Laboratory ESTEC Noordwijk, Netherlands	1

Continued on next page

[11] https://www.esa.int/Enabling_Support/Space_Engineering_Technology/ESA_partnering_on_UK_s_new_space_thruster_test_site

[12] https://www.eoportal.org/other-space-activities/test-campaign-of-space-batteries#test-campaign-of-space-batteries-to-destr

[13] https://www.esa.int/Education/CubeSats_-_Fly_Your_Satellite/SOURCE_team_of_Fly_Your_Satellite!_conduct_electromagnetic_susceptibility_test_campaign

Table 7.5 – *Continued from previous page*

Components	Test to perform	Rationale	Testing facility	Estimated time [days]
	Electrical test	Verify that the PCDU remains operational after making it undergo electrical shocks.	Electromagnetic Compatibility Laboratory ESTEC Noordwijk, Netherlands	1
Cable harness	Resistance test	Verify the quality of the insulation of all the cables to make sure they can properly transmit all the data from one component to another.	ESTEC, Noordwijk Netherlands [14]	1
CMG	Rotation test	Verify that the CMG still functions properly when rotating it at its maximum rotation rate with respect to all its axes.	ESTEC, Noordwijk Netherlands	1
	Vibration test	Verify that the CMG still works properly after undergoing critical vibrations.	Airbus, Defence & Space Toulouse, France [15]	1
Sensors	Radiation test	Verify that sensors can still operate properly when subjected to important radiation flux from the Sun.	Shock test facilities ESTEC Noordwijk Netherlands	1
	Shock tests	Verify that sensors still function properly after subjecting them to important shocks that could occur during the launch or the mission.	QEC radiation test facilities ESTEC Noordwijk Netherlands [16]	1
Computer	Vibration test	Verify that the computer can still compute the necessary data when subjected to important vibrations.	Airbus, Defence & Space Toulouse, France	1
	Heat test	Verify that the computer can still compute the necessary data when heated up beyond its maximum temperature operational range.	Thermal Data Handling Facilities ESTEC Noordwijk Netherlands [17]	1
Antenna	Transmission test	Verify that the antenna and the laser gimbal function properly when directed towards a test antenna.	Compact Antenna Test Range (CATR) ESTEC Noordwijk Netherlands [18]	1

Continued on next page

[14] https://www.weetech.com/actual-applications/wiring-of-satellites
[15] https://triasrnd.com/l/400-80-kn-shaker
[16] https://escies.org/webdocument/showArticle?id=230&groupid=6
[17] https://www.esa.int/Enabling_Support/Space_Engineering_Technology/Test_centre/Thermal_Data_Handling_Facilities
[18] https://www.esa.int/Enabling_Support/Space_Engineering_Technology/Test_centre/Antenna_Test_Facilities

Table 7.5 – *Continued from previous page*

Components	Test to perform	Rationale	Testing facility	Estimated time [days]
Radiators	Thermal test	Verify that the radiators still work properly when subjected to more than their maximum operational temperature.	Thermal Data Handling Facilities ESTEC Noordwijk Netherlands	1
	Vibration test	Verify that the radiators are not damaged when subjected to high vibration loads, especially provided they are located outside the satellite.	Airbus, Defence & Space Toulouse, France	1
Heaters	Vibration test	Verify that heaters still function properly when subjected to high vibration loads.	Airbus, Defence & Space Toulouse, France	1

Second Testing Campaign

The second testing campaign focuses more on the later stages of the satellite design. The first remark that must be made is about the design of models that are subjected to tough test conditions. Usually, an Engineering as well as a Structural and Thermal Model (EM and STM) are manufactured to test excessively different aspects of the future satellite.

Another comment to be made is that the same way the GIOVE-A and GIOVE-B were launched before the actual Galileo constellation was set in place, the first satellite that will be sent for the Navigating the Moon mission is a prototype version. This means that the first manufacturing phase will only involve the production of one satellite, along with the STM and EM models. The assigned time for manufacturing, assembly and integration was therefore set to two years.

In addition to that, some components are already assembled before they are integrated into the satellite. These assembled components, such as the propulsion or structures system must undergo some testing as well (see subsection 7.7.1).

To finish with, each fully assembled spacecraft must be tested as well. Unlike the STM and EM, the testing conditions applied are not as tough. The testing facilities are mostly performed at ESTEC again. Testing facilities used to verify the good state of assemblies or the spacecraft are listed below:

- Large Space Simulator (LSS), ESTEC[19]: Can perform thermal and mechanical testing.
- Maxwell Test Chamber, ESTEC [20]: Can perform electromagnetic testing
- Large European Acoustic Facility (LEAF), ESTEC [21]: Can perform acoustic testing that allows to verify that the satellites does not show anomalies during the launch.

It should also be mentioned that these tests are non-destructive and mainly aim to verify that the satellites and its assemblies can survive the harsh conditions of space. Other tests that must be performed entail the verification that all components work together (integration testing) and that the tasks done by the satellite are done properly (functional testing).

Concluding Remarks

The most important aspect that must be kept in mind is that the production plan involves numerous uncertainties which can delay the entire manufacturing, assembly and integration process of the spacecraft. In addition to that, regulations implemented by the government can seriously slow down the production process of each of the satellites. These are factors that can only be mentioned and for which the time estimation is extremely convoluted. Another critical aspect that has not been accounted for is the coordination of several tests at the same location and at the same time.

[19] https://www.esa.int/Enabling_Support/Space_Engineering_Technology/Test_centre/Large_Space_Simulator_LSS

[20] https://www.esa.int/ESA_Multimedia/Images/2015/02/Maxwell_Test_Chamber

[21] https://www.esa.int/Enabling_Support/Space_Engineering_Technology/Test_centre/Large_European_Acoustic_Facility_LEAF

7.8. Mission Cost

The mission cost estimation is a crucial part in the design of the LNSS. It plays a critical role in assessing the feasibility of the mission from a financial perspective. Furthermore, it helps in efficient resource allocation and it allows the stakeholder to evaluate the cost effectiveness. The total mission cost should not exceed $10\,\mathrm{B}\,\$$ [FY2023] as set by ESA [120].

This section will give an overview of the evaluation of the cost estimations. The initial cost estimation is performed based on empirical data of multiple Earth and Lunar satellites. Afterwards, the initial cost is broken down into different phases according to empirical data of the Galileo satellite constellation. Lastly, a more accurate cost and breakdown estimation is performed as an accurate design of the LNS was available.

7.8.1. Initial Cost Estimation

By C.A.G.C. Spichal

The initial cost estimation will perform the first order estimation of the mission cost. This task is complex given that no LNSS is operational currently, meaning that the cost estimation can not be set upon missions that had the exact same purpose. This means that the cost estimation will be made using navigation and observation satellites around the Earth and Lunar missions that served purposes slightly different to the Navigating the Moon one's. The reason why Earth observation satellites are also used is to compensate for the fact that the satellites around the Moon do not fully serve navigation purposes. A cross referencing can therefore be applied. The price of one Galileo satellite was estimated using its approximate launch mass of $700\,\mathrm{kg}$ ([121]) and an empirical relation approximating the cost of a navigation spacecraft per kg [35]:

$$C_{S/C} = 40 - 45FY2000\ \mathrm{k\$\,kg^{-1}} \tag{7.1}$$

To be conservative regarding the cost, the upper limit of $45\,\mathrm{k\$\,kg^{-1}}$ was taken. In order to keep consistency, all the prices obtained were converted into the fiscal year 2000 (FY2000) prices using an online Cost Performance Index (CPI) converter [122]. Each satellite's individual cost is indicated in Table 7.6:

Table 7.6: Past satellite costs

Satellite name	Orbited celestial body/ Purpose	Launch Year	Cost [M $]	Cost in FY 2000[M $]
GPS Block I	Earth/ Navigation	1996	20 [35]	21.3 [35]
GPS Block IIA	Earth/ Navigation	1996	40 [35]	41.8 [35]
GPS Block IIR	Earth/ Navigation	1989	28.75 [35]	37.3 [35]
GPS Block III	Earth/ Navigation	1995	41.5 [35]	45.2 [35]
Galileo satellite	Earth/Navigation	2011	-	31.5
Clark	Earth/ Science	1994	41.5 [35]	45.2 [35]
Lewis	Earth/ Science	1994	59 [35]	65.5 [35]
AEOLUS	Earth/ Science	2005	210.6 [35]	190.9 [35]
Lunar Reconnaissance Orbiter (LRO)	Moon/ Science	2009	583 [123]	472.7
Lunar Atmosphere and Dust Environment Explorer (LADEE)	Moon/ Science	2013	280 [124]	208.2
Kaguya	Moon/ Science	2017	480 [125]	356.9

To obtain the total constellation cost for the GPS and the Galileo, the prices obtained Table 7.6 were multiplied by the number of satellites in service around the Earth. This seals a total constellation cost of $1003\,\mathrm{M}\,\$$ for the GPS (the most expensive GPS satellite from Table 7.6 was taken and then multiplied by the 24 operational GPS satellites) and $945\,\mathrm{M}\,\$$ for the Galileo (the Galileo constellation has 24 active and 6 passive satellites and each one was taken into account for the cost estimation). Finally, a cost estimation of the Navigating the Moon constellation itself needs to be made. Table 7.6 gives an idea on how much Earth navigation constellations cost compared to Earth scientific spacecrafts. This ratio can then be combined with the cost of Lunar scientific spacecraft to obtain an idea of how much a Lunar constellation would approximately cost. From Table 7.6, Earth navigation constellations cost 10 times more than Earth observation satellites. Given that the

Lunar scientific spacecraft cost on average $345.9\,\mathrm{M\,\$}$, this means that the Lunar Navigation Spacecraft System would approximately cost $3.36\,\mathrm{B\,\$}$. If this price is converted into the fiscal year 2023 price, this corresponds to $5.46\,\mathrm{B\,€}$. Given that no similar missions have been performed previously, the level of uncertainty is assumed to be high, meaning that the margin level is set to be at $25\,\%$ [126]. This results in a cost budget margin of $4.10\,\mathrm{B\,€} - 6.83\,\mathrm{B\,€}$.

7.8.2. Initial Cost Breakdown

By M. Vereycken

The next step is to perform a breakdown of the initial cost estimation. The cost of the Moon constellation can be divided in 3 main categories, namely R&D phase, deployment phase and exploitation phase. This is done based on the Galileo navigation satellite constellation.

From subsection 7.8.1, the average satellite cost was estimated $140\,\mathrm{M\,\$}$ [FY2000] without margins. However, this was then multiplied with the total amount of satellites to get the total mission cost of $3.36\,\mathrm{B\,\$}$ [FY2000]. Using the percentages provided in [127], the total cost can then be split up in the three different phases. The development phase and exploitation phase are considered accurate enough and will not be modified as it is similar for the Moon as for the Earth. The deployment phase should be modified as deploying satellites around Earth is different than around the Moon.

For now, only the launch vehicle is considered as in this design stage only limited information of the conceptual design is known. The chosen launcher is the Falcon Heavy and 6 launches are needed which has a launch cost $64.12\,\mathrm{M\,\$}$ [FY2000] per launch[22]. This will have a total launch cost of $384.7\,\mathrm{M\,\$}$ [FY2000], which is 11.45 % of the total budget. A small margin of $5\,\%$ is taken as the first launch will only take place in 2028. The following division of the cost budget for the Moon constellation is given in Table 7.7 with the $25\,\%$.

Table 7.7: Overview of Cost of the Moon Constellation where Launch Vehicle Cost and Others are a breakdown of the Deployment Phase

Phase	Cost in FY 2000[M $]	Percentage of Total Cost [%]
R&D Phase	668.3 +/- 167.1	19.89 +/- 4.97
Deployment Phase	1731.1 +/- 355.8	51.52 +/- 10.59
Launch Vehicle Cost	384.7 +/- 19.2	11.45 +/- 0.57
Other	1346.4 +/- 336.6	40.07 +/- 10.02
Exploitation Phase	960.6 +- 240.2	28.59 +/- 7.15
Total	3360 +/- 763.1	100.0 +/- 22.71

7.8.3. Final Cost Estimation & Breakdown

By M. Vereycken, J.K. Geijsberts

The final cost estimation and breakdown is performed based on the final design of the LNS. First, a cost estimation of the clock is performed as it is one of the most specific and expensive components of the satellite. Furthermore, the cost of the remaining navigation payload is estimated. Afterwards, the launch cost is revised as the constellation is changed with respect to the last launch cost estimation. Additionally, empirical relation are used to determine the cost of the remaining subsystem and other phases of the mission. Lastly, all information is combined for a clear cost estimation and breakdown overview.

Clocks

J.K. Geijsberts

In the design of a LNSS, the clocks, which are crucial for the functioning of the navigation service, have been looked into with special detail. The clocks being used are unique and no price could be found. Therefore, to estimate the price of the clock, a linear parametric estimation method was used. For this the performance of previously used clocks were compared to the performance of the clock used on the spacecraft. The clocks and their prices used can be found in Table 7.8

[22] https://spacenews.com/spacexs-new-price-chart-illustrates-performance-cost-of-reusability/

Table 7.8: Data of historical clocks used.[128]

Clock	Performance (Ratio of time it takes to deviate 1 sec from true time)	Price ($) FY2006
TCXO	1.00E+07	100
OCXO	6.67.E+08	1000
Rubidium	2.40E+13	3000
Cesium	4.32E+13	20000

Using Excel, a linear parametric estimation formula can be set up using the data from Table 7.8, with the usage of the least squares method.
Doing this, Equation 7.2 emerges.

$$C[\$] = 4 \times 10^{-10} \cdot P - 769.44, \tag{7.2}$$

Where C is the clock cost, and P is the performance of the clock. Then, the cost can be estimated using the performance of the actual clock used [16]. The amount for this is then,

$$4 \times 10^{-10} \cdot 8.64 \times 10^{14} - 769.44 = \$344830.56.$$

Turning this value into FY2023, and taking all clocks, an amount of 105, with a learning curve of $95\,\%$, which is calculated in Equation 7.3 [101],

$$L = N^{(1+log(S)/log(2))} \tag{7.3}$$

where L is the correction coefficient, N the number of units and S the average learning curve, the costs of all clocks is **$M38.74** with a total standard deviation of **$M0.2537**. Apart from the clocks, the remaining navigation payload should be estimated, which is done with Equation 7.4 [101].

$$Y = 189 \cdot m_{NAV} \cdot L \tag{7.4}$$

Here, Y is the navigation payload cost in FY2010 $K, m_{NAV} the remaining navigation payload mass and L the correction factor which is calculated with a learning curve of $95\,\%$ for 34 units (number of satellites). The equation has a standard deviation of $39\,\%$.

Launch
By J.K. Geijsberts

The launch cost can be estimated using existing launchers. First, the number of launches needs to be estimated. This is done by looking at the orbital planes present in the mission, as well as how many spacecraft fit into a payload fairing. Then, the cost of the launches can be estimated by adding the number of launches up.
The launchers considered are shown in Table 7.9. Other launchers are not considered due to their TRL or as they are not in service anymore (i.e. Saturn V, which is not in service anymore, or Starship, which at the current moment does not have a high enough TRL, and cannot be expected to have reached a high enough TRL by 2028).

Table 7.9: Launch vehicles considered in the mission.

Launch vehicle	Mass possible [kg]	Height [m]	Diameter [m]	Cost per launch in millions FY2023	Cost with margin in FY2023
Falcon Heavy (to Mars) [129]	16800	13.1	5.2	108.63	114.0615
Falcon 9 (to Mars) [129]	4020	13.1	5.2	69.72	73.206
Long March 5 [23]	9400	-	-	-	-
Ariane 6 [24]	3000	20	5.4	115.11	120.8655

[23] https://web.archive.org/web/20200809052829/http://www.xinhuanet.com/english/2019-12/27/c_138662139.htm
[24] https://www.arianespace.com/vehicle/ariane-6/

As can be seen in Table 7.9, four total launchers that are ready are considered. What must be noted is that Long March 5 is from the CALT (China Academy of Launch Vehicle Technology), which is not a partner of ESA and therefore not considered.
That leaves us with 3 possible choices for launch vehicles. It is known that there are six orbital planes, where five have six spacecraft and one has 4 spacecraft. Therefore, a launch vehicle is needed that must be able to carry at least 6 spacecraft, as this is optimal per orbit plane. The spacecraft that are in one orbital plane can all be deployed through the same launch vehicle. As the Falcon 9 has the smallest payload fairing, that one is checked in terms of fitting the spacecraft (which is around 2 × 2 × 1 m in its dimensions (shown in section B.1)). This checking can visually be done in a figure which has been done already and can be seen in Figure 6.17a. From Figure 6.17a, one can see that just on the bottom level, three spacecraft already fit in the fairing. This can be stacked once to reach a total of six spacecraft per launch. Knowing that the 6 spacecraft fit in the Falcon 9, the other launch vehicles considered have larger dimensions and will also fit the six spacecraft.
Next, the mass must be checked. The mass for six spacecraft is the mass of one spacecraft times six, equalling **6287.5 kg**, which is more than the Falcon 9 can handle to Mars. The Falcon Heavy is feasible for this job as it can carry 16800 kg to Mars. Therefore, Falcon Heavy is used for those launches with six spacecraft. For four spacecraft, the mass of the spacecraft will be **4191.7 kg**, which is more than the allowed for Falcon 9, but only by a small margin, which can be seen in Equation 7.5.

$$4191.7 - 4020 = 171.7\text{kg} \tag{7.5}$$

This difference is relatively small, and as the payload to Mars for the Falcon 9 is 4020 kg, it is assumed that for the Moon, which is much closer and therefore should not need as much propellant in the launch vehicle, the Falcon 9 suffices.
It must be noted that one extra launch is added for a prototype spacecraft, which means an additional Falcon 9 launch will occur.
Then one can calculate the lowest-cost launch configuration for the mission. The Falcon 9 has the lowest cost, so will be used on the prototype launch as well as the launch with four spacecraft. The Falcon Heavy will be used for the other launches. Both launchers have reuse-able lower stages, which makes them more sustainable as well. The launch configuration can then be calculated and is shown to be the configuration as follows:

Five Falcon Heavy launches (with six satellites), and one Falcon 9 launch (with four satellites for the low inclination orbit), as well as one Falcon 9 launch (with one satellite as a prototype) at a cost of **$716 million FY2023**

Empirical Relations
By M. Vereycken
Using empirical relations derived from previous space mission, the cost can be divided into numerous categories. Because the satellite constellation consists of 34 satellites (N) and a learning curve (S) of 95 % is used, the cost for all satellites can be determined by multiplying the cost of the first satellite (T1) with the learning curve constant (L), which is 26.19. Table 7.10 provides all relations used to determine the cost estimation for the different phases of the mission [101]. The IA&T cost includes the prototype cost, but not the launch cost to the Moon. Furthermore, if no SSD percentage or value is given, a 25 % SSD will be assumed.

Table 7.10: Cost estimation for the different phases of the mission based on empirical relations [101]. The production, IA&T and operating cost should be multiplied with the correction factor due to the learning curve.

Mission Phase	Cost FY2010 $K	SSD [%]
Development	$1022 \cdot m_{dry}$	
Production		
TT&C	$883.7 \cdot m_{TT\&C}^{0.491}$	18
EPS	$32.4 \cdot m_{EPS}$	31
CDH	$658 + 75 \cdot m_{CDH}^{1.35}$	854 FY2010 $K
TCS + Structure	$22.6 \cdot (m_{TCS} + m_{Structure})$	21
ADCS	$795 \cdot m_{ADCS}$	36
Propulsion	$20.0 \cdot V_{Prop_{Tank}}^{0.485}$	35
Navigation Payload	Previously Determined.	
IA&T	$0.124 \cdot C_{Production}$	34
Operation	5850	

The satellite production cost can be checked by using empirical relation from another cost estimation book [130]. The comparison does not include the navigation payload production cost, as it is omitted in the book. The average satellite production cost without the navigation payload according to Table 7.10 is 38.1 M $ FY2023 and from '*Guidelines and Metrics for Assessing Space System Cost Estimates [130]*', a cost of 38.1 M $ FY2023. As these values are very similar, it gives a high confidence in the production cost estimation.

Costs of Offsetting for Atmospheric Pollution

By J.K. Geijsberts, K. Scherpenzeel. Written by J.K. Geijsberts

An important user requirement is requirement **NTM-USER-07**. This one states that costs need to include costs for atmospheric pollution. Therefore, all the greenhouse gases that are emitted into the atmosphere need to be counteracted with carbon credits. The carbon credits that are being used are the European carbon credits that one can buy to offset pollution. This offset is done by the program investing money into carbon capturing solutions and, therefore, allowing companies to mitigate their carbon production[25]. To find how much needs to be paid in carbon credits, the amount of carbon emitted into the atmosphere needs to be determined. Normally, the carbon emissions for the whole project need to be estimated, and the amount that needs to be paid for that needs to be calculated. However, this includes development and transportation costs, as well as costs for the production of the spacecraft and of course launcher emissions. For development and transportation, no estimation methods could be found. Therefore, a margin on the values calculated was used instead.
The carbon emissions for the spacecraft can be calculated through the materials used. For the structure, aluminium, and titanium are used. The total carbon per kg of aluminium and titanium can be used to then calculate the amount of carbon. This is shown in Table 7.11.

Table 7.11: The carbon footprint of the structure of the spacecraft.

Material	Mass in Spacecraft [kg]	Carbon [kg/kg]	Total Amount of Carbon [kg]
Titanium	14.87 [131]	49	728.6
Aluminium	258.2 [131]	13	3356.6

Next to the carbon footprint of the spacecraft structure, the carbon footprint of the launch can be incorporated. The amount of carbon emitted by the launch is already given in subsection 7.6.2. These values can then be incorporated together with the amount of carbon of the spacecraft, to get the total amount of carbon. Then the number of dollars per kg of carbon can be used to calculate the total amount of costs. This is shown in Table 7.12.

Table 7.12: The total amount of carbon footprint of the launches and spacecraft, as well as the number of dollars it costs to offset this footprint.

Two Falcon 9 Launches [kg]	Five Falcon Heavy Launches [kg]	Carbon spacecraft [kg]	Total amount of carbon [kg]
673104	2337000	4085	3014189
Euros per tonne [€] (17 June) [26]	**Dollar [$] per Euro [€]** [27]	**Dollars [$] per kg**	**Total cost + 900% in Dollars [$] FY2023**
92.35	1.09115	0.101	3037329

As can be seen in Table 7.12, the total costs for offsetting the carbon footprint is around $ 3 million dollars, including a 1000% margin for the fact that development and transport costs were not included.

Final Values

Performed by M. Vereycken, J.K. Geijsberts. Written by J.K. Geijsberts

All the values found for all the subsystems and other parts of the mission are summarised and can be seen in Table 7.13.

[25] https://climate.ec.europa.eu/eu-action/eu-emissions-trading-system-eu-ets_en
[26] `https://ember-climate.org/data/data-tools/carbon-price-viewer/`
[27] `https://www.xe.com/currencyconverter/convert/?Amount=1&From=EUR&To=USD`

Table 7.13: The finalised cost breakdown of the mission. All values in dollars [$].

ID	Item section	Fiscal Year	Level	FY2023 (Millions)	SSD (FY2023 Millions)	+ 2 SSD (FY2023 Millions)	+ 1 SSD (FY2023 Millions)
1.0	Mission total	2023	1	$ 6192	$ 1461	$ 9115	$ 7653
1.1	Development	2023	2	$ 1134	$ 283	$ 1701	$ 1417
1.2	Spacecraft	2023	2	$ 1538	$ 418	$ 2373	$ 1956
1.2.2	TT&C	2023	3	$ 112	$ 20	$ 152	$ 132
1.2.3	Navigation	2023	3	$ 242	$ 80	$ 401	$ 322
1.2.3.1	Clocks	2023	4	$ 39	-	-	-
1.2.3.2	Other	2023	4	$ 203	-	-	-
1.2.4	EPS	2023	3	$ 314	$ 97	$ 508	$ 411
1.2.5	CDH	2023	3	$ 91	$ 22	$ 136	$ 113
1.2.6	TCS & Struct.	2023	3	$ 315	$ 66	$ 447	$ 381
1.2.7	ADCS	2023	3	$ 213	$ 77	$ 367	$ 290
1.2.8	Propulsion	2023	3	$ 252	$ 55	$ 362	$ 307
1.3	IA&T	2023	2	$ 263	$ 89	$ 442	$ 353
1.4	Launch	2023	2	$ 717	$ 36	$ 788	$ 753
1.5	Operations	2023	2	$ 2537	$ 634	$ 3806	$ 3172
1.6	Carbon Footprint	2023	2	$ 3	$ 1	$ 5	$ 4

As can be seen Table 7.13, the total cost of the mission including a 2 SSD margin is **9115 $FY2023 millions**.

7.8.4. Return on Investment (ROI)

Performed by Kyle Scherpenzeel, L.D. van der Peet. Written by Kyle Scherpenzeel,L.D. van der Peet

The ROI is usually a ratio of the total net income over the accumulated cost. However, this usually concerns for-profit organisations. Since ESA is a non-profit organisation[28], this definition of ROI may not hold. Instead, the mission focuses on enabling science. Therefore, a more accurate definition of the ROI is: 'a ratio of the value of science missions enabled over the accumulated cost'. With the total cost of the design and market analysis having been performed, the return on investment can be quantified. As the total estimated mission cost with 2σ confidence is $9110\,\mathrm{M}\,\$$(FY2023), the mission cost is below the initial budget with $890\,\mathrm{M}\,\$$(FY2023) remaining. The market analysis in section 3.3 discussed some of the potentials that this project will create, however, they have not been weighed against the cost of this project. The 2σ $9110\,\mathrm{M}\,\$$(FY2023) is minuscule compared to the $100\,\mathrm{B}\,\$$ that is already currently being invested into different Moon missions[7]. This investment also allows ESA to take a large role in the global Lunar economy, as they will be one of the largest initial service providers in that area and will put Europe on the map in terms of Lunar exploration. This allows ESA to stand out and be very visible to the public, which in turn, could lead to more funding for the program.

As discussed in section 3.3 there are many missions with different goals planned currently. These new missions can be created much cheaper by the initial investment in an initial navigation service. The cost savings for these missions also allow much smaller companies, with smaller budgets, to have a stake in the future Lunar market. These companies would require less investment in navigation determination because of this system and would allow them to create much more autonomous vehicles. Many of these companies could be situated in Europe, which is why this design can be very beneficial to taxpayers in Europe, as the public can also utilise these systems once they are available. The new opportunities created by this design are much greater than the initial investment, causing the return on investment to be much greater than one.

Recommendations

For the calculation of costs of offsetting the carbon footprint created by the mission, no estimation method was used for the development and transportation costs. Instead, a margin was included to account for this. A more in-depth analysis should be done into estimation methods for finding the costs for this. As an example, some estimation methods found in literature [132] can be used for further analysis.

[28] https://www.esa.int/About_Us/Business_with_ESA/Business_Opportunities/Eurospace

8
Conclusion

By N. Ricker, S. Nedelcu, L.D. van der Peet
The Navigating the Moon project analysed the possibility of developing a Lunar Navigation Satellite System (LNSS). It is based on a similar mission currently being developed by ESA known as Moonlight Project. This report aimed to develop a viable mission design concept and a preliminary design of a satellite in the constellation. It discussed both technical and non-technical aspects, mainly delving into navigation requirements and their effect on the entire system.

The primary goal of the project was to produce a robust system capable of supporting future Lunar missions. The mission concept chosen met most of the defined requirements. It is a self-controlled satellite constellation of 34 modules orbiting in seven different frozen orbits to reduce propellant and improve sustainability. This constellation delivers a $10\,\mathrm{m}$, $0.4\,\mu\mathrm{s}$, and $1\,\mathrm{m\,s^{-1}}$ accuracy for surface Moon users. Furthermore, redundancy is also provided up to two satellites, without any ΔV required. Inter-satellite communication is possible through lasers. Monitoring from the Earth is available through the Lunar Pathfinder mission acting as a relay satellite. The concept included a market analysis, sustainability approach, mission timeline and operations & logistics. The total approximated cost for the mission is $ 6.192 billion dollars and aims to be fully operational by 2037.

The second goal was to perform a preliminary design of one satellite. It is a worst-case scenario for the entire mission. It was designed to have a 12-year lifetime, have enough fuel for orbit control, and be capable of providing service continuously throughout the whole period. Each spacecraft has a mass of $1047.9\,\mathrm{kg}$, a BOL power $1605\,\mathrm{W}$, and an average production cost per module of $ 45.24 million dollars.

The report proved the feasibility of the project, along with the potential it has as a tool for future Lunar missions. The focus was mainly on establishing a solid foundation for future stages. Initial critical factors were addressed, such as orbit determination, updating frequency, and preliminary spacecraft sizing. In the next stages, the design must be further developed. This includes refining the design, performing sufficient testing and analysis, developing communication protocols, and ensuring compatibility within the system components. Based on these outcomes, the Navigating the Moon project is on track to becoming a vital component of the upcoming lunar missions, illuminating the Moon's hidden realms and guiding exploration to unprecedented depths.

References

[1] Moonlight Team. *MOONLIGHT LCNS ESA SERVICE CONCEPT OF OPERATIONS*. 2023.

[2] ESA Navipedia. *BeiDou Space Segment*. 2014. URL: https://gssc.esa.int/navipedia/index.php/BeiDou_Space_Segment (visited on 05/04/2023).

[3] Filipe Pereira and Daniel Selva. "Exploring the Design Space of Lunar GNSS in Frozen Orbit Conditions". In: *Arxiv Conference* 17 (Oct. 2020). DOI: https://doi.org/10.48550/arXiv.2010.08706.

[4] Todd A. Ely. "Stable Constellations of Frozen Elliptical Inclined Lunar Orbits". In: *The Journal of the Astronautical Sciences* 53.3 (July 2005), pp. 301–316. DOI: 10.1007/BF03546355.

[5] Matei Dinescu; Jasper Geijsberts; Ian Maes; Serban Nedelcu; Andreas Van Parys; Lennart van der Peet; Nikolaus Oliver Ricker Chong; Kyle Scherpenzeel; Carl Spichal; Mathijs Vereycken. *Navigating the Moon Midterm Report*. May 2023.

[6] Matei Dinescu; Jasper Geijsberts; Ian Maes; Serban Nedelcu; Andreas Van Parys; Lennart van der Peet; Nikolaus Oliver Ricker Chong; Kyle Scherpenzeel; Carl Spichal; Mathijs Vereycken. *Navigating the Moon Baseline Report*. Apr. 2023.

[7] ESA. *MOONLIGHT PROGRAMME*. Oct. 2022. URL: https://esamultimedia.esa.int/docs/telecom/22.09.26_Moonlight_White_Paper.pdf.

[8] Nelly Philips et al. “Tweeting from the Moon”. In: *36th annual small satellite conference* (2021). URL: https://digitalcommons.usu.edu/cgi/viewcontent.cgi?article=5307&context=smallsat.

[9] Luigi Scatteia and Yann Perrot. “Lunar market assessment: market trends and challenges in the development of a lunar economy”. In: (2021).

[10] Jos Sinke. “Reader Production of Aerospace Systems (AE3211-II)”. Unpublished.

[11] Melahat Cihan et al. “Design and analysis of an innovative modular cubesat structure for ITU-pSAT II”. In: July 2011, pp. 494–499. DOI: 10.1109/RAST.2011.5966885.

[12] Angel David et al. “Methodology for optimizing a Constellation of a Lunar Global Navigation System with a multi-objective optimization algorithm”. In: *Acta Astronautica* 204 (2023), pp. 348–357. DOI: doi.org/10.1016/j.actaastro.2023.01.003.

[13] Moonlight Team. *MOONLIGHT LCNS ESA SERVICE REQUIREMENTS DOCUMENT (ESRD)*. 2023.

[14] Interagency Operations Advisory Group. *The Future Lunar Communications Architecture, Final Version, V1.3*. Jan. 31, 2022. URL: https://www.ioag.org/Public%5C%20Documents/Lunar%5C%20communications%5C%20architecture%5C%20study%5C%20report%5C%20FINAL%5C%20v1.3.pdf.

[15] Elliott Kaplan and Christopher Hegarty. *Understanding GPS/GNSS: Principles and Applications, Third Edition*. 2017.

[16] National Aeronautics and Space Administration. *Deep Space Atomic Clock (DSAC)*. 2021. URL: https://www.nasa.gov/mission_pages/tdm/clock/index.html (visited on 06/15/2023).

[17] Pietro Giordano et al. “Moonlight navigation service - how to land on peaks of eternal light”. In: Oct. 2021.

[18] Magdy A. Sirwaha et al. “A study of the moderate altitude frozen orbits around the Moon”. In: *Results in Physics* 17 (June 2020). DOI: https://doi.org/10.1016/j.rinp.2020.103148.

[19] Peter Teunissen and O Montenbruck, eds. *Springer Handbook of Global Navigation Satellite Systems*. English. Vol. XXXI. Springer, 2017. ISBN: 978-3-319-42926-7.

[20] June Chul Roh and Deric Wayne Waters. *POSITION AND VELOCITY UNCERTAINTY METRICS IN GNSS RECEIVERS*. US PATENT 8,525,727 B2, Texas Instruments Incorporated, Dallas, TX. Sept. 2013. URL: https://patentimages.storage.googleapis.com/2d/7d/59/2c1efbaf74db58/US8525727.pdf.

[21] P.N.A.M Visser. *Experimental Design & Data Analysis Space Topic*. AE2223-II course, Faculty of Aerospace Engineering, Delft University of Technology. Jan. 2022. URL: https://brightspace.tudelft.nl/d2l/le/content/419884/viewContent/2367628/View.

[22] A. Joseph. *GNSS solutions : Measuring GNSS Signal Strength*. Inside GNSS. Nov. 2010. URL: https://insidegnss.com/wp-content/uploads/2018/01/novdec10-Solutions.pdf.

[23] Zhitao Lyu and Yang Gao. *An SVM Based Weight Scheme for Improving Kinematic GNSS Positioning Accuracy with Low-Cost GNSS Receiver in Urban Environments*. Dec. 2020. DOI: 10.3390/s20247265.

[24] S Gaglione. *GNSS solutions : How does a GNSS receiver estimate velocity*. Inside GNSS. Apr. 2015. URL: https://insidegnss.com/wp-content/uploads/2018/01/marapr15-SOLUTIONS.pdf.

[25] Antonio Elipe and Martin Lara. “Frozen Orbits About the Moon”. In: *Pre-publicaciones del Seminario Matemático* 12 (Mar. 2003). DOI: DOI:10.2514/2.5064.

[26] Todd Ely. *Mission Countdown for Deep Space Atomic Clock*. Dec. 2018. URL: https://www.gps.gov/governance/advisory/meetings/2018-12/ely.pdf.

[27] Todd Ely et al. “Deep Space Atomic Clock Technology Demonstration Mission Results”. In: *2022 IEEE Aerospace Conference (AERO)*. 2022, pp. 1–20. DOI: 10.1109/AERO53065.2022.9843303.

[28] “IEEE Standard Definitions of Physical Quantities for Fundamental Frequency and Time Metrology-Random Instabilities”. In: *IEEE Std 1139-1999* (1999), pp. 1–40. DOI: 10.1109/IEEESTD.1999.90575.

[29] Jet Propulsion Laboratory. *Deep Space Atomic Clock A New Frontier in Ultra-Precise Space Navigation*. Aug. 2019. URL: https://d2pn8kiwq2w21t.cloudfront.net/documents/DSAC-factsheet.pdf.

[30] Todd A. Ely et al. *Deep space atomic clock mission overview*. Version V1. 2019. URL: https://hdl.handle.net/2014/51659.

[31] Ignacio Romero. *The Receiver Independent Exchange Format Version 4.00*. Dec. 2021. URL: https://files.igs.org/pub/data/format/rinex_4.00.pdf.

[32] T. Nie and P. Gurfil. “Lunar frozen orbits revisited”. In: *Celestial Mechanics and Dynamical Astronomy 130* 61 (2018). DOI: https://doi.org/10.1007/s10569-018-9858-0.

[33] Justyna Tomaszewskaa et al. *Comparative analysis of vitality of GPS and GLONASS satellite systems*. 8th International Conference on Air Transport - INAIR. 2019. URL: https://insidegnss.com/wp-content/uploads/2018/01/novdec10-Solutions.pdf.

[34] TU Delft. *Spacecraft Design and Sizing*. 2021. URL: https://brightspace.tudelft.nl/d2l/le/content/292964/viewContent/1767758/View.

[35] James Wertz and Wiley Larson. *Space Mission Analysis and Design*. Vol. -1. Jan. 1999. ISBN: 978-0-7923-0971-0. DOI: 10.1007/978-94-011-2692-2.

[36] Jorge Amaya et al. “The PAC2MAN mission: A new tool to understand and predict solar energetic events”. In: *Journal of Space Weather and Space Climate* 5 (Feb. 2015), A5. DOI: 10.1051/swsc/2015005.

[37] André Guerra et al. “Magrathea: Dust growth experiment in micro-gravity conditions”. In: (Mar. 2018).

[38] ThalesAleniaSpace. *TRIS NSGU*. 2012. URL: https://www.thalesgroup.com/sites/default/files/database/d7/asset/document/TRIS_NSGU-092012.pdf.

[39] kongsberg. *Frequency Generator and Upconverter Unit*. 2014. URL: https://www.kongsberg.com/kmagazine/2014/9/board-galileo/.

[40] Airbus. *Clock Monitoring and Control Unit*. 2014. URL: https://www.airbus.com/sites/g/files/jlcbta136/files/2021-11/Publication-sce-PP-NAV-CMCU-old.pdf.

[41] Nitin Kumar Suyan et al. “Design of Circularly Polarized IRNSS Receiver Antenna using Characteristic Mode Analysis”. In: July 2020. DOI: 10.1109/conecct50063.2020.9198683. URL: https://doi.org/10.1109/conecct50063.2020.9198683.

[42] Jianxing Li et al. “Design of Low RCS Circularly Polarized Patch Antenna Array Using Metasurface for CNSS Adaptive Antenna Applications”. In: *Materials* 12.12 (2019). ISSN: 1996-1944. DOI: 10.3390/ma12121898. URL: https://www.mdpi.com/1996-1944/12/12/1898.

[43] The European Space Agency. *ESA LUNAR NAVIGATION PLANS: LUNAR PATHFINDER & MOONLIGHT*. URL: https://www.unoosa.org/documents/pdf/icg/2022/ICG16/WG-B/ICG16_WG-B_05.pdf.

[44] S. Speretta. “Aerospace Design and Systems Engineering Elements II - Spacecraft Telecommunications Slides”. 2021.

[45] Zachary Warren and Renny A. Fields. “Optical crosslinks and satellite synchronization for GNSS, communications, and beyond”. In: *GPS Solutions* 26.3 (Apr. 2022). DOI: 10.1007/s10291-022-01233-3. URL: https://doi.org/10.1007/s10291-022-01233-3.

[46] NXP Semiconductors. *UWB Minutes: Ranging Technics*. Nov. 2020. URL: https://www.youtube.com/watch?v=5KN4dJdkHUk.

[47] Jeongrae Kim and Byron D. Tapley. “Simulation of Dual One-Way Ranging Measurements”. In: *Journal of Spacecraft and Rockets* 40.3 (May 2003), pp. 419–425. DOI: 10.2514/2.3962. URL: https://doi.org/10.2514/2.3962.

[48] Jun Zhu et al. “Performance of dual one-way measurements and precise orbit determination for BDS via inter-satellite link”. In: *Open Astronomy* 31.1 (Jan. 2022), pp. 276–286. DOI: 10.1515/astro-2022-0034. URL: https://doi.org/10.1515/astro-2022-0034.

[49] Michael Vacek et al. “Single photon laser altimeter data processing, analysis and experimental validation”. In: *Advances in Space Research* 56.7 (Oct. 2015), pp. 1307–1318. DOI: 10.1016/j.asr.2015.06.039. URL: https://doi.org/10.1016/j.asr.2015.06.039.

[50] Jintao Liang et al. “Link Budget Analysis for Free-Space Optical Satellite Networks”. In: June 2022. DOI: 10.1109/wowmom54355.2022.00073. URL: https://doi.org/10.1109/wowmom54355.2022.00073.

[51] PVEducation. *Energy of Photon*. URL: https://www.pveducation.org/pvcdrom/properties-of-sunlight/energy-of-photon.

[52] Reinald Kallenbach et al. “Space-qualified laser system for the BepiColombo Laser Altimeter”. In: *Appl. Opt.* 52.36 (Dec. 2013), pp. 8732–8746. DOI: 10.1364/AO.52.008732. URL: https://opg.optica.org/ao/abstract.cfm?URI=ao-52-36-8732.

[53] Dominic Dirkx et al. “Influence of atmospheric turbulence on planetary transceiver laser ranging”. In: *Advances in Space Research* 54.11 (Dec. 2014), pp. 2349–2370. DOI: 10.1016/j.asr.2014.08.022. URL: https://doi.org/10.1016/j.asr.2014.08.022.

[54] Christoph Althaus et al. “BELA transmitter performance and pointing stability verification campaign at DLR-PF”. In: *Acta Astronautica* (Jan. 2019). DOI: 10.1016/j.actaastro.2018.09.032. URL: https://doi.org/10.1016/j.actaastro.2018.09.032.

[55] K. Gunderson, N. Thomas, and M. Rohner. “A Laser Altimeter Performance Model and Its Application to BELA”. In: *IEEE Transactions on Geoscience and Remote Sensing* 44.11 (2006), pp. 3308–3319. DOI: 10.1109/TGRS.2006.880623.

[56] Kai Weidlich, Markus Rech, and Reinald Kallenbach. “Qualification testing of the laser transmitter part for ESA’s BepiColombo Laser Altimeter (BELA)”. In: Sept. 2011. DOI: 10.1117/12.893071. URL: https://doi.org/10.1117/12.893071.

[57] Rafael Rodrigo. “The BepiColombo Laser Altimeter (BELA): Concept and baseline design”. In: *csic* (Jan. 2007). URL: https://www.academia.edu/74560577/The_BepiColombo_Laser_Altimeter_BELA_Concept_and_baseline_design.

[58] Universität Bern. *BepiColombo Laser Altimeter - BELA*. URL: https://www.bela.space.unibe.ch/.

[59] H. Hussmann et al. “The Ganymede Laser Altimeter (GALA)”. In: *ResearchGate* (Sept. 2014). URL: https://www.researchgate.net/publication/312171398_The_Ganymede_Laser_Altimeter_GALA.

[60] Keigo Enya et al. “The Ganymede Laser Altimeter (GALA) for the Jupiter Icy Moons Explorer (JUICE): Mission, science, and instrumentation of its receiver modules”. In: *Advances in Space Research* 69.5 (Mar. 2022), pp. 2283–2304. DOI: 10.1016/j.asr.2021.11.036. URL: https://doi.org/10.1016/j.asr.2021.11.036.

[61] DLR Institute of Planetary Research. *The Ganymede Laser Altimeter (GALA)*. URL: https://www.dlr.de/pf/en/desktopdefault.aspx/tabid-10617/18438_read-43017/.

[62] Hiroshi Araki et al. “Performance Model Simulation of Ganymede Laser Altimeter (GALA) for the JUICE Mission”. In: *Transactions of the Japan Society for Aeronautical and Space Sciences, aerospace technology Japan* (Jan. 2019). DOI: 10.2322/tastj.17.150. URL: https://doi.org/10.2322/tastj.17.150.

[63] Tom Murphy. *Lunar Retroreflectors*. URL: https://tmurphy.physics.ucsd.edu/apollo/lrrr.html.

[64] Sergey A. Kaplev et al. “Lunar PNT system concept and simulation results”. In: *Open Astronomy* 31.1 (Jan. 2022), pp. 110–117. DOI: 10.1515/astro-2022-0014. URL: https://doi.org/10.1515/astro-2022-0014.

[65] Jürgen L. Müller et al. “Lunar Laser Ranging: a tool for general relativity, lunar geophysics and Earth science”. In: *Journal of Geodesy* 93.11 (Sept. 2019), pp. 2195–2210. DOI: 10.1007/s00190-019-01296-0. URL: https://doi.org/10.1007/s00190-019-01296-0.

[66] Erwan Mazarico et al. “First two-way laser ranging to a lunar orbiter: infrared observations from the Grasse station to LRO’s retro-reflector array”. In: *Earth, Planets and Space* 72.1 (Aug. 2020). DOI: 10.1186/s40623-020-01243-w. URL: https://doi.org/10.1186/s40623-020-01243-w.

[67] Thomas E. Murphy et al. “Lunar eclipse observations reveal anomalous thermal performance of Apollo reflectors”. In: *Icarus* 231 (Mar. 2014), pp. 183–192. DOI: 10.1016/j.icarus.2013.12.006. URL: https://doi.org/10.1016/j.icarus.2013.12.006.

[68] Scott D. Goodrow and Thomas W. Murphy. “Effects of thermal gradients on total internal reflection corner cubes”. In: *Appl. Opt.* 51.36 (Dec. 2012), pp. 8793–8799. DOI: 10.1364/AO.51.008793. URL: https://opg.optica.org/ao/abstract.cfm?URI=ao-51-36-8793.

[69] Hang Li et al. “A compact and lightweight two-dimensional gimbal for inter-satellite laser communication applications”. In: *Opt. Express* 27.17 (Aug. 2019), pp. 24060–24071. DOI: 10.1364/OE.27.024060. URL: https://opg.optica.org/oe/abstract.cfm?URI=oe-27-17-24060.

[70] Moog Inc. *Type 33 Biaxial Gimbal*. 2021. URL: https://www.moog.com/products/space-mechanisms/antenna-pointing-mechanisms/type-33.html.

[71] Surrey Satellite Technology. *Lunar Pathfinder, Data relay satellite in orbit around the Moon, Service Guide*. 2022.

[72] Endurosat. *S-BAND TRANSCEIVER I*. 2023. URL: https://www.endurosat.com/cubesat-store/cubesat-communication-modules/s-band-transceiver/#request-step-modal.

[73] Abdelati Reha and Marouane Bouchouirbat. “A Dual-Band Rectangular CPW Folded Slot Antenna for GNSS Applications”. In: *International Journal of Advanced Research in Electrical, Electronics and Instrumentation Engineering* (2014).

[74] Elliott Kaplan and Christopher Hegarty. In: *Understanding GPS/GNSS: Principles and Applications*. 2017, p. 243.

[75] Mohammed A. Alzabidi et al. “Broadband High Gain Helical Antenna for Satellite Communication Applications”. In: *Institute of Electrical and Electronics Engineers* (2022). DOI: 10.1109/AP-S/USNC-URSI47032.2022.9886926.

[76] Nursinem Handan Şahan. “Why Do Satellites Mostly Operate In L Band?” In: *Surveying Group* (Dec. 2020). URL: https://surveyinggroup.com/why-do-satellites-mostly-operate-in-l-band/.

[77] Jose-Angel Avila-Rodriguez et al. “A Vision on New Frequencies, Signals and Concepts for Future GNSS Systems”. In: *Proceedings of the 20th International Technical Meeting of the Satellite Division of The Institute of Navigation (ION GNSS 2007)* (Sept. 2007), pp. 517–534. URL: https://www.ion.org/publications/abstract.cfm?articleID=7550.

[78] Isidre Mateu et al. “Exploration of possible GNSS signals in S-band”. In: French National Centre for Scientific Research, Sept. 2009. URL: https://hal-enac.archives-ouvertes.fr/hal-01022157.

[79] NASA. *LunaNet: Empowering Artemis with Communications and Navigation Interoperability*. 2021. URL: https://www.nasa.gov/feature/goddard/2021/lunanet-empowering-artemis-with-communications-and-navigation-interoperability.

[80] Tom Murphy. *APOLLO*. URL: https://tmurphy.physics.ucsd.edu/apollo/apollo.html.

[81] Barry Zandbergen. *AE1222-II: Aerospace Design & Systems Engineering Elements I, Part: Spacecraft (bus/platform) design and sizing*. 2015.

[82] Beyond Gravity. *Next Generation On Board Computer*. Jan. 2022. URL: https://products.beyondgravity.com/d/SVq1aavsDmtE/library/show/eyJpZCI6MTM5NywidGltZXN0YW1wIjoiMTY4NjY2OTY3OCJ9:beyond-gravity:XhxYPso6HlA66Xalk-rVWbqO-koFKmh3eVIgYHLdeEU.

[83] NASA. *RINEX Version 3 data*. 2021. URL: https://cddis.nasa.gov/Data_and_Derived_Products/GNSS/RINEX_Version_3.html.

[84] James Wertz and Wiley Larson. *Space Mission Analysis and Design*. Vol. -1. Jan. 1999, pp. 656–657. ISBN: 978-0-7923-0971-0. DOI: 10.1007/978-94-011-2692-2.

[85] NASA. *GEODYN Systems Description Volume 1*. 2015. URL: https://space-geodesy.nasa.gov/techniques/tools/GEODYN/geodyn_vol1.pdf.

[86] Alan Quan et al. “A ground-based memory state tracker for satellite on-board computer memory”. In: (Feb. 1993). DOI: 10.2514/6.1993-4550.

[87] Dan Lev et al. *The technological and commercial expansion of electric propulsion*. Mar. 2019. URL: https://www.sciencedirect.com/science/article/pii/S0094576518319672.

[88] B.T.C Zandbergen. *Modern Liquid Propellant Rocket Engines, 2000 Outlook*. 2000. URL: https://www.researchgate.net/publication/267047129_Modern_Liquid_Propellant_Rocket_Engines_2000_Outlook.

[89] Hugo Nguyen, Johan Köhler, and Lars Stenmark. *The merits of cold gas micropropulsion in state-of-the-art space missions*. Jan. 2002. URL: https://www.diva-portal.org/smash/get/diva2:75729/FULLTEXT01.pdf.

[90] Martin B. Houghton, Craig R. Tooley, and Jr Richard S. Saylor. *Mission design and operations considerations for NASA’s Lunar Reconnaissance Orbiter*. 2008. URL: https://lunar.gsfc.nasa.gov/library/IAC-07-C1_7_06.pdf.

[91] Melissa L. McGuire, Steven L. McCarty, and Laura M. Burk. *Power and Propulsion Element (PPE) Spacecraft Reference Trajectory Document*. 2020. URL: https://ntrs.nasa.gov/api/citations/20200002143/downloads/20200002143.pdf.

[92] J. A. Gonzalez del Amo. *Electric Propulsion Activities*. 2017. URL: https://epic-src.eu/wp-content/uploads/ESA-EP-Activities-2017-DRESDEN.pdf.

[93] Angelo Pasini Ahmed E. S. Nosseir Angelo Cervone. “Review of State-of-the-Art Green Monopropellants: For Propulsion Systems Analysts and Designers”. In: Jan. 2021, p. 21.

[94] Daniel A. Herman and Kenneth G. Unfried. *Xenon acquisition strategies for high-power electric propulsion NASA missions*. Jan. 2015. URL: https://ntrs.nasa.gov/api/citations/20150023080/downloads/20150023080.pdf.

[95] JPL. "Transfers to low-lunar orbits". In: (2023). URL: https://descanso.jpl.nasa.gov/monograph/series12/LunarTraj--05Chapter4TransferstoLowLunarOrbits.pdf.

[96] LLC Advanced Space. *BLT (Ballistic Lunar Transfer) Cheat Sheet*. 2021. URL: https://s3-us-west-2.amazonaws.com/advspace.publicshare/BLT+(Ballistic+Lunar+Transfer)+Cheat+Sheet.pdf.

[97] Ron Noomen. *Maneuvers*. 2022. URL: https://brightspace.tudelft.nl/d2l/le/content/419886/viewContent/2623293/View.

[98] Nosseir A.E.S., A. Cervone, and Pasini A. *Modular impulsive green-monopropellant propulsion system for micro/nano satellites highthrust orbital maneuvers (MIMPS-G)*. Oct. 2020. URL: https://pure.tudelft.nl/ws/portalfiles/portal/85733983/Nosseir_et_al_IAC2020.pdf.

[99] Daniel Cavender. *Emerging low toxicity "green" chemical propulsion technologies for smallsats*. 2018. URL: https://plasmapros.com/wp-content/uploads/S3VI-Webinar-Presentation-Emerging-Green-Prop-Technology_UPDATED_02.10.21-1-1.pdf.

[100] SRE-PA & D-TEC staff. *Margin philosophy for science assessment studies*. 2012.

[101] *Space mission engineering : the new SMAD*. eng. Space technology library ; v. 28. Hawthorne, CA: Microcosm Press, 2011. ISBN: 9781881883159.

[102] Marcin Kaczmarzyk, Marcin Gawronski, and Grzegorz Piatkowski. "Global database of direct solar radiation at the Moon's surface for lunar engineering purposes". In: *E3S Web of Conferences* 49 (Jan. 2018), p. 00053. DOI: 10.1051/e3sconf/20184900053.

[103] Mohammad Asadnezhad, Abdollah Eslamimajd, and Hassan Hajghassem. "Optical system design of star sensor and stray light analysis". In: *Journal of the European Optical Society-Rapid Publications* 14.9 (2018). URL: https://doi.org/10.1186/s41476-018-0078-8.

[104] T.E Girish and S Aranya. "Moon'S Radiation Environment and Expected Performance of Solar Cells During Future Lunar Missions". In: (2010). URL: https://arxiv.org/ftp/arxiv/papers/1012/1012.0717.pdf.

[105] Fred Cunningham. "Calculation of the eclipse factor for elliptical satellite orbits". In: *ARS Journal* 32 (Jan. 1962).

[106] Mukund Patel. *Spacecraft Power Systems*. Vol. 1. CRC Press, 2004. ISBN: 9781420038217.

[107] Seyyed Ali Pourmousavi Kani, Ratnesh Sharma, and Babak Asghari. "A framework for real-time power management of a grid-tied microgrid to extend battery lifetime and reduce cost of energy". In: *2012 IEEE PES Innovative Smart Grid Technologies, ISGT 2012* (Jan. 2012). DOI: 10.1109/ISGT.2012.6175707.

[108] Bruce Yost and Sasha Weston. "State-of-the-Art Small Spacecraft Technology". In: (2021). URL: https://www.nasa.gov/sites/default/files/atoms/files/soa%5C_2021%5C_0.pdf.

[109] Marc Malagoli and Laurence Cosquéric. "Space Harness Design Optimization Opportunities on ECSS derating rules". In: *ESCIES* (2013).

[110] Shuaishuai Lv et al. "The Influence of Temperature on the Capacity of Lithium Ion Batteries with Different Anodes". In: *Energies* 15 (Dec. 2021), p. 60. DOI: 10.3390/en15010060.

[111] Kalaivanan Thirupathi, Pal Barzcy, and Béla Somosvári. "The Study of Chromate Conversion Coating on Space Metallic Hardwares". In: May 2016.

[112] Lonny Kauder. *Spacecraft Thermal Control Coatings References*. 2005. URL: https://ntrs.nasa.gov/api/citations/20070014757/downloads/20070014757.pdf.

[113] Sara E. Kline Donald A. Jaworske. *Review of End-of-Life Thermal Control Coating Performance*. 2008. URL: https://ntrs.nasa.gov/api/citations/20080018585/downloads/20080018585.pdf.

[114] NASA Ames Research Center. *State-of-the-Art Small Spacecraft Technology*. 2023. URL: https://www.nasa.gov/sites/default/files/atoms/files/2022_soa_full.pdf.

[115] Alberto Riverola et al. "Mid-infrared emissivity of crystalline silicon solar cells". In: *Solar Energy Materials and Solar Cells* 174 (Jan. 2018), pp. 607–615. DOI: 10.1016/j.solmat.2017.10.002.

[116] GEMMA SAURA CARRETERO. *Study of a lunar satellite navigation system*. Tech. rep. Universitat Politècnica de Catalunya, 2012. URL: https://upcommons.upc.edu/bitstream/handle/2099.1/17684/Project%5C%20Report.pdf.

[117] Wouter van der Wal. *Introduction to Satellite Navigation*. 2019. URL: https://brightspace.tudelft.nl/d2l/le/content/512955/viewContent/2888769/View.

[118] Eurospace. *REACH - Eurospace*. Jan. 13, 2023. URL: https://eurospace.org/working-bodies/reach/.

[119] A. F. Norman et al. *Advanced manufacturing of titanium propellant tanks for space applications part 1: tank design and demonstrator manufacturing*. Oct. 2021. URL: https://link.springer.com/article/10.1007/s12567-021-00397-x.

[120] Wouter van der Wal. *Project Guide Design Synthesis Exercise: Navigating the Moon*. Apr. 2023.

[121] ESA. *Galileo satellites*. 2023. URL: https://www.esa.int/Applications/Navigation/Galileo/Galileo_satellites (visited on 05/02/2023).

[122] U.S Bureau of Labor Statistics. *CPI Inflation Calculator*. 2023. URL: https://www.bls.gov/data/inflation_calculator.htm (visited on 05/02/2023).

[123] CNET. *Atlas 5 rocket launches NASA moon mission*. 2009. URL: https://web.archive.org/web/20131103112957/http://news.cnet.com/8301-19514_3-10268241-239.html (visited on 05/02/2023).

[124] Space.com. *LADEE: NASA's Moon Mission to Study Lunar Dust Secrets*. 2018. URL: https://www.space.com/22452-ladee-nasa-moon-mission.html (visited on 05/02/2023).

[125] Space.com. *Japan Launches Kaguya Probe on Moon Mission*. 2020. URL: https://www.space.com/4345-japan-launches-kaguya-probe-moon-mission.html (visited on 05/02/2023).

[126] Project Management Institute. *A Guide to the Project Management Body of Knowledge (PMBOK Guide)*. Project Management Institute, 2021.

[127] European court of auditors. *EU space programmes Galileo and Copernicus*. Tech. rep. 2021. URL: https://www.eca.europa.eu/Lists/ECADocuments/SR21_07/SR_EUs-space-assets_EN.pdf.

[128] Pratap Misra and Per Enge. *Global Positioning System, Signal, Measurements, and Performance*. 2006, pp. 112–113. ISBN: 0-9709544-1-7.

[129] SpaceX. *FALCON USER'S GUIDE*. Sept. 2021. URL: https://www.spacex.com/media/falcon-users-guide-2021-09.pdf.

[130] Fox Bernard, Kevin Brancato, and Brien Alkire. *Guidelines and Metrics for Assessing Space System Cost Estimates*. Santa Monica, CA: RAND Corporation, 2008.

[131] Mike Ashby, Hugh Shercliff, and David Cebon. *Materials: engineering, science, processing and design*. 2019, p. 745. ISBN: 978-0-08-102376-1.

[132] Ioannis W. Kokkinakis and Dimitris Drikakis. "Atmospheric pollution from rockets". In: *Journal of the European Optical Society-Rapid Publications* (2022).

[133] Artemis Team. *LunaNet Interoperability Specification Document*. 2023.

A

Subsystem Requirements

The appendix includes all requirements developed for several sub-/systems. They are listed as separate tables per system. The first column includes the ID for each requirement, followed by a description. The final column studies the compliance of the requirement, where 'yes' means the requirement is fulfilled, 'no' means it is not fulfilled, and '-' implies the requirement was not considered in the design. A sample table is introduced in Table A.1

Table A.1: Requirements for ... Subsystem

	Title for Requirement Section	
NTM-SYS-TEMP-01:	Requirement description	Yes/No/-

Table A.2: Navigation Payload Requirements

	General Navigation (NAV) Requirements	
NTM-SYS-NAV-01:	The LNSS shall provide a navigation service for lunar surface stationary, surface mobile, descending, ascending, orbiting users to ESA, ESA's partners and third parties.	Yes
NTM-SYS-NAV-02:	The LNSS shall inform the ULS about expected quality and availability.	Yes
NTM-SYS-NAV-03:	The navigation service shall allow the users to determine their position and velocity with respect to the selenocentric frame.	Yes
NTM-SYS-NAV-04:	The navigation service shall allow the users to determine their position and velocity with respect to the lunar inertial reference frame.	Yes
NTM-SYS-NAV-05:	The navigation service shall allow the users to determine the local clock offset with respect with the lunar reference time.	Yes
NTM-SYS-NAV-06:	Navigation real time services (except TWM) shall be provided in SV1 and SV2 at least.	Yes
NTM-SYS-NAV-07:	Navigation real time services (except TWM) shall be provided continuously.	Yes
	One Way Ranging (OWR) Requirements	
NTM-SYS-NAV-OWR-01:	The OWR service shall result in provider nodes position error smaller or equal to $10\,\mathrm{m}$ with a two sigma confidence interval (95% of the time over 24 h).	Yes
NTM-SYS-NAV-OWR-02:	The OWR service shall result in provider nodes velocity error smaller or equal to $0.1\,\mathrm{m\,s^{-1}}$ with a two sigma confidence interval (95% of the time over 24 h).	Yes
NTM-SYS-NAV-OWR-03:	The availability of the OWR service shall be greater or equal to 95% of the time, computed over 3 months.	-
NTM-SYS-NAV-OWR-04:	The OWR service shall be available at least 20 min without interruption with a probability of over 99%, computed over a year.	-
	Two Way Measurements (TWM) Requirements	
NTM-SYS-NAV-TWM-01:	The TWM service shall provide coverage to ULS located in SV1 and SV2.	Yes
NTM-SYS-NAV-TWM-02:	The TWM service shall provide coverage to ULS in a service window of 18 hours of any earth day.	Yes
NTM-SYS-NAV-TWM-03:	The TWM service shall allow the user to move the centre of the service window by ± 3 hours at least once in any 12-month period with more than 8 weeks of user notice.	-
NTM-SYS-NAV-TWM-04:	The TWM service shall provide the measurements to the user within 1 min from their generation.	Yes
NTM-SYS-NAV-TWM-05:	The TWM service shall be available to multiple collocated ULS.	-
NTM-SYS-NAV-TWM-06:	The TWM shall be in line with the LunaNet Interoperability Specification Document [133].	Yes
NTM-SYS-NAV-TWM-07:	The TWM service shall result in provider nodes position error smaller or equal to $10\,\mathrm{m}$ with a two sigma confidence interval (95% of the time over 24 h).	Yes
NTM-SYS-NAV-TWM-08:	The TWM service shall result in provider nodes velocity error smaller or equal to $0.1\,\mathrm{m\,s^{-1}}$ with a two sigma confidence interval (95% of the time over 24 h).	Yes

NTM-SYS-NAV-TWM-09:	The TWM service shall provide the necessary data and measurements (at least clock and ephemeris data) for the user to obtain its PVT.	Yes
	Position, Velocity, and Time (PVT) Requirements	
NTM-SYS-NAV-PVT-01:	The PVT service shall allow a user to compute position and velocity and calculate time offset of local clock with respect to the LNSS time using AFS at least once per second.	Yes
NTM-SYS-NAV-PVT-02:	The Navigation PVT services shall provide a time coverage of at least 15 continuous hours, computed over any 24-hour period.	Yes
NTM-SYS-NAV-PVT-03:	The PVT service shall ensure a Height constrained Horizontal Dilution of Precision (HHDOP defined in [13]) less than 3.5.	Yes
NTM-SYS-NAV-PVT-04:	The PVT service availability shall be at least 95%, computed over 3 months.	-
NTM-SYS-NAV-PVT-05:	When the PVT service is available it shall work for 20 minutes without interruption with a probability of 99.9% over a yearly period.	-
NTM-SYS-NAV-PVT-06:	The PVT service shall allow position, velocity, and time solution for the surface to be computed in 60 s from initialisation of the Navigation User Terminal.	-
NTM-SYS-NAV-PVT-07:	The position error arising from the PVT service for orbiting users shall be smaller than $100\,\mathrm{m}$ (in 3 dimensions; 95% of the time).	Yes
NTM-SYS-NAV-PVT-08:	The velocity error arising from the PVT service for orbiting users shall be smaller than $1\,\mathrm{m\,s^{-1}}$ (in 3 dimensions; 95% of the time).	Yes
NTM-SYS-NAV-PVT-09:	The timing error arising from the PVT service for orbiting users shall be smaller than $15\,\mathrm{ms}$ (95% of the time).	Yes
NTM-SYS-NAV-PVT-10:	The horizontal position error arising from the PVT service for landing users shall be smaller than $50\,\mathrm{m}$ (95%).	Yes
NTM-SYS-NAV-PVT-11:	The vertical position error arising from the PVT service for landing users shall be smaller than $100\,\mathrm{m}$ (95%).	Yes
NTM-SYS-NAV-PVT-12:	The horizontal velocity error arising from the PVT service for landing users shall be smaller than $1\,\mathrm{m\,s^{-1}}$ (95%).	Yes
NTM-SYS-NAV-PVT-13:	The vertical velocity error arising from the PVT service for landing users shall be smaller than $2\,\mathrm{m\,s^{-1}}$ (95%).	Yes
NTM-SYS-NAV-PVT-14:	The timing error arising from the PVT service for landing users shall be smaller than $15\,\mathrm{ms}$ (95%).	Yes
NTM-SYS-NAV-PVT-15:	The position error arising from the PVT service for surface users shall be smaller than $10\,\mathrm{m}$ (95%).	Yes
NTM-SYS-NAV-PVT-16:	The velocity error arising from the PVT service for surface users shall be smaller than $1\,\mathrm{m\,s^{-1}}$ (95%).	Yes
NTM-SYS-NAV-PVT-17:	The timing error arising from the PVT service for surface users shall be smaller than $0.4\,\mu\mathrm{s}$ (95%).	Yes
	Time Dissemination (TS) Requirements	
NTM-SYS-NAV-TS-01:	The TS service shall allow the user to obtain the bias between the local clock and the lunar reference time.	Yes
NTM-SYS-NAV-TS-02:	The TS service shall allow the user to obtain the bias between the local clock and the UTC.	Yes
NTM-SYS-NAV-TS-03:	The TS service accuracy shall be greater or equal to $1\,\mu\mathrm{s}$.	Yes
NTM-SYS-NAV-TS-04:	The TS service shall be available over 95% of the time, computed over 3 months.	-

Table A.3: Requirements for the Propulsion Subsystem

	General Propulsion Requirements	
NTM-SYS-PROP-01:	The propulsion subsystem shall have a max delta V of $620\,\mathrm{m\,s^{-1}}$.	Yes
NTM-SYS-PROP-02:	The propulsion subsystem shall not use hydrazine.	Yes
NTM-SYS-PROP-03:	The propulsion subsystem shall have a maximum mass of $265\,\mathrm{kg}$.	Yes
NTM-SYS-PROP-04:	The propulsion subsystem shall have a propellant margin of $5\,\%$ for each mission phase.	Yes
NTM-SYS-PROP-05:	The thrusters shall be capable of counteracting all three axis rotations of the spacecraft.	Yes
NTM-SYS-PROP-06:	The thrusters shall have the capability to be throttled down to at least $80\,\%$ of maximum thrust.	Yes
NTM-SYS-PROP-07:	The propulsion subsystem shall be redundant by a factor of 2.	Yes
NTM-SYS-PROP-08:	The propulsion subsystem shall provide $200\,\mathrm{km\,s^{-1}}$ of Δ V to insert the NTM constellation into the final mission orbit.	Yes

Table A.4: Requirements for the Attitude Determination & Control Subsystem

	General ADCS Requirements	
NTM-SYS-ADCS-01:	The ADCS shall be able to determine the attitude of the spacecraft with an accuracy of $0.23°$.	Yes
NTM-SYS-ADCS-02:	The ADCS shall be able to calculate the output based on the input with an accuracy of $0.46°$, 2 sigma interval	Yes
NTM-SYS-ADCS-03:	The ADCS subsystem shall be able to correct the attitude of the spacecraft with a frequency of $1\,\mathrm{s^{-1}}$.	Yes
NTM-SYS-ADCS-04:	The ADCS subsystem shall be able to make adjustments to the orbit of the spacecraft based on the inputs from Navigation subsystem.	-
NTM-SYS-ADCS-05:	The ADCS subsystem shall be in service for at least the complete designed mission duration of 12 years.	-
NTM-SYS-ADCS-06:	The ADCS shall be redundant by a factor of 2	Yes

Table A.5: Requirements for the Electrical Power Subsystem

	Power Generation Requirements	
NTM-SYS-EPS-GEN-01	The EPS shall provide continuous power for at least $15\,\mathrm{h}$.	Yes
NTM-SYS-EPS-GEN-02	The EPS shall generate more than $1461\,\mathrm{W}$ of power at EOL with two sigma confidence interval ($95\,\%$).	Yes
NTM-SYS-EPS-GEN-03	The solar array shall be rotatable.	-
	Power Storage Requirements	
NTM-SYS-EPS-STR-01	The EPS shall provide more than $926\,\mathrm{W}$ during eclipse at EOL.	Yes
NTM-SYS-EPS-STR-02	The first battery shall have a capacity higher than $2394\,\mathrm{W\,h}$ at BOL with a two sigma confidence interval ($95\,\%$).	Yes
NTM-SYS-EPS-STR-03	The second battery shall have a capacity of $4895\,\mathrm{W\,h}$ at BOL with a two sigma confidence interval ($95\,\%$).	Yes
NTM-SYS-EPS-STR-04	The batteries shall store $1000\,\mathrm{W\,h}$ during launch to initialise the satellite once in orbit.	Yes
NTM-SYS-EPS-STR-05	The first battery shall accommodate at least 9800 cycles during its 12 year lifetime.	Yes
NTM-SYS-EPS-STR-06	The second battery shall accommodate at least 200 cycles during its 12 year lifetime.	Yes
	Sustainable Power Requirements	

NTM-SYS-EPS-SUS-01	The EPS shall not use Radioisotope Thermoelectric Generators RTGs.	Yes

Table A.6: Requirements for the Thermal Control Subsystem (TCS)

	General TCS Requirements	
NTM-SYS-TCS-01:	The operative temperature range of the spacecraft's body shall be between $0\,^{\circ}$C an $40\,^{\circ}$C.	Yes
NTM-SYS-TCS-02:	The operative temperature range of the solar arrays shall be between $-230\,^{\circ}$C an $110\,^{\circ}$C.	Yes
NTM-SYS-TCS-03:	The TCS shall use passive thermal control as much as possible.	Yes
NTM-SYS-TCS-04:	The TCS shall not use power during eclipse.	Yes
NTM-SYS-TCS-05:	The TCS shall not use toxic materials.	Yes
NTM-SYS-TCS-06:	The TCS shall measure the temperature of critical components within $1\,^{\circ}$C accuracy.	Yes

Table A.7: Requirements for the Structures Subsystem

	General Structures Requirements	
NTM-SYS-STR-01:	The structure subsystem shall provide a structural interface for all other subsystems.	-
NTM-SYS-STR-02:	The structure subsystem shall safeguard the other subsystems from external risks.	Yes
NTM-SYS-STR-03:	The structure subsystem shall be designed using a safety margin on performance requirements.	Yes
NTM-SYS-STR-04:	The primary structure shall have dimensions below 2 x 3.5 x 3.5 [m].	Yes
	Structure Interface Requirements	
NTM-SYS-STR-INT-01:	The structure subsystem shall provide the launcher interface.	Yes
NTM-SYS-STR-INT-02:	The structure subsystem shall provide the solar array deployment mechanism.	Yes
NTM-SYS-STR-INT-03:	The structure subsystem shall have the solar array rotating mechanism.	Yes
NTM-SYS-STR-INT-04:	The structure subsystem shall have a rotating transceiver mechanism.	Yes
NTM-SYS-STR-INT-05:	The structure subsystem shall have a structural ADCS interface.	Yes
NTM-SYS-STR-INT-06:	The solar panels interface shall withstand 8.5g loads in bending.	Yes
NTM-SYS-STR-INT-07:	The structure subsystem elements shall have a maximum allowable deformation of 2%.	Yes
NTM-SYS-STR-INT-08:	The structure subsystem shall provide signal insulation to the payload to reduce noise.	-
NTM-SYS-STR-INT-09:	The structure subsystem shall not deform under the launcher's internal fairing pressure.	-
	Structure Performance Requirements	
NTM-SYS-STR-PERF-01:	The structure subsystem shall be able to withstand 8.5g axial acceleration during launch without yielding.	Yes
NTM-SYS-STR-PERF-02:	The structure subsystem shall be able to withstand 3g lateral acceleration during launch without yielding.	Yes
NTM-SYS-STR-PERF-03:	The structure subsystem shall have an axial eigenfrequency higher than 25 Hz.	Yes
NTM-SYS-STR-PERF-04:	The structure subsystem shall have a lateral eigenfrequency higher than 10 Hz.	Yes

NTM-SYS-STR-PERF-05:	The secondary structures minimum resonance frequency shall be above 35 Hz.	-
NTM-SYS-STR-PERF-06:	The structure subsystem shall not buckle under launch loads.	Yes
NTM-SYS-STR-PERF-07:	The structure subsystem shall be able to withstand the loads caused by an environment temperature range of -120 and 130°C.	Yes
NTM-SYS-STR-PERF-08:	The structure subsystem shall protect other subsystems from external radiation.	-
NTM-SYS-STR-PERF-09:	The propellant tank shall withstand 4 MPa of pressure.	Yes
NTM-SYS-STR-PERF-10:	The structure shall withstand periodical loads from nominal operation for 12 years.	Yes
	Structure Manufacturing Requirements	
NTM-SYS-STR-MAN-01:	The structure subsystem shall be accesible for assembly.	-
NTM-SYS-STR-MAN-02:	The materials used shall be readily manufacturable, considering ease of production and sustainable methods.	Yes
	Structure Sustainability Requirements	
NTM-SYS-STR-SUS-01:	Upon failure, the structure subsystem shall maintain its integrity without fragmentation.	-
NTM-SYS-STR-SUS-02:	The subsystem material shall not be toxic.	Yes

Table A.8: Requirements for TT&C Subsystem

	General TT&C Requirements	
NTM-SYS-TTC-GEN-01	The LNSS shall provide the same access hardware architecture for all Lunar missions	Yes
NTM-SYS-TTC-GEN-02	Monitoring shall be possible in worst case conditions on Earth	-
NTM-SYS-TTC-GEN-03	The TT&C system shall be designed, developed, and produced before the first launch, which is at the latest in 2028	Yes
NTM-SYS-TTC-GEN-04	The lifetime of the TT&C system shall be at least 12 years.	-
	Signal Requirements	
NTM-SYS-TTC-SIG-01	The navigation real time services (except TWM) shall be broadcast with a radio signal (AFS).	Yes
NTM-SYS-TTC-SIG-02	The navigation signal data rate shall be at least 1000 bit/s.	-
NTM-SYS-TTC-SIG-03	The monitoring signal data rate shall be at least 1000 bit/s	Yes
NTM-SYS-TTC-SIG-04	The crosslink signal shall be detectable upon arrival at the receiver.	Yes
	Performance Requirements	
NTM-SYS-TTC-PRF-01	The TWM service shall provide the measurements to the user within 1 min from their generation.	Yes
NTM-SYS-TTC-PRF-02	The laser pointing error of the LNS shall be smaller than 0.5°.	Yes
	Sustainable Requirements	
NTM-SYS-TTC-SUS-01	The LNSS shall rely on heritage from Earth GNSS systems where possible.	Yes
	Legal Requirements	
NTM-SYS-TTC-LEG-01	The Service to User MOC interface shall at least implement the terrestrial interfaces defined in accordance with [4]	Yes
NTM-SYS-TTC-LEG-02	The LNSS shall comply with the LunaNet Interoperability specifications [4].	Yes
NTM-SYS-TTC-LEG-03	The LNSS shall comply with the Future Lunar Communications Architecture and Solar System Internetwork (SSI) Architecture as specified in [5].	Yes
NTM-SYS-TTC-LEG-04	The LNSS shall be designed to use frequency bands that are available and allocated for Lunar Navigation Systems.	Yes

NTM-SYS-TTC-LEG-04A	The frequency band used for downlink to the user from the LNS shall be in the following range: 2483.5 - 2500 MHz.	Yes
NTM-SYS-TTC-LEG-04B	The frequency band used for downlink from LNS to relay shall be in the following range: 2025-2110 MHz.	Yes
NTM-SYS-TTC-LEG-04C	The optical links shall not interfere with other missions.	Yes
NTM-SYS-TTC-LEG-04D	The coding used for the signal to the user from the LNS shall be convolutional or LDPC.	Yes
NTM-SYS-TTC-LEG-05	The AFS shall adhere to the LunaNet Interoperability Specification Document [4].	Yes
	External Requirements	
NTM-SYS-TTC-EXT-01	The LNSS shall establish, validate, and maintain over the lifetime of the mission interfaces with external entities.	Yes
	User Requirements	
NTM-SYS-TTC-USER-01	The OWR, PVT and TS shall be accessed in real time on a Navigation User Terminal that operates within the following envelope: • Size <30 x 30 x 10 cm or 9 L. • Weight <4 kg. • Power <15 W (25 W peak).	-
NTM-SYS-TTC-USER-02	The OWR, PVT and TS shall be accessed in real time on a User Terminal Antenna that operates within the following envelope: • Size <10 x 10 x 5 cm or 0.5 L. • Weight <0.3 kg.	Yes
NTM-SYS-TTC-USER-03	The LNSS shall define, establish, and maintain a standardised interface to users	-

Table A.9: Requirements for CDH Subsystem

	General CDH Requirements	
NTM-SYS-CDH-GEN-01	The CDH shall protect confidentiality, integrity, availability and accountability of the Service infrastructure.	Yes
NTM-SYS-CDH-GEN-02	The CDH shall prevent unauthorised access (corruption, interception, loss) of services.	Yes
NTM-SYS-CDH-GEN-03	The CDH shall provide protection from intentional attacks to undermine services (confidentiality, integrity, availability and accountability).	Yes
NTM-SYS-CDH-GEN-04	The CDH shall authenticate the navigation message data required for the PVT service.	Yes
NTM-SYS-CDH-GEN-05	The CDH shall make sure users do not lose access due to lack of data required for authentication.	-
NTM-SYS-CDH-GEN-06	The CDH shall guarantee the confidentiality of users' sensitive data. This can include positional and research data.	Yes
NTM-SYS-CDH-GEN-07	The CDH shall define, establish, and maintain a standardised interface to users.	Yes
NTM-SYS-CDH-GEN-08	The CDH shall establish, validate, and maintain over the lifetime of the mission interfaces with external entities.	Yes
NTM-SYS-CDH-GEN-09	The lifetime of the CDH system shall be at least 12 years.	Yes
NTM-SYS-CDH-GEN-10	The CDH system shall be designed, developed, and produced before the first launch, which is at the latest in 2028.	Yes
NTM-SYS-CDH-GEN-11	The CDH system shall be able to recover from single event effects, which includes upsets.	Yes
NTM-SYS-CDH-GEN-12	The onboard computer shall be the centralized computer commanding all daughterboards.	Yes
NTM-SYS-CDH-GEN-13	The CDH system must be able to work in accordance with the spacecrafts clock.	-
	Performance Requirements	
NTM-SYS-CDH-PRF-01	The TWM service shall provide the measurements to the user within 1 min from their generation.	-

NTM-SYS-CDH-PRF-02	The PVT service shall allow position, velocity and time solution for the surface to be computed in 60 s from initialisation of the Navigation User Terminal.	-
NTM-SYS-CDH-PRF-03	The reliability of the CDH system shall be higher than 0.9.	Yes
NTM-SYS-CDH-PRF-04	The onboard hard drive shall have at least 81600 Mbit of storage.	Yes
NTM-SYS-CDH-PRF-05	The CDH shall have a processing memory higher than 1.125 Mbit.	Yes
NTM-SYS-CDH-PRF-06	The CDH system shall have a computer power required for computing ODTS that is higher than 53.85 MIPS.	Yes
	Legal Requirements	
NTM-SYS-CDH-LEG-01	The CDH shall comply with the LunaNet Interoperability specifications.	Yes
NTM-SYS-CDH-LEG-02	The CDH shall comply with the Future Lunar Communications Architecture and Solar System Internetwork (SSI) Architecture.	Yes
	Sustainability Requirements	
NTM-SYS-CDH-SUS-01	The CDH shall rely on heritage from Earth GNSS systems where possible.	-

B

Diagrams

This chapter includes the diagrams of the design.

B.1. Technical drawing

The technical drawing shows the external layout of the spacecraft together with its main dimensions. *By I. Maes*

B.2. Mission Diagrams

The appendix includes diagrams to clarify the mission. It starts with a Functional Flow Diagram and a Functional Breakdown Structure. It is followed by the Production Plan, to finally conclude with a Project Gantt Chart showing a timeline.

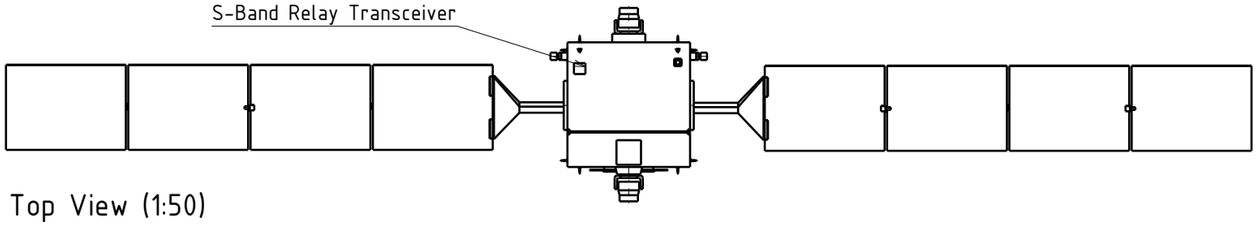

Top View (1:50)

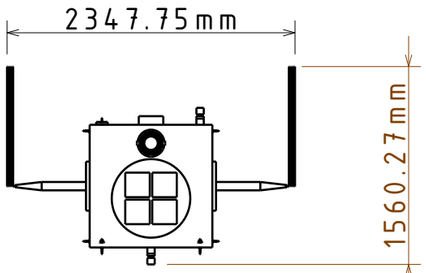

Front View Stowed (1:50)

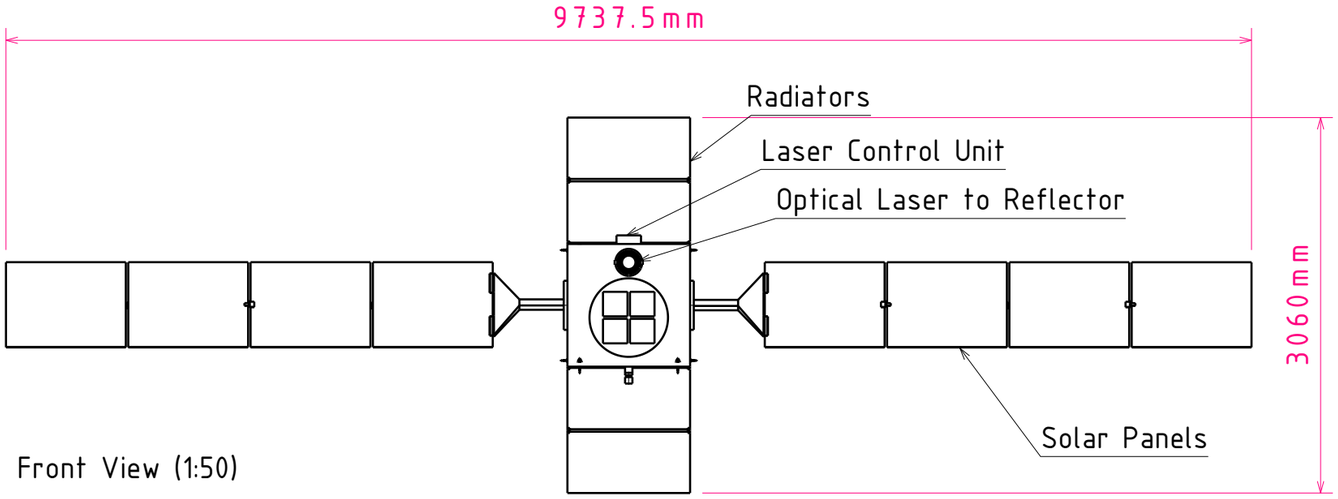

Front View (1:50)

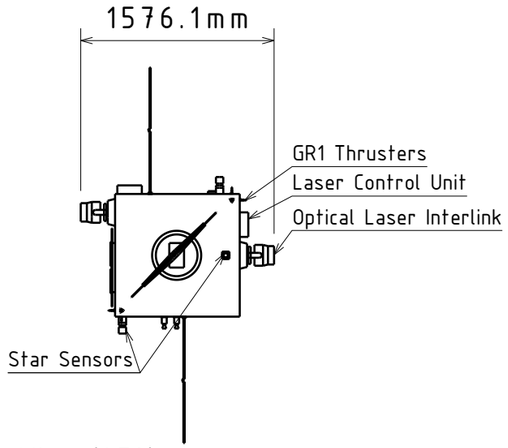

Right View (1:50)

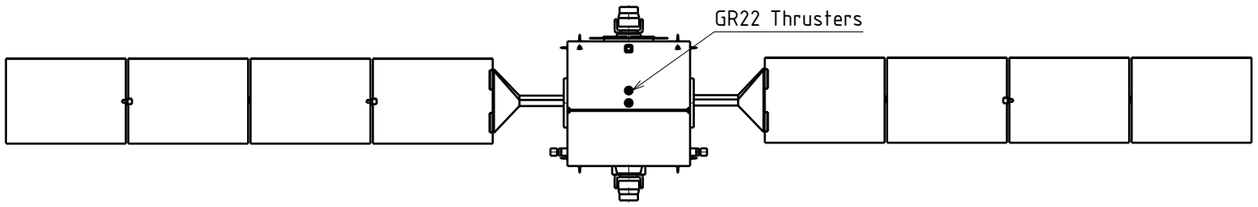

Bottom View (1:50)

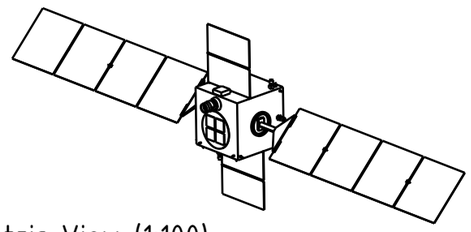

Isometric View (1:100)

DESIGNED BY: Group 22 DATE: 17/06/2023		LUNAV Satellite	
CHECKED BY: XXX DATE: XXX			
SIZE A3		Tu Delft	
SCALE	WEIGHT (kg)	DRAWING NUMBER	SHEET
1:50	XXX	001	1/1

Functional Flow Block Diagram

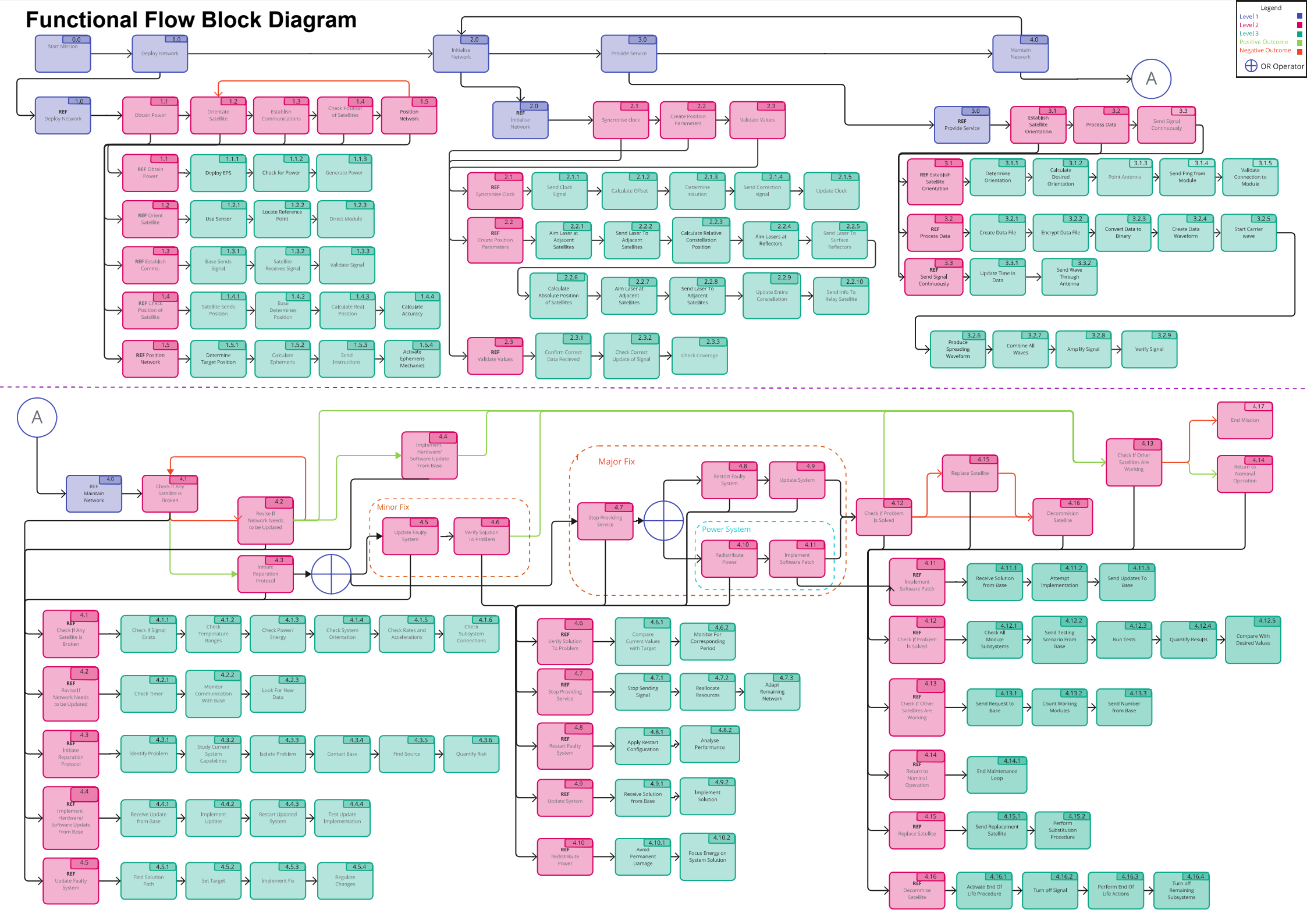

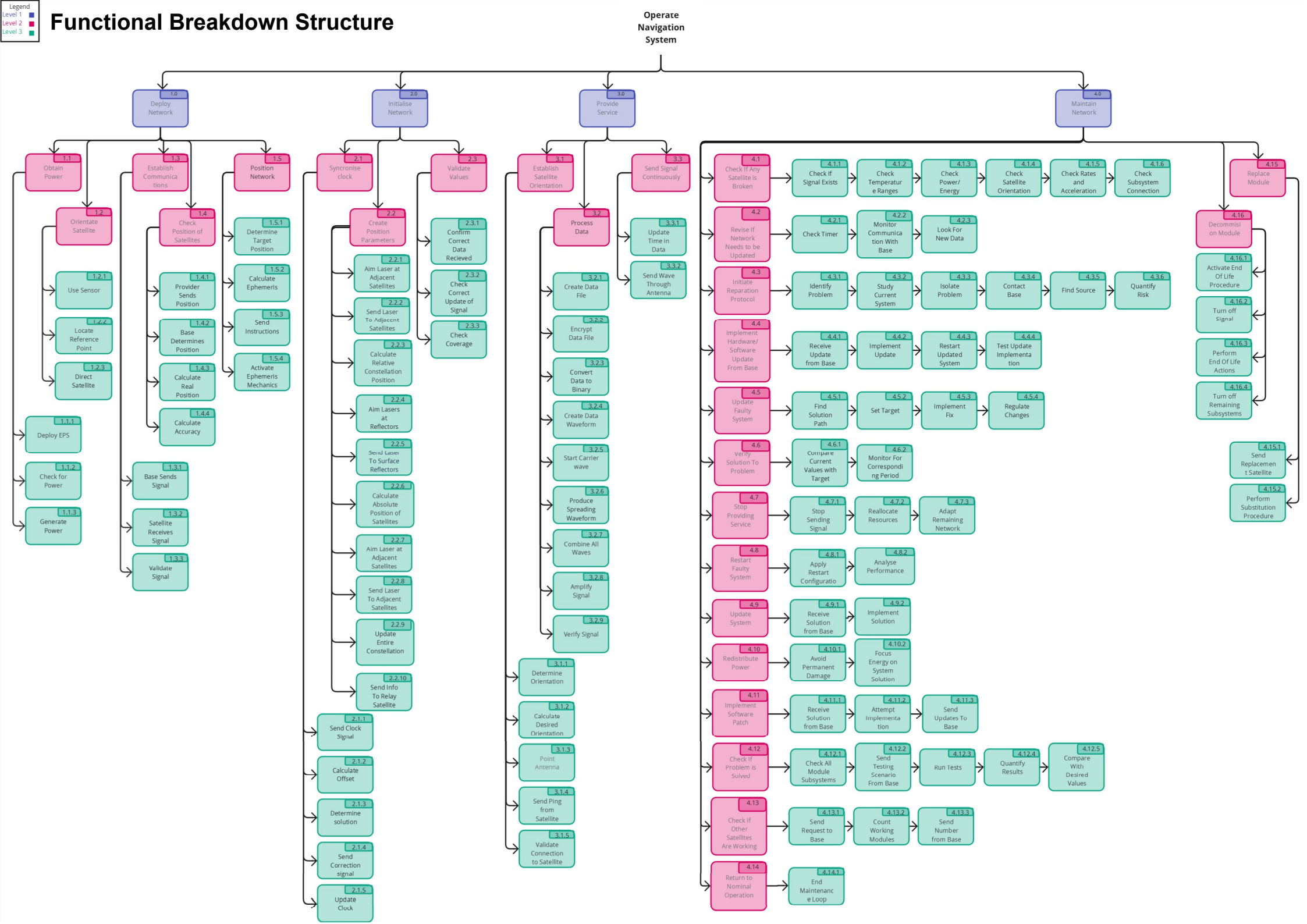
Legend
Level 1
Level 2
Level 3
Functional Breakdown Structure
Operate Navigation System
1.0 Deploy Network
2.0 Initialise Network
3.0 Provide Service
4.0 Maintain Network
1.1 Obtain Power
1.1.1 Deploy EPS
1.1.2 Check for Power
1.1.3 Generate Power
1.2 Orientate Satellite
1.2.1 Use Sensor
1.2.2 Locate Reference Point
1.2.3 Direct Satellite
1.3 Establish Communications
1.3.1 Base Sends Signal
1.3.2 Satellite Receives Signal
1.3.3 Validate Signal
1.4 Check Position of Satellites
1.4.1 Provider Sends Position
1.4.2 Base Determines Position
1.4.3 Calculate Real Position
1.4.4 Calculate Accuracy
1.5 Position Network
1.5.1 Determine Target Position
1.5.2 Calculate Ephemeris
1.5.3 Send Instructions
1.5.4 Activate Ephemeris Mechanics
2.1 Syncronise clock
2.1.1 Send Clock Signal
2.1.2 Calculate Offset
2.1.3 Determine solution
2.1.4 Send Correction signal
2.1.5 Update Clock
2.2 Create Position Parameters
2.2.1 Aim Laser at Adjacent Satellites
2.2.2 Send Laser To Adjacent Satellites
2.2.3 Calculate Relative Constellation Position
2.2.4 Aim Lasers at Reflectors
2.2.5 Send Laser To Surface Reflectors
2.2.6 Calculate Absolute Position of Satellites
2.2.7 Aim Laser at Adjacent Satellites
2.2.8 Send Laser To Adjacent Satellites
2.2.9 Update Entire Constellation
2.2.10 Send Info To Relay Satellite
2.3 Validate Values
2.3.1 Confirm Correct Data Recieved
2.3.2 Check Correct Update of Signal
2.3.3 Check Coverage
3.1 Establish Satellite Orientation
3.1.1 Determine Orientation
3.1.2 Calculate Desired Orientation
3.1.3 Point Antenna
3.1.4 Send Ping from Satellite
3.1.5 Validate Connection to Satellite
3.2 Process Data
3.2.1 Create Data File
3.2.2 Encrypt Data File
3.2.3 Convert Data to Binary
3.2.4 Create Data Waveform
3.2.5 Start Carrier wave
3.2.6 Produce Spreading Waveform
3.2.7 Combine All Waves
3.2.8 Amplify Signal
3.2.9 Verify Signal
3.3 Send Signal Continuously
3.3.1 Update Time in Data
3.3.2 Send Wave Through Antenna
4.1 Check If Any Satellite is Broken
4.1.1 Check If Signal Exists
4.1.2 Check Temperature Ranges
4.1.3 Check Power/ Energy
4.1.4 Check Satellite Orientation
4.1.5 Check Rates and Acceleration
4.1.6 Check Subsystem Connection
4.2 Revise If Network Needs to be Updated
4.2.1 Check TImer
4.2.2 Monitor Communication With Base
4.2.3 Look For New Data
4.3 Initiate Reparation Protocol
4.3.1 Identify Problem
4.3.2 Study Current System
4.3.3 Isolate Problem
4.3.4 Contact Base
4.3.5 Find Source
4.3.6 Quantify Risk
4.4 Implement Hardware/ Software Update From Base
4.4.1 Receive Update from Base
4.4.2 Implement Update
4.4.3 Restart Updated System
4.4.4 Test Update Implementation
4.5 Update Faulty System
4.5.1 Find Solution Path
4.5.2 Set Target
4.5.3 Implement Fix
4.5.4 Regulate Changes
4.6 Verify Solution To Problem
4.6.1 Compare Current Values with Target
4.6.2 Monitor For Corresponding Period
4.7 Stop Providing Service
4.7.1 Stop Sending Signal
4.7.2 Reallocate Resources
4.7.3 Adapt Remaining Network
4.8 Restart Faulty System
4.8.1 Apply Restart Configuratio
4.8.2 Analyse Performance
4.9 Update System
4.9.1 Receive Solution from Base
4.9.2 Implement Solution
4.10 Redistribute Power
4.10.1 Avoid Permanent Damage
4.10.2 Focus Energy on System Solution
4.11 Implement Software Patch
4.11.1 Receive Solution from Base
4.11.2 Attempt Implementation
4.11.3 Send Updates To Base
4.12 Check If Problem Is Solved
4.12.1 Check All Module Subsystems
4.12.2 Send Testing Scenario From Base
4.12.3 Run Tests
4.12.4 Quantify Results
4.12.5 Compare With Desired Values
4.13 Check If Other Satellites Are Working
4.13.1 Send Request to Base
4.13.2 Count Working Modules
4.13.3 Send Number from Base
4.14 Return to Nominal Operation
4.14.1 End Maintenance Loop
4.15 Replace Module
4.15.1 Send Replacement Satellite
4.15.2 Perform Substitution Procedure
4.16 Decommision Module
4.16.1 Activate End Of Life Procedure
4.16.2 Turn off Signal
4.16.3 Perform End Of Life Actions
4.16.4 Turn off Remaining Subsystems

Production Plan

Satellite	Subsystem	Components	Component acronym	Year 1 Jan-Feb	Mar-Apr	May-Jun	Jul-Aug	Sep-Oct	Nov-Dec	Year 2 Jan-Feb	Mar-Apr	May-Jun	Jul-Aug	Sep-Oct	Nov-Dec	Year 3 Jan-Feb	Mar-Apr	May-Jun	Jul-Aug	Sep-Oct	Nov-Dec
6 satellites	NTM-NAV	Clock (x3)	CLO	Place the orders of each component	Manufacture CLO (from external companies)			Ship CLO	CLO accuracy test V campaign ESTEC		CLO vibration Test V ESTEC	Manufacturing Buffer time	Assembly of the Clock subsystem ESTEC		Assembly test V Clock subsystem ESTEC		Integration of the 6 NTM spacecraft subsystems		Final integration tests of the 6 NTM spacecraft subsystems		Integration Buffer time
		Signal Generation Unit	CSG			Manufacture CSG (from external companies)				Ship CSG	CFG magnetic test V ESTEC										
		Frequency generator	CFG		Manufacture CFG (from external companies)				Ship CFG	CFG vibration test V Airbus D&S	CFG thermal test V ESTEC										
		Clock control unit	CCU			Manufacture CCU(from external companies)				CCU vibration test Airbus D&S	CCU software and thermal test ESTEC										
	NTM-ADCS	Control Moment Gyro (x2)	CMG								Manufacture CMG (from ext. comp.)		Manufacture CMG (from ext. comp.)	Ship CMG	CMG vibr. test V Airbus D&S	CMG rotation test V ESTEC					
		Star sensor (x4)	STS										Manufacture STS (OTS)	Ship STS	STS radiation and shock test V ESTEC						
		Sun sensor (x15)	SUS										Manufacture SUS (OTS)	Ship SUS	SUS radiation and shock test V ESTEC						
		Ring laser gyroscope (x4)	RLG								Manufacture RLG (from ext. comp.)		Manufacture RLG (from ext. comp.)	Ship RLG	RLG vibration test V Airbus D&S	CCU performance test V ESTEC					
	NTM-CDH	Computer	COM					Manufacture COM (from external companies)					COM vibration test V Airbus D&S	COM thermal test V ESTEC	COM software test V ESTEC						
	NTM-EPS	Power Control/ Distribution Unit	PCD				Manufacture PCD OTS (from external companies)		Ship PCD	PCD power, electromagnetic, electrical test V ESTEC			Establish cable connections with other components		Cable connection test V campaign ESTEC						
		Cable harness	CAH					Manufacture CAH (from external companies)		Ship CAH	CAH resistance test V ESTEC										
		Batteries (x2)	BAT					Manufacture BAT (from external companies)		Ship BAT	BAT heat and charge test V ESTEC capacity										
		Solar array (x4)	SOA					Manufacture SOA (from external companies)					CFG vibration test V Airbus D&S	CFG thermal test V ESTEC	SOA Deployment test ESTEC						
	NTM-PROP	Propellant Tank	PTK				Manufacture PTK (Internally)			PTK Tensile & Fracture test V NSPTF			Assembly of the Propulsion subsystem NSPTF		Assembly test V Propulsion subsystem NSPTF						
		Thrusters (x14)	THR					Manufacture THR (from external companies)	Ship THR	THR vibration test V Airbus D&S											
		Filters & Valves	FV				Manufacture FV (from external companies)			Ship FV	FV dry run test										
	NTM-TTC	Patch Antenna Array (x4)	ANT								Manufacture ANT (from ext. comp.)		Manufacture ANT (from ext. comp.)	Ship ANT	ANT vibration test V Airbus D&S	ANT thermal test V ESTEC					
		Transceiver	TRA								Manufacture TRA (from ext. comp.)		Manufacture TRA (from ext. comp.)	Ship TRA	TRA vibration test V Airbus D&S	TRA thermal test V ESTEC					
		2D gimbal	2DG					Manufacture 2DG (from external companies)		Ship 2DG	2DG vibration test V Airbus D&S		Assembly of LAS & 2DG		Assembly test V of LAS & 2DG						
		Laser Altimeter (x2)	LAS			Manufacture LAS (from external comapnies)			Ship LAS	LAS transmission test ESTEC											
	NTM-STR	Primary Structure	PST			Manufacture PST (from external companies)		Ship PST	PST vibration test V Airbus D&S	PST thermal and shock test V ESTEC			Structures subsystem assembly		Structures test V subsystem assembly						
		Propellant Tank support	PTS				Manufacture PTS (from external companies)		Ship PTS	PTS vibration test V Airbus D&S	PTS thermal test V ESTEC										
		Secondary Structure	SST				Manufacture SST (from external companies)		Ship SST	SST vibration test V Airbus D&S	SST thermal test V ESTEC										
	NTM-TC	Fluid Pump	FPU			Manufacture FPU(from external companies)			Ship FPU	FPU vibration test V Airbus D&S	FPU thermal test V Airbus D&S		Radiator subsystem assembly		Radiator test V subsystem assembly						
		Deployable Radiator	DRA				Manufacture DRA (from external companies)		Ship DRA	DRA vibration test V Airbus D&S	DRA deployment test V Airbus D&S										
		Thermal Storage Unit	TSU					Manufacture TSU (from external companies)		Ship TSU	TSU thermal test V ESTEC										
		Heater (x22)	HEA						Manufacture HEA (from external companies)				Ship HEA	HEA vibration test V Airbus D&S		HEA electric test V ESTEC					

Project Gantt Chart